ORIGINAL ARTICLE

CrossMark

Utility of Ruxolitinib in a Child with Chronic Mucocutaneous Candidiasis Caused by a Novel STAT1 Gain-of-Function Mutation

Markéta Bloomfield[1,2,3] · Veronika Kanderová[4] · Zuzana Paračková[1] · Petra Vrabcová[1] · Michael Svatoň[4] · Eva Froňková[4] · Martina Fejtková[4] · Radana Zachová[1] · Michal Rataj[1] · Irena Zentsová[1] · Tomáš Milota[1] · Adam Klocperk[1] · Tomáš Kalina[4] · Anna Šedivá[1]

Abstract

Purpose Signal transducer and activator of transcription 1 gain-of-function (STAT1 GOF) mutations are the most common cause of chronic mucocutaneous candidiasis (CMC). We aim to report the effect of oral ruxolitinib, the Janus kinase (JAK) family tyrosine kinase inhibitor, on clinical and immune status of a 12-year-old boy with severe CMC due to a novel STAT1 GOF mutation.

Methods Clinical features and laboratory data were analyzed, particularly lymphocyte subsets, ex vivo IFNγ- and IFNα-induced STAT1, 3, 5 phosphorylation dynamics during the course of JAK1/2 inhibition therapy, and Th17-related, STAT1- and STAT3-inducible gene expression before and during the treatment. Sanger sequencing was used to detect the STAT1 mutation. Literature review of ruxolitinib in treatment of CMC is appended.

Results A novel STAT1 GOF mutation (c.617T > C; p.L206P), detected in a child with recalcitrant CMC, was shown to be reversible in vitro with ruxolitinib. Major clinical improvement was achieved after 8 weeks of ruxolitinib treatment, while sustained suppression of IFNγ- and IFNα-induced phosphorylation of STAT1, STAT3, and STAT5, as well as increased STAT3-inducible and Th17-related gene expression, was demonstrated ex vivo. Clinical relapse and spike of all monitored phosphorylated STAT activity was registered shortly after unplanned withdrawal, decreasing again after ruxolitinib reintroduction. No increase of peripheral CD4$^+$ IL17$^+$ T cells was detected after 4 months of therapy. No adverse effects were noted.

Conclusion JAK1/2 inhibition with ruxolitinib represents a viable option for treatment of refractory CMC, if HSCT is not considered. However, long-term administration is necessary, as the effect is not sustained after treatment discontinuation.

Keywords Chronic mucocutaneous candidiasis · candida · signal transducer and activator of transcription 1 · Janus kinase inhibitor · ruxolitinib

Abbreviations

AD	Autosomal dominant
AR	Autosomal recessive
CARD9	Caspase recruitment domain-containing protein 9
CMC	Chronic mucocutaneous candidiasis

✉ Markéta Bloomfield
marketa.bloomfield@fnmotol.cz

[1] Department of Immunology, 2nd Faculty of Medicine, Charles University and University Hospital in Motol, Prague, Czech Republic

[2] Department of Paediatrics, Thomayer's Hospital, 1st Faculty of Medicine, Charles University, Prague, Czech Republic

[3] Department of Immunology, Motol University Hospital, V Úvalu 84, Prague 150 06, Czech Republic

[4] CLIP - Childhood Leukaemia Investigation Prague, Department of Paediatric Haematology and Oncology,Second Faculty of Medicine, Charles University and University Hospital Motol, Prague, Czech Republic

CMCD   Chronic mucocutaneous candidiasis disease
GAPDH   Glyceraldehyde-3-phosphate dehydrogenase
GOF   Gain-of-function
HSCT   Hematopoietic stem cell transplantation
JAK   Janus kinase
LPS   Lipopolysaccharide
PBMC   Peripheral blood mononuclear cell
PD-1   Programmed cell death protein 1
PD-L1   Programmed cell death ligand 1
PHA   Phytohaemagglutinin
PMA   Phorbol myristate acetate
RORC   RAR-related orphan receptor gene
RORγt   Thymus-specific RAR-related orphan
            receptor gamma
SOSC3   Suppressor of cytokine signaling 3
STAT1, 3, 5 Signal transducer and activator of
            transcription 1, 3, 5
Treg   Regulatory T cell
Tyr   Tyrosine

Introduction

Chronic mucocutaneous candidiasis (CMC), defined as a persistent or recurrent skin, nail, and mucosal infection with Candida species, may arise as a consequence of secondary T cell deficiency or as an inborn error of immunity [1]. Several genetic etiologies have been identified to convey a complex syndromic phenotype with abnormal fungal susceptibility, such as the autosomal dominant (AD) hyper IgE syndrome, autosomal recessive (AR) autoimmune polyendocrinopathy-candidiasis-ectodermal dystrophy, AR CARD9, IL-12Rβ1, IL-12p40, and RORγt deficiencies. Other gene defects, such as AR IL-17RA, AR IL-17RC, ACT1, and AD IL-17F deficiencies result in isolated superficial candidiasis in non-syndromic chronic mucocutaneous candidiasis disease (CMCD) due to disturbed IL-17 signaling [2–4]. Signal transducer and activator of transcription 1 gain-of-function (STAT1 GOF) mutations have recently been established as the most common cause of inherited syndromic CMC, with well over 300 cases identified worldwide to date [5]. The exact mechanism underlying CMC in STAT1 hyperfunction is not yet fully understood. Peripheral blood lymphocytes of STAT1 GOF patients exhibit skewed Th17 (CD4$^+$IL-17$^+$) differentiation in more than 80% of investigated cases [5], while some but not all patients display increased levels of circulating Th1 (CD4$^+$IFNγ$^+$) [6–8]. Previous reports indicate that disturbed functional equilibrium of STAT1/STAT3 signaling results in impaired Th17 development via reduced transcription of Th-17-related genes (RORC, IL-17A, IL-22) and STAT3-dependent genes (IL-10, c-Fos, SOCS3, c-Myc) [9, 10]. This is most likely due to altered STAT3 promoter binding precipitated by reduced

histone acetylation status as a result of abnormally strong, antagonizing IFNα-, IFNγ-, and IL-27-induced STAT1 response [10, 11]. The diminished Th17 response entails low levels of IL-17A, IL-17F, and IL-22, the key mediators in skin and mucosal antifungal protection [1, 3, 12].

Lately, STAT1 GOF mutations have been shown to convey a much broader clinical phenotype than previously appreciated, ranging from isolated CMC to complex combined immune deficiencies often associated with infectious, autoimmune, and neoplastic complications and aneurysms [5, 12, 13] prompting the need for more complex management. Newly gained insights into functional impact of the hypermorphic STAT1 mutations expose promising therapeutic targets along the dysregulated STAT1/STAT3/IL-17 pathways [14], such as Janus kinases (JAKs). JAKs are intracellular proteins, constitutively associated with cytokine receptors, which recruit STATs upon receptor stimulation and facilitate signal transduction, which may be inhibited with various JAK inhibitors [15].

In this report, we describe a child with a novel STAT1 GOF mutation presenting as an isolated mucocutaneous candidiasis and the outcome of treatment with oral selective JAK1 and JAK2 inhibitor ruxolitinib.

Methods

Informed consents were obtained from the patient and his guardians in accordance with the Declaration of Helsinki and according to the procedures established by the Ethical Committee of our institution.

STAT1 Sequencing

Sanger sequencing of the patient's STAT1 gene was originally performed in Debrecen, Hungary, as reported here [12]. Later, targeted Sanger sequencing of STAT1 gene was repeated for the patient and performed for his parents on 3730xl DNA Analyzer instrument (Thermo Fisher Scientific, Rockford, IL) in our facility. DNA was isolated from peripheral blood samples using QIAamp DNA Mini Kit (Qiagen, Hilden, Germany). Analysis of the trace files was performed with SnapGene® software (from GSL Biotech).

Immunophenotyping

Immunophenotyping of lymphocyte subpopulations was performed using CD27-Brilliant Violet (BV) 421, IgD-FITC, and IgM-PerCP-Cy5.5 (Biolegend, San Diego, CA, USA); CD45RA-BV510, CD16-PE, CD4-PerCP-Cy5.5, TCRgd-PE-Cy7, CD3-APC, and CD45-APC-H7 (BD Biosciences, San Jose, CA, USA); CD19-PE-Cy7 and HLA-DR-Pacific Blue (Beckman Coulter, Miami, FL, USA); and CD8-FITC

and CD56-PE (Cytognos, Salamanca, Spain). The samples were acquired on LSR II cytometer (BD Biosciences), and the data analysis was performed using FlowJo (TreeStar, Ashland, OR, USA).

CD4+ Subset Analysis (IL-17+Th, IFNγ+Th, Tregs)

PBMCs were stimulated with phorbol myristate acetate (PMA, 50 ng/ml) and ionomycin (750 ng/ml) (both from Sigma Aldrich, Darmstadt, Germany); 1 h later, brefeldin A (10 mg/ml) (Biolegend) was added for 3 h. Cells were harvested and stained with CD3-Alexa Fluor 700, CD8-PE-Dy594 (Exbio Praha, Vestec, Czech Republic), and CD4-PE-Cy7 (eBioscience, San Diego, CA, USA) before being fixed and permeabilized using eBioscience Fixation/Permeabilization solutions. The following Abs were added: IFNγ-FITC (BD Biosciences) and IL-17-Alexa Fluor 647 (Biolegend). Cells were incubated at 4 °C for 30 min, washed, and resuspended in FACS buffer. Data were collected using FACS Aria II, Diva software was used for signal acquisition (both from BD Biosciences), and data analysis was performed using FlowJo (Treestar).

For T regulatory cell (Tregs) analysis, protocol previously published elsewhere was used [16]. In short, PBMCs were stained with CD3-Alexa Fluor 700, CD8-PE-Dy594 (Exbio), CD4-PE-Cy7 (eBioscience), CD25-PerCP-Cy5.5, and CD127-APC (BioLegend), then fixed and permeabilized using eBioscience solutions and stained for intracellular markers using FoxP3-Alexa Fluor 488 (eBioscience) and Helios-PE (BioLegend) antibodies. Data were collected using FACS Aria II (BD Biosciences).

Western Blotting

PBMCs were stimulated w/wo IFNγ (1 μg/ml, R&D Systems, Minneapolis, MN) for 30 min at 37 °C; the cells were lysed using lysis buffer containing 50 mM HEPES, 10 mM MgCl2, 140 mM NaCl, pH 8, supplemented with 0.1% Tween 20, 1% n-dodecyl beta-D-maltoside, 2 mM PMSF, proteinase inhibitors, and phosphatase inhibitors (all from Sigma Aldrich). The lysates were sonicated 4× for 10 s, incubated for 60 min on ice, and centrifuged at 21.255 g for 10 min at 4 °C. Supernatants were diluted 1:1 with Laemmli reducing sample buffer (Sigma Aldrich) and heated to 90 °C for 5 min. Proteins were separated in SDS-PAGE gels and transferred to nitrocellulose membranes (Bio-Rad, Hercules, CA). The membranes were blocked in 7.5% low-fat bovine milk in PBS with 0.05% Tween 20 at 8 °C overnight. To detect STAT1 proteins, primary antibodies against phospho-STAT1 (Tyr701) and STAT1 (Cell Signaling Technologies, Danvers, MA) were used together with the peroxidase-conjugated secondary antibodies (Jackson Immunoresearch, West Grove, PA)

and the SuperSignal West Pico Chemiluminescent Substrate (Thermo Fischer). For in vitro ruxolitinib inhibition test, PBMCs were cultured with ruxolitinib (Seleckchem, Houston, TX) for 30 min at 37 °C prior to IFNγ stimulation.

Phospho-Flow

Whole peripheral blood was stimulated w/wo IFNα (1 μg/ml, Abcam, Cambridge, UK) or IFNγ (0,5-1 μg/ml, R&D Systems) for 5, 10, 15, or 30 min at 37 °C; intracellular signaling was stopped using 4% formaldehyde for 10 min at 25 °C; erythrocytes were lysed using 0.1% Triton X-100 for 15 min at 37 °C; and the leukocytes were permeabilized using 80% ice-cold methanol. B cells and T cells were discriminated using anti-CD45-Pacific Blue, anti-CD3-PerCP-Cy5.5 (Exbio Praha), and anti-CD19-PE-Cy7 (Beckman Coulter), and intracellular signaling was detected using anti-phospho-STAT1(Tyr701)-Alexa Fluor 647, anti-phospho-STAT3(Tyr705)-Alexa Fluor 488, and anti-phospho-STAT5(Tyr694)-PE (all from BD Biosciences). The samples were acquired on LSR II cytometer (BD Biosciences), and the data analysis was performed using FlowJo (TreeStar). For in vitro ruxolitinib inhibition test, whole blood was cultured with ruxolitinib (Seleckchem) for 30 min at 37 °C prior IFNα or IFNγ stimulation.

Gene Expression by qRT-PCR

PBMCs were isolated by density gradient centrifugation, pre-cultivated in RPMI medium supplemented with 10% fetal bovine serum and antibiotics in the presence of phytohaemagglutinin (2μg/ml) and IL-2 (20 U/ML) for 72 h, and then stimulated for 4 h with IFNγ (1 μg/ml) for CXCL10 expression, IL-27 (100 ng/ml) (both Peprotech, New Jersey, USA) for SOCS3, and cFOS expression or left without cytokines for IL-17A and RORC expression. Total RNA was isolated using RNeasy Mini Kit following manufacturer's instructions (Qiagen), and complementary DNA (cDNA) was synthetized using M-MLV Reverse Transcriptase (Thermo Fisher). RT-PCR was performed in duplicates using the cDNA and Platinum Taq polymerase (Thermo Fisher), 200 nM dNTP (Promega, Southampton, UK), 50 mM MgCl2 (Thermo Fisher), and TaqMan primer/probe sets (Thermo Fisher). Samples were matched to a standard curve generated by amplifying serially diluted products using the same PCR reaction and normalized to GAPDH (TIB MOLBIOL, Berlin, Germany) to obtain the relative expression value. Real-time assays were run on iQ5 Cycler (Bio-Rad). Primer sequences are available upon request at the author.

Intracellular Cytokine Detection

Intracellular detection of IL-1β was performed in heparinized whole blood stimulated with 100 ng/ml LPS (lipopolysaccharide, Sigma Aldrich) 4 h in a presence of brefeldin A. For analysis of IL-6 and TNF-α production, heparinized whole blood was stimulated with 100 ng/ml LPS, brefeldin A was added after 2 h, and samples were left for another 4 h in 37 °C. Cells were labeled with anti CD14⁻PE-Cy7 (Exbio). Following the lysis of RBC using BD lysing solution (BD Biosciences) and fixation/permeabilization using eBioscience protocol, cells were stained with antibodies against respected cytokines: IL-1β-PE (Thermo Fisher), IL-6-APC, or TNF-α-BV421 (BioLegend) for 30 min. Samples were washed and acquired on Canto II instrument (BD Biosciences). Results were expressed as mean fluorescence intensity (MFI) of a given cytokine within CD14⁺ population.

Results

Case Report

A healthy Czech newborn developed treatment-resistant oral thrush at the age of 2 months. By the end of the first year, he suffered seven middle ear infections, mostly bacterial, and one uncomplicated pneumonia, which resolved with standard course of antibiotics. Later, increased susceptibility to cutaneous staphylococcal infections was noted and prominent onychomycosis appeared. No gross immunodeficiency was initially discovered, but in time, the patient developed progressive CD4⁺ and CD8⁺ T cell lymphopenia with Th17 and T regulatory cell (Treg, CD4⁺CD25⁺FOXP3⁺) deficiency, CD19⁺ switched memory B cell lymphopenia, and low IgG2, IgG4, and IgM levels. Extensive screening excluded autoimmune and vascular complications (Table 1). Treatment with prophylactic azoles (fluconazole alternated with itraconazole), trimethoprim/sulfamethoxazole, and subcutaneous immunoglobulins was initiated; however, the increasing antifungal resistance eventually rendered azoles altogether ineffective and allowed massive spread of the yeast infection. At this point, a novel sporadic mutation in STAT1 gene was discovered (Fig. 1), and its gain-of-function property was verified (Figs. 2 and 3). Next, the IFN-induced augmented STAT1 phosphorylation in patient's circulating T and B cells was shown to be reversible in vitro with JAK1/2 inhibitor ruxolitinib as demonstrated in previous reports (Figs. 2 and 3) [7, 8]. Based on this, treatment with ruxolitinib was initiated when the patient was 12 years of age. The dose was increased gradually over 4 weeks to a target dose 10 mg twice daily (20 mg/m²/day), in adherence to previously reported well-tolerated dose in children with solid tumors/hematologic malignancies [17], and decreased by 50% for ruxolitinib's

pharmacologic interaction with concomitantly administered itraconazole on cytochrome CYP3A4. At the end of week 4, first improvement of the cutaneous (and partially oral) candidiasis was noted, which culminated at week 8 (Fig. 5) when the treatment had to be interrupted for non-medical reasons. Within 2 weeks from the abrupt withdrawal, the previously achieved amelioration of CMC was almost completely lost (Fig. 5). Four weeks after ruxolitinib discontinuation, the treatment was resumed at the same dose with gradual, but this time much less, pronounced improvement (Fig. 5). During the treatment, skin and mucosal swabs continued to yield candida strains. No adverse reactions were noted throughout the treatment; the patient's full blood count, liver, renal functions, blood cholesterol, and triacylglycerol levels remained unaltered; and the patient suffered only one episode of mild upper respiratory tract infection.

Detection of STAT1 Mutation

Sanger sequencing revealed novel heterozygous mutation in STAT1 gene leading to amino acid substitution of proline for leucine (c.617T > C; p.L206P). This mutation occurred de novo in the patient; neither of his parents are affected (Fig. 1). The mutation is located in the coiled-coil domain of STAT1 protein, which is essential for STAT1 dimerization and STAT1 nuclear dephosphorylation [18].

STAT Phosphorylation Dynamics

To evaluate functional impact of the mutation in STAT1 gene, we first examined STAT1 protein expression and IFNγ-induced STAT1 phosphorylation (p-) at Tyr 701 in patient's PBMCs using Western blot. We found mildly increased constitutive STAT1 expression and threefold higher phosphorylation of STAT1 in response to IFNγ compared to patient's unaffected mother and unrelated healthy control. Interestingly, IFNγ activated not only STAT1α isoform, but also STAT1β isoform in patient in contrast to healthy controls (Fig. 2). The results were confirmed at a single-cell level; following IFNγ stimulation, higher phosphorylation of STAT1 was detected in patient's CD3⁺ T cells (Fig. 3a) and CD19⁺ B cells (Fig. 3b) compared to healthy controls. Moreover, pre-treatment of the patient's cells with ruxolitinib suppressed IFNγ-induced p-STAT1 signal to levels seen in IFNγ-stimulated control cells (Fig. 3a, b). Additionally, IFNα was also shown to induce abnormally high p-STAT1 activation compared to controls in both cell types (Fig. 3a, b). Flow cytometry-based test for evaluation of p-STAT1 (Tyr701), p-STAT3 (Tyr705), and p-STAT5 (Tyr694) in whole blood on a single-tube platform was optimized for ex vivo monitoring of response to IFNα and IFNγ. After just 7 days on initial dose of ruxolitinib (10 mg/m²/day), p-STAT1 response to IFNα was reduced

Table 1 Immunologic characteristics of STAT1 GOF $^{c.617T>C}$ patient before ruxolitinib and after 4 months of treatment

Patient 12 years of age		Pre-ruxolitinib	16 weeks on ruxolitinib	Age-matched reference values
Leukocytes (cells/μL)		11,600	7500	4500–13,500
Lymphocytes (cells/μL)		*850* ↓	*1360* ↓	1500–4100
Neutrophils (cells/μL)		*9690* ↑	5230	1500–5900
Monocytes (cells/μL)		1010	870	150–1280
Eosinophils (cells/μL)		0	0	0–460
CD3$^+$ (%[a], cells/μL)		*73/621* ↓	*70/952* ↓	56–84/1200–2600
CD3$^+$ CD4$^+$ (%[a], cells/μL)		*12/102* ↓	*17/231* ↓	20–65/400–2100
CD3$^+$ CD8$^+$ (%[a], cells/μL)		*8.6/73* ↓	*13/177* ↓	14–40/300–1300
Naïve CD4$^+$ (%[b]) (CD3$^+$CD4$^+$CD45RA$^+$CD27$^+$)		40	59	37–97
Central memory CD4$^+$ (%[b]) (CD3$^+$CD4$^+$CD45RA$^-$CD27$^+$)		51	38	13–76
Effector memory CD4$^+$ (%[b]) (CD3$^+$CD4$^+$CD45RA$^-$CD27$^-$)		3.6	2.4	0.49–25
Terminally diff. CD4$^+$ (%[b]) (CD3$^+$CD4$^+$CD45RA$^+$CD27$^-$)		5.4	0.2	0.0042–5.8
Naïve CD8$^+$ (%[c]) (CD3$^+$CD8$^+$CD45RA$^+$CD27$^+$)		34	48	20–95
Central memory CD8$^+$ (%[c]) (CD3$^+$CD8$^+$CD45RA$^-$CD27$^+$)		*27* ↑	17	0.42–18
Effector memory CD8$^+$ (%[c]) (CD3$^+$CD8$^+$CD45RA$^-$CD27$^-$)		12	13	4–100
Terminally diff. CD8$^+$ (%[c]) (CD3$^+$CD8$^+$CD45RA$^+$CD27$^-$)		23	20	9–65
CD19$^+$ (%[a], cells/μL)		18/153	20/272	6–23/110–570
Naïve CD19$^+$ (%[d]) (CD19$^+$CD27$^-$IgD$^+$)		92	97	49–100
Switched memory CD19$^+$ (%[d]) (CD19$^+$CD27$^+$IgD$^-$)		*0.7* ↓	*0.3* ↓	8.7–25.6
CD16$^+$/CD56$^+$ (%[a], cells/μL)		11/123	7.7/105	4–51/92–1200
CD4$^+$IL17$^+$ (%[b])		*0.26* ↓	*0.19* ↓	1.05–5.97
$^+$IFNγ$^+$ (%[b])		9.47	*4.4* ↓	7.2–41.9
Regulatory T cells (%[b]) (CD4$^+$CD25$^+$FOXP3$^+$)		*1.11* ↓	*1.04* ↓	4.0–8.0
Immunoglobulins (on SCIG) IgG (g/l)		7.52	8.52	6.20–11.50
IgG1 (g/l)		6.06	6.60	4.23–10.60
IgG2 (g/l)		*0.97* ↓	1.30	0.98–3.55
IgG3 (g/l)		0.76	0.69	0.17–1.73
IgG4 (g/l)		*< 0.080* ↓	*< 0.080* ↓	0.030–1.150
IgA (g/l)		0.55	*0.35* ↓	0.50–1.70
IgM (g/l)		*0.33* ↓	*0.29* ↓	0.55–1.55
IgE (IU/ml)		1.3	1.0	0.0–200
Autoantibodies (ANA, ENA, ANCA, ASCA, a-dsDNA, AMA, ASMA, GPCA, LKM, a-TPO, a-TG)		neg	ND	NA
LPS-induced intracellular cytokine production in CD14$^+$			8 weeks on RX	Reference ranges
	IL-6	1232	1806	1489 ± 1050
	TNF-α	*5315* ↓	*9372* ↓	32,306 ± 19,218
	IL-1	5388	5755	3949 ± 2142

values beyond normal reference values are shown in italics

RX ruxolitinib, ND not done, NA not applicable, SCIG subcutaneous immunoglobulins, LPS lipopolysaccharide, ANA antinuclear antibodies, ENA extractable nuclear antigen antibodies, ANCA anti-neutrophil cytoplasm antibodies, ASCA anti-saccharomyces cerevisiae antibodies, a-dsDNA anti-double stranded DNA antibodies, AMA anti-mitochondrial antibodies, ASMA anti-smooth muscle antibodies, GPCA gastric parietal cell antibodies, LKM liver kidney microsome antibodies, a-TPO anti-thyreoperoxidase antibodies, a-TG anti-thyreoglobulin antibodies, ↑, ↓ value above and below reference range, respectively
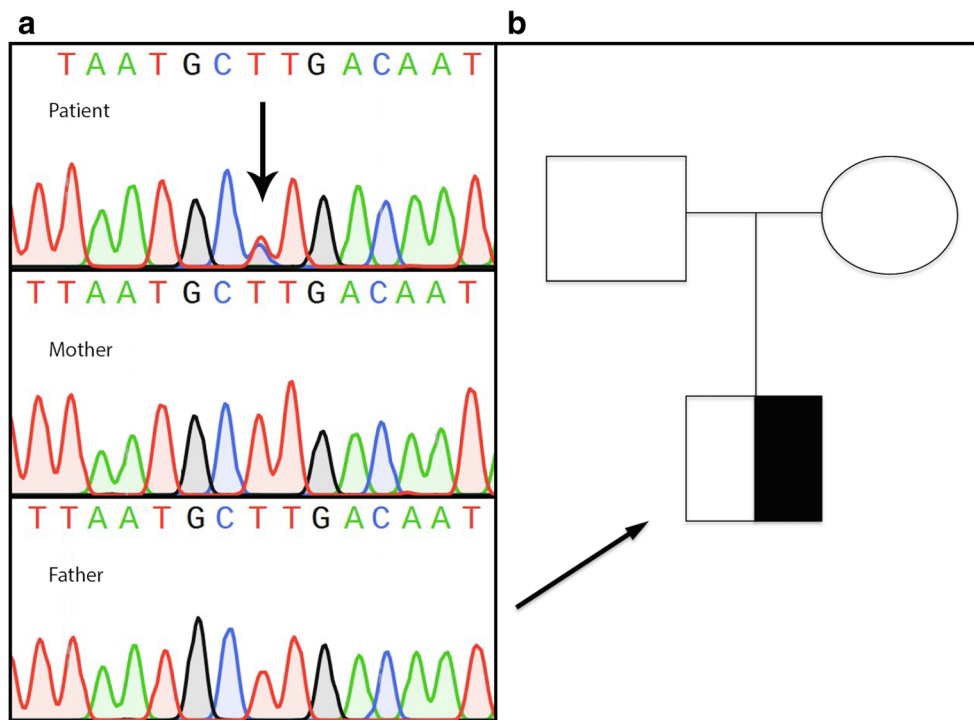
[a] % of total peripheral lymphocytes

[b] % of CD4$^+$

[c] % of CD8$^+$

[d] % of CD19$^+$

Fig. 1 Novel heterozygous STAT1$^{c.617T>C}$ leading to p.P206L amino acid change in STAT1 gene detected by Sanger sequencing in the patient. **a** DNA chromatogram of patient and his parents (wild-type) and **b** family tree are shown

to 32 and 57% of pre-treatment values in patient's CD3$^+$ and CD19$^+$ cells, respectively. Similarly, IFNγ-induced p-STAT1 activation was reduced to 17 and 14% of pre-treatment values in patient's CD3$^+$ and CD19$^+$ cells, respectively. Compared to healthy control, patient's p-STAT1 signal upon IFNα stimulation decreased from 274 to 87% in CD3$^+$ cells and from 208 to 137% in CD19$^+$ cells (Fig. 4) while IFNγ-stimulated p-STAT1 signal was reduced from

105 to 25% of control values in CD3$^+$ cells and from 404 to 53% of control values in CD19$^+$ cells (Fig. 5). Pre-treatment p-STAT3 and p-STAT5 responses were similar to healthy controls, and their parallel milder decrease was observed after ruxolitinib introduction (Fig. 4). During the following 7 weeks of ruxolitinib treatment, a dose-dependent suppression of all monitored p-STAT molecules was observed (Figs 4 and 5). Sudden withdrawal of ruxolitinib reverted
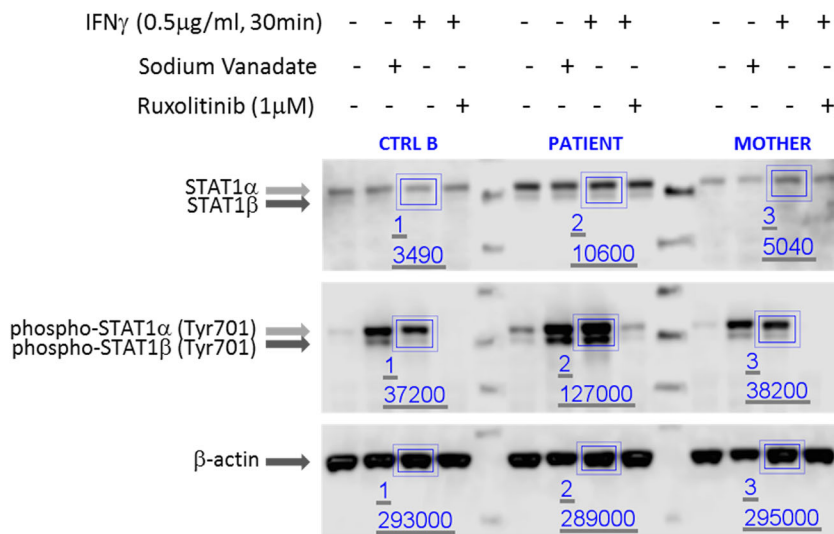

Fig. 2 Western blot analyses of STAT1 expression and phosphorylation confirms gain-of-function effect of STAT1$^{c.617T>C}$ which is rescued with ruxolitinib. Patient's PBMCs were analyzed for STAT1 expression and STAT1 phosphorylation response to IFNγ and ruxolitinib and compared to healthy mother and additional healthy control (quantification indicated by numbers in figure). In the patient, mildly increased constitutive STAT1 is shown, markedly high activation of p-STAT1 after IFNγ, and abnormal presence of p-STAT1β isoform, along with p-STAT1 reversal to pre-stimulation levels after ruxolitinib are demonstrated
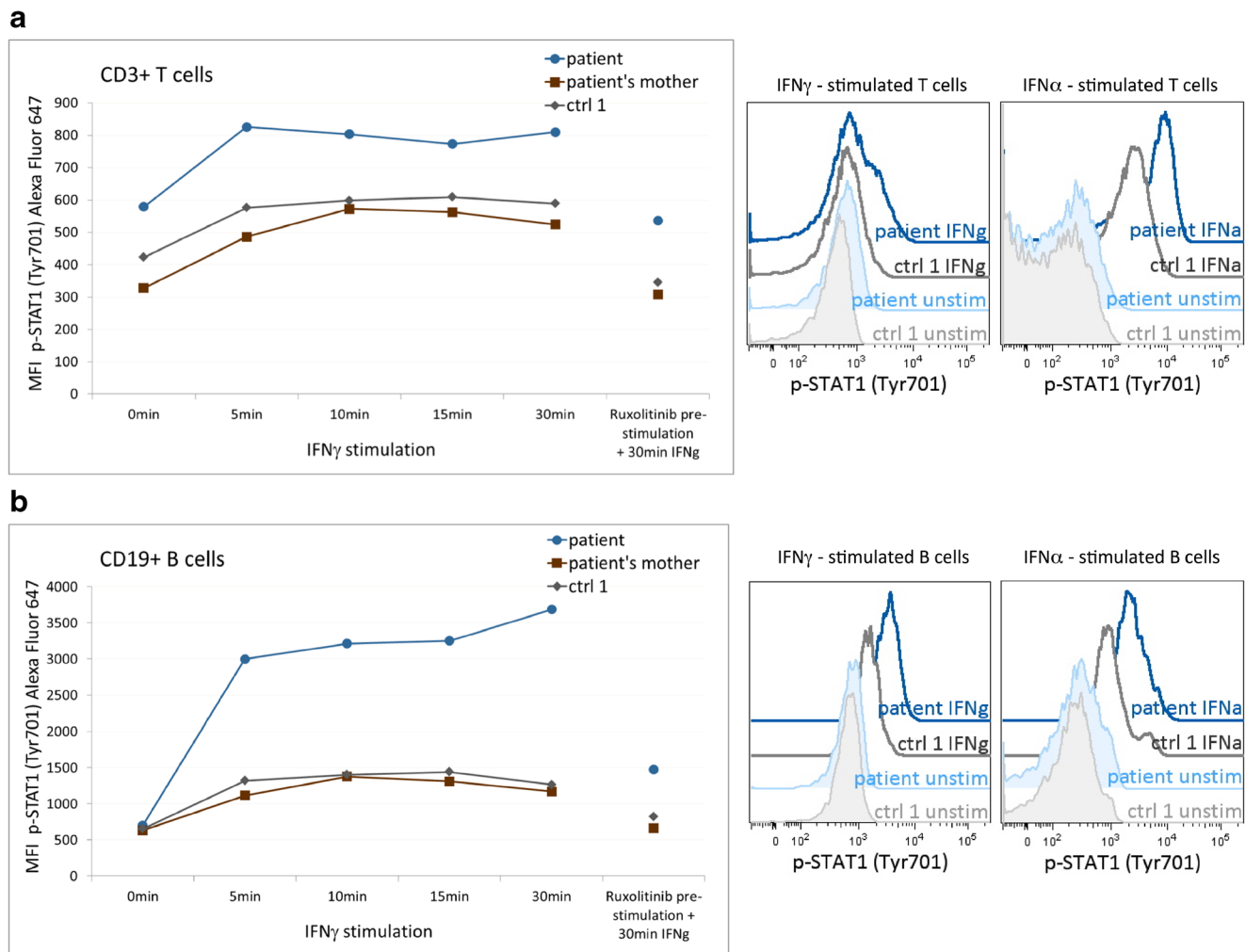
Fig. 3 Flow cytometric trace of p-STAT1 (Tyr701) ascertains GOF property of STAT1$^{c.617T>C}$ and confirms its reversibility with ruxolitinib. Time-dependent IFNγ-induced hyperphosphorylation of p-STAT1 (Tyr701) is shown in patient's CD3$^+$ T cells (a) and in CD19$^+$ B cells (b) compared to healthy controls. Pre-treatment of the patient's cells with ruxolitinib suppresses the stimulated p-STAT1 (Tyr701) response to IFNγ-stimulated control levels. Histograms (right) show hyperphosphorylation of p-STAT1 (Tyr701) in patient's cells 10 min upon IFNγ or IFNα stimulation. MFI median fluorescence intensity

p-STAT1 response to its augmented state, reflected by clinical deterioration. Concurrently, restoration of p-STAT3 and p-STAT5 signals was registered. Similar patterns of p-STAT suppression were later observed after ruxolitinib treatment was restarted (Figs 4 and 5). The remarkable correlation between the ruxolitinib dose, the IFNγ-induced p-STAT1 activity, and the clinical condition of the patient is shown in Fig. 5. The basal levels of p-STATs are available as a supplementary figure.

STAT1/STAT3-Dependent/Th17-Related Gene Transcription Alteration

In order to evaluate changes in transcription of relevant genes during treatment with JAK1/2 inhibitor, qRT-PCR was performed on patient's PHA and IL-2-stimulated PBMCs before treatment and after 16 weeks on ruxolitinib (Fig. 6). Before treatment, abnormally heightened IFNγ-induced transcription of STAT1-dependent gene CXCL10 was noted compared to healthy control, which was markedly reduced with ruxolitinib treatment. Conversely, expression of IL-27-induced STAT3-dependent genes cFOS and SOCS3, as well as Th17-related genes IL-17A and RORC, was prominently suppressed in the setting of extremely high STAT1 activity before treatment and increased upon reduction of STAT1 signaling with the JAK inhibitor.

Lymphocyte Subpopulation Profile

Consistent with previous observations in STAT1 GOF patients, diminished peripheral Th17 population (CD4$^+$IL17$^+$) was detected in our patient, while IFNγ producing Th1 cells (CD4$^+$IFNγ$^+$) were not increased compared to age-matched healthy donors (Table 1, Fig. 7). Despite apparent clinical
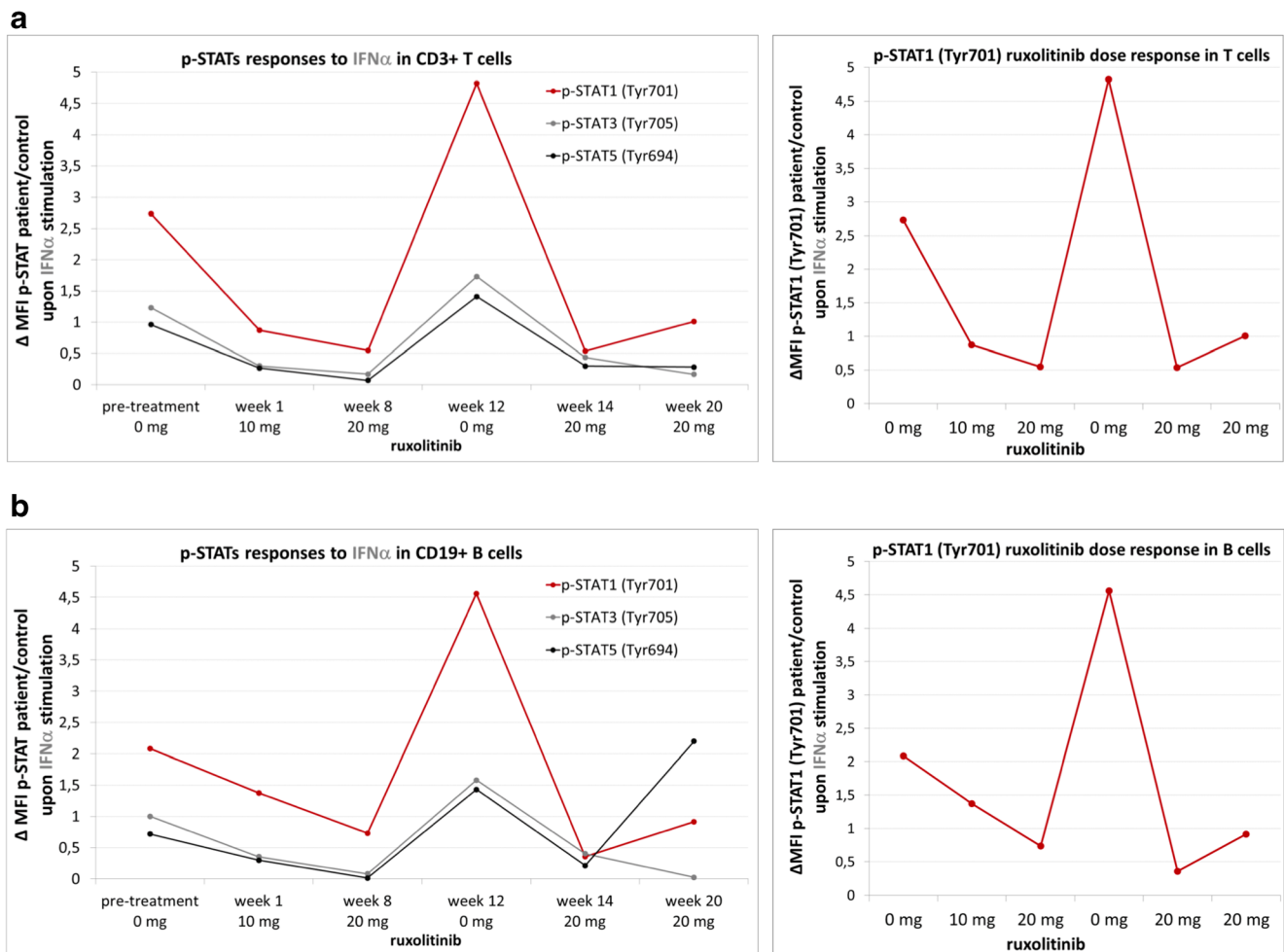
Fig. 4 Phospho-Flow analysis of IFNα-induced p-STAT1 (Tyr701), p-STAT3 (Tyr705), and p-STAT5 (Tyr694) activation in CD3^{+} cells (**a**) and in CD19^{+} cells (**b**) of STAT1[c.617T > C] patient and the response to ruxolitinib. Ruxolitinib suppresses IFNα-induced augmented p-STAT1 (Tyr701) in a dose-dependent manner, which was particularly marked in CD19+ B cells (bottom right). Pre-treatment p-STAT3 (Tyr705) and p-STAT5 (Tyr694) levels corresponded to healthy controls and were mildly suppressed with ruxolitinib during treatment. Daily dose of ruxolitinib is indicated on the x-axis; the y-axis represents a quantitative relation between the median fluorescence intensity (MFI) of the patient's IFNα-induced p-STATs and that of a healthy control

improvement, the CD4^{+}IL17^{+} peripheral counts remained low throughout the treatment with ruxolitinib, while IFNγ^{+}Th1 population dropped below the reference values (Table 1, Fig. 7). Additionally, decreased numbers of Tregs were noted and remained low on treatment. Mild, yet progressive T cell lymphopenia and decreased switched memory B cell compartment, as well as low IgG2, IgG4, and IgM, were detected prior to ruxolitinib treatment (Table 1), corresponding to similar irregularities in other STAT1 GOF patients [19]. Although the absolute CD3^{+} counts improved during the treatment on the account of both CD4^{+} and CD8^{+} lymphocytes, they remained below the age-matched reference values. The relative count of CD4^{+} effector memory cells and CD4^{+} central memory cells declined on treatment by 1.2 and 13%, respectively (Table 1). Lastly, the low relative proportion of switched memory B cells within the CD19^{+} compartment decreased even further on treatment.

Cytokine Production

To assess mononuclear phagocyte ability to produce pro-inflammatory cytokines in our patient before treatment, we measured LPS-induced TNF-α, IL-6, and IL-1β production in CD14^{+} monocytes, yielding mildly decreased TNF-α response; otherwise, similar results compared to healthy controls (Table 1). The test was repeated after 8 weeks on ruxolitinib with a similar result.

Discussion

We report a child with treatment-resistant chronic mucocutaneous candidiasis due to a novel STAT1 GOF mutation, who improved significantly during treatment with JAK1/2 inhibitor ruxolitinib. To our knowledge, this is only a fourth
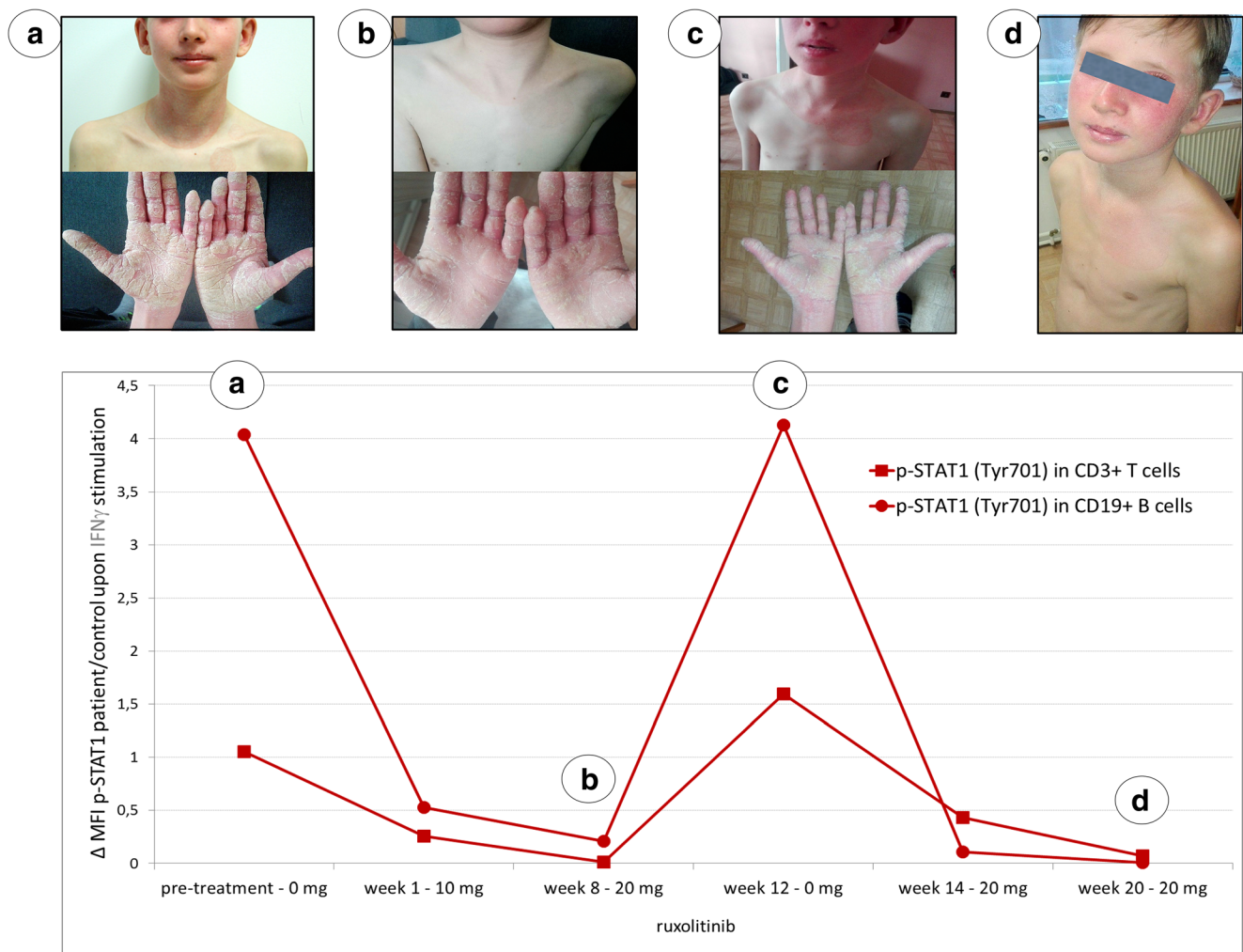
Fig. 5 Clinical progress paralleled to IFNγ-induced p-STAT1 (Tyr701) activation during ruxolitinib treatment of STAT1$^{c.617T>C}$ patient. Sustained suppression of p-STAT1 (Tyr701) in CD3$^+$ T cells and CD19$^+$ B cells along with marked improvement of CMC (**a**, **b**) is detected during ruxolitinib administration. Increase of p-STAT1 signal and clinical decay is noted shortly after discontinuation (**c**) and reversed again after ruxolitinib is restarted (**d**). Daily dose of ruxolitinib is indicated on the *x*-axis; the *y*-axis represents the quantitative relation between the median fluorescence intensity (MFI) of the patient's IFNγ-induced p-STAT1 (Tyr701) and that of a healthy control

child with STAT1 GOF CMC reported to receive this treatment [8, 20, 21].

STAT1 GOF CMC patients are currently managed with long-term administration of systemic antifungal drugs; some patients benefit from prophylactic antibiotics, antivirotics, and replacement/immunomodulatory immunoglobulins. The diverse phenotype often renders such treatment insufficient, particularly when autoimmune phenomena are present. Moreover, development of antifungal resistance frequently necessitates use of second-line drugs with higher toxicity and heralds poorer outcome [5]. An initially promising effect of granulocyte macrophage colony-stimulating factor and granulocyte colony-stimulating factor on CMC [22] was regrettably not replicable in four other patients [5, 23, 24]. In 2017, the first multi-center experience with hematopoietic stem cell transplantation (HSCT) in 15 STAT1 GOF patients was reported [21]. Despite having curative potential, only 40% overall post-transplant survival was achieved.

Recently, systemic administration of JAK1 and JAK2 inhibitor ruxolitinib, approved by European Commission for treatment of myelofibrosis and polycythemia vera [25], has been shown to rapidly improve STAT1 GOF-driven oral candidiasis and alopecia in adult female [26], indicating its capacity to ameliorate associated autoimmune symptoms. Similar to our experience, the candidiasis flared up 2 weeks after ruxolitinib withdrawal, while, remarkably, the hair regrowth was sustained for 6 months. Of note, the relapse in our patient after the drug withdrawal was mirrored by p-STAT1 rebound to levels almost twofold higher than pre-treatment values related to healthy control in IFNα-induced cells, perhaps resonating with the abrupt clinical deterioration during ruxolitinib withdrawal syndrome reported in patients with myelofibrosis
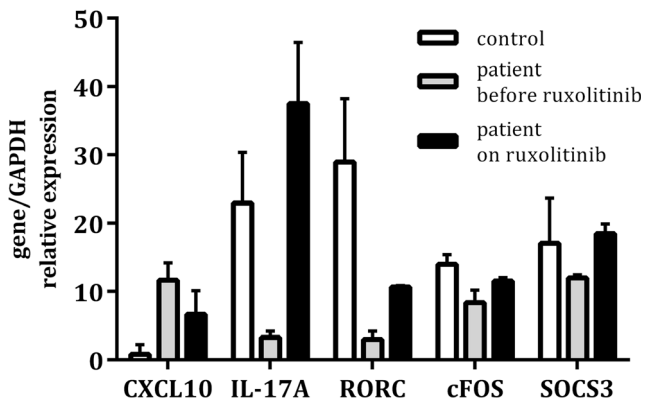
Fig. 6 qRT-PCR of Th17-related STAT1 and STAT3-induced genes in STAT1$^{c.617T > C}$ patient before and during ruxolitinib treatment. Ruxolitinib-näive phytohaemagglutinin (PHA) and IL-2-stimulated IFNγ-induced CXCL10 expression in PBMCs surmounts values seen in healthy control and significantly decreases after 16 weeks on ruxolitinib; ruxolitinib-näive PHA and IL-2-stimulated expression of IL-17A and RORC, as well as identically pre-treated IL-27-induced cFOS and SOCS3 expression are suppressed and increase markedly on treatment. Individual gene expressions are related to housekeeping gene GAPDH. Data are expressed as mean significant deviation of the indicated gene/GAPDH

[27]. In another adult male patient, ruxolitinib induced remission of severe oro-esophageal candidiasis after 6 months of treatment [24], albeit with slower and only partial effect, while increased IL-17A/F secretion and dose-dependent decrease of serum IL-6 were observed. Another intriguing utility of ruxolitinib was reported in a patient who received the compound 2 weeks prior to HCST for STAT1 GOF CMC [21] and was one of the six survivors of the procedure, out of 15 recipients. The fourth patient treated with ruxolitinib cleared his CMC as well as severe autoimmune cytopenias after more than 1 year of uninterrupted therapy [8]. Curiously, the

patient's originally increased peripheral IFNγ$^+$Th1 cells decreased within first 4 months, while increase in Th17 wasn't registered until the 12th month of therapy, despite months of prominent clinical improvement. Another group reported a 7-year-old male with STAT1 GOF mutation who improved his IPEX-like enteropathy and chronic norovirus enteritis after 3 months of ruxolitinib therapy [20]. In contrast to these reports, two adult patients with severe dermatophytosis and disseminated coccidioidomycosis due to STAT1 GOF mutation were recently reported to fail to respond to ruxolitinib [28]. Despite having achieved near-normal STAT1 phosphorylation by dose titration in one of the patients, the downstream STAT1-induced gene expression remained high and Th17 population more or less unchanged. The other patient failed to improve his Th17 levels after 2 weeks despite the use of currently approved adult therapeutic dose of ruxolitinib (40 mg/daily).

In our case, we demonstrated ruxolitinib-induced suppression of STAT1, STAT3, and STAT5 phosphorylation ex vivo. Despite having achieved a profound suppression of p-STAT1 within days from treatment initiation, the clinical improvement was first seen when p-STAT1 had been reduced to subnormal level for 4 weeks. As such, the clinical effect may not only be due to dose increments but also to longer time-to-improvement interval required. For unknown reason, the rate and extend of candidiasis clearance was less prominent when ruxolitinib was reintroduced after an unintended interruption of treatment, in spite of using the same target dose (20 mg/daily) and achieving similar levels of p-STAT1. Parallel to p-STAT1 suppression, rescued STAT3-dependent gene expression was demonstrated; however, the anticipated CD4$^+$IL17$^+$ restoration was not observed after 4 months, suggesting longer duration of ruxolitinib treatment may be required to achieve
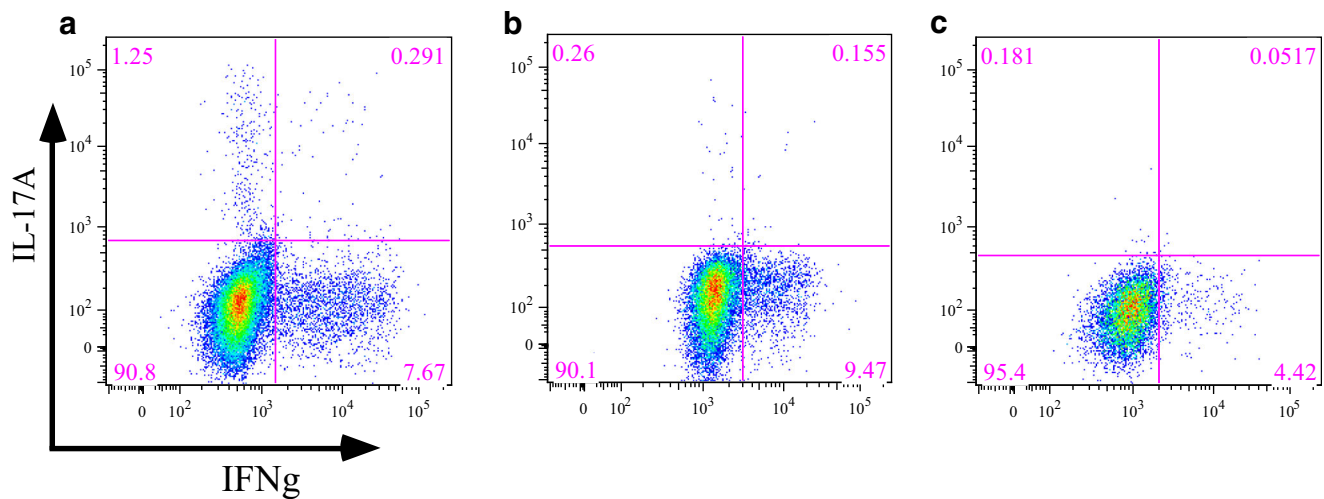

Fig. 7 Flow cytometric analyses of IL-17 and IFNγ producing peripheral CD4$^+$ lymphocytes **a** from a healthy age-matched subject and **b** from patient before ruxolitinib; low CD4$^+$IL17$^+$ count and normal CD4$^+$IFNγ$^+$ are shown **c** from patient after 16 weeks on ruxolitinib; no increase of CD4$^+$IL17$^+$ count is registered

this. The reason for this delay is obscured. Differentiation of Th17 cells requires precisely orchestrated actions of multiple cytokines, signal transducers, and transcription factors (known or unknown) [2, 9, 29], which may be affected by JAK inhibition. Crucial pro-Th17 cytokines, IL-6, and IL-23, require JAK2-mediated STAT3 recruitment [30]. It is therefore conceivable that ruxolitinib itself might restrain Th17 development via concomitant STAT3 suppression. However, we showed that during suppression of the augmented STAT1 activity, an increase of STAT3-inducible/Th17-related gene transcription was achieved, despite the parallel p-STAT3 suppression, corresponding with a previous observation that the disturbed Th17 development in STAT1 GOF patients results from altered signaling downstream of STAT3 [10]. Curiously, another set of experiments demonstrated that in addition to the canonical STAT3-driven Th17 induction, STAT3 inhibition may also, under certain conditions, cause amplification of IL-17$^+$ T cells within memory T cell population, depending on the kinetics of STAT3 activation [31], foreshadowing the intricate and still largely unknown regulations at play. Furthermore, naïve CD4$^+$ T cells of a set of STAT1 GOF patients were shown to overexpress PD-L1 protein [19]. STAT1-invoked PD-L1 overexpression was demonstrated to skew Th17 differentiation via PD-1/PD-L1 interaction [32], exposing another potential mechanism for disrupted Th17 lineage commitment which might be reversible with ruxolitinib with unknown dynamics.

On a side note, the finding of non-rescued CD4$^+$IL17$^+$ does not allow an unequivocal interpretation of Th17 dynamics because the Th17 lymphocytes should be more accurately assessed as proportion of CD4$^+$ memory cells, the principal IL-17 producing T cells. Adherence to commonly used enumeration of Th17 population as percentage of total CD4$^+$ cells in our experiments allows comparison across the previously published studies but limits the interpretability of the intra-individual data due to physiologic fluctuation of memory cell compartments. Nevertheless, as the CD4$^+$ memory cell frequencies decreased slightly in our patient at the time of CD4$^+$IL17$^+$ measurements, no major increase of the IL17$^+$ memory cells may be anticipated.

While the Th17 functional integrity is indisputably important in mucosal antifungal immunity, other aspects may be affected with ruxolitinib in STAT1 GOF patients and contribute to the clinical improvement even in the absence of peripheral blood Th17 restoration. For example, defective NK cell cytotoxicity due to aberrant STAT5 signaling was recently demonstrated in STAT1 GOF patients and shown to be partially reversible ex vivo with ruxolitinib [20]. The impairment of STAT5 activity may be at least in part due to augmented STAT1-induced SOCS1-mediated suppression of STAT5 [33] which would be ameliorated during ruxolitinib-induced p-STAT1 suppression. The restoration of NK cytotoxicity may attribute for the improvement of both antiviral and antifungal susceptibility in these patients [34]. It is also important to emphasize that our experiments were performed on peripheral blood lymphocytes, yet the antifungal response in mucosal and skin microenvironment may be modulated by other mechanisms, such as tissue-resident cytotoxic CD8$^+$ lymphocytes [35], IL-17-secreting γδ T cells [36, 37], or even keratinocytes, in which the IFN-STAT1-SOCS1 negative feedback loop is implicated in antiviral protection [38].

In our patient, no autoimmune complications were present, but low levels of circulating Tregs were noted. Such reduction may be, at least in part, due to IL-6 inhibitory effect on the induction of Tregs [39, 40], as serum levels of IL-6 were shown to be highly elevated in some STAT1 GOF patients [24]. Nevertheless, autoimmune features of STAT1 GOF patients most likely do not result from Tregs deficiency as indicated by unaltered Treg compartment in patients with IPEX-like manifestation of STAT1 GOF [41] but rather from stronger response to IFNα/β signaling in interferonopathy-like manner [42] and/or naïve CD4$^+$ T cell priming towards differentiation into Th1 lineage under both Th1 and Th17 polarizing conditions [8]. How ruxolitinib should tackle autoimmunity in STAT1 GOF CMC is not precisely understood. Evidently, a part of rescuing Th17 development, thus facilitating an effective protection against candida, ruxolitinib also suppresses exaggerated Th1 and follicular T helper cell responses and reverses the IFNγ$^+$Th1-biased priming of naïve T cells [8]. In our patient, ruxolitinib induced sustained suppression of p-STAT5, one of the non-redundant players in Tregs development [43]. Although Treg counts did not decrease significantly on treatment, such suppression of the kinase activity further supports the notion of Treg-independent mechanism of development of autoimmune features in STAT1 GOF patients.

Experience with prolonged use of ruxolitinib in children with CMC is scarce, and close monitoring of adverse reactions is essential. These are mainly related to off-target effects of JAK1 and JAK2 inhibition and include increased susceptibility to infections, dose-dependent anemia, thrombocytopenia, neutropenia (due to inhibited erythropoietin, thrombopoietin, and granulocyte colony-stimulating factor signaling via JAK2), and dyslipidemia [44–46]. Additionally, supported by our observation of parallel p-STAT5 inhibition, the risk of growth failure due to disturbed growth hormone-JAK2-STAT5 signaling [47] is a major concern in pediatric population. In our patient, no such events were noted after 4 months of treatment; serum levels of insulin-like growth factor and insulin-like growth factor-binding protein 3 were undisturbed. Our original concern that ruxolitinib might compromise TNF-α production and thus increase infectious susceptibility [48] proved to be unsubstantiated in our patient.

Conclusion

In summary, this paper expands evidence of ruxolitinib's efficacy in control of the profound immune disbalance caused by STAT1 GOF mutation. From our experience, we conclude that the effect of ruxolitinib on mucocutaneous candidiasis is short-lived after discontinuation and long-term administration is required to maintain disease control; therefore, careful dose titration is necessary to avoid adverse effects. However, efficacy and safety of prolonged treatment of STAT1 GOF patients with ruxolitinib is yet to be ascertained. Alternatively, ruxolitinib may be a useful tool to bridge time to HSCT and possibly improve its outcome. Further experience is needed to draw conclusions about its role in CMC management and optimal pediatric dose.

Compliance with Ethical Standards

Conflicts of Interest All authors declare that they have no conflicts of interest.

References

1. Liu L, Okada S, Kong X-F, Kreins AY, Cypowyj S, Abhyankar A, et al. Gain-of-function human STAT1 mutations impair IL-17 immunity and underlie chronic mucocutaneous candidiasis. J Exp Med. 2011;208:1635–48.

2. Puel A, Cypowyj S, Maródi L, Abel L, Picard C, Casanova J-L. Inborn errors of human IL-17 immunity underlie chronic mucocutaneous candidiasis. Curr Opin Allergy Clin Immunol. 2012;12:616–22.

3. Okada S, Puel A, Casanova J-L, Kobayashi M. Chronic mucocutaneous candidiasis disease associated with inborn errors of IL-17 immunity. Clin Transl Immunol. 2016;5:e114.

4. Boisson-Dupuis S, Kong XF, Okada S, Cypowyj S, Puel A, Abel L, et al. Inborn errors of human STAT1: allelic heterogeneity governs the diversity of immunological and infectious phenotypes. Curr Opin Immunol. 2012;24:364–78.

5. Toubiana J, Okada S, Hiller J, Oleastro M, Gomez ML, Becerra JCA, et al. Heterozygous STAT1 gain-of-function mutations underlie an unexpectedly broad clinical phenotype. Blood. 2016;127:3154–64.

6. Ma CS, Wong N, Rao G, Avery DT, Torpy J, Hambridge T, et al. Monogenic mutations differentially affect the quantity and quality of T follicular helper cells in patients with human primary immunodeficiencies. J Allergy Clin Immunol. 2015;136:993–1006e1.

7. Baris S, Alroqi F, Kiykim A, Karakoc-Aydiner E, Ogulur I, Ozen A, et al. Severe early-onset combined immunodeficiency due to

8. Weinacht KG, Charbonnier LM, Alroqi F, Plant A, Qiao Q, Wu H, et al. Ruxolitinib reverses dysregulated T helper cell responses and controls autoimmunity caused by a novel signal transducer and activator of transcription 1 (STAT1) gain-of-function mutation. J Allergy Clin Immunol. 2017;139:1629–1640.e2.

9. Maródi L, Cypowyj S, Tóth B, Chernyshova L, Puel A, Casanova JL. Molecular mechanisms of mucocutaneous immunity against Candida and Staphylococcus species. J Allergy Clin Immunol. 2012;130:1019–27.

10. Zheng J, van de Veerdonk FL, Crossland KL, Smeekens SP, Chan CM, Al Shehri T, et al. Gain-of-function STAT1 mutations impair STAT3 activity in patients with chronic mucocutaneous candidiasis (CMC). Eur J Immunol. 2015;45:2834–46.

11. Krämer OH, Knauer SK, Greiner G, Jandt E, Reichardt S, Ghrs KH, et al. A phosphorylation-acetylation switch regulates STAT1 signaling. Genes Dev. 2009;23:223–35.

12. Soltész B, Tóth B, Shabashova N, Bondarenko A, Okada S, Cypowyj S, et al. New and recurrent gain-of-function STAT1 mutations in patients with chronic mucocutaneous candidiasis from Eastern and Central Europe. J Med Genet. 2013;50:567–78.

13. Sharfe N, Nahum A, Newell A, Dadi H, Ngan B, Pereira SL, et al. Fatal combined immunodeficiency associated with heterozygous mutation in STAT1. J Allergy Clin Immunol. 2017;133:807–17. Elsevier

14. van de Veerdonk FL, Netea MG. Treatment options for chronic mucocutaneous candidiasis. J Inf Secur. 2017;72:S56–60. Elsevier

15. Furumoto Y, Gadina M. The arrival of JAK inhibitors: advancing the treatment of immune and hematologic disorders. BioDrugs. 2013;27:431–8.

16. Parackova Z, Kayserova J, Danova K, Sismova K, Dudkova E, Sumnik Z, et al. T regulatory lymphocytes in type 1 diabetes: impaired CD25 expression and IL-2 induced STAT5 phosphorylation in pediatric patients. Autoimmunity. 2016;49:523–31. Taylor & Francis

17. Loh ML, Tasian SK, Rabin KR, Brown P, Magoon D, Reid JM, et al. A phase 1 dosing study of ruxolitinib in children with relapsed or refractory solid tumors, leukemias, or myeloproliferative neoplasms: a children's oncology group phase 1 consortium study (ADVL1011). Pediatr Blood Cancer. 2015;62:1717–24.

18. Chen X, Vinkemeier U, Zhao Y, Jeruzalmi D, Darnell JE, Kuriyan J. Crystal structure of a tyrosine phosphorylated STAT-1 dimer bound to DNA. Cell. 1998;93:827–39.

19. Romberg N, Morbach H, Lawrence MG, Kim S, Kang I, Holland SM, et al. Gain-of-function STAT1 mutations are associated with PD-L1 overexpression and a defect in B-cell survival. J Allergy Clin Immunol. 2017;131:1691–3. Elsevier

20. Vargas-Hernandez A, Mace EM, Zimmerman O, Zerbe CS, Freeman AF, Rosenzweig S, et al. Ruxolitinib partially reverses functional NK cell deficiency in patients with STAT1 gain-of-function mutations. J Allergy Clin Immunol. 2017; Accepted for print.

21. Leiding JW, Okada S, Hagin D, Abinun M, Shcherbina A, Balashov DN, et al. Hematopoietic stem cell transplantation in patients with gain-of-function signal transducer and activator of transcription 1 mutations. J Allergy Clin Immunol. 2017; Accepted for print.

22. Shahar E, Wildbaum G, Katz R, Karin N, Etzioni A, Pollack S. Continuous G-CSF Ttreatment induces complete clinical remission and restoration of IL-17 secretion in autosomal dominant chronic mucocutaneous candidiasis. J Allergy Clin Immunol. 2017;131:AB231. Elsevier.

23. van de Veerdonk FL, Koenen HJPM, van der Velden WJFM, van der Meer JWM, Netea MG. Immunotherapy with G-CSF in

patients with chronic mucocutaneous candidiasis. Immunol Lett. 2015;167:54–6.

24. Mössner R, Diering N, Bader O. Ruxolitinib induces interleukin 17 and ameliorates chronic mucocutaneous candidiasis caused by STAT1 gain-of-function mutation. Clin Infect Dis. 2016;62:951–3.

25. Verstovsek S, Safety PD. Efficacy of INCB018424, a JAK1 and JAK2 inhibitor, in myelofibrosis safety and efficacy of INCB018424, a JAK1 and JAK2 inhibitor, in myelofibrosis. N Engl J Med. 2010;363:1117–27.

26. Higgins E, Al Shehri T, McAleer MA, Conlon N, Feighery C, Lilic D, et al. Use of ruxolitinib to successfully treat chronic mucocutaneous candidiasis caused by gain-of-function signal transducer and activator of transcription 1 (STAT1) mutation. J Allergy Clin Immunol. 2017;135:551–553.e3. Elsevier.

27. Tefferi A, Pardanani A. Serious adverse events during ruxolitinib treatment discontinuation in patients with myelofibrosis. Mayo Clin Proc. 2011;86:1188–91.

28. Zimmerman O, Rösler B, Zerbe CS, Rosen LB, Hsu AP, Uzel G, et al. Risks of ruxolitinib in STAT1 gain-of-function-associated severe fungal disease. Open Forum Infect Dis. 2017;4:ofx202. US: Oxford University Press.

29. Casanova JL, Holland SM, Notarangelo LD. Inborn errors of human JAKs and STATs. Immunity. 2012;36:515–28.

30. Yang XO, Panopoulos AD, Nurieva R, Seon HC, Wang D, Watowich SS, et al. STAT3 regulates cytokine-mediated generation of inflammatory helper T cells. J Biol Chem. 2007;282:9358–63.

31. Purvis HA, Anderson AE, Young DA, Isaacs JD, CMU H. A negative feedback loop mediated by STAT3 limits human Th17 responses. J Immunol. 2014;193:1142–50.

32. Zhang Y, Ma CA, Lawrence MG, Break TJ, O'Connell MP, Lyons JJ, et al. PD-L1 up-regulation restrains Th17 cell differentiation in STAT3 loss- and STAT1 gain-of-function patients. J Exp Med. 2017;1:1–11.

33. Tabellini G, Vairo D, Scomodon O, Tamassia N, Ferraro RM, Patrizi O, et al. Impaired natural killer cell functions in patients with signal transducer and activator of transcription 1 (STAT1) gain-of-function mutations. J Allergy Clin Immunol. 2017;140: 553–564.e4.

34. Voigt J, Hünniger K, Bouzani M, Jacobsen ID, Barz D, Hube B, et al. Human natural killer cells acting as phagocytes against Candida albicans and mounting an inflammatory response that modulates neutrophil antifungal activity. J Infect Dis. 2014;209:616–26.

35. Cheuk S, Schlums H, Gallais Sérézal I, Martini E, Chiang SC, Marquardt N, et al. CD49a expression defines tissue-resident CD8+ T cells poised for cytotoxic function in human skin. Immunity. 2017;46:287–300.

36. Jones-Carson J, Vazquez-Torres A, van der Heyde HC, Warner T, Wagner RD, Balish E. Gamma delta T cell-induced nitric oxide production enhances resistance to mucosal candidiasis. Nat Med. 1995;1:552–7.

37. Fenoglio D, Poggi A, Catellani S, Battaglia F, Ferrera A, Setti M, et al. Vdelta1 T lymphocytes producing IFN-gamma and IL-17 are expanded in HIV-1-infected patients and respond to Candida albicans. Blood. 2009;113:6611–8.

38. Dai X, Sayama K, Yamasaki K, Tohyama M, Shirakata Y, Hanakawa Y, et al. SOCS1-negative feedback of STAT1 activation is a key pathway in the dsRNA-induced innate immune response of human keratinocytes. J Invest Dermatol. 2018;126:1574–81. Elsevier.

39. Korn T, Mitsdoerffer M, Croxford AL, Awasthi A, Dardalhon VA, Galileos G, et al. IL-6 controls Th17 immunity in vivo by inhibiting the conversion of conventional T cells into Foxp3+ regulatory T cells. Proc Natl Acad Sci. 2008;105:18460–5.

40. Fujimoto M, Nakano M, Terabe F, Kawahata H, Ohkawara T, Han Y, et al. The influence of excessive IL-6 production in vivo on the development and function of Foxp3+ regulatory T cells. J Immunol. 2011;186:32–40.

41. Uzel G, Sampaio EP, Lawrence MG, Hsu AP, Hackett M, Dorsey MJ, et al. Dominant gain-of-function STAT1 mutations in FOXP3 wild-type immune dysregulation-polyendocrinopathy-enteropathy-X-linked-like syndrome. J Allergy Clin Immunol. 2013;131:1611–23.

42. Crow YJ. Type I interferonopathies: a novel set of inborn errors of immunity. Ann N Y Acad Sci. 2011;1238:91–8.

43. Cohen AC, Nadeau KC, Tu W, Hwa V, Dionis K, Bezrodnik L, et al. Cutting edge: decreased accumulation and regulatory function of CD4+ CD25(high) T cells in human STAT5b deficiency. J Immunol. 2006;177:2770–4.

44. Verstovsek S, Mesa RA, Gotlib J, Levy RS, Gupta V, Dipersio JF, et al. Efficacy, safety, and survival with ruxolitinib in patients with myelofibrosis: results of a median 3-year follow-up of COMFORT-I. Haematologica. 2015;100:479–88.

45. Sonbol MB, Firwana B, Zarzour A, Morad M, Rana V, Tiu RV. Comprehensive review of JAK inhibitors in myeloproliferative neoplasms. Ther Adv Hematol. 2013;4:15–35.

46. Kantarjian HM, Silver RT, Komrokji RS, Mesa RA, Tacke R, Harrison CN. Ruxolitinib for myelofibrosis-an update of its clinical effects. Clin Lymphoma, Myeloma Leuk. 2013;13:638–45.

47. Baik M, Yu JH, Hennighausen L. Growth hormone-STAT5 regulation of growth, hepatocellular carcinoma, and liver metabolism. Ann N Y Acad Sci. 2011;1229:29–37.

48. Tefferi A. Challenges facing JAK inhibitor therapy for myeloproliferative neoplasms. N Engl J Med. 2012;366:844–6.

ORIGINAL ARTICLE

Impact of JAK Inhibitors in Pediatric Patients with STAT1 Gain of Function (GOF) Mutations—10 Children and Review of the Literature

Angela Deyà-Martínez[1,2,3] · Jaques G. Rivière[4,5,6] · Pérsio Roxo-Junior[7] · Jan Ramakers[8,9] · Markéta Bloomfield[10,11] · Paloma Guisado Hernandez[12] · Pilar Blanco Lobo[12] · Soraya Regina Abu Jamra[7] · Ana Esteve-Sole[1,2,3] · Veronika Kanderova[13] · Ana García-García[1,2,3] · Mireia Lopez-Corbeto[14] · Natalia Martinez Pomar[15,16] · Andrea Martín-Nalda[4,5,6] · Laia Alsina[1,2,3,17] · Olaf Neth[12,18] · Peter Olbrich[12,18,19]

Abstract

Introduction Since the first description of gain of function (GOF) mutations in signal transducer and activator of transcription (STAT) 1, more than 300 patients have been described with a broad clinical phenotype including infections and severe immune dysregulation. Whilst Jak inhibitors (JAKinibs) have demonstrated benefits in several reported cases, their indications, dosing, and monitoring remain to be established.

Methods A retrospective, multicenter study recruiting pediatric patients with STAT1 GOF under JAKinib treatment was performed and, when applicable, compared with the available reports from the literature.

Results Ten children (median age 8.5 years (3–18), receiving JAKinibs (ruxolitinib ($n=9$) and baricitinib ($n=1$)) with a median follow-up of 18 months (2–42) from 6 inborn errors of immunity (IEI) reference centers were included. Clinical profile and JAKinib indications in our series were similar to the previously published 14 pediatric patients. 9/10 (our cohort) and 14/14 patients (previous reports) showed partial or complete responses. The median immune deficiency and dysregulation activity scores were 15.99 (5.2–40) pre and 7.55 (3–14.1) under therapy ($p=0.0078$). Infection, considered a likely adverse event of JAKinib therapy, was observed in 1/10 patients; JAKinibs were stopped in 3/10 children, due to hepatotoxicity, pre-HSCT, and absence of response.

Conclusions Our study supports the potentially beneficial use of JAKinibs in patients with STAT1 GOF, in line with previously published data. However, consensus regarding their indications and timing, dosing, treatment duration, and monitoring, as well as defining biomarkers to monitor clinical and immunological responses, remains to be determined, in form of international prospective multicenter studies using established IEI registries.

Keywords Primary immunodeficiency disease · Inborn errors of immunity · Pediatrics · Children · JAK-STAT pathway · Chronic mucocutaneous candidiasis · Ruxolitinib · Baricitinib · STAT1 GOF · JAK inhibitors

Introduction

Since its first description in 2011 [1, 2], gain of function (GOF) mutations in signal transducer and activator of transcription (STAT) 1 have been identified in more than

300 patients worldwide. Most mutations are localized in the Src homology 2 (SH2) or DNA-binding domains [3]. STAT1 is mainly activated via the binding of type I, II, and III interferons to their respective cytokine receptors, resulting in JAK1, JAK2, and JAK3 activation and phosphorylation, followed by the recruitment of STAT molecules from the cytoplasm. The STAT molecules are then phosphorylated (pSTAT) and form homo- or heterodimers that translocate to the nucleus where they regulate gene transcription [4]. STAT1 GOF patients show higher pSTAT1 levels after stimulation with activating cytokines (mainly interferons), which represents the molecular hallmark of the disease [1, 2]. Whether this

Olaf Neth and Peter Olbrich contributed equally and shared last authors.

✉ Olaf Neth
oneth-ibis@us.es

✉ Peter Olbrich
polbrich@us.es; peter.olbrich.sspa@juntadeandalucia.es

Extended author information available on the last page of the article

is the result of altered dephosphorylation dynamics, prolonged binding of STAT1, increased availability of total STAT1 molecules, or other mechanisms remains to be elucidated [1, 2, 5].

From a clinical perspective, the phenotype of STAT1 GOF patients is broadly heterogenous. The most common symptom is early-onset chronic mucocutaneous candidiasis (CMC). However, (myco-) bacterial, viral, and fungal infections, (multiorgan) autoimmunity or autoinflammation, vascular malformations, and malignancies have also been reported [6]. The management of these complex patients is therefore challenging and often requires a balanced use of antimicrobial and immunosuppressive therapies. Hematopoietic stem cell transplantation (HSCT) is a potential curative procedure but graft failure as well as secondary graft rejection is common and resulted in a 40% overall survival rate only [7].

In recent years, case reports have described JAK inhibition as an effective targeted treatment option for STAT1 GOF patients [3, 8–12]. JAK inhibitors (JAKinibs) are small molecules interfering with the process of cytokine-dependent JAK activation. In patients with STAT1 GOF, ruxolitinib®, as well as baricitinib®, have been used [13, 14]. However, the clinical experience with these drugs in the field of inborn errors of immunity (IEI) is still limited and important questions including indications, dosing, and monitoring remain, especially in pediatric patients.

Here, we present the experience with JAK inhibition in 10 pediatric STAT1 GOF patients under the care of six IEI reference centers. We provide detailed information regarding indications, dosing regimens, side effects, and complications as well as the clinical effects on the most relevant disease manifestations. In addition, we reviewed all previously published pediatric STAT1 GOF cases treated with JAKinibs and compared main characteristics with our cohort, when applicable.

Methods

Patients and Study Design

Pediatric patients (age < 18 years at treatment initiation) with functionally confirmed or previously described STAT1 GOF mutations receiving JAKinibs for a minimum of two consecutive months were recruited from six IEI reference centers. The protocol of this study was reviewed and approved by the local ethics committees of the participating centers. Informed consents were obtained from study participants and/or their legal guardians according to the requirements of the local ethics committees.

Data Collection

A questionnaire (available on reasonable request) designed to retrospectively collect demographic, molecular, and clinical data was prepared and distributed. Additionally, the responsible physicians were contacted to verify and discuss the extracted data for each patient.

Genetic Analysis and Functional Variant Validation

All patients were tested at their corresponding institutions. Sanger sequencing was performed for all patients and novel variants were functionally validated by means of STAT1 phosphorylation assays as previously described [1, 2].

Response Evaluation

For our cohort, the attending physicians were asked to categorize the clinical response of their patients before and after starting JAK inhibition in the following categories: (1) complete response, (2) partial response, (3) no response, (4) manifestation not present. Due to the limited data information extracted from the literature review, the treatment response of the published cases was categorized as follows: (1) resolution of symptoms or partial response, (2) manifestation present in the patient but response to JAKinib not specified, (3) transitory response, (4) no response, (5) manifestation not present.

Immune Deficiency and Dysregulation Activity (IDDA) Score

The IDDA score is a promising tool to assess disease activity and burden in the setting of immune deregulatory diseases [15, 16]. It allows for intraindividual, longitudinal monitoring by using a number of relevant clinical parameters. Items required to calculate the score were part of a questionnaire. The patients' scores were calculated as previously described [15] by their attending physician before starting JAK inhibition (retrospectively) and at the last clinical follow-up.

Literature Review

STAT1 GOF patients less than 18 years old treated with JAK inhibitors were identified via a systematic literature search in EMBASE and PUBMED using the following search terms: primary immunodeficiency disease, inborn errors of immunity, pediatrics, children, JAK-STAT pathway, chronic mucocutaneous candidiasis, STAT1 GOF, JAK inhibitors, STAT1, gain of function, JAKinib, JAK inhibitor, ruxolitinib and baricitinib. All articles and references were screened for

other eligible publications. To avoid case duplications, those patients mentioned in more than one publication were identified and relevant data was extracted from all corresponding publications (Table S-1).

Statistical Analysis

Variables were described as percentages or median values with ranges (min–max), respectively. Normality for quantitative variables was evaluated using the Shapiro–Wilk test. For inferential statistics, the Wilcoxon test was applied. A p-value lower than 0.05 was considered statistically significant.

Results

Baseline Characteristics and Disease Manifestations Before Starting JAK Inhibition

Ten patients were included in our cohort (Table 1). Of note, patient 9 (P9) was treated with ruxolitinib during two time periods. Whilst the first episode has been previously published [11], we here provide extended data on the second treatment course. The baseline characteristics of the cohort are presented in Table 1 and a detailed description for each patient is given in Table S-1 and Table S-2.

The median age of disease onset and at study entry of our cohort was 6 months (range 1–48 months) and 8.5 years (3–18 years), respectively, with a predominance of female patients (8/10).

Infections were common and CMC was present in all patients, being the only infectious manifestation in two of them. Bacterial infections, mainly of the lower respiratory tract, were frequently reported; 6/10 patients developed bronchiectasis. At least one episode of symptomatic *herpesviridae* infection was observed in 6 out of 10 children prior to starting JAK inhibition.

All patients showed at least one autoimmune and/or autoinflammatory manifestation. Oral aphthae (8/10) were the most common feature, followed by scleritis/keratitis (4/10) and autoimmune cytopenia (3/10). Lymphoproliferation was not observed in our cohort. One patient suffered from pulmonary hypertension due to a chronic interstitial lung disease. Failure to thrive was noted in 3/10 patients, and in two patients, aneurysms of the central nervous system were identified.

Features of antibody deficiency were reported for 5/10 patients. Six of ten patients received immunoglobulin replacement treatment (IGRT).

A systematic literature review identified 14 additional pediatric STAT1 GOF patients under JAKinib therapy (see Table 1 and Table S-2. Median age was 10 years

(7 months–17 years); 50% were female. Almost all children suffered infections, CMC (13/14) and bacterial (11/14) infections being most commonly reported. Autoimmune/autoinflammatory complications were often reported, with cytopenia being the most common (9/14), followed by enteropathy (8/14) and autoimmune hepatitis (6/14). One patient presented with lymphoproliferation and most showed failure to thrive (9/14).

JAKinib Treatment Indications and Monitoring

In our cohort, 9 patients received ruxolitinib and one patient baricitinib. Dosing is detailed for each patient in Table S-1. The main reasons to start JAK inhibition were immune dysregulation (10/10), manifested as oral aphthae, keratitis, enteropathy and autoimmune hepatitis, followed by uncontrolled CMC (6/10). The baseline studies performed prior to treatment initiation and during the follow-up, as well as the monitoring frequency of the treatment, are detailed in Table 1, Figure S-1, Table S-1 and Table S-2. The median treatment follow-up time for our cohort was 18 months (2–42 months); with a total follow-up time of 197 months.

Although specific information was not available for all previously published cases the main reason to start treatment were autoimmune complications.

JAKinib Treatment Responses

An overview summarizing the treatment responses for each disease manifestation in our patients and previously published pediatric cases is shown in Fig. 1. Under JAKinib therapy, most clinical manifestations showed at least partial improvement except for P2, in whom CMC and stomatitis/aphthae persisted despite good treatment adherence. Time to response after treatment initiation appears to depend on the clinical manifestation. In our cohort, early responses were observed for cytopenia (1–2 weeks), CMC (1–8 weeks), dermatitis (2–4 weeks) and improvement of oral aphthae and enteropathy after 6–12 weeks of treatment. In contrast, keratitis, autoimmune hepatitis, or pulmonary hypertension required prolonged treatment (3–8 months) and cerebral aneurysms did not show any treatment responses during the time of follow up. In the reviewed cases from the literature, the variable "time to response" was not consistently reported (Figure S-1). In those cases where specific information was available, hemolytic autoimmune anemia ($n = 1$) responded after 1 month of treatment initiation [17] and enteropathy improved between 2 weeks and 2 months in three patients [8], whereas a singular more severe case required up to 12 months of therapy [18]. Resolution of

Table 1 Summary of baseline characteristics of our cohort (*n*=10) and of previously described pediatric STAT1 GOF patients under Jakinib therapy (*n*=14)

	n = **10***	Literature review *n* = 14
Age (years) at time of study entry: mean	8.5 y (3y–18y)	10y (7 m–17y)
Gender (female)	8/10	7/14
Age (months) at symptom onset	6 (1–48)	4 (0.5–10)**
Mutations localization		
Coiled coil domain	4/10	2/14
DNA-binding domain	5/10	8/14
Linker domain	0/10	2/14
SH2 domain	1/10	1/14
Tail segment domain	0/10	1/14
Infections prior to JAK inhibitor	10/10	14/14
Viral	7/10	5/14
Fungal	10/10	13/14
Bacterial	8/10	11/14
Only Chronic mucocutaneous candidiasis	2/10	0/14
Immune dysregulatory symptoms	10/10	12/14
Cytopenia	3/10	9/14
Enteropathy	2/10	8/14
Autoimmune hepatitis	1/10	6/14
Endocrinopathy	0/10	4/14
Oral aphtha	8/10	2/14
Arthritis	1/10	0/14
Keratitis/episcleritis	4/10	1/14
Dermatitis/eczema	2/10	2/14
Fatigue	2/10	1/14
Alopecia	0/10	2/10
Lymphoproliferation	0/10	1/14
Pulmonary disease	6/10	5/14**&**
Bronchiectasis	6/10	5/14
Interstitial lung disease	0/10	0/14
Pulmonary hypertension	1/10	0/14
Failure to thrive	3/10	9/14
Vasculopathy	2/10	1/14
Heart	0	0/14
Central nervous system	2/2	1/14
Antibody deficiency***	5/10	3/14
Subclasses deficiency and hypo IgM and IgA	1	0
Subclasses deficiency and hypo IgA	1	0
Isolated low IgM	1	0
SPAD	1	0
Hypo IgG and SPAD	1	0
Isolated low IgG	0	1
Subclasses deficiency	0	1
Isolated low IgA	0	1
HSCT	2/10	4/14
Mortality	1/10	0/14
JAK inhibitor information		
Type of JAK inhibitor		
Ruxolitinib	9/10	14/14
Baricitinib	1/10	0/14

Table 1 (continued)

	$n = 10^*$	Literature review $n = 14$
Starting dosage: median (range)		
Ruxolitinib	0.28 (0.2–0.6) mg/kg/day	20 (5–50) mg/day 11/14
Baricitinib	2 mg/day	5 (5–5) mg/m²/day 3/14
Maximum dosage: median (range)		
Ruxolitinib	0.6 (0.25–0.78) mg/kg/day	20 (5–50) mg/day (11/14)
Baricitinib	4 mg/day	10 (10–15) mg/m²/day (3/14)
Reason to start JAK inhibitors&&		
Uncontrolled immune dysregulation		
Oral aphtha	4/10	3/14
Keratitis/iritis	1/10	1/14
Enteropathy	1/10	6/14
Autoimmune hepatitis	1/10	2/14
Autoimmune cytopenia	1/10	4/14
Fatigue	0/10	1/14
Type I diabetes mellitus	0/10	2/14
Alopecia	0/10	1/14
Failure to thrive	0/10	2/14
Life-threatening infections	1/10	0/10
Recurrent bacterial infections	0/10	1/14
Chronic mucocutaneous candidiasis	6/10	4/14
Azole resistant	2/10	ND
Azole susceptible	4/10	ND
Vasculopathy progression	2/10	1/14
Lung disease progression/decline lung function	2/10	0/14
Bridge to HSCT	1/10	1/14
Median follow-up in months (range)	18 (2–42)	ND
Median IDDA score (range)		
Before treatment	15.99 (5.2–40)	
Under treatment	7.55 (3–14.1) $p = 0.0078$	ND
Side effects	4/10	
Infectious	1/4	4/14
Other	3/4	4/14
JAK inhibitor discontinued /stopped	3/10	ND

CVID, common variable immunodeficiency; *HSCT*, hematopoietic stem cell transplantation; *IDDA*, immune deficiency and dysregulation activity; *m*, months; *ND*, no detailed information was available for this variable; *SPAD*, specific polysaccharide antibody deficiency; *y*, year

[*]The results are expressed by median and range (min–max) and percentage if not stated otherwise

[**]Information available only from 4 patients

[***]Some patients presented more than one humoral defect

[&]One of these patients was stated to suffer from an unspecified chronic lung disease

[&&]Patients may have more than one reason to start ruxolitinib

diabetes mellitus was observed after 12 months of ruxolitinib treatment in 1 case [10].

The IDDA score significantly decreased under ruxolitinib therapy (median pre: 15.99, median post: 7.55, $p = 0.0078$), whilst P2 (patient under baricitinib) and P7 did not improve at 2 and 7 months, respectively (Table 1, Fig. 2).

A summary of treatment responses reported for the previously published cases is shown in Fig. 1. Although detailed descriptions were not available for all patients and symptoms, most patients showed improvement under therapy for the most prevalent disease manifestations such as CMC, enteropathy, cytopenias, and lung disease.

	Deya et al (this cohort)											Forbes et al [8]									Moriya et al [9]	Chaimowitz et al [10]	Al Shehri et al [3]	Kayaoglu et al [17]	Acker et al [18]	Overall response rate*
Patient number in publication	1	2	3	4	5	6	7	8	9.1	9.2	10	1	3	4	5	7	8	9	10	11	1	1	1	1	1	
Follow up (m)	28	2	39	42	18	4**	7	30	8	10	9	ND														
CMC	1&		4	4	4	4		2-4	4-8	4-8#	4-8															18/22
Enteropathy/Diarrhea			6	6																						11/12
Stomatitis/Ulcers	12		4	4	8				4-8	4-8																7/8
Urticaria/ skin rash			4	4																						5/5
Lung disease			24	24						8-12																5/5
Cytopenia								1-2	4-8																	3/9
Aneurysm																										0/3
Alopecia																										1/2
LFTs /AI hepatitis						12																				3/5
Keratitis /Iritis	22									4-8																3/3
Fatigue								2		2	2-4															5/5
DM type 1																										1/3

This cohort:
Dark Green: Complete response
Green: Partial response
Red: No response
Literature review:
Black: Complete or partial response
Gray: Symptom or manifestation present in the patient but response to Jakinib not specified
White: Symptom or manifestation not present at time of Jakinib initiation
Blue: Transient response

AI: autoimmune; CMC: chronic mucocutaneous candidiasis; DM: diabetes mellitus; LFT: liver function tests; m: month; ND: No detailed information was available for this variable.
*Overall response rate was defined as sustained improvement of symptoms (when present) stated by the investigators.
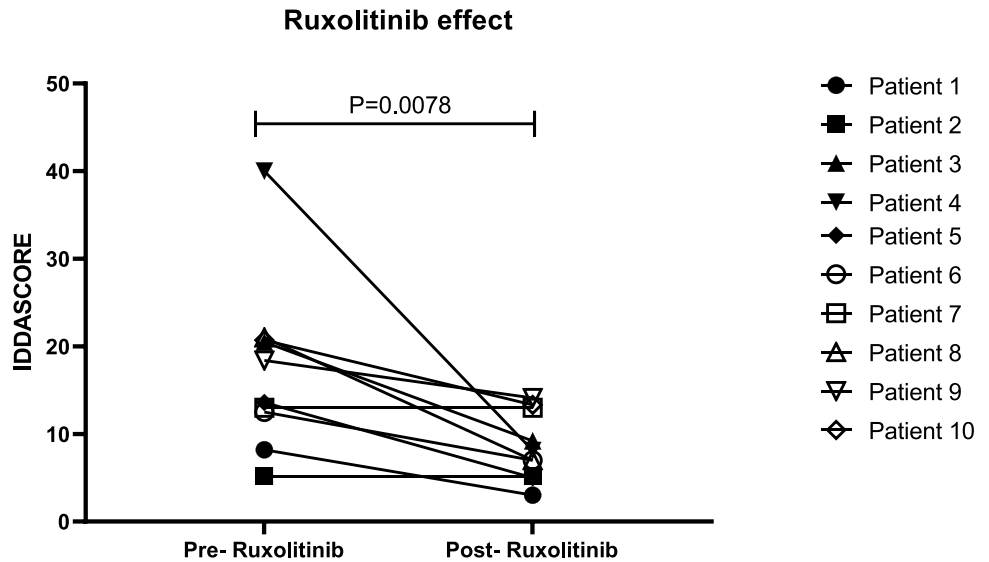**4 months after Ruxolitinib and 8 years post hematopoietic stem cell transplantation
&Numbers appearing in the colored squares indicate the time to obtain a clinical response to Jakinibs in weeks
#Onychomycosis: P9: 8-12 weeks; P10 24: weeks

Fig. 1 Response to JAK inhibitor treatment. AI, autoimmune; CMC, chronic mucocutaneous candidiasis; DM, diabetes mellitus; LFT, liver function tests; m, month; ND, no detailed information was available for this variable. *Overall response rate was defined as sustained improvement of symptoms (when present) stated by the investigators. **4 months after ruxolitinib and 8 years post hematopoietic stem cell transplantation. &Numbers appearing in the colored squares indicate the time to obtain a clinical response to JAKinibs in weeks. #Onychomycosis: P9: 8–12 weeks; P10: 24 weeks

Fig. 2 Effect of JAKinibs on Immune deficiency and dysregulation activity (IDDA) score

Ruxolitinib effect

P=0.0078

IDDASCORE

Pre- Ruxolitinib   Post- Ruxolitinib

- Patient 1
- Patient 2
- Patient 3
- Patient 4
- Patient 5
- Patient 6
- Patient 7
- Patient 8
- Patient 9
- Patient 10

Prophylaxis and Adverse Events

Antibacterial (5/10) and antiviral (2/10) prophylaxis and immunoglobulin replacement therapy (5/10) were initiated prior to JAKinibs as part of the routine clinical management. In addition, antimicrobial prophylaxis was started after JAKinib initiation in two patients: in P1 due to recurrent bacterial lower respiratory tract infections and in P8 due to anticipated increased viral infection risk.

Bacterial infections (4 episodes during a 6-month period: 1 pneumonia and 3 episodes of upper respiratory tract infections with fever and acute reactants elevation), vertigo, sleep disturbances, and transitory liver enzyme elevation were attributed by the attending physicians to the JAKinib as probable but not proven side effects (Table S-1). Treatment was discontinued in 3/10 patients. P6 and P9 stopped ruxolitinib due to hepatotoxicity just before HSCT and loss of effect on CMC respectively. P2 discontinued baricitinib as no treatment benefit was observed after 2 months of therapy.

In the previously reported 14 patients, 8 presented adverse events potentially related to JAKinibs: 4/8 infections (2 cases *varicella zoster* virus, 1 *herpes simplex virus*, and 1 *cytomegalovirus* (CMV) and 4/8 suffered from other complications (one each from thrombocytopenia and neutropenia and two from pancreatitis).

Ruxolitinib and HSCT

P6 (matched sibling donor) and P9 (matched unrelated donor) underwent HSCT. P5 is currently in the process of HSCT preparation. P6 was successfully transplanted and remains healthy and stable 4 years post-HSCT. P9 was treated twice with ruxolitinib therapy for 8 months prior to HSCT; however, the patient sadly deceased in the context of an uncontrollable thrombocytopenia and invasive aspergillosis 75 days post-HSCT (complete donor chimerism, no signs of graft-versus-host disease).

In three of the previously published 14 patients, ruxolitinib was stopped prior to HSCT. In this setting, HSCT was successful in all reported cases.

Discussion

To the best of our knowledge, this is the most extensive pediatric case series describing patients with STAT1 GOF mutations under JAKinib therapy to date. Our study provides a detailed description of the clinical experience with this treatment approach in children and highlights the heterogeneity in terms of indications, dosing schedules, and follow-up practices.

Disease Manifestations

Infections were common in our cohort, correlating well with previous reports [3, 8–10, 17, 18, 12]. Before starting JAKinibs, most infections had been controlled; only P3 suffered from CMV stomatitis. The previously published cases showed overall a more severe phenotype, with higher prevalence and severity of autoimmune manifestations and failure to thrive (Table 1, Table S-2). In addition, these patients had also received other immunosuppressive drugs. Thus, in most of them, JAKinibs were not used as "first-line" therapy. In our series, JAKinibs were initiated at earlier disease stages, possibly reflecting the positive experiences reported in the previous studies [3, 8–10, 17, 18, 12].

Indications

Reasons to start JAKinibs stated by the attending physicians of our cohort were similar to previous reports [3, 8–10, 17, 18]. Beyond CMC, these included refractory autoimmune complications, progressive vasculopathy, and lung disease (Table 1, Table S1). Furthermore, one patient received ruxolitinib for 4 months as a bridge to a subsequent HSCT procedure [8, Table S-2].

Treatment, Dosing, and Treatment Response

In the setting of IEI, the appropriate dosing and interval for JAKinibs remain to be established, as experience with these small molecule inhibitors in the pediatric age is very limited. Whilst the European Medicine Agency (EMA) has not yet approved ruxolitinib in children [19], the Food and Drug Administration (FDA) indicates their use for steroid-refractory acute graft-versus-host disease (GVHD) in children older than 12 years of age in 2019 (recommended dose 5 mg every 12 h) [20]. Of note, 50mg/m^2/day has been indicated to be the maximum well-tolerated dose in children [21]. Based on serial drug level determination and functional assays, 8-h dose intervals have been recently suggested in a child with STAT3 GOF mutation associated with immune dysregulation (type 1 diabetes mellitus and interstitial lung disease). Interestingly, the dose needed and tolerated in this case report was high (2.2 mg/kg/day), being more than twice the dose compared to previous reports [8, 22] and those used in our own cohort (see Table S-1 and S-2).

In our patients, ruxolitinib was used in 9/10 and baricitinib in 1/10 children, respectively. The attending physicians preferred ruxolitinib, given the larger literary experience in STAT1 GOF setting. We provide detailed dosing information (Table 1 and Table S-1) for our patients, including the starting and maximum doses. Our starting (0.28 mg/kg/day vs 0.8 mg/kg/day) and maximum (0.6 mg/kg/day vs 1.05 mg/

kg/day) doses were lower than previously reported [3, 8–10, 17]. However, the absence of homogenous protocols (and dosing reported diversely as mg/kg/day, mg/day, and/or m^2/day) in the literature limits conclusive comparisons and should be unified in future studies. Dose adjustments in our cohort were performed mainly according to the clinical effect and absence of adverse events and in three cases supported by functional analysis using pSTAT1 stimulation assays (P3, P4, P9).

Collectively, CMC was the most prevalent disease manifestation ($n = 23$) and JAKinib treatment was effective in almost all patients (overall response rate 20/22, Fig. 1) within 2–8 weeks of treatment. Contrastingly, Acker et al. recently described a patient with only transient responses to JAKinib, administered for CMC, enteropathy, and cytopenia [18]. Importantly, in our cohort, the only patient receiving baricitinib did not show clinical improvement resulting in its discontinuation and switch to ruxolitinib.

In the absence of controlled prospective data, we suggest starting pediatric patients on 0.3–0.5 mg/kg/day of ruxolitinib twice per day and then progressively increasing the dose by 0.1–0.2 mg/kg/day every 2–4 weeks until achieving the expected clinical effect or occurrence of relevant side effects keeping in mind the suggested maximum dose of 50 mg/m^2/day by Loh et al. [21].

For the clinician, the patients, and family, it is important to know how long it takes to achieve a JAKinib treatment response. In our cohort, the cytopenias and CMC responded rather promptly (1–8 weeks), whereas others, such as keratitis and autoimmune hepatitis, required prolonged treatment courses (4–8 months). No improvement or worsening of cerebral aneurysms was observed in two patients. Unfortunately, the information available in the literature regarding treatment responses is often unspecific and incomplete. Where such data were provided, the time to response was similar to what was observed in our cohort requiring several weeks of therapy to achieve improvement (Table S-1).

Despite the combined data presented here, the number of pediatric STAT1 GOF patients treated with JAKinibs is still small. Furthermore, it is likely that the time to response might vary depending on the organ involved, severity and duration of the disease, and JAKinib dosage. Therefore, larger, detailed, and prospective patient cohorts will need to address these aspects more consistently.

Baricitinib, a potent JAK1/JAK2 inhibitor, has shown good tolerability in rheumatologic diseases and other monogenic interferonopathies [23, 24]. To date, one case report indicated efficacy in an adult patient with STAT1 GOF suffering from recurrent aphthae, as well as oral and esophageal CMC [25]. Contrastingly, in our cohort, P2 failed to show any improvement after 2 months of treatment with 4mg/day. However, upon, upon switching to ruxolitinib, a fast, complete, and sustained remission of CMC and partial remission of aphthae after 3 months of treatment were observed. Whether baricitinib is inferior or not in the control of the disease manifestations in STAT1 GOF compared to ruxolitinib remains to be determined.

Assessing Disease Activity Using Immune Deficiency and Dysregulation Activity (IDDA) Score

The IDDA score is a promising tool to assess disease activity and burden in the setting of immune dysregulatory diseases [15, 16]. It allows for intraindividual, longitudinal monitoring by using a number of relevant clinical parameters and has been added as a voluntary option to the European Society for Immunodeficiencies (ESID) registry [26]. We applied the score for the first time to patients with STAT1 GOF obtaining lower numbers (15.99) when compared to those reported for lipopolysaccharide (LPS)-responsive and beige-like anchor protein (LRBA)-deficient patients proceeding to transplant (32.9) or those remaining under conventional immunosuppressive therapy (20.8) (Table 1, [15]). A significant reduction in the IDDA score was observed after initiation of JAKinib therapy for all patients with initial IDDA score > 10, suggesting a substantial decline in the disease activity after JAKinib introduction (Fig. 2).

Adverse Events and Monitoring

Overall, the occurrence of adverse events potentially related to JAK inhibition was rare in our cohort. In fact, only one patient experienced an increased frequency of bacterial infections. Contrastingly, the reports in the literature for STAT1 GOF on JAKinib mention higher rates of urinary infections [27, 28] and other less frequent infectious complications, such as herpes virus reactivation [28], tuberculosis and/or other atypical mycobacterial infections [27–29], *JC virus* (four fatal cases) [30–33], *Pneumocystis jirovecii* [34], hepatitis B [35, 36], and toxoplasmosis [37]. This discrepancy might be attributed to an earlier introduction of JAKinibs in our cohort compared to their predominant use as a rescue strategy following the failure of other immunosuppressive regimens in the previously reported cases [3, 8, 10, 17, 18].

Although no published guidelines exist, we observed a surprisingly consistent approach chosen by the individual participating centers in terms of investigations performed prior to and during JAKinib therapy (Fig. S1, Table S1). These parameters most likely reflect concerns based on the published experience with JAKinibs in other scenarios, such as myelofibrosis, arthritis, and graft-versus-host disease (GVHD), as well as STAT1 GOF cases

[8, 27, 28], FDA and EMA recommendations [19, 20]. They include screening for infectious complications and monitoring for organ toxicity. In the absence of an easy-to-perform assay to determine ruxolitinib serum levels and the lack of the well-defined correlation between drug levels and clinical response, other biomarkers have been explored to monitor the drug effect/clinical response, such as phosphorylated STAT1 levels (pSTAT1) and IL17 production in T lymphocytes. Whilst some studies suggest a correlation between normalization of these markers [3, 11, 38], others reported a clear discrepancy [5]. This might be due to differences in timing of sampling, sample preparation, and assay protocols. In future studies, harmonized treatment and monitoring protocols are needed to consistently evaluate the role of these and other biomarkers in patients with IEI under JAKinib therapy.

In our cohort, drug levels were not performed. All participating centers stated an overall interest to perform JAKinibs level testing but did not have test availability at their institutions.

Importantly, none of the patients described here experienced severe adverse events such as thromboembolism or pulmonary hypertension. Interestingly, one patient (P4), who was started on ruxolitinib despite suffering from pulmonary hypertension, showed a marked improvement allowing the reduction of chronic medication for pulmonary hypertension, as well as the suspension of long-term oxygen supplementation.

Our recommendation prior to starting the JAK inhibition in pediatric patients with STAT1 GOF is to obtain a complete medical history, aiming to identify previous, active, or chronic infections and potential underlying organ damage. We also suggest applying early and extensive diagnostic and therapeutic strategies when suspecting viral, bacterial, and/or fungal infections including blood, urine, stool, aspirate samples, and biopsies from affected tissues/organs, if indicated, to minimize the risk of severe and preventable infectious complications.

In the specific setting of JAK inhibition in (pediatric) STAT1 GOF patients, the role of primary or secondary antimicrobial, antiviral, and antifungal prophylaxis remains to be established. Most authors suggest antimicrobial prophylaxis in patients with recurrent (respiratory) infections [39]. Systematic prevention of herpes virus infections is more controversial but should be considered in those patients with a history of systemic infection and severe lymphopenia as well as a history of long-term immunosuppression. In our cohort, immunoglobulin replacement therapy and antimicrobial and antiviral prophylaxis were prescribed according to the initial immunological workup and were not part of a specific strategy to prevent infections under JAKinib therapy.

Conclusions

We provide a comprehensive overview of the spectrum of pediatric STAT1 GOF patients that have been treated with JAK inhibitors to date, thereby highlighting the heterogeneity in terms of treatment indication, dosing, and monitoring. Based on our experience and previously published reports, we have stated recommendations regarding dosing, monitoring, and follow-up to help guide the attending clinicians. Application of a standardized methodology aimed to systematically assess the JAKinib indications, role of biomarkers, and drug level determination as well as clinical responses is needed and should be included in future studies. In this regard, the European Society for Immunodeficiency (ESID) and European Society for Blood and Marrow Transplantation (EBMT) have recently launched a multicentric retrospective study on JAKinib treatment in patients with inborn errors of the JAK/STAT pathways [40].

Declarations

Ethics Approval and Consent to Participate The protocol of this study was reviewed and approved by the local ethics committees of the participating centers. Informed consent was obtained from study participants and/or their legal guardians according to the requirements of the local ethics committees.

Consent for Publication The authors affirm that human research participants provided informed consent for publication of their individual details.

Conflict of Interest The authors declare no competing interests.

Open Access This article is licensed under a Creative Commons Attribution 4.0 International License, which permits use, sharing, adaptation, distribution and reproduction in any medium or format, as long as you give appropriate credit to the original author(s) and the source, provide a link to the Creative Commons licence, and indicate if changes were made. The images or other third party material in this article are included in the article's Creative Commons licence, unless indicated otherwise in a credit line to the material. If material is not included in the article's Creative Commons licence and your intended use is not permitted by statutory regulation or exceeds the permitted use, you will need to obtain permission directly from the copyright holder. To view a copy of this licence, visit http://creativecommons.org/licenses/by/4.0/.

References

1. van der Veerdonk FL, Plantinga TS, Hoishchen A, Smeekens SP, Joosten LAB, Gilissen C, et al. STAT1 mutations in autosomal dominant chronic mucocutaneous candidiasis. N Engl J Med. 2011;365(1):54–61. https://doi.org/10.1056/NEJMoa1100102.

2. Liu L, Okada S, Hong XF, Kreins AY, Cypowyj S, Abhyankar A, et al. Gain-of-function human STAT1 mutation impair IL-17 immunity and underlie chronic mucocutaneous candidaisis. J Exp Med. 2011;208:1635–48. https://doi.org/10.1084/jem.20110958.

3. Al Shehri T, Gilmour K, Gothe F, Loughlin S, Bibi S, Rowan AD, et al. Novel gain-of-function mutation in Stat1 sumoylation site leads to CMC/CID phenotype responsive to ruxolitinib. J Clin Immunol. 2019;39(8):776–85. https://doi.org/10.1007/s10875-019-00687-4.

4. Kiu H, Nicholson SE. Biology and significance of the JAK/STAT signaling pathways. Growth Factors. 2012;30(2):88–106. https://doi.org/10.3109/08977194.2012.660936.

5. Zimmerman O, Olbrich P, Freeman AF, Rosen LB, Uzel G, Zerbe CS, et al. STAT1 gain-of-function mutations cause high total STAT1 levels with normal dephosphorylation. Front Immunol. 2019;10(10):1433. https://doi.org/10.3389/fimmu.2019.01433.

6. Toubiana J, Okada S, Hiller J, Oleastro M, Lagos Gomez M, Aldave Becerra JC, et al.. Heterozygous STAT1 gain-of-function mutations underlie an unexpectedly broad clinical phenotype. Blood. 2016; ;127(25):3154–64. https://doi.org/10.1182/blood-2015-11-679902.

7. Leiding JW, Okada S, Hagin D, Abinun M, Shcherbina A, Balashov DN, et al. Hematopoietic stem cell transplantation in patients with gain-of-function signal transducer and activator of transcription 1 mutations. J Allergy Clin Immunol. 2018;141(2):704-717.e5. https://doi.org/10.1016/j.jaci.2017.03.049.

8. Forbes LR, Vogel TP, Cooper MA, Castro-Wagner J, Schussler E, Weinacht KG, et al. JAKinibs for the treatment of immune dysregulation in patients with gain-of-function signal transducer and activator of transcription 1 (STAT1) or STAT3 mutations. J Allergy Clin Immunol. 2018;142(5):1665–9. https://doi.org/10.1016/j.jaci.2018.07.020.

9. Moriya K, Suzuki T, Uchida N, Nakano T, Katayama S, Irie M, Rikiishi T, Niizuma H, Okada S, Imai K, Sasahara Y, Kure S. Ruxolitinib treatment of a patient with steroid-dependent severe autoimmunity due to STAT1 gain-of-function mutation. Int J Hematol. 2020;112(2):258–62. https://doi.org/10.1007/s12185-020-02860-7.

10. Chaimowitz NS, Ebenezer SJ, Hanson IC, Anderson M, Forbes LR. STAT1 gain of function, type 1 diabetes, and reversal with JAK inhibition. N Engl J Med. 2020t 8;383(15):1494–1496.https://doi.org/10.1056/NEJMc2022226.

11. Bloomfield M, Kanderová V, Paračková Z, Vrabcová P, Svatoň M, Froňková E, et al. A. Utility of ruxolitinib in a child with chronic mucocutaneous candidiasis caused by a novel STAT1 gain-of-function mutation. J Clin Immunol. 2018;38(5):589–601. https://doi.org/10.1007/s10875-018-0519-6

12. Vargas-Hernández A, Mace EM, Zimmerman O, Zerbe CS, Freeman AF, Rosenzweig S, Leiding JW, Torgerson T, Altman MC, Schussler E, Cunningham-Rundles C, Chinn IK, Carisey AF, Hanson IC, Rider NL, Holland SM, Orange JS, Forbes LR. Ruxolitinib partially reverses functional natural killer cell deficiency in patients with signal transducer and activator of transcription 1 (STAT1) gain-of-function mutations. J Allergy Clin Immunol. 2018 Jun;141(6):2142–2155.e5. https://doi.org/10.1016/j.jaci.2017.08.040.

13. Neven B, Al Adba B, Hully M, Desguerre I, Pressiat C, Boddaert N, et al. JAK inhibition in the Aicardi-Goutières syndrome. N Engl J Med Mass Med Soc. 2020;383(22):2190–3. https://doi.org/10.1056/NEJMc2031081.

14. Hadjadj J, Frémond ML, Neven B. Emerging place of JAK inhibitors in the treatment of inborn errors of immunity. Front Immunol. 2021;17(12): 717388. https://doi.org/10.3389/fimmu.2021.717388.

15. Tesch VK, Abolhassani H, Shadur B, Zobel J, Mareika Y, Sharapova S, et al. Long-term outcome of LRBA deficiency in 76 patients after various treatment modalities as evaluated by the immune deficiency and dysregulation activity (IDDA) score. J Allergy Clin Immunol. 2020;145(5):1452–63. https://doi.org/10.1016/j.jaci.2019.12.896.

16. Seidel MG, Tesch VK, Yang L, Hauck F, Horn AL, Smolle MA, et al The immune deficiency and dysregulation activity (IDDA2.1 'kaleidoscope') score and other clinical measures in inborn errors of immunity. J Clin Immunol. 2021 Nov 19. https://doi.org/10.1007/s10875-021-01177-2. Epub ahead of print

17. Kayaoglu B, Kasap N, Yilmaz NS, Charbonnier LM, Geckin B, Akcay A, et al. Stepwise reversal of immune dysregulation due to STAT1 gain-of-function mutation following ruxolitinib bridge therapy and transplantation. J Clin Immunol. 2021;41(4):769–79. https://doi.org/10.1007/s10875-020-00943-y.

18. Acker KP, Borlack R, Iuga A, Remotti HE, Soderquist CR, Okada S, et al. Ruxolitinib response in an infant with very-early-onset inflammatory bowel disease and gain-of-function STAT1 mutation. J Pediatr Gastroenterol Nutr. 2020;71(4):e132–3. https://doi.org/10.1097/MPG.0000000000002854.

19. Full prescribing information JAKAVI EMA. https://www.ema.europa.eu/en/documents/product-information/jakavi-epar-product-information_es.pdf. Accessed 04/08/2021.

20. Full prescribing information FDA: JAKAVI https://www.accessdata.fda.gov/drugsatfda_docs/label/2019/202192s017lbl.pdf. Accessed 04/08/2021.

21. Loh ML, Tasian SK, Rabin KR, Brown P, Magoon D, Reid JM, et al. A phase 1 dosing study of ruxolitinib in children with relapsed or refractory solid tumors, leukemias, or myeloproliferative neoplasms: a Children's Oncology Group phase 1 consortium study (ADVL1011). Pediatr Blood Cancer. 2015;62(10):1717–24. https://doi.org/10.1002/pbc.25575.

22. Wegehaupt O., Muckenhaupt T., Johnson M.B. et al. Ruxolitinib controls lymphoproliferation and diabetes in a STAT3-GOF patient. J Clin Immunol 40, 1207–1210 (2020).https://doi.org/10.1007/s10875-020-00864-w

23. Sanchez GAM, Reinhardt A, Ramsey S, Wittkowski H, Hashkes PJ, Berkun Y, et al. JAK1/2 inhibition with baricitinib in the treatment of autoinflammatory interferonopathies. J Clin Invest. 2018;128(7):3041–52. https://doi.org/10.1172/JCI98814.

24. Vanderver A, Adang L, Gavazzi F, McDonald K, Helman G, Frank DB, et al. Janus kinase inhibition in the Aicardi-Goutières syndrome. N Engl J Med. 2020;383(10):986–9. https://doi.org/10.1056/NEJMc2001362.

25. Meesilpavikkai K, Dik WA, Schrijver B, Nagtzaam NMA, Posthumus-van Sluijs SJ, van Hagen PM, et al. Baricitinib treatment in a patient with a gain-of-function mutation in signal transducer and activator of transcription 1 (STAT1). J Allergy Clin Immunol. 2018;142(1):328-330.e2. https://doi.org/10.1016/j.jaci.2018.02.045.

26. Registry Working Party. Immune deficiency and dysregulation activity (IDDA) score. https://esid.org/Working-Parties/Registry-Working-Party/Studies/IDDA-Score. Accessed: 20 December 2021

27. Przepiorka D, Luo L, Subramaniam S, Qiu J, Gudi R, Cunningham LC, et al. FDA approval summary: ruxolitinib for treatment of steroid-refractory acute graft-versus-host disease. Oncologist. 2020;25(2):e328–34. https://doi.org/10.1634/theoncologist.2019-0627.

28. Saeed I, McLornan D, Harrison CN. Managing side effects of JAK inhibitors for myelofibrosis in clinical practice. Expert Rev Hematol. 2017;10(7):617–25. https://doi.org/10.1080/17474086.2017.1337507.

29. Sant'Antonio E, Bonifacio M, Breccia M, Rumi E. A journey through infectious risk associated with ruxolitinib. Br J Haematol. 2019;187(3):286–295. https://doi.org/10.1111/bjh.16174.

30. Ballesta B, González H, Martín V, Ballesta JJ. Fatal ruxolitinib-related JC virus meningitis. J Neurovirol. 2017;23(5):783–78. https://doi.org/10.1007/s13365-017-0558-4.

31. Nakayama K, Nakamura M, Konishi A, Kaneko S, Nakamichi K, Saijo M, Yakushiji Y, Kusaka H. JC virus granule cell neuronopathy associated with ruxolitinib: a case report and review of the literature. eNeurologicalSci. 2020;21:100269 . https://doi.org/10.1016/j.ensci.2020.100269

32. Reoma LB, Trindade CJ, Monaco MC, Solis J, Montojo MG, Vu P, et al A. Fatal encephalopathy with wild-type JC virus and ruxolitinib therapy. Ann Neurol. 2019;86(6):878–884. https://doi.org/10.1002/ana.25608

33. Wathes R, Moule S, Milojkovic D. Progressive multifocal leucoencephalopathy associated with ruxolitinib. N Engl J Med. 2013;369:197–8. https://doi.org/10.1056/NEJMc1302135.

34. Lee SC, Feenstra J, Georghiou PR. Pneumocystis jiroveci pneumonitis complicating ruxolitinib therapy. BMJ Case Rep. 2014;2014. pii: bcr2014204950. https://doi.org/10.1136/bcr-2014-204950

35. Gill H, Leung GMK, Seto WK, Kwong YL. Risk of viral reactivation in patients with occult hepatitis B virus infection during ruxolitinib treatment. Ann Hematol. 2019;98(1):215–8. https://doi.org/10.1007/s00277-018-3405-7.

36. Caocci G, Murgia F, Podda L, Solinas A, Atzeni S, La Nasa G. Reactivation of hepatitis B virus infection following ruxolitinib treatment in a patient with myelofibrosis. Leukemia. 2014;28(1):225–7. https://doi.org/10.1038/leu.2013.235.

37. Goldberg RA, Reichel E, Oshry LJ. Bilateral toxoplasmosis retinitis associated with ruxolitinib. N Engl J Med. 2013;369:681–3. https://doi.org/10.1056/NEJMc1302895.

38. Weinacht KG, Charbonnier LM, Alroqi F, Plant A, Qiao Q, Wu H, et al. Ruxolitinib reverses dysregulated T helper cell responses and controls autoimmunity caused by a novel signal transducer and activator of transcription 1 (STAT1) gain-of-function mutation. J Allergy Clin Immunol. 2017;139(5):1629-1640.e2. https://doi.org/10.1016/j.jaci.2016.11.022.

39. Cordero E, Goycochea-Valdivia W, Mendez-Echevarria A, Allende LM, Alsina L, Bravo García-Morato M, et al. Executive summary of the Consensus Document on the diagnosis and management of patients with primary immunodeficiencies. J Allergy Clin Immunol Pract. 2020;8(10):3342–7. https://doi.org/10.1016/j.jaip.2020.05.008.

40. Registry Working Party. Resources. https://esid.org/Working-Parties/Inborn-Errors-Working-Party-IEWP/Studies/Multicentric-retrospective-study-on-JAKinib-treatment-of-patients-with-IEI-of-the-JAK-STAT-pathway. Accessed 21 December 2021

Authors and Affiliations

Angela Deyà-Martínez[1,2,3] · Jaques G. Rivière[4,5,6] · Pérsio Roxo-Junior[7] · Jan Ramakers[8,9] · Markéta Bloomfield[10,11] · Paloma Guisado Hernandez[12] · Pilar Blanco Lobo[12] · Soraya Regina Abu Jamra[7] · Ana Esteve-Sole[1,2,3] · Veronika Kanderova[13] · Ana García-García[1,2,3] · Mireia Lopez-Corbeto[14] · Natalia Martinez Pomar[15,16] · Andrea Martín-Nalda[4,5,6] · Laia Alsina[1,2,3,17] · Olaf Neth[12,18] · Peter Olbrich[12,18,19]

1   Study Group for Immune Dysfunction Diseases in Children (GEMDIP), Institut de Recerca Sant Joan de Déu, Barcelona, Spain

2   Clinical Immunology and Primary Immunodeficiencies Unit, Pediatric Allergy and Clinical Immunology Department, Hospital Sant Joan de Déu, Barcelona, Spain

3   Clinical Immunology Program Hospital, Sant Joan de Déu-Hospital Clínic Barcelona, Barcelona, Spain

4   Infection in Immunocompromised Pediatric Patients Research Group, Vall d'Hebron Institut de Recerca (VHIR), Hospital Universitari Vall d'Hebron, Vall d'Hebron Barcelona Hospital Campus, Barcelona, Catalonia, Spain

[5] Pediatric Infectious Diseases and Immunodeficiencies Unit, Hospital Universitari Vall d'Hebron, Vall d'Hebron Barcelona Hospital Campus, Barcelona, Catalonia, Spain

[6] Jeffrey Modell Diagnostic and Research Center for Primary Immunodeficiencies, Barcelona, Spain

[7] Division of Immunology and Allergy, Dept of Pediatrics, Ribeirão Preto Medical School, University of São Paulo, Ribeirão Preto, Brazil

[8] Department of Pediatrics, Hospital Universitari Son Espases, Palma, Spain

[9] Multidisciplinary Group for Research in Peadiatrics, Hospital Universitari Son Espases, Balearic Islands Health Research Institute (IdISBa), Palma, Spain

[10] Department of Immunology, 2nd Faculty of Medicine, Charles University and University Hospital Motol, Prague, Czech Republic

[11] Department of Pediatrics, 1st Faculty of Medicine, Charles University in Prague, Thomayer University Hospital, Prague, Czech Republic

[12] Laboratorio de Alteraciones Congénitas de La Inmunidad, Instituto de Biomedicina de Sevilla (IBiS), Laboratorio 205, Seville, Spain

[13] Inborn Errors of Immunity Group, Laboratory 205, Instituto de Biomedicina de Sevilla (IBiS), Seville, Spain

[14] Pediatric Rheumatology Unit, Rheumatology Department, Hospital Universitari Vall d'Hebron, Vall d'Hebron Barcelona Hospital Campus, Barcelona, Catalonia, Spain

[15] Immunology Department, Hospital Universitari Son Espases, Palma, Spain

[16] Human Immunopathology Research Laboratory, Institut d'Investigació Sanitària de Les Illes Balears (IdISBa), Palma, Spain

[17] Universitat de Barcelona, Barcelona, Spain

[18] Pediatric Infectious Diseases, Rheumatology and Immunology Unit, Hospital Universitario Virgen del Rocio, Sevilla, Spain

[19] Departamento de Farmacología, Pediatría y Radiología. Facultad de Medicina, Universidad de Sevilla, Seville, Spain

Immunogenicity and Safety of COVID-19 mRNA Vaccine in STAT1 GOF Patients

Marketa Bloomfield[1,2] · Zuzana Parackova[1] · Jana Hanzlikova[3] · Jan Lastovicka[1] · Anna Sediva[1]

To the Editor,

STAT1 gain-of-function (STAT1 GOF) mutations underlie chronic mucocutaneous candidiasis (CMC), a phenotypically diverse inborn error of immunity, ranging from isolated infectious susceptibility to complex immune deficiency [1]. The hypermorphic effect of the STAT1 mutation is likely due to reduced STAT3 promoter binding as a result of strong antagonizing type I and II interferon (IFN-I, IFN-II)-driven STAT1 recruitment [2]. Recently, JAK inhibitors, such as ruxolitinib, operating upstream from STATs, were shown to suppress the STAT1 response to IFNs and ameliorate the immune dysregulation [3].

The host immune response to SARS-CoV-2 infection, the cause of COVID-19 disease, is largely governed by the innate viral sensing mechanisms [4, 5]. Following their activation in the infected cells, the upregulation of the downstream transcription factors leads to increased production of IFNs. IFNs act as ubiquitous alarm triggers for the neighboring cells, activating the JAK/STAT pathways to augment the anti-viral defenses [6].

Recently, the most severe forms of COVID-19 were shown to be associated with disrupted IFN-I signaling, either due to inborn genetic errors or the presence of anti-IFN antibodies [7, 8]. Moreover, the early therapeutic enhancement of IFN response may be beneficial in preventing the infection and lowering mortality [9].

✉ Marketa Bloomfield
marketa.bloomfield@fnmotol.cz

1 Department of Immunology, 2nd Faculty of Medicine, Charles University in Prague and University Hospital in Motol, V Uvalu 84, Prague 15006, Czech Republic

2 Department of Pediatrics, 1st Faculty of Medicine, Charles University in Prague and Thomayer University Hospital, Prague, Czech Republic

3 Department of Immunology and Allergology, Faculty of Medicine and Faculty Hospital in Pilsen, Charles University in Prague, Pilsen, Czech Republic

Hypothetically, STAT1 GOF patients may be to some degree protected from SARS-CoV-2 infection/severe COVID-19 via the pre-emptive overactivation of IFN-I signaling, despite their otherwise immune deficient status. On the other hand, abnormally augmented IFN response may contribute to the catastrophic cytokine-driven hyperinflammation in delayed stages of COVID-19 [10]. So far, three STAT1 GOF patients were reported to suffer COVID-19 (one on ruxolitinib), all experiencing a mild course [11–13].

The mRNA-based SARS-CoV-2 vaccines activate the mechanisms of innate immunity, resulting in the production of multiple inflammatory mediators, including IFNs, which effectively promote both T and B cell-mediated response and antigen-specific immune memory [14]. The introduction of such agents into an IFN-biased environment in STAT1 GOF might amplify the immune dysregulation-related symptoms. Conversely, STAT1 GOF patients receiving JAK inhibitors, such as ruxolitinib, may have blunted vaccine response, due to the artificially suppressed JAK/STAT pathway. Recently, two STAT1 GOF CMC patients were reported to mount a normal vaccine-specific anti-spike 1 antibody response and one who failed to do so [15, 16].

Here, we report seven adult STAT1 GOF patients (two with novel mutations) with an uneventful course of COVID-19 vaccination, and/or SARS-CoV-2 infection, including two patients receiving JAK inhibitor ruxolitinib.

Results

Seven adult Czech STAT1 GOF CMC patients (previously described p.Y68C, p.A267V, p.M390T and novel p.T288N and p.E29A; cohort characteristics detailed in Supplementary Table 1) received SARS-CoV-2 spike 1 protein-encoding mRNA vaccine (Comirnaty®, Pfizer/BioNTech). All seven received two doses, six of them 3 to 6 weeks apart, one patient 4 months apart. Two patients were receiving ruxolitinib at the time of vaccination. No adverse events were

noted during 1–4-month follow-up. The antibody response was determined prior to the vaccination (Enzyme immunoassay COVID-19 RBD by TestLine Clinical Diagnostics, Czech Republic) and 3–5 weeks after the second vaccine dose (Microblot-Array COVID-19 by TestLine Clinical Diagnostics, Czech Republic). Four seronegative patients achieved vaccine-specific receptor-binding domain spike protein (RBD) IgG seroconversion (median 1211.5, range 999–1347 U/ml), which was comparable to vaccinated healthy controls ($N=100$, median 985.5, range 470–1924 U/ml). Only two patients responded with anti-RBD IgA, compared to 76 out of 100 healthy controls. This may be an important efficacy parameter, as serum IgA was shown to be an early SARS-CoV-2–neutralizing agent [17]. Despite the absence of any previous COVID-19 symptoms, one patient (P5[M390T]) was found to be S1-spike protein seropositive before vaccination, and one patient (P4[A267V], unavailable for testing prior to vaccination) had anti-nucleocapsid, as well as anti-RBD antibodies after vaccination, suggestive of past infections in both patients. One patient did not mount an antibody response after vaccination (P7[E29A]) (Fig. 1A). Regardless of the serologic status, six out of seven patients (one patient not tested), including the two ruxolitinib receivers, were found to mount a virus-specific (S1-spike protein) cellular immune response (median 1192.5, range 585–4115 mIU/ml), which was comparable to vaccinated healthy controls ($N=7$, median 1830, range 675–1735 mIU/ml), detected by whole blood IFN-γ release assay (EUROIMMUN SARS-CoV-2 IGRA, Germany) (Fig. 1B). The summary of the humoral and cellular COVID-19-related immune parameters is listed in Table 1.

Within the cohort, two patients were of particular interest. An 18-year-old female P5[M390T] with CMC and severe pulmonary damage had asymptomatic COVID-19 infection, as evident by anti-S1 seropositivity prior to vaccination. Despite that, the anti-nucleocapsid antibodies were not detectable. This patient has been on ruxolitinib (0.4 mg/kg/day, dose titered to healthy control's phosphorylated STAT1 level) for the past 6 months; however, it is unknown whether the infection occurred prior or after the JAK inhibitor initiation.

The second patient, a 45-year-old male P7[E29A] with CMC, severe pneumopathy, and multiple autoimmune phenomena, was vaccinated while COVID-19 naïve and 5 months on ruxolitinib (0.2 mg/kg/day, dose titered to healthy control's phosphorylated STAT1 level). The patient failed to produce detectable SARS-CoV-2 antibodies. However, this may be attributed to continuing B cell impairment after previous CD20-depletion therapy (rituximab) 18 months prior to vaccination; while the overall CD19 B cells count represented 5.7% of lymphocytes, the B cell pool constituted predominantly of CD27 negative naïve B cells prior to vaccination. In fact, such skewed antibody response to primary antigen exposure post-rituximab has been reported by multiple studies, including, recently, the impaired response to SARS-CoV-2 vaccines [16, 18]. Nevertheless, the patient developed a strong S1-peptide-specific T cell immune response in IGRA, interestingly, the strongest in our cohort (4115 mIU/ml; Fig. 1B).

In summary, while limited by the cohort size and the absence of antibody-neutralization assays, our observations indicate that SARS-CoV-2 mRNA vaccination in

Fig. 1 Immune responses to SARS-CoV-2 mRNA vaccine (Pfizer/BioNTech) in STAT1 GOF patients evaluated 3–5 weeks after the second vaccine dose. A Antibody titers in 7 patients determined by Microblot-Array COVID-19 (TestLine Clinical Diagnostics, Brno, Czech Republic); results are compared to vaccinated healthy controls ($N=100$) and considered positive if value is > 210 U/ml. B S1-spike protein-specific T cell immune response in 6 patients determined by EUROIMMUN SARS-CoV-2 IGRA, Lübeck, Germany; results are compared to vaccinated healthy controls ($N=7$) and considered positive if value > 200 mIU/ml. CMC, chronic mucocutaneous candidiasis; RBD, receptor-binding domain spike protein; S1, spike 1 protein
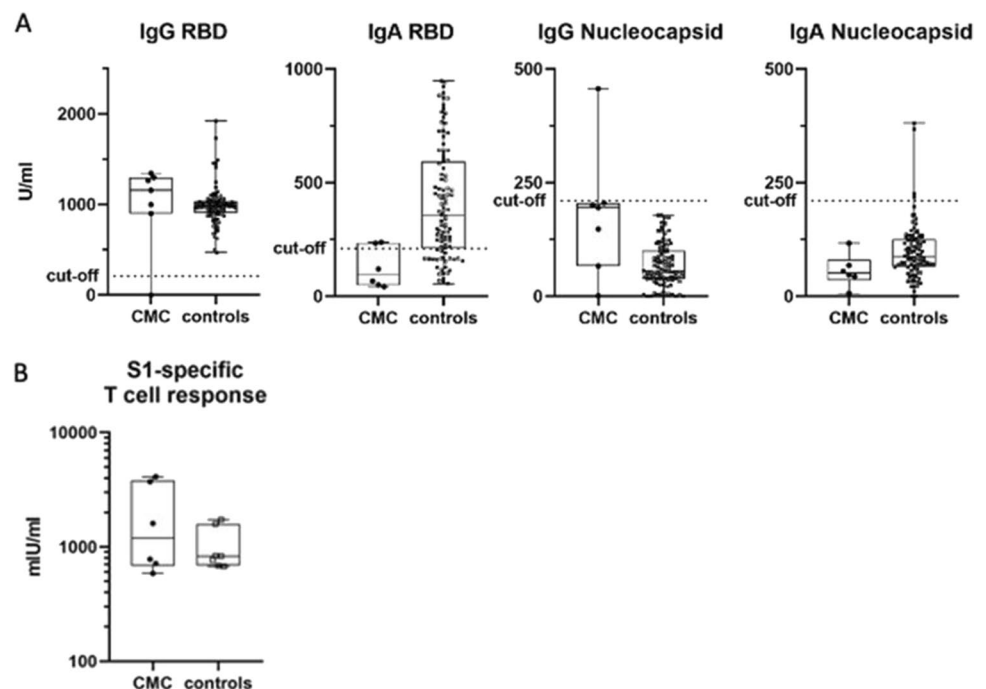
Table 1 Overview of COVID-19-related immune status of 7 STAT1 GOF patients

	Past COVID-19 symptoms/ confirmed infection	Pre-vaccination SARS-CoV-2 anti-RBD	Post-vaccination SARS-CoV-2 anti-RBD IgG	Post-vaccination SARS-CoV-2 anti-RBD IgA	Post-vaccination SARS-CoV-2 anti-NC IgG	Post-vaccination SARS-CoV-2 anti-NC IgA	Post-vaccination S1-specific IGRA	Interval between 2nd vaccine dose and testing (weeks)	Immune therapy at time of vaccination
P1[Y68C]	−	−	+	+	−	−	+	3	−
P2[Y68C]	−	−	+	+	−	−	+	3	IgRT
P3[A267V]	−	−	+	−	−	−	ND	5	−
P4[A267V]	−	ND	+	−	+	−	+	3	−
P5[M390T]	−	IgG+/IgA+	+	−	−	−	+	3	Ruxolitinib IgRT
P6[T288N]	−	−	+	−	−	−	+	3	−
P7[E29A]	−	−	−	−	−	−	+	4	Ruxolitinib IgRT Rituximab 18 months pre-vaccination

+, positive; −, negative; *RBD*, receptor-binding domain spike protein; *NC*, nucleocapsid protein; *ND*, not done; *IGRA*, IFN-γ release assay; *IgRT*, immunoglobulin replacement therapy

STAT1 GOF is immunogenic and may be safe, even during treatment with JAK inhibitor and after past infection. Furthermore, we affirm that COVID-19 disease may take a mild/asymptomatic course in STAT1 GOF CMC. This data may help guide clinical counselling for patients with STAT1 GOF CMC.

Declarations

References

1. Toubiana J, Okada S, Hiller J, Oleastro M, Gomez ML, Becerra JCA, Ouachée-Chardin M, Fouyssac F, Girisha KM, Etzioni A, et al. Heterozygous STAT1 gain-of-function mutations underlie an unexpectedly broad clinical phenotype. Blood. 2016;127:3154–64. https://doi.org/10.1182/blood-2015-11-679902.

2. Zheng J, van de Veerdonk FL, Crossland KL, Smeekens SP, Chan CM, Al Shehri T, Abinun M, Gennery AR, Mann J, Lendrem DW, et al. Gain-of-function STAT1 mutations impair STAT3 activity in patients with chronic mucocutaneous candidiasis (CMC). Eur J Immunol. 2015;45:2834–46. https://doi.org/10.1002/eji.201445344.

3. Forbes LR, Vogel TP, Cooper MA, Castro-Wagner J, Schussler E, Weinacht KG, Plant AS, Su HC, Allenspach EJ, Slatter M, et al. Jakinibs for the treatment of immune dysregulation in patients with gain-of-function signal transducer and activator of transcription 1 (STAT1) or STAT3 mutations. J Allergy Clin Immunol. 2018;142. https://doi.org/10.1016/j.jaci.2018.07.020.

4. Lim Y, Ng Y, Tam J, Liu D. Human coronaviruses: a review of virus–host interactions. Diseases. 2016;4. https://doi.org/10.3390/diseases4030026.

5. Fitzgerald KA, Kagan JC. Toll-like receptors and the control of immunity. Cell. 2020;180. https://doi.org/10.1016/j.cell.2020.02.041.

6. Li SF, Gong MJ, Zhao FR, Shao JJ, Xie YL, Zhang YG, Chang HY. Type i interferons: distinct biological activities and current applications for viral infection. Cell Physiol Biochem. 2018;51. https://doi.org/10.1159/000495897.

7. Bastard P, Rosen LB, Zhang Q, Michailidis E, Hoffmann HH, Zhang Y, Dorgham K, Philippot Q, Rosain J, Béziat V, et al. Autoantibodies against type I IFNs in patients with life-threatening COVID-19. Science (80-). 2020;370. https://doi.org/10.1126/science.abd4585.

8. Zhang Q, Liu Z, Moncada-Velez M, Chen J, Ogishi M, Bigio B, Yang R, Arias AA, Zhou Q, Han JE, et al. Inborn errors of type I IFN immunity in patients with life-threatening COVID-19. Science (80-). 2020;370. https://doi.org/10.1126/science.abd4570.

9. Jirjees F, Saad AK, Al Hano Z, Hatahet T, Al Obaidi H, Dallal Bashi YH. COVID-19 treatment guidelines: do they really reflect best medical practices to manage the pandemic? Infect Dis Rep. 2021;13:259–84. https://doi.org/10.3390/idr13020029.

10. Wang N, Zhan Y, Zhu L, Hou Z, Liu F, Song P, Qiu F, Wang X, Zou X, Wan D, et al. Retrospective multicenter cohort study shows early interferon therapy is associated with favorable clinical responses in COVID-19 patients. Cell Host Microbe. 2020;28:455-464.e2. https://doi.org/10.1016/j.chom.2020.07.005.

11. Guisado Hernández P, Blanco Lobo P, Villaoslada I, de Felipe B, Lucena JM, Martín Gutierrez G, Castro MJ, Gutiérrez Valencia A, Sánchez Codez MI, Gaboli M, et al. SARS-CoV-2 infection in a pediatrics STAT1 GOF patient under ruxolitinib therapy-a matter of balance? J Clin Immunol. 2021;1–5. https://doi.org/10.1007/s10875-021-01081-9.

12. Meyts I, Bucciol G, Quinti I, Neven B, Fischer A, Seoane E, Lopez-Granados E, Gianelli C, Robles-Marhuenda A, Jeandel P-Y, et al. Coronavirus disease 2019 in patients with inborn errors of immunity: an international study. J Allergy Clin Immunol. 2021;147:520–31. https://doi.org/10.1016/j.jaci.2020.09.010.

13. Esenboga S, Ocak M, Akarsu A, Bildik HN, Cagdas D, Iskit AT, Tezcan I. COVID-19 in patients with primary immunodeficiency. J Clin Immunol. 2021. https://doi.org/10.1007/s10875-021-01065-9.

14. Pardi N, Hogan MJ, Porter FW, Weissman D. mRNA vaccines — a new era in vaccinology. Nat Rev Drug Discov. 2018;17:261–79. https://doi.org/10.1038/nrd.2017.243.

15. Hagin D, Freund T, Navon M, Halperin T, Adir D, Marom R, Levi I, Benor S, Alcalay Y, Freund NT. Immunogenicity of Pfizer-BioNTech COVID-19 vaccine in patients with inborn errors of immunity. J Allergy Clin Immunol. 2021;148:739–49. https://doi.org/10.1016/j.jaci.2021.05.029.

16. Delmonte OM, Bergerson JRE, Burbelo PD, Durkee-Shock JR, Dobbs K, Bosticardo M, Keller MD, McDermott DH, Rao VK, Dimitrova D, Quiros-Roldan E, Imberti L, Ferrè EMN, Schmitt M, Lafeer C, Pfister J, Shaw D, Draper D, Truong M, Ulrick J, DiMaggio T, Urban A, FA. Antibody responses to the SARS-CoV-2 vaccine in individuals with various inborn errors of immunity. J Allergy Clin Immunol. 2021; 4:0091-6749(21)01356–7.

17. Delphine S, Alexis M, Makoto M, Audrey M, François A, Laetitia C, Paul Q, Jehane F, Hervé D, Pascale G, et al. IgA dominates the early neutralizing antibody response to SARS-CoV-2. Sci Transl Med. 2021;13:abd2223. https://doi.org/10.1126/scitranslmed.abd2223.

18. Mrak D, Tobudic S, Koblischke M, Graninger M, Radner H, Sieghart D, Hofer P, Perkmann T, Haslacher H, Thalhammer R, et al. SARS-CoV-2 vaccination in rituximab-treated patients: B cells promote humoral immune responses in the presence of T-cell-mediated immunity. Ann Rheum Dis. 2021;annrheumdis-2021-220781. https://doi.org/10.1136/annrheumdis-2021-220781.

Mutual alteration of NOD2-associated Blau syndrome and IFNγR1 deficiency

Zuzana Parackova[1] · Marketa Bloomfield[1,2] · Petra Vrabcova[1] · Irena Zentsova[1] ·
Adam Klocperk[1] · Tomas Milota[1] · Michael Svaton[3] · Jean-Laurent Casanova[4,5,6,7,8] ·
Jacinta Bustamante[4,5,6,9] · Eva Fronkova[3] · Anna Sediva[1]

Abstract

Blau syndrome (BS) is an auto-inflammatory granulomatous disease that possibly involves abnormal response to interferon gamma (IFNγ) due to exaggerated nucleotide-binding oligomerization domain containing 2 (NOD2) activity. Mendelian susceptibility to mycobacterial diseases (MSMD) is an infectious granulomatous disease that is caused by impaired production of or response to IFNγ. We report a mother and daughter who are both heterozygous for $NOD2^{c.2264C>T}$ variant and dominant-negative $IFNGR1^{818del4}$ mutation. The 17-year-old patient displayed an altered form of BS and milder form of MSMD, whereas the 44-year-old mother was completely asymptomatic. This experiment of nature supports the notion that IFNγ is an important driver of at least some BS manifestations and that elucidation of its involvement in the disease immunopathogenesis may identify novel therapeutic targets.

Keywords NOD2 · IFNγR1 · IFNγ · WES · MSMD · Blau syndrome · methotrexate

Introduction

Blau syndrome (BS) (OMIM, #186580) is a rare, autosomal-dominant (AD) childhood-onset systemic auto-inflammatory disorder classically characterized by a triad of arthritis, dermatitis, and uveitis, and the presence of non-caseating sterile granulomas [1–3]. It is caused by mutations in nucleotide-binding oligomerization domain containing 2 (NOD2), also

---

Zuzana Parackova and Marketa Bloomfield contributed equally to this work.

✉ Zuzana Parackova
  zuzana.parackova@fnmotol.cz

1   Department of Immunology, 2nd Faculty of Medicine, Charles University and Motol University Hospital, V Uvalu 84, 15006 Prague 5, Czech Republic

2   Department of Pediatrics, 1st Faculty of Medicine Charles University and Thomayer's Hospital, Prague, Czech Republic

3   CLIP - Childhood Leukaemia Investigation Prague, Department of Paediatric Haematology and Oncology, 2nd Faculty of Medicine, Charles University and Motol University Hospital, Prague, Czech Republic

4   Laboratory of Human Genetics of Infectious Diseases, Necker Branch, INSERM U1163, Necker Hospital for Sick Children, Paris, France

5   Imagine Institute, Paris Descartes University, Paris, France

6   St. Giles Laboratory of Human Genetics of Infectious Diseases, Rockefeller Branch, The Rockefeller University, New York, NY, USA

7   Howard Hughes Medical Institute, New York, NY, USA

8   Pediatric Hematology-Immunology Unit, Necker Hospital for Sick Children, AP-HP, Paris, France

9   Study Center for Primary Immunodeficiencies, AP-HP, Necker Children Hospital, Paris, France

known as *CARD 15* (caspase activation and recruitment domain 15) [1, 2]. NOD2 is an innate immune system pattern-recognition receptor expressed mostly by not only monocytes, macrophages, and dendritic cells but also hepatocytes, preadipocytes, and pulmonary and intestinal epithelial cells [4, 5]. The three-domain protein recognizes and binds peptidoglycans contained in bacterial cell walls, chiefly muramyl dipeptide (MDP), and various other bacterial and viral products [6]. After ligand recognition, NOD2 activates the transcription factor NFκB and MAPKs (mitogen-activated protein kinases), thereby promoting inflammatory responses against pathogens [1, 2]. In particular, NOD2-mediated signaling can be triggered by mycobacteria [7, 8], including the attenuated vaccinal substrains *Bacillus Calmette-Guérin* (BCG) [9].

The importance of NOD2 in human health has been intensively studied. Heterozygous mutations in *NOD2* gene were first identified in Blau syndrome patients in 2001 [10]. Since then, twenty-seven variants have been found in patients with Blau syndrome (Infevers https://infevers.umai-montpellier.fr/web/). Most mutations occur at or near the NACHT domain of the protein, which is important for ATP-dependent self-oligomerization [11], while several other mutations are located within the leucine-rich repeat (LRR) motif or between the two domains. However, pathophysiologic mechanisms and genotype-phenotype correlation have yet not been ascertained. Even an argument of the gain-of-function (GOF) vs. loss-of-function (LOF) effect of the mutations remains unresolved.

Due to the granulomatous character of BS, the GOF phenotype was originally proposed and this was supported by studies using in vitro transient transfection assays with overexpressed NOD2 which demonstrated an elevated basal NFκB activation [3, 12]. However, this hypothesis was not confirmed by consecutive ex vivo experiments, as other studies fail to demonstrate the supposed exaggerated cytokine release by patients' peripheral blood mononuclear cells (PBMCs) after MDP stimulation [13, 14]. In parallel, the murine Blau syndrome model also showed reduced cytokine production and NFκB signaling and overall reduced response to MDP [15]. Nevertheless, the most recent evidence suggests that the proinflammatory state in BS may, indeed, be due to an increased NOD2 response and that interferon gamma (IFNγ) might play a crucial role in the disease pathophysiology. In healthy cells, IFNγ acts as a priming signal to upregulate NOD2 expression in order to mount an efficient inflammatory response against pathogens containing peptidoglycans [16]. In BS, such priming with IFNγ was shown to result in an abnormal spontaneous NOD2 activation even in the absence of infectious ligand [17].

AD (autosomal dominant) partial IFNγR1 deficiency is one of the genetic etiologies of Mendelian susceptibility to mycobacterial disease (MSMD; OMIM, #209950) [18–20]. The majority of MSMD genetic etiologies impair IFNγ

immunity, either by impairing its production or by diminishing cellular responses to it [18–30]. MSMD patients suffer from increased susceptibility to intra-macrophagic pathogens, especially weakly virulent mycobacteria, such as environmental mycobacteria (EM) and attenuated BCG vaccinal substrains. Infections with *Salmonella* spp. are also commonly seen, whereas infections by *Nocardia* spp., *Histoplasma capsulatum*, and other microorganisms are rarer [21].

Twenty-nine genetic etiologies of MSMD have been discovered, with 12 "isolated MSMD"–causing loci (*IFNGR1*, *IFNGR2*, *STAT1*, *IL12RB1*, *IL-12B2*, *IL-12p40*, *IL-23R*, *TYK2*, *IRF8*, *SPPL2A*, *CYBB*, and *NEMO*) and with three "syndromic-MSMD" loci (*RORC*, *JAK1*, and *ISG15*) [22–28]. AD partial IFNγR1 deficiency is one of the most common causes of MSMD, in part because it is due to a mutation that is recurrent by hotspot [29]. As many as 45 unrelated kindreds have already been reported since 1999 and many more have been diagnosed [20–22, 27–30]. It is due to heterozygous mutations that truncate the cytoplasmic domain of the protein. The mutated receptor accumulates on the cellular surface due to a lack of recycling motif and exerts a dominant-negative effect over the wild-type receptors. This results in weakened, but not abolished, downstream signaling [29, 30]. This form of AD partial IFNγR1 deficiency causes a clinical susceptibility to environmental mycobacteria (EM) and non-typhoid *Salmonellae*. In over 70% of cases, the infections affect the bones [21]. Overall, the presentation is less severe than patients with complete IFNγR1 deficiency, which is a fatal condition with an early onset and a poor prognosis. Patients with AD partial IFNγR1 are treated with prolonged courses of antimycobacterial drugs and IFNγ [27, 30].

We were intrigued by a 17-year-old patient whose clinical features were reminiscent of both BS and MSMD who was found to harbor *NOD2*[c.2264C>T] and *IFNγR1*[818del4] mutation. The patient's mother is completely asymptomatic despite carrying both mutations. Here, we describe the clinical and immunological phenotype of the kindred, as well as their *NOD2* and *IFNGR1* genotypes.

Materials and methods

Informed consent was obtained from all subjects involved in the study and all controls in accordance with the Declaration of Helsinki and according to the procedures established by the Ethical Committee of our institution.

Whole exome sequencing

DNA was isolated with QIAamp DNA Mini Kit (Qiagen, Hilden, Germany) and sequencing libraries were prepared using SureSelectXT Human All Exon + UTRs V6 kit (Agilent Technologies, Santa Clara, CA) and sequenced on

the NextSeq 500 instrument with the High Output V2 kit (Illumina, San Diego, CA). The reads in resulting FASTQ files were aligned against the human reference genome hg19 with BWA [31]. Genomic variants were called with samtools [32] and VarScan [33]. Variant annotation was performed using SnpEff [34]. Identification of causal variants was performed with Ingenuity® Variant Analysis™ software (https://www.qiagen-bioinformatics.com/products/ingenuity-variant-analysis, Qiagen).

IFNγR1 expression

Peripheral blood drawn into EDTA-coated tubes was labeled with antibodies against lineage-specific markers (CD3 clone MEM-57, CD19 clone LT19, CD20 clone LT20, CD16 clone LNK16, CD56 clone MEM-188) - FITC, CD14 - PEDy594 (clone MEM-15), CD11c - APC (clone BU15) (Exbio, Prague, Czech Republic), CD123 - PC7 (clone 6H6), HLA-DR - A700 (clone L243), IFNγR1 - PE (clone GIR-2018) (BioLegend, San Diego, CA, USA) for 20 min at room temperature and then lysed with hypotonic solution. Samples were acquired on AriaII (BD Biosciences, San Jose, CA, USA), analyzed using FlowJo (TreeStar, Ashland, OR, USA) and IFNγR1 was shown as MFI (mean fluorescence intensity).

Intracellular signaling and phospho flow

For IFNγR1 signaling, peripheral blood was stimulated with 1 μg/ml IFNγ (R&D, Minneapolis, MN, USA) (or with 100 ng/ml and 10 μg/ml when indicated) or 1 μg/ml IFNα (Abcam, Cambridge, UK) for 5 min (or for 30 or 60 min when indicated) at 37 °C. For MAPK phosphorylation, peripheral blood was left unstimulated. Subsequently, the cells were fixed using 4% formaldehyde for 10 min at 25 °C; erythrocytes were lysed using 0.1% Triton X-100 (Sigma-Aldrich, Darmstadt, Germany) for 15 min at 37 °C and the leukocytes were permeabilized using 80% ice-cold methanol for 30 min.

Samples for IFNγR1 signaling were labeled with antibodies against lineage-specific markers (CD3, CD19, CD20, CD16, CD56) - FITC, CD14 - PEDy594, CD11c - APC (Exbio), CD123 - PC7, HLA-DR - A700 (BioLegend) and intracellular signaling was detected using anti-phospho-STAT1 (Tyr701) - BV421 (clone 4a) antibody (BD Bioscience).

Samples for MAPK phosphorylation were labeled with antibodies against CD3 - A700 (clone MEM-57), CD14 - PEDy594 (Exbio), and CD19 - PC7 (clone J3-119) (Immunotech) and intracellular signaling was detected using anti-phospho-p38 (Thr180) - A647 (#4552S), anti-phosphoErk1/2 (Thr202/Tyr204) - A488 (#4374S), and anti phospho-SAPJ/JNK (Thr183/185) - PE (#5755S) antibody (Cell Signaling, Denvers, MA, USA).

Data were collected using BD FACSAria II, and BD FACSDiva (BD Biosciences) software was used for signal acquisition and then they were analyzed using FlowJo (Treestar) analysis platform.

Cytokine production

2×10^5 peripheral blood mononuclear cells (PBMCs) were resuspended in 200 μl of complete media and were stimulated with muramyl dipeptide (MDP) (10 μg/ml) (Invivogen, San Diego, CA) and E. coli lipopolysaccharide (LPS) (1 μg/ml) (Sigma-Aldrich) or left untreated. When indicated, prestimulation with IFNγ (R&D) was used. After 24-h incubation at 37 °C, the supernatants were harvested and the cytokines were determined using multiplex Luminex cytokine fluorescent bead-based immunoassay (Merck Millipore, Beerlington, MA). Data were collected using Luminex-100 system (Luminex, Austin, TX). A five-parameter regression formula was used to calculate the sample concentrations from standard curves.

CD4+ subset analysis

PBMCs were stimulated with phorbol 12-myristate 13-acetate (PMA) (50 ng/ml) and ionomycin (750 ng/ml) (both from Sigma-Aldrich, Darmstadt, Germany); 1 h later, brefeldin A (10 mg/ml) (BioLegend) was added for additional 3 h. Cells were harvested and stained with CD3 - A700, CD8 - PEDy594 (clone MEM-31) (Exbio), CD4 - PC7 (clone RPA-T4) (eBioscience, San Diego, CA), before being fixed and permeabilized using eBioscience fixation/permeabilization solutions. The following Abs were added: IFNγ - FITC (clone 4S.B3) (BD Biosciences) and IL-17A - A647 (clone BL168) (Biolegend). Samples were acquired on AriaII and analyzed using FlowJo software.

RT-PCR gene expression analysis

PBMCs were stimulated with IFNγ (1 μg/ml) (R&D) for 5 h for IRF1 (Hs00971965_m1) and CXCL10 (Hs00171042_m1) detection, or left untreated for c-Fos (Hs04194186_s1) and c-Jun (Hs99999141_s1) detection. Total RNA was isolated using RNeasy Mini Kit following manufacturer's instructions (Qiagen, MD, USA) and complementary DNA (cDNA) was synthetized using M-MLV reverse transcriptase (Thermo Fisher Scientific, Waltham, MA). RT-PCR was performed in duplicates using the cDNA and platinum Taq polymerase (Thermo Fisher Scientific), 200 nM dNTP (Promega, Southampton, UK), 50 mM MgCl₂ (Thermo Fisher Scientific), and TaqMan primer/probe sets (Thermo Fisher Scientific). Samples were matched to a standard curve generated by amplifying serially diluted products using the same PCR reaction and normalized to GAPDH (forward primers GAAGGTGAAGGTCGGAGTC; reverse primers GAAGATGGTGATGGGATTTC; FAM/TAMRA CAAGCTTCCCGTTCTCAGCC) (TIB MOLBIOL, Berlin, Germany) to obtain the relative expression value. Real-time assays were run on iQ5 Cycler (Bio-Rad, CA, USA).

NFκB translocation and Image Stream analysis

PBMCs were stimulated with MDP (10 μg/ml) (Invivogen) for 30 min or left untreated, then fixed and permeabilized following manufacturer's instructions described in protocol III of the BD phosphoflow protocols (BD Bioscience). The cells were then stained with anti CD14 - PEDy594 (Exbio), NFκB - A488 (#532301) (R&D system), Draq5 fluorescent probe solution (Thermo Fisher Scientific) and then washed. The data were acquired using ImageStream (Merck Millipore) and analyzed using IDEAS software's guided analysis for nuclear translocation (Merck Millipore). The data are expressed as similarity score and value of co-expressed NFκB and Draq5.

Western blot analysis of NFκB signaling

PBMCs were stimulated for 20 min with MDP (10 μg/ml) or left untreated. The cells were then washed and lysed in RIPA lysis buffer and PMSF (Cell Signaling), placed on ice, sonicated, and then centrifuged at $14000g$ to remove cell debris. For western blot analysis, samples were resuspended on Laemli buffer (Sigma-Aldrich) at 1:1 ratio and boiled for 5 min. Proteins were separated by SDS-PAGE and transferred to PVDF membrane. After blocking with 5% BSA in TBST (TBS and 0.1%Tween, both from Bio-Rad), membranes were incubated with the primary antibodies anti-IκB (#4814S), IKK (#2682S and #2370), phospho IKK (S176/S177) (#2078S), and β-actin (#8457S) (all from Cell Signaling) overnight, followed by incubation with peroxidase-conjugated anti-rabbit or anti-mouse secondary antibodies for 2 h. Membranes were developed using SuperSignal West Femto (Thermo Fisher Scientific). Densitometry was performed with ImageJ software (National Institutes of Health, USA). Band area values were used for semi-quantification. Graphs are expressed as ratio of stimulated/unstimulated cells of band area value calculated from band area of phosphorylated forms/band area of unphosphorylated forms.

Results

Case report

The proband (P1) is a 17-year-old female born to non-consanguineous Czech parents. Her father has rheumatoid arthritis and her maternal grandmother had reportedly suffered from frequent skin ulcerations, while her mother (P2) and sister are healthy. At the age of 6 weeks, the proband developed a post-vaccination BCGitis that was treated with isoniazid and rifampicin. The originally increased inflammatory markers decreased slightly but after 2 months of treatment, only partial improvement of the BCGitis was achieved. A new increase of inflammatory parameters (CRP 55 mg/l, erythrocyte sedimentation rate - ESR 120 mm/h, leukocytes 23,500/mm³) prompted further investigation, which revealed anterior uveitis and severe osteomyelitis of mandible. Oral prednisone 1 mg/kg and clindamycin were added to the treatment. The symptoms regressed completely after 6 months of therapy and she appeared healthy until the age of 6 years. She then started experiencing recurrent flares of high-grade fever, accompanied with aseptic arthritis of sternoclavicular joints, knees, and elbows, developed maculopapular rash, often progressing into pustulosis of face and palms, and vasculitis-like rash on lower extremities. She also suffered from recurrent erythema nodosum and cervical lymphadenitis. Multiple biopsies from the lymph nodes showed well-formed granulomas with epithelioid and multinucleated giant cells; some of the granulomas also contained areas of non-caseating necrosis. Microbiologic investigations, including mycobacterial detection (acid-fast staining, PCR for tuberculous and non-tuberculous mycobacteria and cultures), were negative on all occasions. Her laboratory evaluation revealed signs of chronic inflammation (mildly increased ESR, increased serum amyloid A, microcytic anemia), along with elevated serum IgG, contrasting with gradually decreasing CD19⁺ B lymphocyte count. A marked increase of activated CD3⁺ HLA-DR⁺ cells was noted (Table 1). A tentative diagnosis of Saphó or Blau syndrome was considered based on the cutaneous and joint features and the history of infantile uveitis. She was initially managed with oral steroids in flares and occasional courses of antibiotics (sulfamethoxazole/trimethoprim – STX/TMP, azithromycin, clindamycin); later she received STX/TMP prophylaxis alone. At 15 years of age, multifocal granulomatous osteomyelitis of hipbone (containing necrosis within some granulomas), multiple vertebrae and ribs, multiple splenic, hepatic lesions, and lymphadenopathy were detected (Fig. 1a, b). No mycobacteria were found in the bone lesions. The inflammatory markers were only mildly elevated, and she reported no pain. At that point, a heterozygous mutation in *IFNGR1* and a variant in *NOD2* (Fig. 2a, b) was discovered. The patient was thus diagnosed with MSMD and BS with extended phenotype. The STX/TMP was discontinued and she was started on methotrexate (MTX) 20 mg weekly which resolved her clinical symptoms within 6 months. A 2-week unplanned withdrawal of methotrexate resulted in a formation of deep ulceration on the foot which healed promptly after the drug reintroduction (Fig. 1c). Twelve months on the treatment, she experienced no further infectious or non-infections complications, including mycobacteriosis, despite the imune suppression.

The patient's mother carries both mutations but has never experienced any BS-related symptoms, nor has she contracted any apparent mycobacteriosis to date, despite being vaccinated with BCG as an infant. Her basic immune phenotype (lymphocytes subpopulations, immunoglobulin levels, etc.) was normal.

The clinical features of our *IFNGR1*[818del14] and *NOD2*[c.2264C>T] proband, as well as comparison with another

Table 1 Laboratory values of proband1 (*NOD2c.2264C>T + IFNGR1818del4*)

	Pre-treatment	3 month on MTX treatment	12 months on MTX treatment	Age-matched reference values
Haemoglobin (g/l)/ MCV (fl)/ MCH (pg)	109↓/69.8↓/21.6↓	114↓/74.3↓/23.4↓	100↓/75.1↓/24.2↓	120–160/82.0–98.0/28.0–34.0
Leukocytes (cells/μl)	9900	9600	7600	4 000–10 000
Lymphocytes (cells/μl)	3440	3350	1820	800–4 000
Neutrophils (cells/μl)	4550	4790	4730	2 000–7 000
Monocytes (cells/μl)	430	500	550	80–1200
Eosinophils (cells/μl)	1410↑	760↑	460	0–500
CD3+ (%a), cells/μl)	87↑/ 2990	89↑ 2150	86↑/1570	60–85/1000–3900
CD3+ CD4+ (%a), cells/μl)	59↑/2030	59↑/ 1430	58↑/1060	27–57/560–2700
CD3+ CD8+ (%a), cells/μl)	24/830	26/630	25/460	18–40/300–1400
CD3+ HLA-DR+ (%a))	37↑	29↑	22↑	0–10
CD19+ (%a), cells/μl)	4↓/140↓	4↓/100↓	5↓/90↓	7–30/200–1500
CD16+/CD56+ (%a), cells/μL)	9/310	5/120	7/130	6–28/50–1000
CD4+ IL17+ (%b))	0.61	0.33ê	0.37ê	0.5–5.97
Regulatory T cells (%b)) CD4+CD25+FOXP3+	5.9	3.9	6.13	3.0–10.0
Immunoglobulins IgG (g/l)	27.40↑	17.70↑	17.2↑	7.65–13.60
IgA (g/l)	2.44	1.86	2.25	0.91–2.90
IgM (g/l)	1.43	1.29	1.26	0.47–1.95
IgD (g/l)	53.5	27.0	-	0.0–100.0
IgE (IU/ml)	102	26	49.2	0.0–150
Circulating immune complexes	149↑	126↑	166↑	10–46 arb.units
Serum amyloid A (mg/l)	52↑	20↑	14.6↑	0.0–10.0
Autoantibodies (ANA , ENA, ANCA, ASCA, a-TPO, a-TG)	Negative	ND	Negative	NA

a % of total peripheral lymphocytes, b % of CD4+ , c % of CD8+ . *ND*, not done; *NA*, not applicable; *ANA*, antinuclear antibodies; *ENA*, extractable nuclear antigen antibodies; *ANCA*, anti-neutrophil cytoplasm antibodies; *ASCA*, anti-saccharomyces cerevisiae antibodies; *a-dsDNA*, anti-double-stranded DNA antibodies; *a-TPO*, anti-thyreoperoxidase antibodies; *a-TG*, anti-thyroglobulin antibodies; *MTX*, methotrexate. ↑↓ value above and below the reference range, respectively

patient with AD IFNGR1[818del4] mutation and a BS patient reported previously by Rosé et al [2] to carry the identical *NOD2[c.2264C>T]* [2] mutation, are summarized in Table 2.

Whole exome sequencing

In the proband, whole exome sequencing performed on PBMCs revealed simultaneously two mutations. A heterozygous mutation c.819_822delTAAT in *IFNGR1* (NM_000416.2, dbSNP rs587776856) leads to a 4-bp deletion and premature stop codon p.N274fs*2. The mutation, arbitrarily designed as c.818del4, was previously reported in patients with AD partial IFNγR1 deficiency and exerts a dominant-negative effect (DN) [29]. The second variant was found in *NOD2* gene c.2264C>T (NM_022162.2, rs61747625) at heterozygous state. It leads to amino acid substitution p.A755V in the LRR domain of the protein (Fig. 2C) and was previously reported in a patient with Blau syndrome [2].

Both mutations were found in heterozygous state in the patient's asymptomatic mother at the age of 44 years (Fig. 2a, b). The father and the proband's sister are wild-type for

both mutations (Fig. 2b). DNA of the maternal grandmother was not available.

The *IFNGR1[818del4]* mutation is dominant-negative and underlies MSMD

In accordance with other AD partial IFNγR1-deficient patients, the proband showed significantly increased expression of IFNγR1 on monocytes and dendritic cells compared with 7 healthy controls (Fig. 3a). To analyze the AD IFNγR1[818del4] downstream signaling, we quantified the STAT1 phosphorylation (pSTAT1) after IFNγ stimulation. IFNα was used as a control STAT1-activating agent. Using phosphoflow, proband's monocytes displayed an impaired responsiveness to IFNγ stimulation compared with healthy donors; conversely, the level of STAT1 phosphorylation after IFNα administration was comparable to that in healthy donors (Fig. 3b), which indicated that the defect was not in STAT1 protein but, indeed, in the IFNγ receptor.

Fig. 1 PET MRI and histology images. **a** Whole-body PET MRI scan of the $NOD2^{p.A755V}$ and $IFNGR1^{818del4}$ proband at the age 17 years showing increased metabolic activity in cervical lymph nodes, hipbone, multiple vertebrae and ribs, and splenic and hepatic lesions. **b** Microscopic image depicting granulomas with non-caseating necrosis in a biopsy sample from hipbone of the proband. **c** The deep ulceration on the foot after 2 weeks of unplanned withdrawal of methotrexate
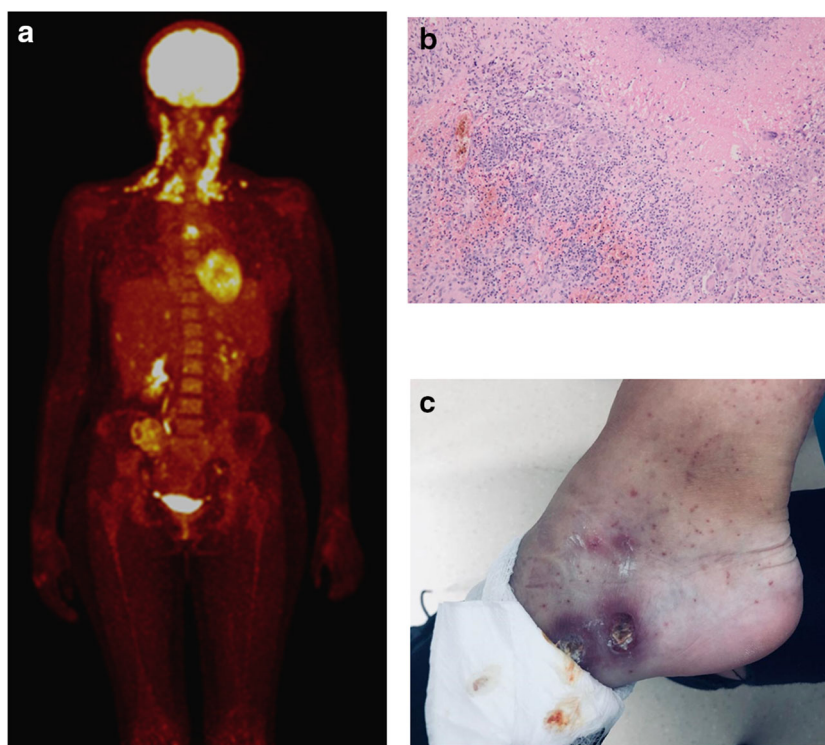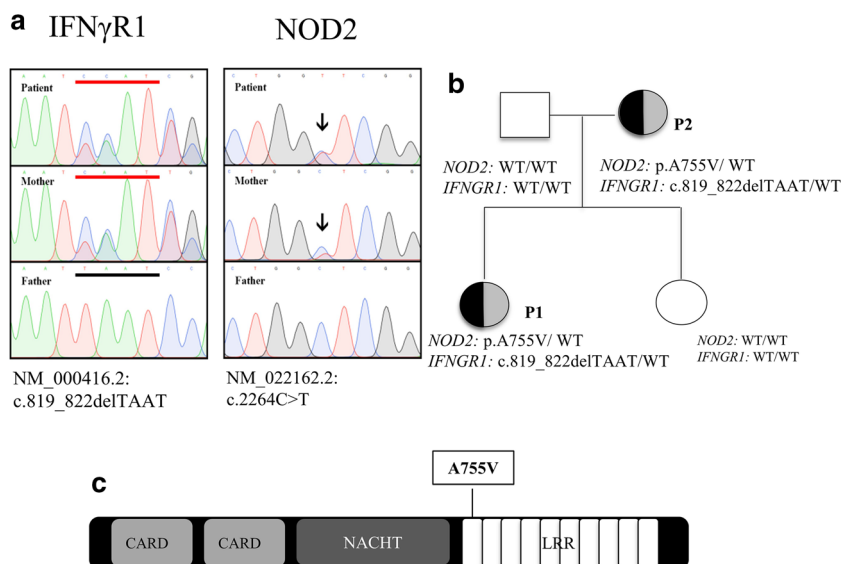
Furthermore, to evaluate the severity of IFNγ signaling defect, we analyzed the expression of IFNγ-inducible genes, *CXCL10* and *IRF1* using RT-PCR. We noticed reduced, but not completely lost, expression of the genes (Fig. 3c) in the proband's PBMCs. In line with previous results, the defective IFNγR1^{818del4} signaling also manifested as decreased IL-12p70 production after simultaneous LPS and IFNγ stimulation (Fig. 3d). Proband's PBMCs were able to produce normal levels of cytokines in response to LPS; however, when simultaneously stimulated with LPS and IFNγ, the cytokine production increased to a much lesser degree than in healthy controls. This was particularly prominent in IL-12p70 production. Next, we analyzed the ability of the CD4$^+$ and CD8$^+$ T cells to produce IFNγ after nonspecific stimulation with PMA (Fig. 3e) and noticed that the proband's lymphocytes produced unexpectedly high amounts of IFNγ compared with seven age-matched healthy controls.

We were also able to perform a series of experiments on the proband's mother (P2) who is healthy, yet carries both mutations. We observed similar results, i.e., increased IFNγR1

Fig. 2 Genetic analysis of the kindred. **a** DNA sequencing chromatograms of the relevant *NOD2* and *IFNGR1* gene regions of the proband (P1), her mother (P2), and father. **b** Pedigree of the kindred showing the familial segregation of the $NOD2^{p.A755V}$ and $IFNGR1^{818del4}$ mutations. **c** NOD2 protein structure highlighting the position of alanine-for-valine substitution in the proband
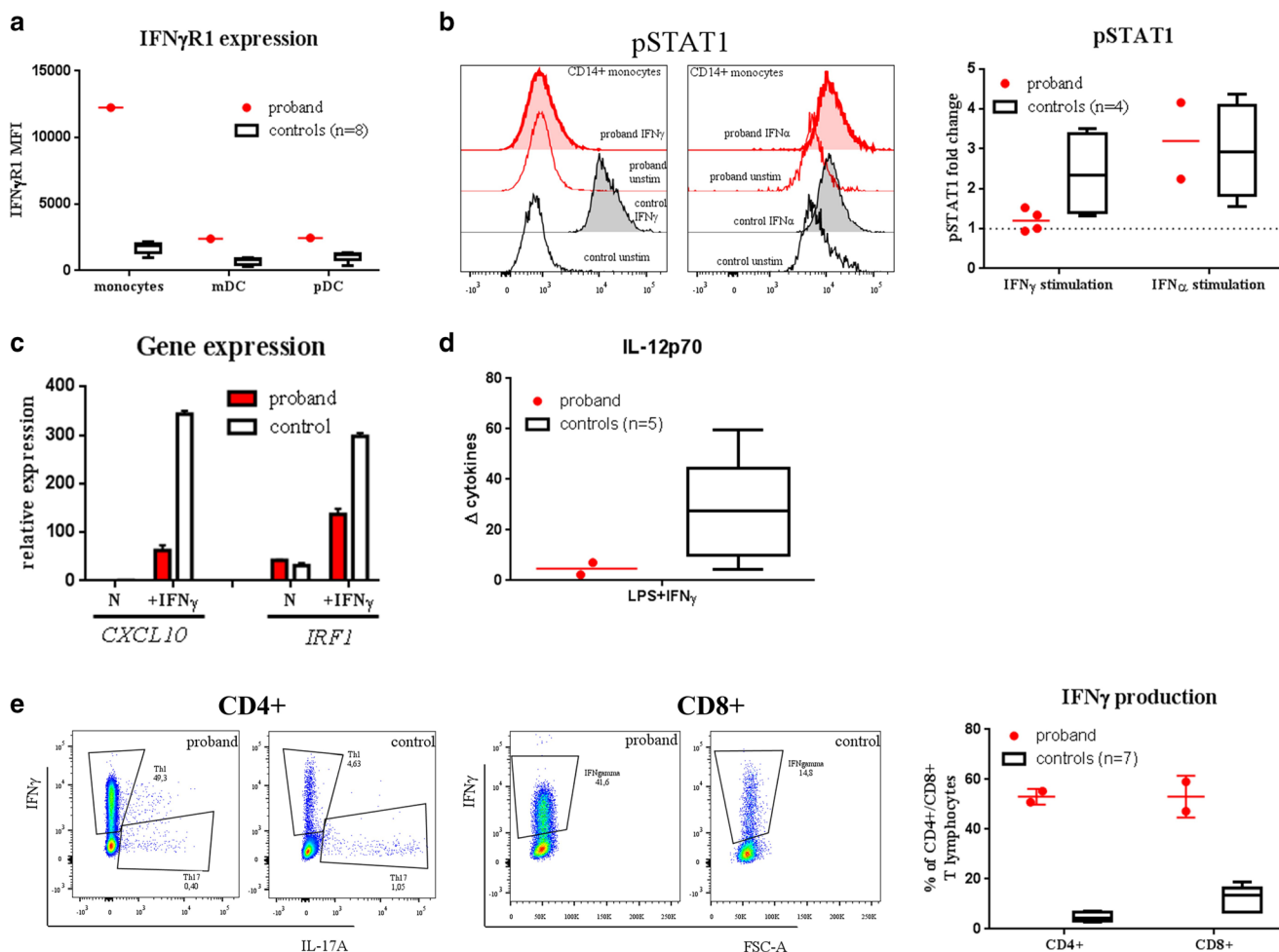
Table 2 Characteristic symptoms of Blau syndrome and partial IFNγR1 deficiency. Specific symptoms in Blau syndrome associated with $NOD2^{c.2264C>T}$ mutation, patient with partial IFNγR1818del14 deficiency, patient with Blau syndrome caused by NOD2p.I37T mutation and AR IFNγR1P268S deficiency and the proband

Characteristics		Blau syndrome	Blau syndrome $NOD2^{c.2264C>T}$	Partial AD IFNGR1 deficiency	Partial $IFNGR1^{818del14}$ deficiency	Blau syndrome $NOD2^{c.2264\,C>T}$ + $IFNGR1^{818del14}$	Blau syndrome $NOD^{c.\,802^{\,C\,>\,T}}$ + $IFNGR1^{c.110T>C}$
						P1	P*
Sex		F > M	Not reported	F = M	Female	Female	Male
Age of onset		< 4 years	Not reported	Mean 13 years	2 months	2 months	11 months
Clinical features	Uveitis	++	Not reported	Not reported	–	+	–
	Arthritis / arthralgia	++	–	–	+	+	+
	Skin rash / dermatitis	++	+	–	–	+	+
	Recurrent fever	++	+	–	–	+	+
	Periodic occurrence	++	+	–	–	+	+
	Infectious susceptibility	–	–	BCG, NTM, Salmonella, Coccidioides, Histoplasma capsule, VZV	BCG, M. avium, M. abscessus—immunogenum	BCG	BCG
	BCGitis/BCGosis	+	–	++	+	+	+
	Multiple osteomyelitis	–	–	++	+	Iliac crest, costae, vertebrae	Iliac crest, costae, humerus
	Lymphadenopathy	+	–	++	+	+	+
	Erythema nodosum	+	+	–	–	+	–
	Hypertension	+	+	–	–	–	–
	Lung involvement	+	Interstitial lung disease	+	–	–	Interstitial lung disease
	Renal disease	+	Interstitial nephritis	–	–	–	Kidney stones
	Hepatosplenomegaly	+	–	+	–	+	+
	Neurological symptoms	+	–	–	–	+	Hepatic lesions, Facial palsy
	Vasculitis	+	–	–	–	Hepatic and splenic lesions	–
Histologic appearance of lesions		Non-caseating granulomas, some fibrinoid necrosis	Not reported	Caseating/non-caseating/granulomas	Caseating/non-caseating granulomas	Likely, unconfirmed Non-caseating granulomas, some with non-caseating necrosis	Granulomatous inflammation

++ common, + reported, – uncharacteristic

BCG, Bacillus Calmette-Guérin; NTM, non-tuberculous mycobacteria; VZV, varicella zoster virus; AD, autosomal dominant; AR, autosomal recessive

Fig. 3 Functional verification of *IFNGR1^818del4* mutation in the proband (P1). **a** Increased IFNγR1 expression on cell surface of proband's monocytes (Lin-, HLA-DR+, CD14+), myeloid (Lin-, HLA-DR+, CD14-, CD11c+), and plasmacytoid (Lin-, HLA-DR+, CD14-, CD123+) dendritic cells compared with healthy controls (*n* = 8). Data are expressed as MFI (mean fluorescence intensity). **b** Reduced STAT1 phosphorylation (Tyr701) after IFNγ (1 μg/ml) stimulation and preserved STAT1 phosphorylation after IFNα (1 μg/ml) stimulation in proband's monocytes compared with healthy controls (*n* = 4). **c** Diminished *CXCL10* and *IRF1* relative expression normalized to *GAPDH* in proband's PBMCs after IFNγ (1 μg/ml) stimulation compared with healthy controls (*n* = 3). **d** Decreased IL-12p70 production in proband's PBMCs in response to LPS (1 μg/ml) or LPS and IFNγ (1 μg/ml) combined compared with healthy controls (*n* = 5). The results are expressed as IFNγ response index (LPS + IFNγ–stimulated/LPS-stimulated PBMCs). **e** Elevated IFNγ production by proband's CD4+ and CD8+ T after PMA (50 ng/ml) and ionomycin (750 ng/ml) stimulation compared with healthy controls (*n* = 7)

expression, diminished STAT1 phosphorylation, reduced IL-12p70 production after LPS and IFNγ stimulation, and increased IFNγ production by T cells (Fig. 5a–d). The only difference between the mother and the proband was detected in IFNγ-induced expression of *CXCL10*; this was comparable to healthy donors in the mother but decreased significantly in the proband (Fig. 5e).

We also had the opportunity to examine samples from another carrier of the same AD *IFNGR1^818del4* mutation and compared the results with the proband. The patient presented with BCGitis and EM osteomyelitis and her laboratory findings were similar to our proband (Suppl. Fig. 1A-D) except of the IFNγ production by T cells, which was only slightly increased, compared to our proband.

The *NOD2^c.2264C>T* variant is hyperactivating and causes augmented NFκB and MAPK signaling

NOD2 stimulation with muramyl dipeptide (MDP) leads to the activation of the NFκB and MAPK signaling pathways. We analyzed cellular responses to MDP stimulation using different approaches. Firstly, we used image cytometry to determine NFκB nuclear translocation after MDP stimulation. We observed increased level of translocation in proband's (P1) cells compared with controls (Fig. 4a). Interestingly, we also noticed higher level of translocation in proband's unstimulated cells, suggesting a ligand-independent activation.

Secondly, using Western blot analysis, we examined the NFκB activation pathway after MDP stimulation, expressed as IκB (inhibitor of κB) degradation and IKK (IκB kinase)
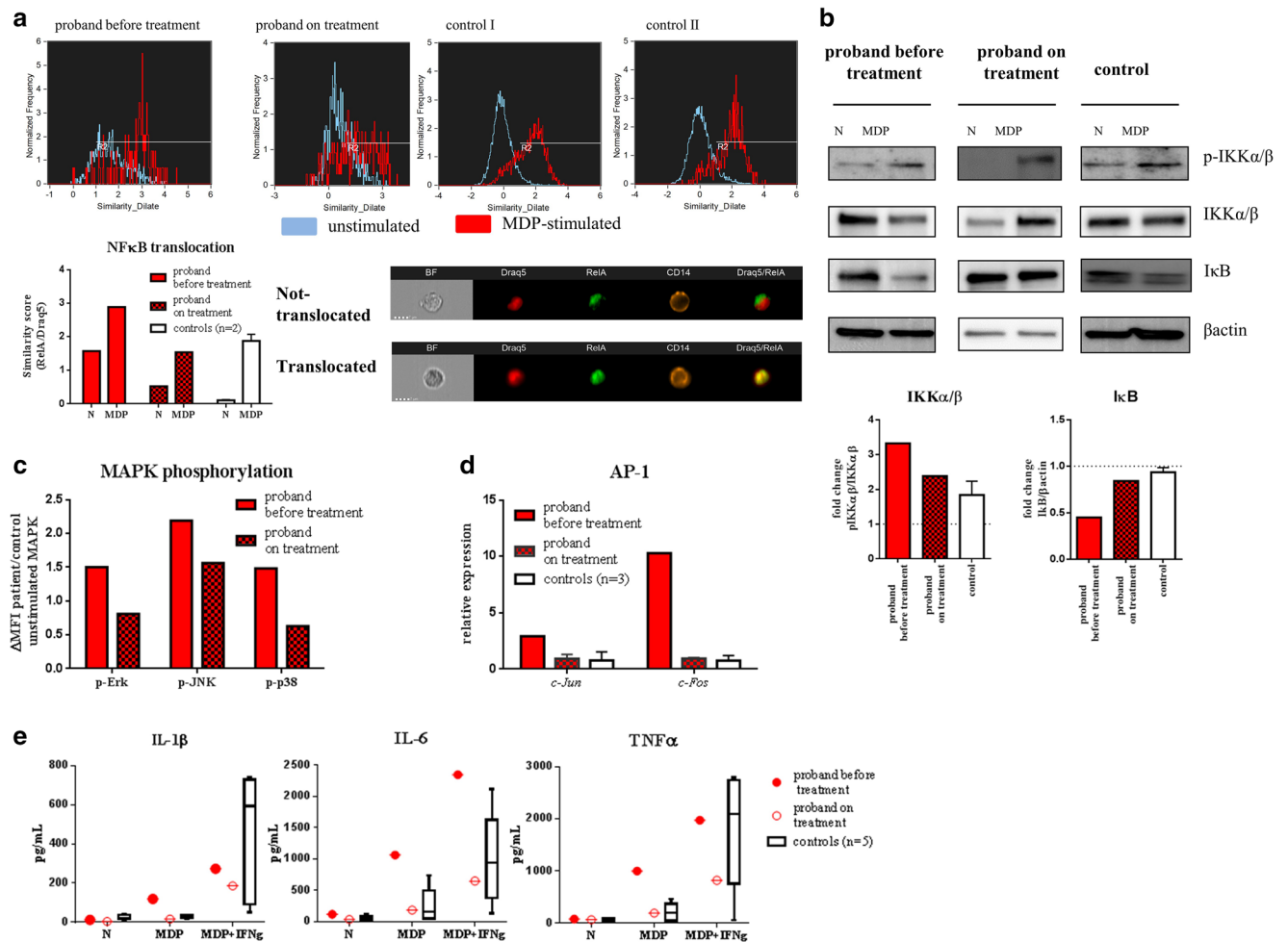
Fig. 4 Functional verification of $NOD2^{p.A755V}$ mutation in the proband (P1) and the effect of methotrexate treatment. **a** Elevated NFκB translocation after MDP (10 μg/ml) stimulation detected by image cytometry in the proband's CD14+ monocytes compared with healthy donors ($n = 2$). Data are expressed as similarity score, i.e., the level of co-expression of NFκB and Draq5-labeled nuclei. **b** Increased NFκB pathway activation after MDP (10 μg/ml) stimulation in proband's PBMCs compared with healthy controls ($n = 2$). The pathway was analyzed through degradation of IκB (inhibitor of κB) and phosphorylation of IKK (IκB kinase α and β) using Western blot. Band area values were used for semi-quantification. Graphs are expressed as a ratio of stimulated/unstimulated cells of band area value calculated from band area of pIKK/IKK or IκB/β-actin ratio, respectively. **c** Elevated ligand-independent Erk, JNK, and p38 MAPK phosphorylation (expressed as MFI-unstimulated proband's MAPK/MFI unstimulated control's MAPK) detected in CD14+ monocytes using phosphoflow cytometry. **d** Increased ligand-independent relative expression of *c-Fos* and *c-Jun* in proband's PBMCs compared with controls ($n = 3$). **e** Cytokine production by proband's and control's ($n = 5$) PBMCs after MDP (10 μg/ml) stimulation or combination of MDP (10 μg/ml) and IFNγ (1 μg/ml) stimulation. All experiments were performed before and after 3 months on treatment with methotrexate

phosphorylation. The activation of IKK leads to phosphorylation of IκB which provides a signal to the inhibitor degradation. Once the inhibitor is degraded, NFκB is activated and translocated to the nucleus. We detect higher intensity of phosphorylated IKK and more intense IκB degradation in proband (Fig. 4b), which was in line with previous observations of higher NFκB activity in the proband's monocytes.

Finally, we focused on phosphorylation of MAP kinases—p38, JNK, and Erk (Fig. 4c). We observed normal levels of phosphorylation of all kinases in response to MDP in proband's monocytes (data not shown), but higher phosphorylation in their unstimulated state, once again suggesting ligand-independent activation. To confirm the observation, we evaluated basal expression of MAPK-inducible genes *c-Fos* and *c-Jun*, which form AP-1 complex and noticed slightly increased ligand-independent expression of these genes compared with controls (Fig. 4d). We observed similar trends in MAPK basal phosphorylation in the proband's mother (Fig. 5F).

Next, we assessed the cytokine production (IL-1β, IL-6, and TNFα) after stimulation of proband PBMCs with MDP, IFNγ, or their combination using Luminex method (Fig. 4e). The proband's cells produced higher levels of cytokines after MDP stimulation compared with healthy controls. IFNγ alone did not induce cytokine release in proband or in healthy donors (data not shown). However, the combination of IFNγ and MDP led to increased cytokine production in both controls
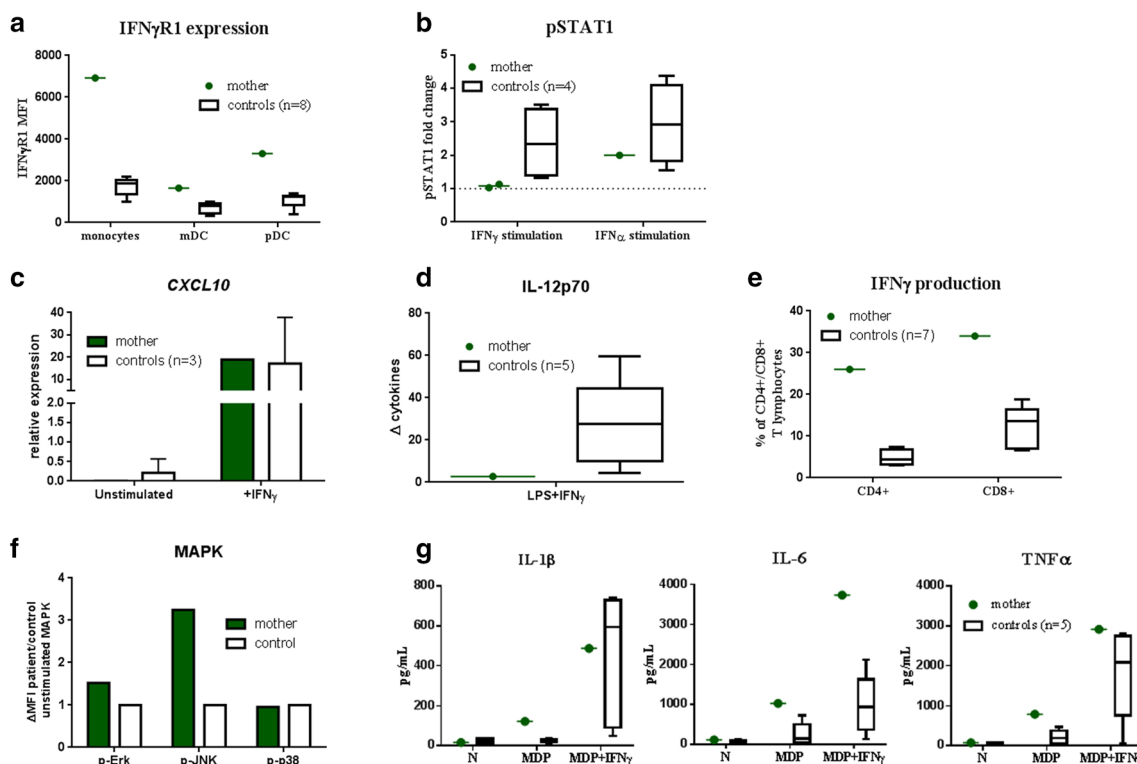
Fig. 5 Functional assays in the proband's mother (P2): **a** Increased IFNγR1 expression on cell surface of P2's monocytes (Lin-, HLA-DR+, CD14+), myeloid (Lin-, HLA-DR+, CD14-, CD11c+), and plasmacytoid (Lin-, HLA-DR+, CD14-, CD123+) dendritic cells compared with healthy controls ($n = 8$). Data are expressed as MFI (mean fluorescence intensity). **b** Reduced STAT1 phosphorylation (Tyr701) after IFNγ (1 μg/ml) stimulation and preserved STAT1 phosphorylation after IFNα (1 μg/ml) stimulation in P2's CD14+ monocytes compared with healthy controls ($n = 4$). **c** Preserved *CXCL10* relative expression normalized to *GAPDH* in P2 PBMCs after IFNγ (1 μg/ml) stimulation compared to healthy controls ($n = 3$). **d** Decreased IL-12p70 production in P2's PBMCs in response to LPS (1 μg/ml) or LPS and IFNγ (1 μg/ml) combined compared with healthy controls ($n = 5$). The results are expressed as IFNγ response index (LPS + IFNγ–stimulated/LPS-stimulated PBMCs). **e** Elevated IFNγ production by P2's CD4+ and CD8+ T lymphocytes after PMA (50 ng/ml) and ionomycin (750 ng/ml) stimulation compared with healthy controls ($n = 7$). **f** Elevated ligand-independent Erk, JNK, and p38 MAPK phosphorylation (expressed as MFI-unstimulated P2's MAPK/MFI-unstimulated control's MAPK) detected in CD14+ monocytes using phosphoflow cytometry

and also in the proband. Given the AD partial IFNγR1 defect, it was surprising to find that the level of proinflammatory cytokines produced by the proband's cells was even slightly higher than in healthy controls. We observed similar results in cells from the proband's mother (Fig. 5g).

Finally, another carrier of the same *IFNGR1*[818del4] mutation was shown to have a normal basal MAPK phosphorylation as well as c-Fos and c-Jun expression (Suppl. Fig. 1E and F), suggesting that the observed increased MAPK signaling in proband and the mother may not be attributed to the *IFNGR1* mutation and is therefore likely due to hyperactivation of NOD2.

A designated set of experiments was repeated 3 and 7 months on MTX treatment in the proband. While no changes in IFNγR1[818del4] signaling (data not shown) were noted a sustained significant decrease of NFκB and MAPK signaling, and the overall cytokine production was detected (Fig. 4a–e) as the proband's symptoms regressed.

Overall, the results suggest that the *NOD2*[c.2264C>T] variant exerts a gain-of-function effect and likely underlies at least some auto-inflammatory features of the proband.

Discussion

In this study, we report a child and her mother harboring two heterozygous mutations in the innate mechanisms of antimicrobial defense, the *IFNGR1*[818del4] and *NOD2*[c.2264C>T], presenting as combined phenotype of altered BS and milder MSMD in the 17-year-old proband, while the proband's mother is asymptomatic.

The *IFNGR1*[818del4] is the most frequent mutation in the "818del4" hotspot, reported in over 80% of patients with AD IFNγR1 deficiency. Both the proband and her mother displayed the corresponding cellular phenotype. The proband's BCGitis represents a classic feature of AD IFNγR1 deficiency, but no infectious pathogens were ever detected in any of her later sites of inflammation. Particularly, thorough investigation was performed to elucidate the etiology of the osteomyelitis, a common feature of AD IFNγR1. Despite the fact that some of the granulomas showed prominent necrotic features, which is characteristic for AD IFNγR1 deficiency and less typical for BS [35], no mycobacteria were detected.

However, it should be stressed out that these pathogens are notoriously difficult to detect in bones. On the other hand, the effect of MTX advocates strongly for non-infectious etiology.

Curiously, the proband's mother received BCG vaccine without any complications (her skin tuberculin test was indicative of having received the BCG vaccine) and remained altogether healthy. This may be due to a phenomenon of incomplete penetrance, which has been reported to some degree in many immune deficiencies [36–40], including AD IFNγR1 [31, 41]. The penetrance of vaccine-associated BCG disease in AD IFNγR1 deficiency appears to be high (uncalculated), but several mutation carriers have been reported to suffer no adverse reactions to BCG. The penetrance of environmental mycobacterial disease was calculated in 2004 to be 21% by 5 years of age and 45% by 10 years of age [30]. The underlying mechanisms of incomplete penetrance are unknown.

The $NOD2^{c.2264C>T}$ allele frequency in general population is 0.2%, according to ExAC database and as such, it is classed as "variant of unknown significance." One other BS patient was previously reported to harbor this mutation, presenting with non-classic phenotype (Table 2). Our experiments demonstrate a hyperactivation of downstream NOD2 signaling via augmented NFκB and MAPK, which corresponds with the findings of some previously published data on the cellular disturbances in BS [3, 17] but is in conflict with others [13]. This hyperactivation may not be attributed to the AD IFNGR1 deficiency. Whereas most of the BS-associated mutations are found in NACHT domain, the $NOD2^{c.2264C>T}$ mutation is located in LRR domain. Taken together, it is therefore possible that this is an atypical BS mutation that does not reflect mechanisms operative in the majority of patients.

In the proband, the hallmark features of BS, e.g., dermatitis and arthritis, were fully expressed. Uveitis, the remaining symptom of the classic BS triad, occurred during the treatment of BCGitis. The fact that it resolved after addition of steroids suggests a non-infection background and we therefore consider it a probable attribute of BS. An additional feature in the proband was multifocal granulomatous osteomyelitis, which responded well to MTX. Again, the mother also carries the heterozygous $NOD2^{c.2264C>T}$ yet suffers no related symptoms. The penetrance of BS-associated NOD2 mutations is not known but appears to be high. Nevertheless, at least 5 asymptomatic mutation carriers have been reported, two of them healthy and well into their adulthood [42–44].

A puzzling excess of IFNγ production by T cells was detected in our kindred. Such overt IFNγ production has not been described in BS [45], nor is the excess of IFNγ found in the sera of patients with partial IFNγR1 deficiency [30, 46]. To confirm this, we evaluated the IFNγ production in another AD IFNγR1 MSMD patient and another NOD2-associated BS patient and found it to be normal in both cases. The overproduction of IFNγ in our patient therefore appears to be the result of a combined effect of both mutations but the underlying

mechanism is unclear. As the patient improved on treatment, the NFKB, MAPK signaling, and the cytokine production decreased but the IFNγR1 signaling and the IFNγ production by T cells remained unaltered. This finding supports the notion that the major culprit in the patient's BS symptoms is the $NOD2^{c.2264C>T}$ downstream hyperresponsiveness and not merely the increased IFNγ.

Several examples of overlapping aspects of BS and AD IFNγR1 MSMD led us to hypothesize that the co-existence of both mutations would exhibit certain functional alterations and that IFNγ is the common denominator. Both diseases present histologically with the formation of granulomas. In BS patients, IFNγ was shown to be overexpressed in cells within the granulomas [35]. Conversely, the inflammatory lesions of patients with complete IFNγR1 signaling arrest, such as the autosomal recessive IFNGR1 mutation, show poorly established granulomas with very few giant cells [47]. The recently published research implies a novel activation pathway in BS, in which IFNγ primes the NOD2-mutated induced pluripotent stem cell-derived macrophages to a pre-activated state, independently of IFNγR/STAT1-mediated signaling [17]. The excessive IFNγ production by T cells found in our proband may therefore account for her altered BS phenotype, even in the setting of impaired IFNγR signaling.

Moreover, both receptors are involved in antimycobacterial immune response [35, 48, 49]. In fact, the BCG was reported as a suspected culprit in triggering or worsening BS in some patients [50–52]. The post-vaccination increase of IFNγ expression [53] suggests a possible mechanism via which the BCG may accentuate the NOD2-driven inflammatory response. In our proband, the BS-associated uveitis, arising after BCG vaccination, resonates with the notion.

On the other hand, given the well-known therapeutic effect of exogenous IFNγ on mycobacterial infections in AD IFNγR1 deficient patients, we suggest that the exaggerated IFNγ production provides a certain protection against mycobacterial infections for the proband and may perhaps compensate for the mother's AD IFNγR1 deficiency. Illustratively, another AD IFNγR1^{818del4} patient, who we examined, suffered three different EM by the age of 9 years, at least one of them shortly after withdrawal of IFNγ treatment (Table 2). This patient showed identically disturbed IFNγR1 signaling but a near-normal IFNγ production.

Interestingly, in 2016, a Turkish patient was briefly reported to harbor heterozygous missense NOD2 mutation (c.802C>T, p.P268S, classed as variant of unknown significance) and homozygous mutation in IFNGR1 gene (c.110T>C, I37T) presenting as BS and AR partial IFNγR1 deficiency [54]. The clinical similarity to our proband is striking (Table 2), including the presence of multifocal osteomyelitis and the response to MTX. Curiously, this patient also developed acute macrophage-activation syndrome (MAS). MAS is thought to result from uncontrolled macrophage

activation due to hypercytokinemia, particularly under the overproduction of IFNγ by T cells [55]. In our proband, such excessive production of IFNγ was a hallmark of her T cell phenotype, although she did not experience MAS.

The presented patient represents a model of BS with impaired IFNγ signaling via IFNγR1. Given the possible role of IFNγ in the pathogenesis of BS, the clinical presentation described here may be of interest to those exploring targeting of its signaling as a therapeutic strategy for BS. However, our study has several limitations; therefore, the findings must be interpreted with care. Because of the dilemmas emphasized above, such as the location and pathogenicity of $NOD2^{c.2264C>T}$ mutation, the nature of the osteomyelitis, or the genotype-phenotype discordance between two carriers, the exact immunopathogenesis of the patient's symptom complex may only be assumed but remains unverified.

In conclusion, we identified a patient with $IFNGR1^{818del4}$ and $NOD2^{c.2264C>T}$ mutations presenting with a unique phenotype and suggest that the functional cross-talk between IFNγ and NOD2 pathways in BS warrants further exploration in future studies.

Compliance with ethical standards

Conflict of interest The authors declare that they have no conflicts of interest.

Ethics statement This study was carried out in accordance with the recommendation of the Ethical Committee of the 2nd Faculty of Medicine, Charles University, in Prague and University Hospital in Motol, Czech Republic. The protocol was approved by the Ethical Committee and all subjects gave informed consent in accordance with the Declaration of Helsinki.

References

1. Wouters CH, Maes A, Foley KP, Bertin J, Rose CD. Blau syndrome, the prototypic auto-inflammatory granulomatous disease. Pediatr Rheumatol Online J. 2014;12:33. https://doi.org/10.1186/1546-0096-12-33.

2. Rose CD, Pans S, Casteels I, Anton J, Bader-Meunier B, Brissaud P, et al. Blau syndrome: cross-sectional data from a multicentre study of clinical, radiological and functional outcomes. Rheumatology. 2015;54:1008–16. https://doi.org/10.1093/rheumatology/keu437.

3. Kanazawa N, Okafuji I, Kambe N, Nishikomori R, Nakata-Hizume M, Nagai S, et al. Early-onset sarcoidosis and CARD15 mutations with constitutive nuclear factor-kappaB activation: common genetic etiology with Blau syndrome. Blood. 2005;105:1195–7. https://doi.org/10.1182/blood-2004-07-2972.

4. Philpott DJ, Sorbara MT, Robertson SJ, Croitoru K, Girardin SE. NOD proteins: regulators of inflammation in health and disease. Nat Rev Immunol. 2014;14:9–23. https://doi.org/10.1038/nri3565.

5. Negroni A, Pierdomenico M, Cucchiara S, Stronati L. NOD2 and inflammation: current insights. J Inflamm Res. 2018;11:49–60. https://doi.org/10.2147/JIR.S137606.

6. Girardin SE, Boneca IG, Viala J, Chamaillard M, Labigne A, Thomas G, et al. Nod2 is a general sensor of peptidoglycan through muramyl dipeptide (MDP) detection. J Biol Chem. 2003;278: 8869–72. https://doi.org/10.1074/jbc.C200651200.

7. Landes MB, Rajaram MVS, Nguyen H, Schlesinger LS. Role for NOD2 in Mycobacterium tuberculosis -induced iNOS expression and NO production in human macrophages. J Leukoc Biol. 2015;97:1111–9. https://doi.org/10.1189/jlb.3A1114-557R.

8. Brooks MN, Rajaram MVS, Azad AK, Amer AO, Valdivia-Arenas MA, Park J-H, et al. NOD2 controls the nature of the inflammatory response and subsequent fate of Mycobacterium tuberculosis and M. bovis BCG in human macrophages. Cell Microbiol. 2011;13: 402–18. https://doi.org/10.1111/j.1462-5822.2010.01544.x.

9. Kleinnijenhuis J, Quintin J, Preijers F, Joosten LAB, Ifrim DC, Saeed S, et al. Bacille Calmette-Guerin induces NOD2-dependent nonspecific protection from reinfection via epigenetic reprogramming of monocytes. Proc Natl Acad Sci. 2012;109: 17537–42. https://doi.org/10.1073/pnas.1202870109.

10. Miceli-Richard C, Lesage S, Rybojad M, Prieur A-M, Manouvrier-Hanu S, Häfner R, et al. CARD15 mutations in Blau syndrome. Nat Genet. 2001;29:19–20. https://doi.org/10.1038/ng720.

11. Rose CD, Martin TM, Wouters CH. Blau syndrome revisited. Curr Opin Rheumatol. 2011;23:411–8. https://doi.org/10.1097/BOR.0b013e328349c430.

12. Ebrahimiadib N, Samra KA, Domina AM, Stiles ER, Ewer R, Bocian CP, et al. A novel NOD2-associated mutation and variant Blau syndrome: phenotype and molecular analysis. Ocul Immunol Inflamm. 2018;26:57–64. https://doi.org/10.1080/09273948.2016.1185529.

13. Martin TM, Zhang Z, Kurz P, Rosé CD, Chen H, Lu H, et al. The NOD2 defect in Blau syndrome does not result in excess interleukin-1 activity. Arthritis Rheum. 2009;60:611–8. https://doi.org/10.1002/art.24222.

14. Son S, Lee J, Woo C-W, Kim I, Kye Y, Lee K, et al. Altered cytokine profiles of mononuclear cells after stimulation in a patient with Blau syndrome. Rheumatol Int. 2010;30:1121–4. https://doi.org/10.1007/s00296-009-1342-4.

15. Dugan J, Griffiths E, Snow P, Rosenzweig H, Lee E, Brown B, et al. Blau syndrome–associated Nod2 mutation alters expression of full-length NOD2 and limits responses to muramyl dipeptide in knock-in mice. J Immunol. 2015;194: 349–57. https://doi.org/10.4049/jimmunol.1402330.

16. Rosenstiel P, Fantini M, Bräutigam K, Kühbacher T, Waetzig GH, Seegert D, et al. TNF-α and IFN-γ regulate the expression of the NOD2 (CARD15) gene in human intestinal epithelial cells. Gastroenterology. 2003;124:1001–9. https://doi.org/10.1053/gast.2003.50157.

17. Takada S, Kambe N, Kawasaki Y, Niwa A, Honda-Ozaki F, Kobayashi K, et al. Pluripotent stem cell models of Blau syndrome reveal an IFN-γ–dependent inflammatory response in macrophages. J Allergy Clin Immunol. 2018;141:339–349.e11. https://doi.org/10.1016/j.jaci.2017.04.013.

18. Newport MJ, Huxley CM, Huston S, Hawrylowicz CM, Oostra BA, Williamson R, et al. A mutation in the interferon-γ –receptor gene and susceptibility to mycobacterial infection. N Engl J Med. 1996;335: 1941–9. https://doi.org/10.1056/NEJM199612263352602.

19. Casanova JL, Ochs H. Interferon-gamma receptor deficiency: an expanding clinical phenotype? J Pediatr. 1999;135:543–5. https://doi.org/10.1016/S0022-3476(99)70050-8.

20. Jouanguy E, Lamhamedi-Cherradi S, Altare F, Fondanèche MC, Tuerlinckx D, Blanche S, et al. Partial interferon-gamma receptor 1 deficiency in a child with tuberculoid bacillus Calmette-Guérin infection and a sibling with clinical tuberculosis. J Clin Invest. 1997;100:2658–64. https://doi.org/10.1172/JCI119810.

21. Bustamante J, Boisson-Dupuis S, Abel L, Casanova J-L. Mendelian susceptibility to mycobacterial disease: genetic, immunological, and clinical features of inborn errors of IFN-γ immunity. Semin Immunol. 2014;26:454–70. https://doi.org/10.1016/j.smim.2014.09.008.

22. Rosain J, Kong X-F, Martinez-Barricarte R, Oleaga-Quintas C, Ramirez-Alejo N, Markle J, et al. Mendelian susceptibility to mycobacterial disease: 2014-2018 update. Immunol Cell Biol. 2018. https://doi.org/10.1111/imcb.12210.

23. Oleaga-Quintas C, Deswarte C, Moncada-Vélez M, Metin A, Krishna Rao I, Kanık-Yüksek S, et al. A purely quantitative form of partial recessive IFN-γR2 deficiency caused by mutations of the initiation or second codon. Hum Mol Genet. 2018;27:3919–35. https://doi.org/10.1093/hmg/ddy275.

24. Boisson-Dupuis S, Ramirez-Alejo N, Li Z, Patin E, Rao G, Kerner G, et al. Tuberculosis and impaired IL-23–dependent IFN-γ immunity in humans homozygous for a common TYK2 missense variant. Sci Immunol. 2018;3:eaau8714. https://doi.org/10.1126/sciimmunol.aau8714.

25. Martínez-Barricarte R, Markle JG, Ma CS, Deenick EK, Ramírez-Alejo N, Mele F, et al. Human IFN-γ immunity to mycobacteria is governed by both IL-12 and IL-23. Sci Immunol. 2018;3:eaau6759. https://doi.org/10.1126/sciimmunol.aau6759.

26. Kong X-F, Martinez-Barricarte R, Kennedy J, Mele F, Lazarov T, Deenick EK, et al. Disruption of an antimycobacterial circuit between dendritic and helper T cells in human SPPL2a deficiency. Nat Immunol. 2018;19:973–85. https://doi.org/10.1038/s41590-018-0178-z.

27. Filipe-Santos O, Bustamante J, Chapgier A, Vogt G, de Beaucoudrey L, Feinberg J, et al. Inborn errors of IL-12/23- and IFN-γ-mediated immunity: molecular, cellular, and clinical features. Semin Immunol. 2006;18:347–61. https://doi.org/10.1016/j.smim.2006.07.010.

28. Rosenzweig SD, Holland SM. Defects in the interferon-gamma and interleukin-12 pathways. Immunol Rev. 2005;203:38–47. https://doi.org/10.1111/j.0105-2896.2005.00227.x.

29. Casanova J-L, Jouanguy E, Lamhamedi-Cherradi S, Lammas D, Dorman SE, Fondanèche M-C, et al. A human IFNGR1 small deletion hotspot associated with dominant susceptibility to mycobacterial infection. Nat Genet. 1999;21:370–8. https://doi.org/10.1038/7701.

30. Dorman SE, Picard C, Lammas D, Heyne K, van Dissel JT, Baretto R, et al. Clinical features of dominant and recessive interferon γ receptor 1 deficiencies. Lancet. 2004;364:2113–21. https://doi.org/10.1016/S0140-6736(04)17552-1.

31. Li H, Durbin R. Fast and accurate short read alignment with Burrows-Wheeler transform. Bioinformatics. 2009;25:1754–60. https://doi.org/10.1093/bioinformatics/btp324.

32. Li H, Handsaker B, Wysoker A, Fennell T, Ruan J, Homer N, et al. 1000 genome project data processing subgroup. The Sequence Alignment/Map format and SAMtools. Bioinformatics. 2009;25: 2078–9. https://doi.org/10.1093/bioinformatics/btp352.

33. Koboldt DC, Zhang Q, Larson DE, Shen D, McLellan MD, Lin L, et al. VarScan 2: Somatic mutation and copy number alteration discovery in cancer by exome sequencing. Genome Res. 2012;22: 568–76. https://doi.org/10.1101/gr.129684.111.

34. Cingolani P, Patel VM, Coon M, Nguyen T, Land SJ, Ruden DM, et al. Using drosophila melanogaster as a model for genotoxic chemical mutational studies with a new program. SnpSift Front Genet. 2012;3:35. https://doi.org/10.3389/fgene.2012.00035.

35. Janssen CEI, Rose CD, De Hertogh G, Martin TM, Bader Meunier B, Cimaz R, et al. Morphologic and immunohistochemical characterization of granulomas in the nucleotide oligomerization domain 2–related disorders Blau syndrome and Crohn disease. J Allergy Clin Immunol. 2012;129:1076–84. https://doi.org/10.1016/j.jaci.2012.02.004.

36. Mitsuiki N, Schwab C, Grimbacher B. What did we learn from CTLA-4 insufficiency on the human immune system? Immunol Rev. 2019;287:33–49. https://doi.org/10.1111/imr.12721.

37. Schwab C, Gabrysch A, Olbrich P, Patiño V, Warnatz K, Wolff D, et al. Phenotype, penetrance, and treatment of 133 cytotoxic T-lymphocyte antigen 4–insufficient subjects. J Allergy Clin Immunol. 2018;142: 1932–46. https://doi.org/10.1016/j.jaci.2018.02.055.

38. La Cava A. Common variable immunodeficiency: two mutations are better than one. J Clin Invest. 2013;123:4142–3. https://doi.org/10.1172/JCI72476.

39. Zhang S-Y, Jouanguy E, Ugolini S, Smahi A, Elain G, Romero P, et al. TLR3 deficiency in patients with herpes simplex encephalitis. Science (80-). 2007, 317:1522–7. https://doi.org/10.1126/science.1139522.

40. Chapgier A, Boisson-Dupuis S, Jouanguy E, Vogt G, Feinberg J, Prochnicka-Chalufour A, et al. Novel STAT1 Alleles in otherwise healthy patients with mycobacterial disease. PLoS Genet. 2006;2: e131. https://doi.org/10.1371/journal.pgen.0020131.

41. Takeda K, Kawai T, Nakazawa Y, Komuro H, Shoji K, Morita K, et al. Augmentation of antitubercular therapy with IFNγ in a patient with dominant partial IFNγ receptor 1 deficiency. Clin Immunol. 2014;151:25–8. https://doi.org/10.1016/j.clim.2014.01.004.

42. Saulsbury FT, Wouters CH, Martin TM, Austin CR, Doyle TM, Goodwin KA, et al. Incomplete penetrance of the NOD2 E383K substitution among members of a pediatric granulomatous arthritis pedigree. Arthritis Rheum. 2009;60:1804–6. https://doi.org/10.1002/art.24532.

43. Rosé CD, Aróstegui JI, Martin TM, Espada G, Scalzi L, Yagüe J, et al. NOD2-associated pediatric granulomatous arthritis, an expanding phenotype: study of an international registry and a national cohort in Spain. Arthritis Rheum. 2009;60:1797–803. https://doi.org/10.1002/art.24533.

44. Harada J, Nakajima T, Kanazawa N. A case of Blau syndrome with NOD2 E383K mutation. Pediatr Dermatol. 2016;33:e385–7. https://doi.org/10.1111/pde.12908.

45. Galozzi P, Negm O, Greco E, Alkhattabi N, Gava A, Sfriso P, et al. Ex vivo and in vitro production of pro-inflammatory cytokines in Blau syndrome. Reumatismo. 2015;66:277–84. https://doi.org/10.4081/reumatismo.2014.772.

46. Fieschi C, Dupuis S, Picard C, Smith CI, Holland SM, Casanova JL. High levels of interferon gamma in the plasma of children with complete interferon gamma receptor deficiency. Pediatrics. 2001;107:E48. https://doi.org/10.1542/PEDS.107.4.E48.

47. J-Fran EMILE, PATEY N, Fr ALTARE, LAMHAMEDI S, JOUANGUY E, Fran BOMAN, et al. MOUSNIER J-Fran, et al. Correlation of granuloma structure with clinical outcome defines two types of idiopathic disseminated BCG infection. J Pathol. 1997;181:25–30. https://doi.org/10.1002/(SICI)1096-9896(199701)181:1<25::AID-PATH747>3.0.CO;2-Z.

48. Xie J, Deng W. NOD2 signaling and role in pathogenic mycobacterium recognition, infection and immunity. Cell Physiol Biochem. 2012;30:953–63. https://doi.org/10.1159/000341472.

49. Ferwerda G, Girardin SE, Kullberg B-J, Le Bourhis L, de Jong DJ, Langenberg DML, et al. NOD2 and toll-like receptors are nonredundant recognition systems of mycobacterium tuberculosis. PLoS Pathog. 2005;1:e34. https://doi.org/10.1371/journal.ppat.0010034.

50. Osborne GEN, Mallon E, Mayou SC. Juvenile sarcoidosis after BCG vaccination. J Am Acad Dermatol. 2003;48:S99–S102. https://doi.org/10.1067/mjd.2003.158.

51. Okafuji I, Nishikomori R, Kanazawa N, Kambe N, Fujisawa A, Yamazaki S, et al. Role of the NOD2 genotype in the clinical phenotype of Blau syndrome and early-onset sarcoidosis. Arthritis Rheum. 2009;60:242–50. https://doi.org/10.1002/art.24134.

52. Sakai H, Ito S, Nishikomori R, Takaoka Y, Kawai T, Saito M, et al. A case of early-onset sarcoidosis with a six-base deletion in the NOD2 gene. Rheumatology. 2010;49:194–6. https://doi.org/10.1093/rheumatology/kep315.

53. Black GF, Weir RE, Floyd S, Bliss L, Warndorff DK, Crampin AC, et al. BCG-induced increase in interferon-gamma response to mycobacterial antigens and efficacy of BCG vaccination in Malawi and the UK: two randomised controlled studies. Lancet. 2002;359:1393–401. https://doi.org/10.1016/S0140-6736(02)08353-8.

54. Çakan M, Keskindemirci G, Aydoğmuş Ç, Akı H, Hatipoğlu N, Kıyak A, et al. Coexistence of early onset sarcoidosis and partial interferon-γ receptor 1 deficiency. Turk J Pediatr. 2016;58:545–9. https://doi.org/10.24953/turkjped.2016.05.015.

55. Henter JI, Elinder G, Söder O, Hansson M, Andersson B, Andersson U. Hypercytokinemia in familial hemophagocytic lymphohistiocytosis. Blood. 1991;78:2918–22 Available at: http://www.ncbi.nlm.nih.gov/pubmed/1954380 [Accessed February 19, 2019].

Karolina DOLEZALOVA[1]
Tomas STRACHAN[2]
Radoslav MATEJ[3]
Dita RICNA[4]
Marketa BLOOMFIELD[5]

[1] Department of Paediatrics, First Faculty of Medicine, Charles University in Prague, Thomayer University Hospital, Prague, Czech Republic
[2] National Institute of Child Tuberculosis and Respiratory Diseases, Dolny Smokovec, Slovakia
[3] Department of Pathology and Molecular Medicine, Third Faculty of Medicine, Charles University in Prague, Thomayer University Hospital, Prague, Czech Republic
[4] Centre for Cardiovascular Surgery and Transplantation, Brno, Czech Republic
[5] Department of Immunology, Second Faculty of Medicine, Charles University in Prague, Motol University Hospital, Prague, Czech Republic

Reprints: Bloomfield Marketa
<marketa.bloomfield@fnmotol.cz>

Manifestations of cutaneous mycobacterial infections in patients with inborn errors of IL-12/IL-23-IFNγ immunity

Background: Inborn errors of IL-12/IL-23-IFNγ immunity underlie Mendelian susceptibility to mycobacterial diseases (MSMD), a group of immunodeficiencies characterized by a highly selective susceptibility to weakly virulent strains of mycobacteria, such as non-tuberculous mycobacteria (NTM) and *bacillus Calmette-Guérin* (BCG). Cutaneous mycobacterial infections are common in MSMD and may represent a red flag for this immunodeficiency. *Objectives:* We present a case series of four paediatric patients with MSMD, specifically with IFNγR1 and STAT1 deficiencies, and cutaneous NTM/BCG infections to increase awareness of this immunodeficiency, which may, in some cases, be intercepted by the dermatologist and thus timely referred to the immunologist. *Materials & Methods*: Clinical, laboratory and genetic investigations of the four paediatric patients with MSMD are presented. *Results:* All four presented patients experienced early complications after BCG vaccination. Two patients suffered recurrent mycobacteriosis, one patient experienced delayed BCG reactivation, and one patient died of disseminated avian mycobacteriosis. The dermatological manifestation in these patients included destructive nasal ulcerations, scrofuloderma of various sites and lupus vulgaris. All patients had a normal basic immune phenotype. *Conclusion:* The presented cases demonstrate that NTM/BCG infections in otherwise seemingly immunocompetent patients should raise suspicion of MSMD. This is of utmost importance as specific therapeutic approaches, such as IFNγ treatment or haematopoietic stem cell transplantation, may be employed to improve the disease outcome.

Keywords: MSMD, mendelian susceptibility to mycobacterial diseases, IFNγR1, STAT1, inborn error of immunity, non-tuberculous mycobacteria, BCG, necrotizing granulomas, antituberculotics

Mendelian susceptibility to mycobacterial disease (MSMD) is an inborn error of immunity due to various monogenic defects in interleukin- (IL) 12/IL-23 - interferon gamma (IFNγ)-mediated communication pathway between mononuclear phagocytes and type 1 helper T cells. To date, several hundreds of patients have been described worldwide to carry one of the 17 known mutations in genes involved in IFNγ production (*e.g. IL12RB1, IL12RB2, IL23R, ISG15, RORC*), responsive to IFNγ (*e.g. IFNGR1, IFNGR2, STAT1, JAK1, CYBB*), or both (*IRF8, NEMO*) [1, 2]. Patients typically suffer from selectively increased susceptibility to mycobacteria, particularly to weakly virulent non-tuberculous mycobacteria (NTM) and attenuated vaccination strains of bacillus *Calmette-Guérin* (BCG), and some also display increased susceptibility to non-typhoid salmonellae or viruses, particularly *Herpesviridae* family. Other antimicrobial defences, however, remain undisturbed and basic parameters of humoral and cellular immune functions

are usually normal. MSMD typically manifests in childhood, particularly in infants who receive the BCG vaccine, but may present later in adolescence/adulthood. The clinical phenotypes range from mild adverse reactions to the BCG vaccine (*i.e.*, vaccination site-limited BCGitis with regional lymphadenopathy), to recurrent NTM lymphadenitis, osteomyelitis, parenchymatous organs and skin infections, such as in patients with partial signal transducer and activator of transcription (STAT1) or partial IFNγ receptor 1 (IFNγR1) deficiency, to treatment-resistant, life-threatening disseminated mycobacteriosis, such as in complete IFNγR1 deficiency or complete IL-12 receptor beta 1 (IL12Rβ1) deficiency [2, 3]. The diagnosis of MSMD is established by genetic testing and genetic counselling is available to the affected families.
NTM are ubiquitous, opportunistic organisms found globally in soil, water reservoirs and vegetation. In general, the weakly virulent NTM may cause localized or disseminated infections, including skin and soft tissue

infections, taking an acute or chronic course. The most frequent NTM are rapidly growing mycobacteria, such as *Mycobacterium fortuitum, Mycobacterium marinum, Mycobacterium abscessus, Mycobacterium chelonae* and *Mycobacterium ulcerans*, and slowly growing NMT, such as *Mycobacterium avium complex*, comprising *Mycobacterium avium* and *Mycobacterium intracellulare*. The typical underlying predispositions in immunocompetent patients are traumatic or surgical wounds which become soiled with contaminated materials [4]. The cutaneous manifestations of NTM and BCG are heterogeneous, including papular lesions, subcutaneous nodules, cellulitis, abscesses, draining sinuses, ulcerations, scrofuloderma or lupus vulgaris [5, 6]. For an early diagnosis of NTM infection, it is necessary to maintain a high degree of suspicion in patients with chronic cutaneous diseases with a history of trauma, risk exposure, and negative results from conventional microbiological studies, as well as those with a history of adverse events after BCG vaccination. Laboratory findings are usually non-specific with just mildly elevated erythrocyte sedimentation rate (ESR), C-reactive protein (CRP) and often normal full blood count; more profound disturbances accompany more severe or disseminated infections. Approaches based on recall immune response, such as IFNγ release assays (IGRA) and intradermal skin testing are also employed for their differential diagnostic value. Specific histochemical acid-fast staining (AFS) methods (Ziehl-Neelsen, auramine-rhodamine fluorescent stain), immunohistochemistry and real-time polymerase chain reaction (PCR) are used for early detection and differentiation of mycobacteria from biopsy or smear specimens. Histopathology is characterized by the presence of necrotising epithelioid granuloma formed by activated macrophages, multinucleated giant cells (predominantly of Langhans type), and CD4+ T cells under the influence of various cytokines, mainly IL-12 and IFNγ [7]. Nevertheless, the mainstay of NTM diagnosis is based on culture studies. Cultivation of mycobacteria requires long-term incubation in special rich media (*e.g.*, Löwenstein-Jensen, Middlebrook 7h10, Ogawa MB/BACT), often as long as six to nine weeks, and inactivation of rapidly growing microorganisms, whose growth impedes the observation of mycobacterial colonies [8, 9]. Treatment of NTM/BCG includes a combination of various antimicrobial agents, second-line antituberculotics are often used due to the natural antibiotic resistance of NTM [10].

In the presented case series, four patients with MSMD and cutaneous mycobacterial infections are portrayed, highlighting the tell-tale signs of the disease. Two patients harboured distinct mutations in genes encoding IFNγ receptor and two in genes encoding STAT1 protein. STAT1 is a cytoplasmic transcription factor that becomes activated in response to interferons, including IFNγ, inducing the expression of multiple genes involved in antimycobacterial immunity [2, 3]. The complex data of the cohort are summarized in *table 1*.

Materials and methods

The data were collected from retrospective analysis of patients' documentation and from interviews with patients/guardians and attending physicians.

Case series

Patient 1: Destructive nasal lesion due to Mycobacterium marinum in partial STAT1 deficiency

The first patient was a 16-year-old Caucasian girl with a history of poor vaccination site healing and axillary lymphadenitis after a BCG vaccine. Since childhood, she has been suffering from cutaneous herpetic reactivations, typically affecting the periocular area, but otherwise she was healthy and thriving. At 14 years of age, a serosanguinous nasal discharge and mucosal crusts obturating the nasal cavity started appearing. Based on a suspected bacterial infection, despite repeatedly negative cultures, topical antibiotics were applied, which were all ineffective. Three months after initial symptoms, an intercurrent herpes simplex infection exacerbated the local disease, with crusts and ulcers expanding further outwards on the tip of the nose (*figure 1A*) and worsening over time (*figure 1B*). Treatment with orally administered acyclovir and antibiotics was ineffective. A comprehensive laboratory workup, including haematological and immunological investigations and oncologic screening, were normal. The intralesional skin biopsy showed a pattern of specific inflammation, *i.e.*, centrally necrotizing granulomas with multinucleated giant cells (*figure 2B*). Suspecting an NTM infection, Ogawa medium was used to culture the samples, yielding *M. marinum* (*figure 2A, C*). The patient disclosed being a keen aquarist, keeping fish in a home aquarium. The combined antituberculous regimen resulted in complete healing after three months (*figure 1C*). Genetic testing revealed a novel, heterozygous mutation in *STAT1* (c.2071A > G; p.Met691Val). Functional assays revealed decreased, but not abolished IFNγ-induced STAT1 phosphorylation, confirming the partial loss-of-function effect of the mutation (data available from authors upon request). The father, who carries the same mutation, suffers only from frequent, yet mild viral respiratory tract infections.

Patient 2: Lupus vulgaris at the site of BCG vaccination due to partial STAT1 deficiency

The second patient was a 12-year-old Caucasian boy, who experienced complications at the site of BCG inoculation at three months of age, requiring a surgical drainage of the colliquated axillary lymph node (samples were AFS-positive and PCR-negative for NTM). Two nodular lesions developed on the shoulder and regressed after six months of treatment with isoniazid alone. Afterwards, the patient was lost to follow-up, supposedly healthy until six years of age when he acquired *varicella zoster virus* (VZV). The otherwise uncomplicated VZV infection (in the VZV unvaccinated child) coincided with a culture positive reactivation for *M. bovis BCG* at the vaccination site, which presented initially as several papulonodular eruptions that merged into a large lupus vulgaris-like elevated erythemato-squamous annular plaque with a well demarcated serpiginous border (*figure 3A*). The lesion biopsy specimen was AFS-negative and PCR-negative for NTM, however, granuloma formation with multinucleated giant cells was found (*figure 3C*). A combined antituber-

Table 1. The characteristics of MSMD patients.

Pt number	Mutation	Disease	Affected family members	Consanquinity	Age at first manifestation	Age at diagnosis of MSMD/year	Clinical manifestation of NTM	Aetiology	Other infections	Histology	Cellular immunity	Humoral immunity	Therapy	Outcome
1	Heterozygous STAT1 (c.2071A>G; p.M691V)*	Autosomal dominant partial STAT1 deficiency	Father (48 years) carrier of c.2071A>G, increased viral susceptibility, no mycobacterial infections	No	3 months	16 years/2021	BCGitis, destructive lesion of the nose	M. bovis BCG, M. marinum	HSV	Cutaneous biopsy from nose: centrally necrotizing granulomas with multinucleated giant cells	Normal	Normal	Moxifloxacin, rifabutin, clarithromycin	Alive
2	Heterozygous STAT1 (c.1921G>A; p.A641T)	Autosomal dominant partial STAT1 deficiency	Father (48 years) and two patients female siblings (adults) - healthy carriers of c.1921G>A; paternal grandfather with suspected BCGitis	No	3 months	6 years/2016	BCGitis, lupus vulgaris	M. bovis BCG	VZV	Cutaneous biopsy from shoulder: granulomas with multinucleated giant cells and partial central necrosis, scarification, mixed inflammatory cellularization; AFS and NTM PCR-negative	Normal	Normal	Isoniasid, rifampicin, ethambutol, local ointments with streptomycin	Alive
3	Heterozygous IFNGR1 (microdeletion 818del4)	Autosomal dominant partial IFNγR1 deficiency	None	No	3 months	4 years/2013	Disseminted BCGitis, multifocal osteomyelitis with scrofuloderma, recurrent lymphadenitis, multiorgan NTM dissemination	M. bovis BCG, M. avium, M. abscessus	Rotavirus, SARS-CoV-2	Biopsy from the skull: specific granulomatous inflammation; AFS and NTM PCR-positive	Normal	Normal	Isoniazid, rifampicin, cycloserin, clarithromycin, amicacin, azithromycin, interferon gamma	Alive
4	Homozygous IFNGR1 (c.523del; p.Tyr175fs)	Autosomal recessive complete IFNγR1 deficiency	Several unexplained deaths of siblings in infancy	Yes	1 month	3 years/2010	Disseminated BCGitis, multifocal osteomyelitis with scrofuloderma, recurrent lymphadenitis, multiorgan NTM dissemination	M. bovis BCG, M. avium - intracellulare	VZV	Biopsy from spleen: non-specific inflammatory process of red pulp, suppurative and fibroproliferative changes in the splenic hilum, no granuloma formation	Normal	Elevated IgG (IgG1, IgG2), otherwise normal	Isoniasid, rifampicin, ethambutol, pyrazinamid, streptomycin, moxifloxacin, amicacin, cycloserin, clofazimin, linesolid	Died at 13 years

*Mutation previously not reported. Cellular immunity = peripheral blood total neutrophil, eosinophil and lymphocyte count; enumeration of lymphocytes subsets CD3+, CD3+4+, CD3+CD8+, CD19+, CD3-CD16+56+; dihydrorhodamine or nitroblue tetrazolium test for oxidative burst. Humoral immunity = IgG, IgG1-4, IgA, IgM, classic/alternative complement pathway activation. AFS: acid-fast stain; HSV: herpes simplex virus; NTM: non-tuberculous mycobacteria; RT-PCR: real-time polymerase chain reaction; SARS-CoV-2: severe acute respiratory syndrome-related coronavirus 2; VZV: varicella-zoster virus.

Figure 1. A 16-year-old female with *Mycobacterium marinum* infection due to partial STAT1 deficiency. **A**) Periocular herpes simplex infection and the incipient nasal lesion. **B**) Swelling and ulcerations of the tip of the nose with haemorrhagic crust. **C**) Healing after three months of combined antituberculous therapy.

culous regimen and local antituberculous ointment with streptomycin was administered for 14 months; the lesion eventually healed with an atrophic scar (*figure 3B*). Since then, the child has been healthy. Genetic testing confirmed a heterozygous mutation in *STAT1* (c.1921G > A; p.Ala641Thr). The mutation was also found in the patient's father and the patient's two adult sisters, all of whom received a BCG vaccine without any complications and remain healthy. The patient's paternal grandfather, unavailable for testing, reportedly suffered with severe BCGitis in infancy.

Patient 3: Multifocal NTM mycobacteriosis with scrofuloderma due to partial IFNγ receptor 1 deficiency

The third patient was a 12-year-old Caucasian girl presenting in infancy with suppurative inflammation at the BCG inoculation site, followed by axillary lymphadenitis and scrofuloderma as a contiguous extension of the infection from the lymph node into the overlying skin (*figure 4A, B*). Further investigations revealed lesions in the lungs and a markedly positive tuberculin skin test (35 mm/72 hours; normal range for a BCG-vaccinated person: 5-10 mm). The lymph node biopsy showed specific granulomatous inflammation with positivity for AFS and PCR-positive NTM, and cultures were positive for *M. bovis BCG*. The total 21 months of combined antituberculous therapy achieved slow but complete remission. At four years of age, the patient returned with non-tender cervical lymphadenitis, multifocal osteomyelitis of the skull (*figure 4C*) (extending per continuitatem to the cutaneous structures) and femur (*figure 4E*), and lesions in the spleen and lungs, as diagnosed by whole-body PET/CT (*figure 4D*). *M. avium* was cultured from the lesion on the skull, but only poorly formed granulomas with incipient central necrosis were presented in the biopsy specimen, despite the PCR-positive NTM and the presence of AFS bacilli. All immunological, haematological and oncological investigations were normal. The family reported keeping a parrot in the household. Suspecting a disturbed IL-12/IL-23-IFNγ axis, the diagnosis
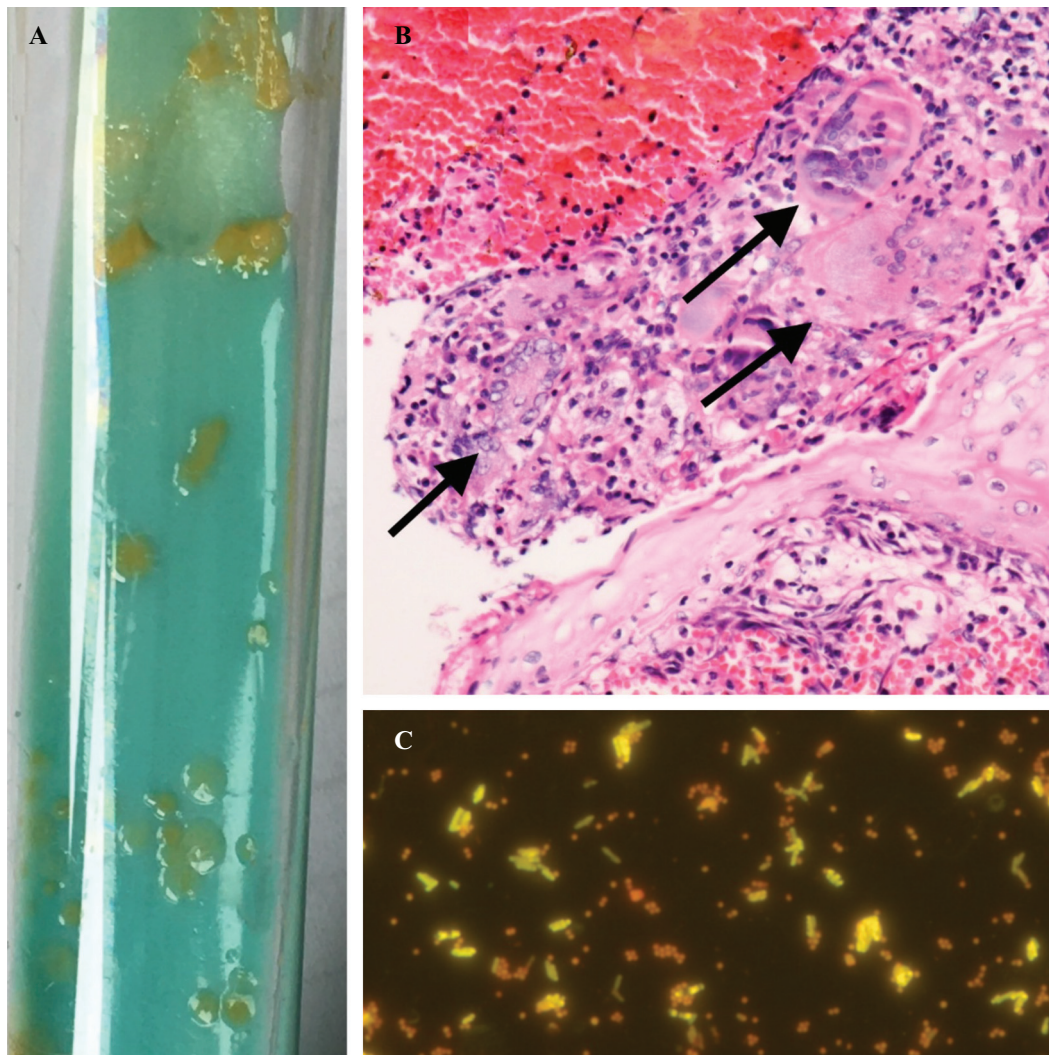
Figure 2. Laboratory evidence of *M. marinum* infection in a patient with partial STAT1 deficiency. **A**) Culture *of M. marinum* on Ogawa medium (image courtesy of Marie Mikulasova MD, Laboratory for Clinical Microbiology and Parasitology, Hospital Ceske Budejovice, Czech Republic). **B**) Granuloma formation with multinucleated giant cells (arrows) from a cutaneous nasal biopsy (H&E staining; 400x magnification) (image courtesy of Marek Grega MD, Department of Pathology and Molecular Medicine, 2nd Faculty of Medicine, University Hospital Motol, Prague, Czech Republic). **C**) Visualization of *M. marinum* by fluorescence microscopy using auramine-rhodamine staining (1000x magnification) showing the presence of contaminating staphylococci (image courtesy of Marie Mikulasova MD, Laboratory for Clinical Microbiology and Parasitology, Hospital Ceske Budejovice, Czech Republic).

of MSMD was established upon the detection of a *de novo* heterozygous microdeletion, 818del4, in *IFNGR1*; a small deletion hotspot region causing a partial defect of the R1 subunit of IFNγ receptor (IFNγR1). Along with multiple antituberculotics, recombinant IFNγ was initiated, allowing slow but complete healing (*figure 4C*). Three years later, at seven years of age, shortly after IFNγ withdrawal, *M. abscessus-immunogenum* cervical lymphadenitis was diagnosed. Another combined regimen with second-line antituberculotics and adjuvant IFNγ was started, again with a slow but favourable outcome after three years of treatment. At 12 years of age, the patient contracted severe acute respiratory syndrome coronavirus 2 (SARS-CoV-2) which manifested with low-grade fever and mild, self-limited respiratory symptoms.

Patient 4: Scrofuloderma in the thorax and fatal disseminated NTM due to complete IFNyR1 deficiency

The fourth patient was a 13-year-old boy from healthy, consanguineous Roma parents. Within the first weeks of life, he developed BCGitis at the vaccination site and axillary lymphadenopathy, which spontaneously drained externally, forming a large scrofuloderma. Despite three months of isoniazid treatment, the lymph node had to be eventually surgically removed. *M. bovis BCG* was cultured from the tissue sample. Two weeks after the discontinuation of antituberculous therapy, fevers and generalized lymphadenopathy appeared and multiple abscesses were detected in the enlarged spleen. The splenic tissue displayed signs of a
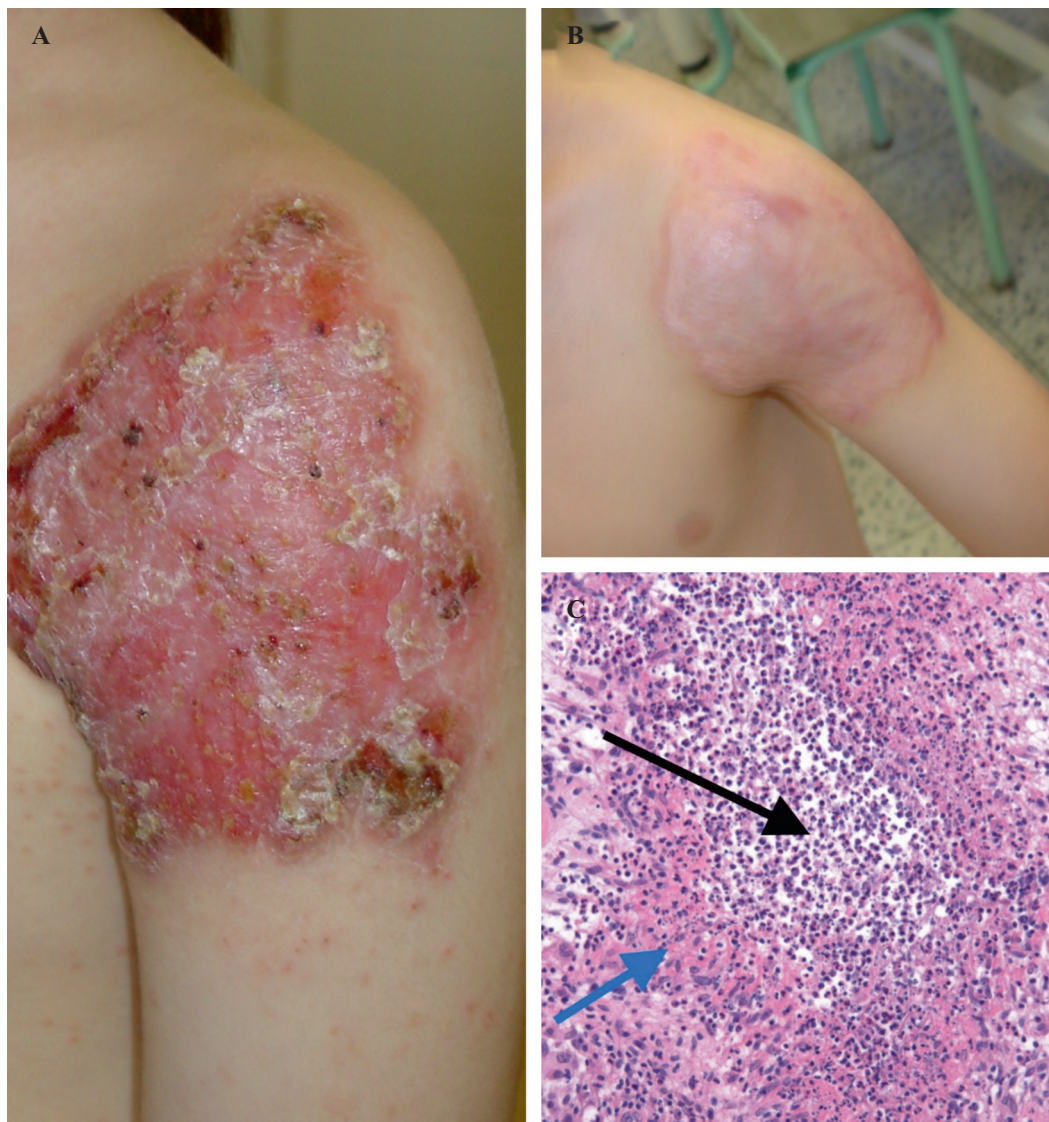
Figure 3. A 12-year-old male with *Mycobacterium bovis BCG* reactivation due to partial STAT1 deficiency. **A)** Lupus vulgaris at the site of BCG vaccination presenting as well-demarcated plastic annular erythemato-squamous plaques with serpiginous edges (aged six years). **B)** Healing with an atrophic scar after 14 months of antituberculous treatment. **C)** Histology of the lesion showing necrotizing granuloma formation; the blue arrow indicates epitheloid macrophages and the black arrow indicates central necrosis (H&E staining; 200x magnification).

non-specific inflammatory process of the red pulp and suppurative and fibroproliferative changes in the splenic hilum, but a surprising absence of granuloma formation. Since the microbiological findings were negative, the tentative diagnosis of disseminated BCG infection was established and a four-drug regimen was continued for 18 months. Again, shortly after therapy cessation, the patient suffered with *M. bovis BCG* osteomyelitis and multifocal suppurative lymphadenopathy. He received continuous antimicrobial treatment, consisting of as many as seven antituberculotics at a time. Despite this, multiple osteolytic lesions of the knee, vertebrae and ribs, and multifocal lymphadenopathy associated with spikes of fever and increased inflammatory markers (particularly ESR, CRP, leukocytosis and thrombocytosis) kept appearing. Subsequently, the infection progressed in a flare-up/regress manner, affecting, per continuitatem, the adjacent pleura and soft tissues of the thorax, eventu-

ally draining through the skin, forming a well-demarcated *M. avium-intracellulare*-positive scrofuloderma (*figure 5 A,B*). At 13 years of age, the VZV unvaccinated patient acquired VZV, complicated with severe immune thrombocytopenia requiring high-dose intravenous immunoglobulin treatment. Six months later, he died due to overwhelming multiorgan dissemination of *M. avium*. Haematopoietic stem cell transplantation was refused by the parents. The consanguinity, absence of susceptibility to other infectious, failure of granuloma formation, as well as negative results of extensive immune phenotyping (excepting the elevated serum IgG) suggested MSMD. At three years of age, a homozygous mutation in the gene encoding IFNγ receptor subunit 1 (c.523del;p.Tyr175fs) was found, establishing the diagnosis of autosomal recessive complete IFNγR1 deficiency. The parents are healthy heterozygous carriers of the mutation. Additionally, several unexplained infant deaths
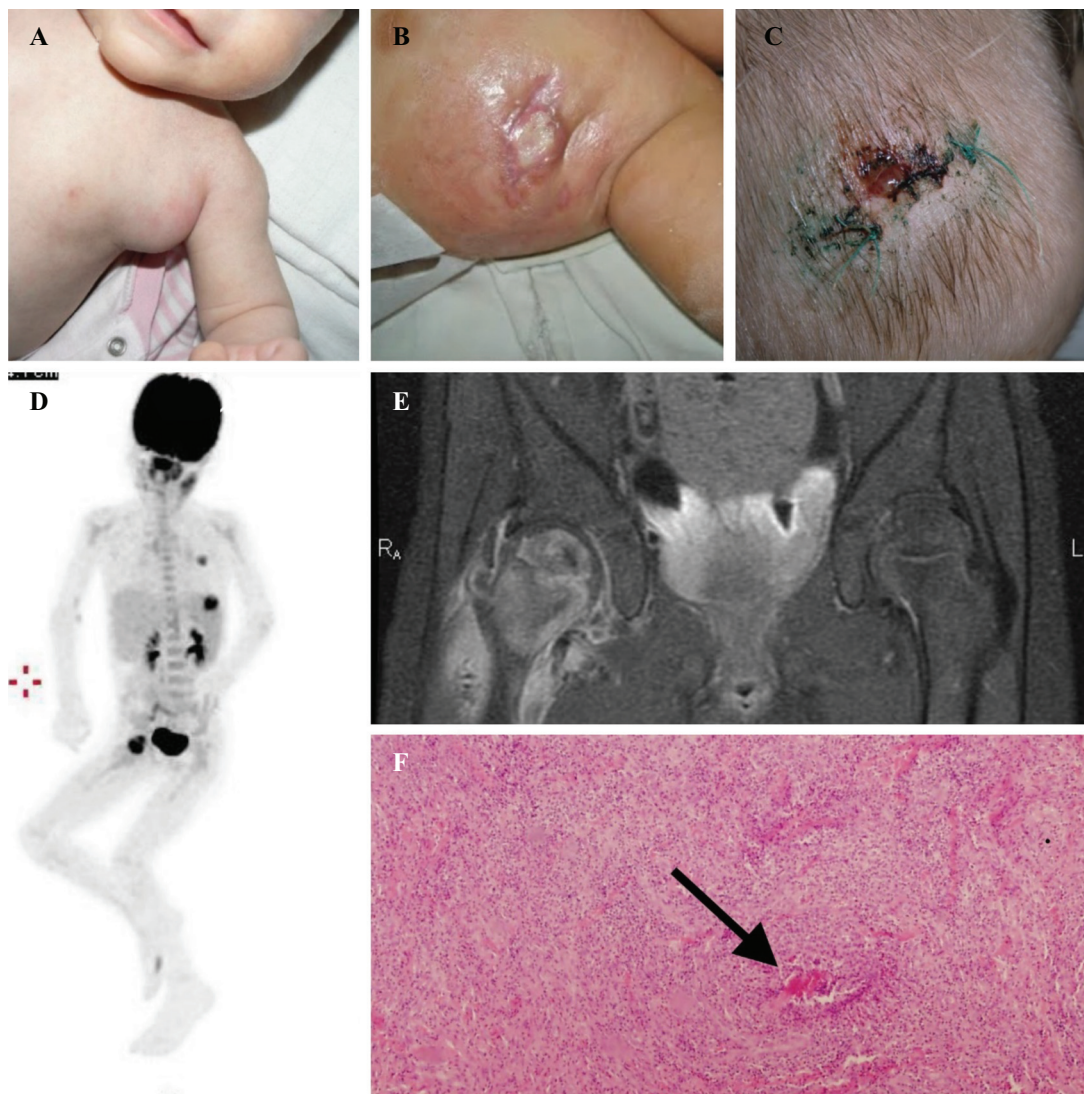
Figure 4. A 12-year-old female with recurrent NTM infections due to partial IFNγR1 deficiency. **A)** Axillary BCG lymphadenitis (aged three months). **B)** Scrofuloderma of the axillary region (aged four months). **C)** Delayed postoperative wound healing of the skull (aged four years). **D)** Whole-body PET/CT with F-18 fludeoxyglucose (FDG) showing anterior projection of increased FDG activity in the cervical lymph nodes, spleen, left lung and right hip (aged four years). **E)** MRI of the pelvis showing osteomyelitis of the right proximal femur, abscess formation in the femoral head, and adjacent soft tissue oedema (aged four years). **F)** Poorly formed granuloma with incipient central necrosis (H&E staining; 200x magnification) (sample was taken from a lesion on the skull; image courtesy of Blanka Rosova MD, Department of Pathology and Molecular Medicine, 3rd Faculty of Medicine, Thomayer University Hospital, Prague, Czech Republic).

within this family were reported, suggestive of disease penetrance in those affected.

Discussion

The presented case series portrays the heterogeneity of cutaneous manifestations of infections with weakly virulent mycobacteria in children with disturbed antimycobacterial defences. These may, in general, arise from both acquired immunodeficiencies (*e.g.*, HIV infection, iatrogenic immunosuppression, treatment with biological agents such as tumour necrosis factor alpha blockers and anti-IL-12/23 monoclonal antibodies, presence of anti-IFNγ autoantibodies) and inborn immunodeficiencies [11, 12]. The latter

include defects in various aspects of cellular immunity, for example, severe combined immunodeficiency (SCID), combined or predominantly T cell, NK cell and phagocytic defects [13]. However, in addition to mycobacteria, these entities convey susceptibility to a wider range of pathogens. Contrastingly, MSMD renders patients selectively susceptible to weakly virulent mycobacteria. All four presented MSMD patients suffered early complications of BCG vaccination and consecutive NTM/BCG infections, yet, with the exception of recurrent or complicated herpetic infections in Patient 1 and 4, no clinical signs of disturbed antimicrobial defences were detectable. All patients had normal results of basic immune investigations, except for Patient 4, who had elevated serum IgG, likely as a result of chronic inflammation. Such clinical settings should alert the physician to
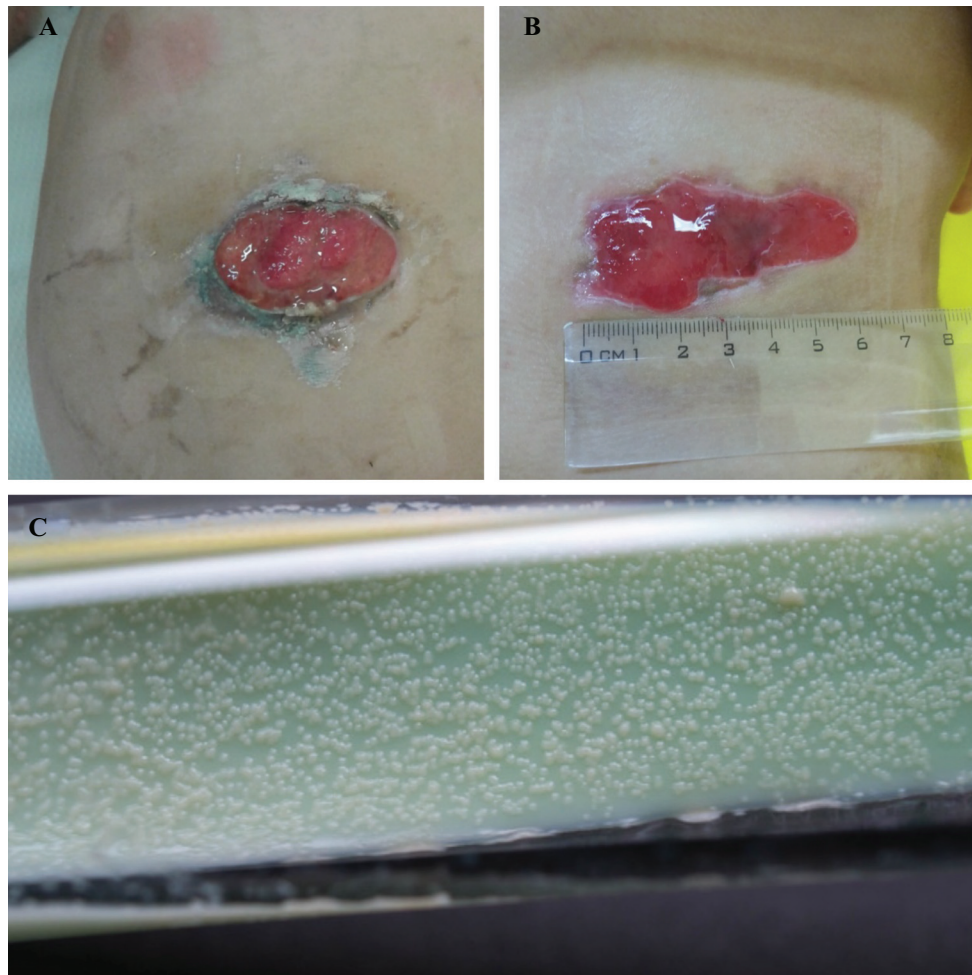
Figure 5. A 13-year-old male with scrofuloderma in the thorax and fatal disseminated NTM due to complete IFNyR1 deficiency **A**, **B**) *M. avium-intracellulare* scrofuloderma due to IFNyR1 deficiency. **C**) Growth of *M. avium* on solid culture.

MSMD. Other warning signs of MSMD may include consanguinity (such as in Patient 4), a history of post-BCG vaccine complications/NTM infections in family members (such as in Patient 2), poorly formed or absence of granulomas in histopathological specimens (such as in Patient 3 and 4), or failure to respond to stimulation in IFNγ-release assays [14]. MSMD may arise from *de novo* mutation or follow autosomal dominant, recessive or X-linked inheritance traits [1, 2]. Given the relatively well-established genotype-phenotype correlation, genetic counselling is an important management tool, yet may be somewhat challenging due to the phenomena of incomplete penetrance and variable expressivity [1, 15] (as seen in the families of Patients 1 and 2). An early diagnosis is of utmost importance, as specific therapeutic approaches may be offered. In patients with MSMD, treatment with antituberculotics is prolonged and may be, in some cases, augmented by subcutaneous administration of human recombinant IFNγ (such as in Patient 3) [2]. In severe patients with a complete lack of signalling, hematopoietic stem cell transplantation was shown to be a curative option, alas with a high mortality and graft rejection rate [16]. Mycobacteria, with over 170 species identified, represent frequently encountered human pathogens [17]. While the classic tuberculosis, caused by *M. tuberculosis*, is still a globally important infection, its incidence in devel-

oped countries is decreasing. Conversely, infections with NTM are on the rise. According to Wenworth *et al.,* the incidence of cutaneous NTM infections increased nearly three-fold during the period 1980-2009 in Minnesota [18]. As such, NTM infection should be considered in the case of any unexplained indolent or suppurative inflammatory process with negative routine bacterial cultures. As NTM often present with cutaneous and soft tissue manifestations, the dermatologist may play a critical role in the diagnosis. The most common clinical manifestation of NTM in childhood is unilateral cervical lymphadenitis caused by *M. avium* [19]. This condition usually affects immunocompetent infants, who have not received the BCG vaccine. In most cases, surgical extirpation of the inflamed lymph node alone is therapeutically sufficient. In contrast, *M. avium* infections in patients with advanced immunosuppression or specific immune defects, such as MSMD, may take on a severe or even life-threatening course, with disseminated disease and systemic symptoms [2, 13]. *M. marinum* infections are typically associated with exposure to water from fish tanks, swimming pools, or brackish water, and may arise even in immunocompetent persons. They typically present as nodular lymphangitis affecting the upper extremities, while nasal localization is scarce. The lesions are non-tender but may erode or ulcerate. They usually respond

well to combined antituberculotic regimens [20]. The extent and atypical localisation of the lesion, as well as the poor healing at the BCG vaccination site, were the key indicators of underlying immunodeficiency in Patient 1. Infections are due to rapidly growing NTM, *i.e.*, *M. fortuitum* affects mostly immunocompetent patients, and are usually associated with plastic surgery and cosmetic procedures. The common presentation is a solitary painful lesion, such as an erythematous nodule, ulcer or abscess, or cellulitis, which appears four to six weeks after inoculation. Similarly, *M. chelonae* and *M. abscessus* present as localized cellulitis or abscesses, typically affecting the extremities at surgical or catheter sites, or as multiple erythematous draining nodules in immunocompromised patients [4, 5].

The diagnosis and targeted treatment of NTM infection relies mostly on culture results. Good communication between the clinician and the microbiologist is therefore essential for the selection of suitable culture media. Moreover, six to nine weeks must be allowed for the incubation time of mycobacterial culture. Histopathological assessment would typically show the formation of specific necrotizing epithelioid granulomas with either caseous or necrobiotic types of necrosis and the presence of tissue-resident macrophages; multinucleated giant cells [21]. Traditional staining for acid-fast bacilli and auramine-rhodamine fluorescent methods may ascertain the presence of mycobacteria, however, they cannot distinguish between individual species. While immunohistochemical staining and real-time PCR-based methods would differentiate between *Mycobacterium tuberculosis* and NTM infections, these methods show limited sensitivity. For specimens obtained by fine needle aspiration biopsy from lymph nodes, the sensitivity is approximately 70% [22], for paraffin-embedded tissue, this is even lower [23]. IFNγ release assays performed on peripheral blood, widely utilized for *M. tuberculosis* infections, have shown good specificity for distinguishing *M. tuberculosis* from NTM with no cross-reactivity with BCG and most NTM. Mycobacterial skin testing for antigens specific to *M. avium*, *M. kansasii* and *M. scrofulaceum*, if available, may also indirectly indicate the presence of NTM infection, with sensitivity and specificity as high as 93%, and 97%, respectively, for *M. avium* cervical lymphadenitis [24].

The treatment of NTM infection consists of a combination of first-line and second-line antituberculous drugs, antibiotics and/or surgical removal of the affected tissue [10]. The selection of antimicrobial drugs should be governed by national guidelines and individual antibiotic sensitivity to the offending pathogen, accounting for the naturally broad multi-drug resistance of NTM.

Conclusion

The diagnosis of weakly virulent mycobacterial infection requires a high level of clinical suspicion and specific microbiological approaches. The cutaneous manifestations of infections with these organisms in otherwise seemingly immunocompetent patients, localisation other than distal extremities, multi-site affections and repeated occurrence should raise a suspicion of Mendelian susceptibility to mycobacterial diseases and the patient should consult an immunologist. The dermatologist may thus facilitate early diagnosis and improved disease outcome, allowing spe-

cific therapeutic approaches to be considered, such as IFNγ treatment or hematopoietic stem cell transplantation. ∎

References

1. Bustamante J. Mendelian susceptibility to mycobacterial disease: recent discoveries. *Hum Genet* 2020; 139: 993-1000.

2. Bustamante J, Boisson-Dupuis S, Abel L, Casanova JL. Mendelian susceptibility to mycobacterial disease: genetic, immunological, and clinical features of inborn errors of IFN-γ immunity. *Semin Immunol* 2014; 26: 454.

3. Taur PD, Gowri V, Pandrowala AA, *et al.* Clinical and molecular findings in mendelian susceptibility to mycobacterial diseases: experience from India. *Front Immunol* 2021; 12: 426.

4. Escalonilla P, Esteban J, Soriano ML, *et al.* Cutaneous manifestations of infection by nontuberculous mycobacteria. *Clin Exp Dermatol* 1998; 23: 214-21.

5. Franco-Paredes C, Marcos LA, Henao-Martínez AF, *et al.* Cutaneous mycobacterial infections. *Clin Microbiol Rev* 2018; 32(1): e00069-18.

6. Alcaide F, Esteban J. Cutaneous and soft skin infections due to non-tuberculous mycobacteria. *Enferm Infecc Microbiol Clin* 2010; 28: 46-50.

7. Kumar SN, Prasad TS, Narayan PA, Muruganandhan J. Granuloma with langhans giant cells: an overview. *J Oral Maxillofac Pathol* 2013; 17(3): 420.

8. Radomski N, Cambau E, Moulin L, Haenn S, Moilleron R, Lucas FS. Comparison of culture methods for isolation of nontuberculous mycobacteria from surface waters. *Appl Environ Microbiol* 2010; 76: 3514.

9. Fonseca L, Moore D, Durier N. *MTB culture and phenotypic drug susceptibility testing-methods inventory inventory of methods for*

mycobacterial culture and Phenotypic Drug Susceptibility Testing (DST) from the culture and phenotypic DST sub-group of the STOP TB Partnership New Diagnostics Working Group Main Tests at a glance solid media liquid media Egg-based Agar-based Automated Manual LJ Ogawa 7H10 7H11 1 BACTE C 460 MBBacT ALERT MGIT ESP II MGIT CRI MODS NRA Culture [Internet]. www.merck.com, 2011. [Accessed on 11/12/2021].

10. Mi Wi Y. Treatment of extrapulmonary nontuberculous mycobacterial diseases. *Infect Chemother* 2019; 51: 245.

11. Henkle E, Winthrop KL. Nontuberculous mycobacteria infections in immunosuppressed hosts. *Clin Chest Med* 2015; 36: 91.

12. Döffinger R, Helbert MR, Barcenas-Morales G, *et al.* Autoantibodies to interferon-gamma in a patient with selective susceptibility to mycobacterial infection and organ-specific autoimmunity. *Clinical Infec Dis* 2004; 38: e10-4.

13. Lee WI, Huang JL, Yeh KW, *et al.* Immune defects in active mycobacterial diseases in patients with primary immunodeficiency diseases (PIDs). *J Formos Med Assoc* 2011; 110: 750-8.

14. Hermansen TS, Thomsen VØ, Lillebaek T, Ravn P. Non-tuberculous mycobacteria and the performance of interferon gamma release assays in Denmark. *PLoS One* 2014; 9: e93986.

15. Casanova JL. Severe infectious diseases of childhood as monogenic inborn errors of immunity. *Proc Natl Acad Sci U S A* 2015; 112: E7128-37.

16. Tovo PA, Garazzino S, Saglio F, *et al.* Successful hematopoietic stem cell transplantation in a patient with complete IFN-γ receptor 2 deficiency: a case report and literature review. *J Clin Immunol* 2020; 40: 1191-5.

17. Falkinham JO. Ecology of nontuberculous mycobacteria. *Microorganisms* 2021; 9: 2262.

18. Wentworth AB, Drage LA, Wengenack NL, Wilson JW, Lohse CM. Increased incidence of cutaneous nontuberculous mycobacterial infection, 1980 to 2009: a population-based study. *Mayo Clin Proc* 2013; 88: 38.

19. Dolezalova K, Maly M, Wallenfels J, Gopfertova D. Nontuberculous mycobacterial infections in children in the Czech Republic in the period 2003-2018. *Biomed Pap Med Fac Univ Palacky Olomouc Czech Repub* 2021; 165: 277-82.

20. Elston D. Nontuberculous mycobacterial skin infections: recognition and management. *Am J Clin Dermatol* 2009; 10: 281-5.

21. Li JJ, Beresford R, Fyfe J, Henderson C. Clinical and histopathological features of cutaneous nontuberculous mycobacterial infection: a review of 13 cases. *J Cutan Pathol* 2017; 44: 433-43.

22. Bruijnesteijn Van Coppenraet ES, Lindeboom JA, Prins JM, Peeters MF, Claas ECJ, Kuijper EJ. Real-time PCR assay using fine-needle aspirates and tissue biopsy specimens for rapid diagnosis of mycobacterial lymphadenitis in children. *J Clin Microbiol* 2004; 42: 2644.

23. Kim YN, Kim KM, Choi HN, *et al.* Clinical usefulness of PCR for differential diagnosis of tuberculosis and nontuberculous mycobacterial infection in paraffin-embedded lung tissues. *J Mol Diagn* 2015; 17: 597-604.

24. Lindeboom JA, Kuijper EJ, Prins JM, Bruijnesteijn Van Coppenraet ES, Lindeboom R. Tuberculin skin testing is useful in the screening for nontuberculous mycobacterial cervicofacial lymphadenitis in children. *Clin Infect Dis* 2006; 43: 1547-51.

Case Report

Mendelian Susceptibility to Mycobacterial Disease: The First Case of a Diagnosed Adult Patient in the Czech Republic

Miroslav Prucha [ID],[1] **Hana Grombirikova** [ID],[2,3] **Pavel Zdrahal** [ID],[4]
Marketa Bloomfield [ID],[5,6] **Zuzana Parackova** [ID],[5] **and Tomas Freiberger** [ID][2,3]

[1]*Department of Clinical Biochemistry, Hematology and Immunology, Na Homolce Hospital, Prague, Czech Republic*
[2]*Centre for Cardiovascular Surgery and Transplantation, Brno, Czech Republic*
[3]*Medical Faculty, Masaryk University, Brno, Czech Republic*
[4]*Department of Vascular Surgery, Na Homolce Hospital, Prague, Czech Republic*
[5]*Department of Immunology, Motol University Hospital and Second Faculty of Medicine, Charles University,*
 Prague, Czech Republic
[6]*Department of Pediatrics, Thomayer's Hospital and First Faculty of Medicine, Charles University, Prague, Czech Republic*

Correspondence should be addressed to Miroslav Prucha; miroslav.prucha@homolka.cz

We present a case of a 42-year-old woman with Mendelian susceptibility to mycobacterial disease. The disease was diagnosed at an adult age with relatively typical clinical manifestations; the skeleton, joints, and soft tissues were affected by nontuberculous mycobacteria: *Mycobacterium lentiflavum*, *M. kansasii*, and *M. avium*. A previously published loss-of-function and functionally validated variant NM_000416.2:c.819_822delTAAT in *IFNGR1* in a heterozygous state was detected using whole-exome sequencing. After interferon-γ therapy was started at a dose of $200\,\mu g/m^2$ three times a week, there was significant clinical improvement, with the need to continue the macrolide-based combination regimen. In the last 4 months, she has been in this therapy without the need for antibiotic treatment.

1. Introduction

Mendelian susceptibility to mycobacterial diseases (MSMD) belongs to the group of primary immunodeficiencies, i.e., a: defects in intrinsic and innate immunity. b: MSMD and viral infection: VI-IUIS update [1]. It is a primary immunodeficiency denoted by molecular defects in the interleukin 12 (IL-12)/interferon γ- (IFN-γ-) dependent signalling pathway. The genetic aetiology of the disease was first demonstrated in 1996 [2], and we currently know of variants in 15 genes that, due to allelic heterogeneity, are the cause of 21 forms of the disease [3, 4]. Patients with this primary immunodeficiency are characterized by a narrow vulnerability to poorly virulent mycobacteria, such as bacillus Calmette–Guérin (BCG)

vaccines and environmental mycobacteria (EM) [5, 6]. IFN-γ is a key player in driving anti-infectious immunity. It is capable of enhancing antigen processing, inducing an antiviral state, and boosting antimicrobial functions. Severe recurrent infections, either disseminated or localized, are typical here [7].

2. Case Report

A 42-year-old female with a suspicion of "immunodeficiency" came to the immunology clinic. The reason at the time was a present active infection by atypical mycobacteria that affected the skeleton with multiple defects of the spine (Th and L vertebrae), skin, and subcutis of the face, lymph nodes, knee joints, calva, paranasal sinuses, and nose.

Immunological investigation revealed normal IgG, IgG subclasses, IgM, and IgA levels. Antibody titres to protein (tetanus, diphtheria) and polysaccharide (pneumococcal) vaccine antigens were normal. The patient had normal lymphocyte subset values, and an oxidation test was normal. A summary of laboratory findings on her first visit to our hospital is presented in Table 1.

The patient's history was long, with the onset of clinical problems in childhood. The chronology of the patient's clinical manifestations is included in Table 2. BCG vaccination in the first month of her life did not cause any immediate complications; however, at 5 years of age, tuberculosis of the lymph node developed, and conventional antituberculous therapy was initiated, i.e., isoniazid and rifampicin were administered. The therapy, which lasted 8 months, was successful and was followed by a long period of remission without any clinical manifestations. The patient was free of clinical complaints until 16 years of age, when an interstitial lung disease was diagnosed. After an erroneous diagnosis of sarcoidosis, the patient was treated with systemic glucocorticoids. During this therapy, dysbacteriosis was clinically manifested. It affected the skin, skeleton, and soft tissues. NTM species were identified using microbiological cultivation methods and subsequently treated according to the proven sensitivity. HIV infection was excluded. From that time, the patient was treated continuously with orally and then parenterally administered antituberculosis drugs (rifampicin, isoniazid, pyrazinamide, streptomycin, and ethambutol) for *Mycobacterium lentiflavum* infection that affected the nasal wings and nasal septum. Th8, Th11, L1, L3, and L5 discitis were etiologically caused by *Mycobacterium kansasii*. The knee joints were affected with *Mycobacterium kansasii* and *Mycobacterium avium intracellulare*.

In view of the clinical picture, we suspected a diagnosis of MSMD. Whole-exome sequencing performed on the NextSeq Illumina platform uncovered a frameshift variant NM_000416.2:c.819_822delTAAT; p.Asn274Hisfs $*$ 2 in the heterozygous state in exon 6 of the *IFNGR1* gene coding IFN-γ receptor 1, which was confirmed using Sanger sequencing. In addition, a heterozygous sequence variant NM_052813.4; c.1434 + 1G > C in the *CARD9* gene was detected. The patient was also submitted to the following laboratory tests: The ability of the proband's CD4 + and CD8 + T cells to produce IFN-γ after nonspecific stimulation with phorbol myristate acetate (PMA) was undisturbed. The proband showed markedly increased expression of IFNγR1 on monocytes, myeloid dendritic cells, and plasmacytoid dendritic cells compared with a healthy control. STAT1 phosphorylation (pSTAT1, Tyr701) assay after IFN-γ stimulation was performed to assess IFNγR1 downstream signalling. The pSTAT1 response was decreased but not absent, compared with a healthy control. Thereafter, the patient was treated with rhIFN-γ and showed significant clinical improvement. rhIFN-γ (Imukin, Boehringer Ingelheim) was started at a dose of 200 μg/m^2 subcutaneously three times per week. The IFN-γ-1b therapy was continued, together with antituberculous treatment. The patient's clinical status stabilized. In the last 4 months, she has been in this therapy without the need for antibiotic treatment.

3. Discussion

MSMD is a rare disease, despite an increase in its incidence [3, 8], that belongs to the category of primary immune deficiencies. The prevalence of this disease is unknown. The affected immunological mechanism involves the Th1 pathway, namely, mononuclear phagocytes and IFN-γ immunity. Localized or systemic infections with nontuberculous mycobacteria are the main clinical manifestations. The defence against mycobacterial infection is mediated by the following mechanism under physiological conditions. Infected mononuclear phagocytes produce IL-12, which stimulates T and natural killer (NK) cells to produce IFN-γ. Upon binding to receptors, IFN-γ stimulates macrophages to produce IL-12, tumour necrosis factor α (TNF-α), and IL-1. Activated macrophages then kill intracellular pathogens, while activated Th1-phenotype T cells proliferate and release IFN-γ. The secreted TNF-α then plays a critical role in the formation of granulomas [9]. In the case of an inherited defect of the IFN-γ receptor, this defensive pathway is disrupted. One of the main groups of etiological agents found with MSMB patients are nontuberculosis bacteria. Currently, more than 170 NTM species are known in clinical practice with different degrees of pathogenicity and importance [10]. A survey of NTM treatment has recently been published [11].

In addition to atypical mycobacteria, the intracellular agent is employed etiologically, where the functionality of the interferon defensive pathway is essential for immunity. These include *Salmonella* spp., *Listeria* spp., leishmaniasis, *Candida*, histoplasmosis, coccidioidomycosis, HHV8, respiratory syncytial virus (RSV), and vesicular stomatitis virus (VSV). For MSMD diagnostics, clinicians can use the combination of different diagnostic approaches, but most have limitations [12]. Genetic analysis is the most powerful approach to a full diagnosis. Our patient carried a heterozygous variant c.819_822delTAAT in the *IFN-γ receptor1* gene, which was evaluated by the ClinVar database as pathogenic.

Jouanguy et al. [13] considered c.819 a small deletion hotspot with two repeats in close proximity, which could cause slipped strand mispairing, further leading to deletion. This variant was repeatedly reported in patients suffering from mycobacterial infection [14–17], and it was confirmed that the variant completely disrupts expression of the receptor [17]. While immunodeficiency caused by *IFNGR1* variants can be inherited in both autosomal recessive (Immunodeficiency 27A, Phenotype MIM number 209950) and autosomal dominant modes (Immunodeficiency 27B, Phenotype MIM number 615978), all pathogenic variants identified so far in exon 6 have led to mycobacterial infection susceptibility with an autosomal dominant mode of inheritance [18]. These nonsense and frameshift variants lead to premature termination of protein synthesis, but they do not affect the IFN-γ binding site and transmembrane domain, so the mutated protein is still capable of binding to the membrane. However, these defects disrupt signalling through STAT1 and internalization of the protein, which results in accumulation of defective IFNGR1 on the cell

Table 1: Summary of laboratory findings.

Summary of laboratory findings	
Test	Patient's result
White cell count x10^9/l (4.0–10.0)	6.2
Neutrophil cells/mm^3	4100
Lymphocyte cells/mm^3	1800
IgA g/l (0.7–4.0)	2.03
IgG g/l (6–16)	13.7
IgM g/l (0.5–2.3)	1.25
IgG1 g/l (4.05–10.1)	7.9
IgG2 g/l (1.65–7.85)	4.12
IgG3 g/l (0.11–0.85)	0.52
IgG4 g/l (0.08–1.4)	1.08
CD3 + cells/mm^3 (700–2100)	1200
CD3 + CD4 + cells/mm^3 (200–900)	850
CD3 + CD8 + cells/mm^3 (200–900)	350
CD19 + cells/mm^3 (100–500)	280
CD16 + 56 + cells/mm^3 (60–600)	320

Table 2: Time sequence of clinical manifestations.

Year of catchment	Localization	Pathogen
1981	Inguinal and cervical lymph nodes	*M. kansasii*
1992	Lungs	Wrongly diagnosed as sarcoidosis
1993	Lymph nodes, Th-7, 8, 9, 11, 12, L1, 2, 5 left femur, maxilla, mandibula	*M. kansasii*
1995	Centre in the distal part of the left femur	*M. avium intracellulare* *M. gordonae*
1997	Granuloma in the right face	*M. lentiflavum*
1998	Left patella Distal part of the femur on the right Granuloma in the right face	*M. lentiflavum* *M. kansasii*
2001	Granuloma of the nasal septum	*M. avium intracellulare*
2002	Left knee	*M. flavescens*
2004	Sputum	*M. lentiflavum*
2007	Granuloma/nasal septum	*M. lentiflavum*
2009	Granuloma/nasal septum	*M. lentiflavum*
2013	Granuloma/nasal septum	*M. avium*
2014	TH 8, 11, L1, L5	*M. avium*
2016	Granuloma of the nasal septum	*M. lentiflavum*
2017	Colliquating granuloma in the nasal septum	*M. avium intracellulare*
2018	Granuloma of the nasal septum Colliquating granuloma in the right face	*M. avium* Start therapy rhIFN-γ
2020	Surgery of the nasal septum Granuloma of the right face healed	Microbiological investigation is negative

membrane [19]. Indeed, we observed an increased amount of IFNGR1 expressed on monocytes and dendritic cells, as well as decreased STAT1 signalling, after IFN-γ stimulation in our patient. As the IFNGR complex comprises two IFNGR1 chains, the variants exert a double-negative effect, which is further emphasized by increased functional IFNGR1 binding to accumulated defective IFNGR1. Still, a small fraction of the IFN-γ receptor is functional, and the disease is manifested as a partial deficiency, typical for Immunodeficiency 27B [19].

In addition, the c.1434 + 1G > C variant in the *CARD9* gene has been shown to disrupt mRNA splicing, thus resulting in out-of-frame exon 11 skipping and production of a truncated, but stable, protein [20]. However, this protein cannot be activated by TRIM62. This variant functions in a

double-negative manner, reducing cytokine production by dendritic cells and acting protectively against inflammatory bowel disease [21]. Although Szymanski et al. [22] suggested this variant to be associated with an increased risk of pulmonary nontuberculous mycobacterial infection, and the evidence supporting its role in MSMD development is missing. We do not consider this variant causative for MSMD; however, its contribution to the patient's phenotype cannot be excluded.

It is necessary to remark that whole-genome sequencing has its limitations. One of the causes of MSMD may be the presence of anti-IFN gamma autoantibodies, in adults in particular. It is an important differential diagnosis which cannot be addressed by whole-exome sequencing. Laboratory tests are very useful in establishing the concentration of

gamma interferon. Its high concentration prompts the suspicion of complete IFNG receptor deficiency [23]. Both functional testing and whole-exome sequencing are, therefore, important.

We were not able to assess our patient's family history. Supposedly, her mother had similar problems but refused examination. The patient has no siblings or children. NTM isolates identified in our patient are typical for MSMD and in agreement with other published studies [24].

In our patient's history, two interesting moments should be mentioned. (i) She was vaccinated against tuberculosis without complications, but at 5 years of age, she developed dysbacteriosis of the lymph nodes. However, the therapy was successful, and there was a long period of remission without any clinical manifestations. (ii) She took a turn for the worse after the use of glucocorticoids at 17 years of age for suspected sarcoidosis. We believe that the diagnosis was incorrect. It was not sarcoidosis but initial signs of dysbacteriosis, which subsequently manifested clinically upon administration of systemic corticosteroids. Clinical problems with affected bones are typical of AR IFNGR1 deficiency [25]. From the patient's perspective and from a practical point of view, it is important that, by using IFN-γ therapy, we significantly influenced the clinical manifestations of the disease and improved our patient's quality of life. Although it was not possible to discontinue the use of antituberculous agents immediately, it was not necessary to continue their parenteral administration. At present, the patient has already been without antibiotic therapy and any clinical problems for 2 months. IFN-γ therapy may be useful for some causes of MSMD [26, 27]. However, the response to IFN-γ treatment is variable, and the mechanism of action remains unclear. There is a lot of uncertainty as far as MSMD IFN-γ is concerned. Apart from not knowing the exact mechanism of the effect, we are lacking sufficient data about the dose which should be administered. Various schemes are used, the general principle being an increased dose in case of an insufficient effect. We applied a higher dose of IFN-γ with our patient as a result of the duration and seriousness of her clinical manifestations. At present, the patient does not exhibit any positive clinical manifestations or positive microbial diagnostics. It should be noted that, for autosomal recessive (AR) complete IFN-γ receptor deficiency, this therapy is not effective [28]. Clinically, the characterization of IFNGR1 deficiency-associated variants translates to important differences in the treatment approach. Complete autosomal recessive IFNGR1 deficiency is characterized by early onset of disseminated life-threatening infections by low-virulent mycobacteria, a lack of response to IFN-γ cytokine replacement therapy, and high mortality [29]. There appears to be some effect for AD partial IFN-γ receptor1 deficiency, IL-12 receptor beta1 deficiency, and IL-12p40 deficiency. The most important points of our casuistry are the following: Diagnosis of the primary immunodeficit must be considered, even in patients with atypical infections, which need not be manifested in the first years of life. Clinically active and inactive periods of disease may take turns. Further extension of the spectrum of these diagnoses with clinically different phenotypes can be supposed.

Molecular biology methods, i.e., whole-gene sequencing, represent a fast and reliable way of diagnosing such patients. IFN-γ treatment is an example of personalized treatment with some of them, even though the mechanism of its effect is not entirely clear.

Summary: primary immunodeficiency can be manifested clinically at an adult age; this must, therefore, be born in mind during its diagnosis. MSMD is a disease that significantly affects the patient's quality of life. Diagnosis is sometimes difficult due to the low prevalence of this disease. Diagnostics using massive parallel sequencing provides clinicians the opportunity to correctly diagnose these patients and allows targeted therapy that positively affects the development of the disease and the patient's quality of life.

Conflicts of Interest

The authors declare that they have no conflicts of interest.

Acknowledgments

References

[1] A. Bousfiha, L. Jeddane, C. Picard et al., "Human inborn errors of immunity: 2019 update of the IUIS phenotypical classification," *Journal of Clinical Immunology*, vol. 40, no. 1, pp. 66–81, 2020.

[2] E. Jouanguy, F. Altare, S. Lamhamedi et al., "Interferon-γ-receptor deficiency in an infant with fatal bacille calmette-guérin infection," *New England Journal of Medicine*, vol. 335, no. 26, pp. 1956–1962, 1996.

[3] J. Rosain, X. F. Kong, R. Martinez-Barricarte et al., "Mendelian susceptibility to mycobacterial disease: 2014-2018 update," *Immunology & Cell Biology*, vol. 97, no. 4, pp. 360–367, 2019.

[4] A. K. Bandari, B. Muthusamy, S. Bhat et al., "A novel splice site mutation in IFNGR2 in patients with primary immunodeficiency exhibiting susceptibility to mycobacterial diseases," *Frontiers in Immunology*, vol. 10, p. 1964, 2019.

[5] J. L. Casanova, S. Blanche, J. F. Emile et al., "Idiopathic disseminated bacillus Calmette-Guérin infection: a French national retrospective study," *Pediatrics*, vol. 98, no. 4 Pt 1, pp. 774–778, 1996.

[6] M. Levin, M. J. Newport, P. Kalabalikis et al., "Familial disseminated atypical mycobacterial infection in childhood: a human mycobacterial susceptibility gene?" *The Lancet*, vol. 345, no. 8942, pp. 79–83, 1995.

[7] G. Kak, M. Raza, and B. K. Tiwari, "Interferon-gamma (IFN-γ): exploring its implications in infectious diseases," *Bio-Molecular Concepts*, vol. 9, no. 1, pp. 64–79, 2018.

[8] M. A. Lake, L. R. Ambrose, M. C. I. Lipman, and D. M. Lowe, ""Why me, why now?" Using clinical immunology and epidemiology to explain who gets nontuberculous mycobacterial infection," *BMC Medicine*, vol. 14, no. 1, 2016.

[9] A. M. Cooper and S. A. Khader, "The role of cytokines in the initiation, expansion, and control of cellular immunity to

tuberculosis," *Immunological Reviews*, vol. 226, no. 1, pp. 191–204, 2008.

[10] S. L. Baldwin, S. E. Larsen, D. Ordway et al., "The complexities and challenges of preventing and treating nontuberculous mycobacterial diseases," *PLoS Neglected Tropical Diseases*, vol. 13, no. 2, Article ID e0007083, 2019.

[11] B. A. Brown-Elliott, K. A. Nash, and R. J. Wallace Jr., "Antimicrobial susceptibility testing, drug resistance mechanisms, and therapy of infections with nontuberculous mycobacteria," *Clinical Microbiology Reviews*, vol. 25, no. 3, pp. 545–582, 2012.

[12] A. Esteve-Solé, I. Sologuren, M. T. Martínez-Saavedra et al., "Laboratory evaluation of the IFN-γ circuit for the molecular diagnosis of Mendelian susceptibility to mycobacterial disease," *Critical Reviews in Clinical Laboratory Sciences*, vol. 55, no. 3, pp. 184–204, 2018.

[13] E. Jouanguy, S. Lamhamedi-Cherradi, D. Lammas et al., "A human IFNGR1 small deletion hotspot associated with dominant susceptibility to mycobacterial infection," *Nature Genetics*, vol. 21, no. 4, pp. 370–378, 1999.

[14] H. Glosli, A. Stray-Pedersen, A. C. Brun et al., "Infections due to various atypical mycobacteria in a Norwegian multiplex family with dominant interferon-receptor deficiency," *Clinical Infectious Diseases*, vol. 46, no. 3, pp. e23–e27, 2008.

[15] B. Glanzmann, C. Uren, N. De Villiers et al., "Primary immunodeficiency diseases in a tuberculosis endemic region: challenges and opportunities," *Genes & Immunity*, vol. 20, no. 6, pp. 447–454, 2019.

[16] A. T. Staines-Boone, C. Deswarte, V. Montoya et al., "Multifocal recurrent osteomyelitis and hemophagocytic lymphohistiocytosis in a boy with partial dominant IFN-γR1 deficiency: case report and review of the literature," *Frontiers in Pediatrics*, vol. 5, p. 75, 2017.

[17] M. A. Rivas, M. Beaudoin, M. Beaudoin et al., "Deep resequencing of GWAS loci identifies independent rare variants associated with inflammatory bowel disease," *Nature Genetics*, vol. 43, no. 11, pp. 1066–1073, 2011.

[18] I. F. A. C. Fokkema, P. E. M. Taschner, G. C. P. Schaafsma, J. Celli, J. F. J. Laros, and J. T. Den Dunnen, "LOVD v.2.0: the next generation in gene variant databases," *Human Mutation*, vol. 32, no. 5, pp. 557–563, 2011.

[19] M. J. Gutierrez, N. Kalra, A. Horwitz et al., "Novel mutation of interferon-γ receptor 1 gene presenting as early life mycobacterial bronchial disease," *Journal Investigative Medicine High Impact Case Report*, vol. 4, pp. 1–5, 2016.

[20] M. Beaudoin, P. Goyette, G. Boucher et al., "Deep resequencing of GWAS loci identifies rare variants in CARD9, IL23R and RNF186 that are associated with ulcerative colitis," *PLoS Genetics*, vol. 9, Article ID e1003723, 2013.

[21] Z. Cao, K. L. Conway, R. J. Heath et al., "Ubiquitin ligase TRIM62 regulates CARD9-mediated anti-fungal immunity and intestinal inflammation," *Immunity*, vol. 43, no. 4, pp. 715–726, 2015.

[22] E. P. Szymanski, J. M. Leung, C. J. Fowler et al., "Pulmonary nontuberculous mycobacterial infection. a multisystem, multigenic disease," *American Journal of Respiratory and Critical Care Medicine*, vol. 192, no. 5, pp. 618–628, 2015.

[23] C. Fieschi, S. Dupuis, E. Catherinot et al., "Low penetrance, broad resistance, and favorable outcome of interleukin 12 receptor β1 deficiency," *Journal of Experimental Medicine*, vol. 197, no. 4, pp. 527–535, 2003.

[24] E. Van De Vosse, "Primary immunodeficiency leading to mycobacterial disease," *International Journal of Mycobacteriology*, vol. 4, pp. 63–68, 2015.

[25] S. E. Dorman, C. Picard, D. Lammas et al., "Clinical features of dominant and recessive interferon γ receptor 1 deficiencies," *The Lancet*, vol. 364, no. 9451, pp. 2113–2121, 2004.

[26] J.-Y. Han, S. D. Rosenzweig, J. A. Church, S. M. Holland, and L. A. Ross, "Variable presentation of disseminated nontuberculous mycobacterial infections in a family with an interferon-receptor mutation," *Clinical Infectious Diseases*, vol. 39, no. 6, pp. 868–870, 2004.

[27] M. T. Milanes-Virelles, I. G. Garcia, Y. S. Herrera et al., "Adjuvant interferon gamma in patients with pulmonary atypical Mycobateriosis: a randomized, double-blind, placebo-controlled study," *BMC Infectious Diseases*, vol. 8, p. 17, 2008.

[28] A. A. Alangari, F. Al-Zamil, A. Al-Mazron et al., "Treatment of disseminated mycobacterial infection with high-dose IFN-Υ in a patient with IL-12Rβ1 deficiency," *Journal Immunology Research*, vol. 2011, Article ID 691956, 5 pages, 2011.

[29] E. Van De Vosse and J. T. Van Dissel, "IFN-γR1 defects: mutation update and description of theIFNGR1variation database," *Human Mutation*, vol. 38, no. 10, pp. 1286–1296, 2017.

Anti-IL6 Autoantibodies in an Infant With CRP-Less Septic Shock

Marketa Bloomfield [1,2*†], Zuzana Parackova [1†], Tamara Cabelova [2], Iva Pospisilova [2,3],
Pavel Kabicek [2], Hana Houstkova [2] and Anna Sediva [1]

[1] Department of Immunology, 2nd Faculty of Medicine, Charles University and Motol University Hospital, Prague, Czechia,
[2] Department of Pediatrics, 1st Faculty of Medicine, Thomayer's Hospital and Charles University, Prague, Czechia,
[3] Department of Clinical Chemistry, 1st Faculty of Medicine, Thomayer's Hospital and Charles University, Prague, Czechia

Background: Interleukin-6 (IL-6) is a pleiotropic cytokine with a multitude of pro-inflammatory effects. Serum C-reactive protein (CRP) is an acute phase protein induced mainly by IL-6 in response to inflammatory conditions, particularly infection. The biological functions of CRP include opsonisation, induction of phagocytosis, complement activation, or chemotaxis enhancement. Factors interfering with IL-6-mediated recruitment of innate immune responses, such as the presence of anti-IL6 antibodies, may therefore compromise the host resistance to microbial pathogens. This has major implications for the use of IL-6-targeting biologics, such as tocilizumab or sarilumab in rheumatologic, immune dysregulation diseases, and cancer.

Case presentation: 20-month-old Czech female developed severe septic shock with clinical and laboratory signs of systemic inflammation but no increase of CRP or IL-6. The offending pathogen was most likely *Staphylococcus aureus,* detected in a throat swab; the response to antibiotic treatment was prompt. A defect in the integrity of IL-6/CRP axis was suspected and verified by the detection of neutralizing IL-6 antibodies in the serum of the child.

Conclusion: We report a first case of systemic bacterial infection in a patient with anti-IL6 autoantibodies. Disturbed IL-6 signaling, whether iatrogenic by targeted IL-6 blockade or endogenous due to the presence of autoantibodies against IL-6, represents a risk factor for increased infectious susceptibility. Patients with severe bacterial infection without elevation of CRP should be examined for the presence of anti-IL6 autoantibodies.

Keywords: interleukin 6, C-reactive protein, anti-IL6 autoantibodies, tocilizumab, siltuximab, sarilumab

BACKGROUND

Interleukin 6 (IL-6), originally described as B-cell stimulatory factor in 1985, is now known as a pleiotropic cytokine with multitude of key biological functions, including inflammatory and immune responses, hematopoiesis, and oncogenesis. It is transiently produced by immune cells, such as monocytes and macrophages, but also by other cell lineages upon various stimuli, e.g. infection or tissue injury (1). IL-6 binds to its receptor, which exists in two forms; a membrane-bound protein or a soluble form. In short, upon IL-6 binding the downstream signaling molecules Janus kinases (JAKs) recruit either signal transducer and activator of transcription 3 (STAT3) or mitogen-activated protein kinases (MAPKs) via receptor-associated molecule gp130. This initiates the transcription of IL-6-inducible genes (2) and results, inter alia, in the production of proteins such as C-reactive protein (CRP), fibrinogen and serum amyloid A.

CRP is an acute phase reactant produced by hepatocyte-derived IL-6-dependent biosynthesis in inflammatory conditions, particularly in response to infection. Its biologic functions are promotion of innate immune processes, including opsonisation, complement activation, induction of release of pro-inflammatory cytokines or promotion of phagocytosis and chemotaxis (3). CRP serum levels begin to rise by 6 hours and peak within 2–3 days from induction (4).

Procalcitonin (PCT) is produced in health in thyroid cells and immediately converted to the hormone calcitonin. On the other hand, the inflammatory PCT is released mainly by adipocytes and white blood cells, triggered by various microbial peptides or inflammatory mediators such as IL-6 or tumor necrosis factor-alpha (TNFα). PCT is utilized as a diagnostically accurate tool for bacterial infection and a useful discriminator of sepsis. Its levels increase more rapidly than CRP, between 2 and 6 hours and peak within 6–24 hours during infection (5).

Sepsis is defined as systemic inflammatory response to infection (6) or, more recently, as life-threatening organ dysfunction caused by a dysregulated host response to infection (7). Septic shock is clinically identified as sepsis with cardiovascular dysfunction (6). During sepsis, an array of cytokines and chemokines is produced, such as interleukin 1β (IL-1β), IL-6, TNF-α, or soluble CD14 (5). Currently, IL-6, CRP and PCT are the most commonly used biomarkers of sepsis, which severity and outcome prediction capacity is of high clinical research interest.

Given the role of IL-6 in immune responses, an enhanced infectious susceptibility is a rational concern in any therapeutic strategy targeting IL-6 signaling, e.g. IL-6 receptor (IL6R) (tocilizumab, sarilumab) or IL-6 (siltuximab), increasingly utilized in treatment of rheumatoid arthritis (RA), juvenile idiopathic arthritis (JIA), or Castleman's disease (8).

To date, three patients only were reported to suffer severe bacterial infections while having detectable neutralizing antibodies to IL-6 and impaired acute phase response (9, 10). The hereby-presented case describes the fourth such patient, who is also the first to present with severe systemic inflammatory response.

CASE PRESENTATION

Clinical Vignette

A Czech female was born in 36th gestational week to a mother with history of intravenous methylamphetamine abuse during

---

Abbreviations: Abs, antibodies; AD HIES, autosomal dominant HyperIgE syndrome; Anti-IL6 abs, antibodies against interleukin 6; Anti-IL6 autoAbs, autoantibodies against interleukin 6; CM, complete medium; CRP, C reactive protein; DOCK8, dedicator of cytokinesis 8; FBS, fetal bovine serum; IFN-γ, interferon gamma; IL12, IL-17A, IL-17F, IL-22, IL-23, interleukin of corresponding enumeration; IL-6, interleukin 6; IL6R, interleukin 6 receptor; IRAK-4, interleukin 1 receptor-associated kinase 4; JAKs, Janus kinases; JIA, juvenile idiopathic arthritis; LPS, lipopolysaccharide; MAPKs, mitogen-activated protein kinases; MyD88, myeloid differentiation primary response 88; NEMO, nuclear factor-kappa B essential modulator; PBMC, peripheral blood mononuclear cells; PBS, phosphate-buffered saline; PCT, procalcitonin; pSTAT3, phosphorylated signal transducer and activator of transcription 3; RA, rheumatoid arthritis; ref.range, reference range; STAT3, signal transducer and activator of transcription 3; TNFα, tumor necrosis factor-alpha.

pregnancy. She suffered severe perinatal asphyxia and multiple ileal perforations requiring a stoma, which was closed at 4 months. At the age of 5 months, she suffered another ileal perforation, during which an increase of CRP (86,7 mg/L) and leucocytosis (19,7 × 10*9/L) were noted. The subsequent infectious susceptibility was inconspicuous; she thrived relatively well, received hexavalent combined vaccine (diphtheria, tetanus, pertussis, poliomyelitis, *Haemophilus influenzae type B*, and hepatitis B) and developed within the neurologic limitations of her perinatal insult. At the age of 20 months, she suffered a short paroxysm of generalized seizures in a second day of fevers of 38, 0–38, 5°C. Upon admission, she presented with dehydration, circulatory instability with hypotension, tachycardia, tachypnea, and anuria. Her laboratory workup showed mild leukopenia 5.8 × 10*9/L (ref. range 6.0–17.5), thrombocytopenia 64 × 10*9/L (ref. range 150–450), severe electrolyte imbalance, increased renal parameters (creatinin 132 umol/L, ref. range 8–45; urea 25 mmol/L, ref. range 3.2–9.0), signs of rhabdomyolysis (increased aspartate aminotransferase, serum creatine kinase, myoglobin) and elevated D-dimers, activated partial thromboplastin time but unincreased fibrinogen 2.82 g/L (ref. range 1.45–3.48). An extreme elevation of PCT 378.0 ug/L (electrochemiluminescence, ref. range 0.0–0.5) but, curiously, no increase of CRP 2.9 mg/L (immunoturbidimetry, ref. range 0.0–5.0) or IL-6 16.2 ng/L (electrochemiluminescence, ref. range 0.0–20.0) were noted. *Staphylococcus aureus* was cultured from throat swabs, other microbiologic investigations were negative, including blood cultures. She was diagnosed with septic shock, required massive intravenous volume expansion and received 10 days of antibiotic treatment (third generation cephalosporin and gentamicin) that controlled the infection and the laboratory parameters normalized. During the following 6 months, she experienced no other infections.

The patient's basic immune profiling suggested no gross abnormality (**Table 1**). However, intrigued by the peculiar dynamics of the inflammatory markers during sepsis, especially the lack of IL-6 and CRP response along the high PCT elevation (**Figure 1A**), we prompted investigation of the integrity of IL-6 signaling axis, which we tested in the following steps.

The Ability to Synthetize IL-6 by Patient's CD14^{+} Monocytes Is Normal

In order to establish a normal cellular ability to produce IL-6, patient's whole blood was stimulated with lipopolysaccharide (LPS) in presence of Brefeldin A. Flow cytometric trace of IL-6 (**Figure 1B**), IL-1β and TNFα (**Supplementary Figure 1**) in CD14^{+} monocytes was analyzed. We observed an increased unstimulated production of IL-6 and IL-1β in the time of sepsis, which further increased after LPS stimulation, demonstrating an unskewed ability to synthetize these cytokines. The production of TNFα was similar to healthy controls.

The Ability to Release IL-6 Into Extracellular Space by Patient's Cells Is Normal

Having established a normal intracellular IL-6 synthesis, we sought to determine the patient's cells ability to release the

TABLE 1 | Patient's basic immune profile.

Patient's immune profile	Value	Age-matched reference values
Leukocytes (cells/μL)	10,100	6,000–17,000
Lymphocytes (cells/μL)	7,180	2,900–12,400
Neutrophils (cells/μL)	1,550	1,300–8,200
Monocytes (cells/μL)	1,010	150–1,280
Eosinophils (cells/μL)	610	0–1,200
CD3^{+} (%[a], cells/μL)	76 ↑/ 5,457 ↑	56–75/1,400–3,700
CD3^{+} CD4^{+} (%[a], cells/μL)	42/3,016 ↑	28–47/700–2,200
CD3^{+} CD8^{+} (%[a], cells/μL)	27/1,939 ↑	16–30/490–1,300
Naïve CD4^{+} (%[b]) (CD3^{+}CD4^{+}CD45RA^{+}CD27^{+})	36	36–97
Naïve CD8^{+} (%[c]) (CD3^{+}CD8^{+}CD45RA^{+}CD27^{+})	19	19–95
CD19^{+} (%[a], cells/μL)	18/1,292	14–33/390–1,400
Naïve CD19^{+} (%[d]) (CD19^{+}CD27^{−}IgD^{+})	91	49–100
Switched memory CD19[+](%[d]) (CD19^{+}CD27^{+}IgD^{−})	3↓	5–25.6
CD16^{+}/CD56^{+} (%[a], cells/μL)	4.4 /316	4–17/130–720
Immunoglobulins		
IgG (g/L)	4.76↓	5.53–10.20
IgG1(g/L)	2.4 ↓	2.90–8.50
IgG2 (g/L)	1.33	0.45–2.60
IgG3 (g/L)	0.42	0.15–1.13
IgG4 (g/L)	0.61	0.01–0.79
IgA (g/L)	0.31↓	0.33–0.91
IgM (g/L)	0.47	0.47–1.55
IgE (IU/mL)	60.6↑	0.0–30.0
IgD (IU/mL)	<5.65	0.0–100.0
a-tetanus, a-diphtheria, a-hemophilus postvaccination IgG	Normal	NA
Autoantibodies (ANA, ENA, a-dsDNA, RF, ANCA, a-TPO, a-TG, a-TSHR, a-EM, a-TTG, a-GD)	Neg	NA
Complement activation (%):		Reference ranges
Classic pathway	94	69–129
Alternative pathway	53.4	30–113
MBL pathway	0.4↓	>10
Burst test PMA and *E.coli,* NBT test	Normal	NA

[a]*% of total peripheral lymphocytes.*
[b]*% of CD4^{+}.*
[c]*% of CD8^{+}.*
[d]*% of CD19^{+}.*

NA, not applicable; SCIG, subcutaneous immunoglobulins; Neg, negative; ANA, antinuclear antibodies; ENA, extractable nuclear antigen antibodies; a-dsDNA, anti-double stranded DNA antibodies; RF, rheumatoid factor IgG, IgA and IgM; ANCA, anti-neutrophil cytoplasm antibodies; a-TPO, anti-thyreoperoxidase antibodies; a-TG, anti-thyreoglobulin antibodies; a-TSHR, TSH receptor antibodies; a-EM, anti-endomisium IgG and IgA antibodies; a-TTG, anti-tissue transglutaminase antibodies IgG and IgA; a-GD, anti-deamidated gliadin IgA and IgG; MBL, mannan binding lectine; PMA, Phorbolmyristate acetate; NBT, nitroblue tetrazolium. ↑,↓, value above, below reference range, respectively.

cytokine extracellularly. Patient's peripheral blood mononuclear cells (PBMCs) were stimulated with LPS overnight. The supernatants were harvested and the IL-6 was determined using a commercial IL-6 Elisa assay. We found the PBMCs of the patient to be capable of substantial IL-6 extracellular release, even if slightly decreased compared to a healthy control (**Figure 1C**).

The Patient's Serum Has IL-6 Neutralizing Property

Because of the patient's uncompromised ability to produce CRP at the age of 5 months, we hypothesized that an induction of anti-IL6 antibodies (abs) may underlie the acquired IL-6/CRP irresponsiveness. The healthy donors' PBMCs were stimulated according to the protocol above or left unstimulated in complete media (CM) supplemented either with patient's serum obtained from 2 different time points (in time of sepsis and 1 month later) or with fetal bovine serum (FBS). We noted a profound decrease of the cytokine in the presence of patient's serum. This indicated that the patient's serum contained a component interfering with the IL-6 detection (**Figure 1D**).

The Patient's Serum Contains Anti-IL6 Autoantibodies

The anti-IL6 abs were detected in the patient's and healthy donors' sera using a commercial Elisa kit (MyBiosource, details available in List of Methods). While the control samples were negative for anti-IL6 abs, the patient's serum was found positive in time of sepsis as well as 1 month after the infection (**Figure 1E**).

The Patient's Serum Decreases the Intracellular IL-6-Mediated Signal Transduction

Finally, we investigated whether the IL-6 abs found in the patient's serum cause a corresponding depression of IL-6 signal transduction downstream of IL-6 receptor (IL6R). To do this, we cultivated recombinant IL-6 in phosphate-buffered saline (PBS) supplemented with patient's serum obtained from 3 different time-points (in sepsis, 1 and 3 months later) or with FBS. Then, control full blood (n = 2) was stimulated with IL-6 in the respective media and STAT3 phosphorylation (pSTAT3) was analyzed in peripheral T cells and monocytes. We observed a significantly lower pSTAT3 signal from samples containing patient's serum from all 3 time-points (**Figure 1F**). The results suggest that the IL-6 abs have a neutralizing effect and indicate the persistence of the IL-6 abs even beyond acute phase of the infection.

DISCUSSION AND CONCLUSIONS

We present a child with septic shock, which most likely developed on the grounds of serum anti-IL6 autoAbs. Based on the lack of detectable IL-6, CRP and fibrinogen response during a clinically manifested systemic inflammation, together with the disturbed IL-6/STAT3-mediated signaling observed in cells exposed to patient's serum, we suggest that these abs have neutralizing property and contributed to the severity of the infection. Meanwhile, the undisturbed functionality of other proinflammatory cytokines, such as IL-1β or TNFα probably explains the patient's retained ability to develop other features of inflammatory response, such as fever or increased PCT. PCT, a strong IL-6 independent biomarker of bacterial infection, rises sooner than CRP. Yet, due to its biologic half-life its increase should later overlap with CRP elevation. Therefore, the
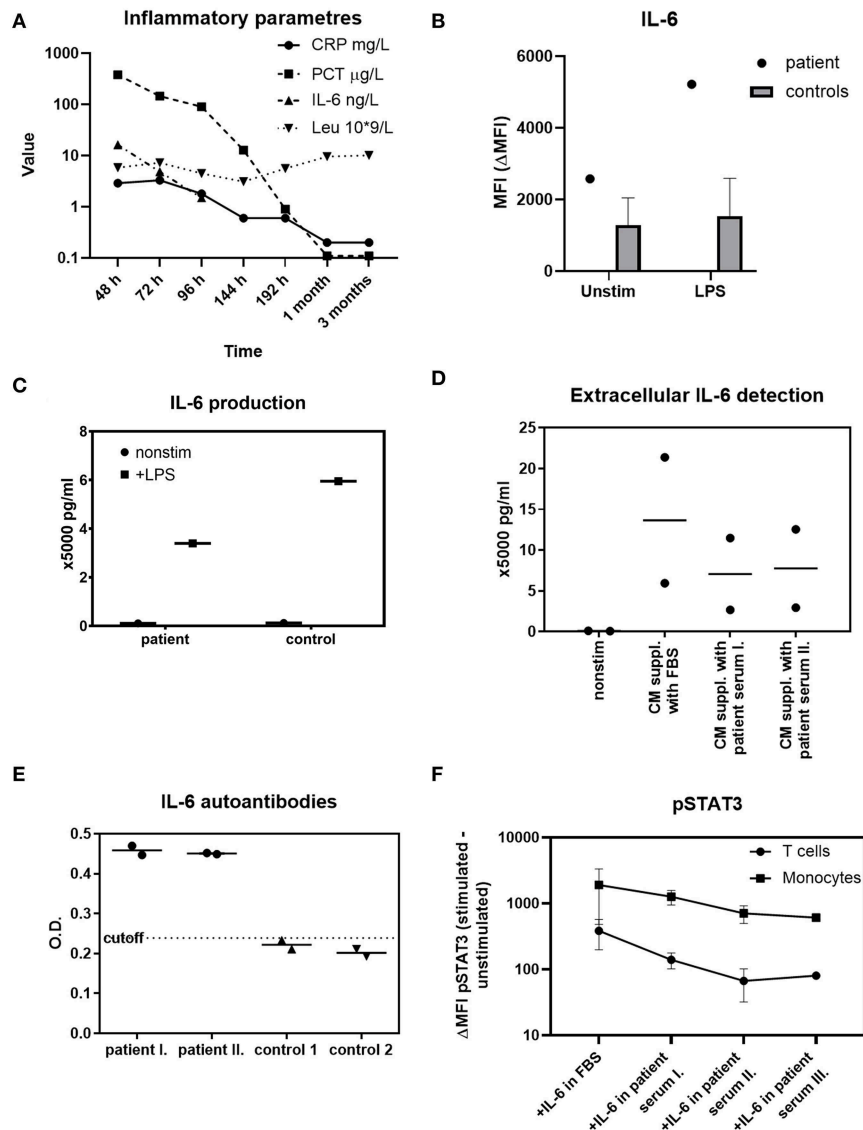
FIGURE 1 | Investigations of IL-6 functions in the patient. **(A)** The dynamics of IL-6, CRP, PCT, and absolute leukocytes count in various time-points during sepsis, 1 and 3 months afterwards (h-hours from onset of fever, m-month/s). An extreme elevation of PCT is not accompanied with IL-6 or CRP increases over the normal reference value. Reference ranges: CRP 0.0–5.0 mg/L; PCT 0.0–0.5 μg/L; IL-6 0.0–20.0 ng/L; Leu 6.0–17.5 × 10⁹/L. **(B)** Intracellular IL-6 production in patient's monocytes at the time of sepsis compared to 59 healthy controls' monocytes after 1 μg/ml LPS determined with flow cytometry. Unstimulated state is expressed as MFI (mean fluorescence intensity). The effect of LPS stimulation is expressed as ΔMFI (stimulated minus unstimulated MFI). The synthesis of IL-6 by patient's monocytes is unskewed. **(C)** Detection of extracellular IL-6 from patient's PBMCs after 1 μg/ml LPS stimulation determined by ELISA. The release of IL-6 into extracellular space by patient's cells is normal. **(D)** Suppression of extracellular IL-6 by patient's serum analyzed by ELISA. Healthy age-matched controls' PBMCs (*n* = 2) were stimulated with LPS, cultivated in complete media (CM) supplemented either with fetal bovine serum (FBS) or 10% patient serum in time of sepsis (I) and 1 month later (II) The amount of IL-6 detected in the presence of patient's serum is decreased in both time-points. **(E)** Anti-IL-6 autoantibodies detection in patient serum obtained in time of sepsis (I), 1 month later (II), and in 2 healthy age-matched controls with ELISA. The patient's serum, but not the control serum, contains anti-IL6 autoantibodies. OD, optical density. **(F)** STAT3 phosphorylation (pSTAT3) in control (*n* = 2) T cells and monocytes after 10 ng/ml recombinant IL-6 stimulation. The peripheral blood was stimulated with IL-6 diluted in PBS containing 20% patient serum obtained in sepsis (I), 1 month later (II), 3 months later (III), or in fetal bovine serum (FBS). The patient's serum decreases the pSTAT3 signal in all three time-points. Data are expressed as ΔMFI (stimulated minus unstimulated MFI). MFI, mean fluorescence intensity.

PCT/IL-6/CRP discrepancy during the acute phase of infection in our patient supports the hypothesis of isolated defect in IL-6-mediated CRP induction.

To our knowledge, this is the first patient with anti-IL6 autoAbs reported to suffer a severe systemic infection. Previously, Puel et al. reported a Haitian boy with recurrent *Staphylococcus aureus* subcutaneous abscesses and cellulitis (9) and Nanki et al. referred two adult Japanese patients presenting with *Staphylococcal aureus cellulitis* and *Streptococcus intermedius* and *Escherichia coli empyema* (10) (**Supplementary Table 1**).

Eventhough very likely, a causative link between the anti-IL6 abs and the infectious susceptibility may not be unequivocally established in our patient. With no human IL-6 deficiency reported to date, the corresponding phenotype and the exact underlying molecular mechanisms of such defects are yet to be elucidated. Nevertheless, some clues may be derived from patients with genetic loss of proteins involved in IL-6/gp130/STAT3 signaling pathway. Two patients were recently reported to harbor homozygous IL6R mutations resulting in a phenotype of recurrent infections, absence of CRP increase during acute phase of clinically apparent infections, elevated IgE and eczema (11). A single case of bilallelic gp130 mutation has been described to present as early onset severe bacterial infections including *Staphylococcus aureus,* eczema, impaired acute phase response and increased IgE (12). Similar features are associated with hypomorphic STAT3 mutations, which constitute the autosomal dominant HyperIgE syndrome (AD HIES) [reviewed in (13)]. Additionally, an IL-6 knockout murine model was shown to develop normally, but the inflammatory acute-phase response after tissue damage or infection was severely compromised (14).

The apparently impeded resistance to *Staphylococcus aureus* in subjects with IL-6 signaling disruption is intriguing. Various primary immunodeficiencies (PIDs) predispose to abnormal, but not selective staphylococcal susceptibility, such as X-linked chronic granulomatous disease, NEMO deficiency syndrome, IRAK-4 deficiency, MyD88 deficiency, or DOCK8 deficiency. Mechanistically, the most relevant to our case is the STAT3 loss-of-function AD HIES, classically hallmarked by recurrent staphylococcal skin and lung infections, and the IL6R deficiency with both reported cases suffering with staphylococcal infections (11). Such similarity strongly suggests that the functional integrity of IL-6/STAT3 pathway is particularly important in antistaphylococcal immunity, however, the exact mechanism is not yet clear. It may involve the lack of CRP-mediated protection or other aspects, such as disturbed Th17 functions or diminished circulating T follicular helper cell induction, which was observed in AD HIES and IL6R deficiency.

Interestingly, several PIDs have recently been coupled with their phenocopies that arise from the presence of anti-cytokine abs. For example, an increased susceptibility to weakly virulent mycobacteria due to IFN-γ autoAbs resembles a rare PID called Mendelian susceptibility to mycobacterial diseases due to monogenic defects in IL-12/IFN-γ circuit. Similarly, abs against Th17-related cytokines IL-17A, IL-17F, IL-22, IL-23 underlie increased susceptibility to fungal infections resembling chronic mucocutaneous candidiasis due to various genetic etiologies [reviewed in (15)].

Naturally occurring anti-IL6 autoAbs were found in 0.1% healthy population but these are likely low concentration and lack the neutralizing property due to their low affinity (16). As with the majority of human autoantibodies, the reason why our patient developed blocking anti-IL6 autoAbs is unknown. A genetic predisposition might play a role. However, having been able to develop a normal acute phase response,

including a CRP increase, at the age of 5 months, a single gene inborn error is unlikely. Of note, the two adult subjects reported previously to produce blocking IL-6 abs were not affected with increased infectious susceptibility until 56 and 67 years of age (10). These aspects suggest that "multiple hits" may be required in the disease pathophysiology. Also, our patient's severe perinatal history may underlie an immune dysbalance, owing to early abnormal exposure to pathogens or self-antigens, which may result in autoAbs induction. Nevertheless, no other clinically relevant abs were detected in the patient's blood.

Finally, two IL6R and one IL-6 blocking agents are currently approved and widely used in diseases such as RA, JIA and Castleman's disease (8). While some studies identified a higher incidence of severe infections in RA patients receiving anti-IL6R blockade compared to anti-TNFα biologics (17, 18), others did not (19). However, the suppression of CRP in RA patients receiving monoclonal anti-IL6R abs has been well-recognized, in fact CRP has been suggested as an outcome predictor and treatment monitoring tool (20). In the same context, CRP has also been reported to be a poor predictor of severe infectious complications (21). Several ongoing clinical trials investigate the efficacy and tolerability of IL-6 targeting in various other immune dysregulation or oncologic diseases and novel compounds interfering with IL-6 signaling are being rapidly developed (8). Therefore, given the severity of presentation in our patient, we suggest that extra care in exercised in patients receiving IL-6 blocking agents, especially when administered together with other immune suppressant drugs.

Of note, an excess of soluble IL-6R, which would bind the IL-6 and interfere with its detection was not excluded in our patient. This is a limitation of our study, however the documented presence of anti-IL6 autoAbs amply explains the observed phenomena.

To conclude, disturbed IL-6/STAT3/CRP axis due to endogenous production of anti-IL6 autoAbs was a likely cause of severe septic shock in our patient who failed to mount an efficient acute phase response. We suggest that patients with severe bacterial infection without elevation of CRP should be examined for the presence of anti-IL6 antibodies.

DATA AVAILABILITY STATEMENT

All data generated or analyzed during this study are included in the article/**Supplementary Material** and are also available from the corresponding author on reasonable request.

ETHICS STATEMENT

Ethical review and approval was not required for the study on human participants in accordance with the local legislation and institutional requirements. Written informed consent to participate in this study and for publication was provided by the participants' legal guardian/next of kin.

AUTHOR CONTRIBUTIONS

MB treated the patient, established the hypothesis and wrote the manuscript. ZP designed and performed the experiments and co-wrote the manuscript. TC treated the patient and revised the manuscript. IP performed the routine tests and revised the manuscript. PK and HH supervised the patient treatment, manuscript preparation and revisions. AS supervised the experiments, manuscript preparation and revisions. All authors have contributed in a substantive and intellectual manner.

FUNDING

ACKNOWLEDGMENTS

SUPPLEMENTARY MATERIAL

The Supplementary Material for this article can be found online at: https://www.frontiersin.org/articles/10.3389/fimmu.2019.02629/full#supplementary-material

Supplementary Figure 1 | Cytokine production by patient's monocytes in time of sepsis: IL-1β and TNFα production determined by flow cytometry compared to 65 and 30 healthy controls, respectively. Unstimulated state is expressed as MFI (mean fluorescence intensity). LPS stimulation is expressed as ΔMFI (stimulated—unstimulated MFI).

Supplementary Table 1 | An overview of reported cases of patients with anti-IL-6 autoantibodies and severe bacterial infections.

REFERENCES

1. Akira S, Taga T, Kishimoto T. Interleukin-6 in biology and medicine. *Adv Immunol.* (1993) 53:1–78. doi: 10.1016/S0065-2776(08)60532-5
2. Wolf J, Rose-John S, Garbers C. Interleukin-6 and its receptors: a highly regulated and dynamic system. *Cytokine.* (2014) 70:11–20. doi: 10.1016/j.cyto.2014.05.024
3. Sproston NR, Ashworth JJ. Role of C-reactive protein at sites of inflammation and infection. *Front Immunol.* (2018) 9:754. doi: 10.3389/fimmu.2018.00754
4. Pepys MB, Hirschfield GM. C-reactive protein: a critical update. *J Clin Invest.* (2003) 111:1805–12. doi: 10.1172/JCI18921
5. Vijayan AL, Vanimaya, Ravindran S, Saikant R, Lakshmi S, Kartik R, G M. Procalcitonin: a promising diagnostic marker for sepsis and antibiotic therapy. *J Intensive Care.* (2017) 5:51. doi: 10.1186/s40560-017-0246-8
6. Goldstein B, Giroir B, Randolph A. International pediatric sepsis consensus conference: definitions for sepsis and organ dysfunction in pediatrics. *Pediatr Crit Care Med.* (2005) 6:2–8. doi: 10.1097/01.PCC.0000149131.72248.E6
7. Singer M, Deutschman CS, Seymour C, Shankar-Hari M, Annane D, Bauer M, et al. The third international consensus definitions for sepsis and septic shock (sepsis-3). *JAMA.* (2016) 315:801–10. doi: 10.1001/jama.2016.0287
8. Kang S, Tanaka T, Narazaki M, Kishimoto T. Targeting interleukin-6 signaling in clinic. *Immunity.* (2019) 50:1007–23. doi: 10.1016/j.immuni.2019.03.026
9. Puel A, Picard C, Lorrot M, Pons C, Chrabieh M, Lorenzo L, et al. Recurrent Staphylococcal cellulitis and subcutaneous abscesses in a child with autoantibodies against IL-6. *J Immunol.* (2008) 180:647–54. doi: 10.4049/jimmunol.180.1.647
10. Nanki T, Onoue I, Nagasaka K, Takayasu A, Ebisawa M, Hosoya T, et al. Suppression of elevations in serum C reactive protein levels by anti-IL-6 autoantibodies in two patients with severe bacterial infections. *Ann Rheum Dis.* (2013) 72:1100–2. doi: 10.1136/annrheumdis-2012-202768
11. Spencer S, Köstel Bal S, Egner W, Lango Allen H, Raza SI, Ma CA, et al. Loss of the interleukin-6 receptor causes immunodeficiency, atopy, and abnormal inflammatory responses. *J Exp Med.* (2019) 216:1986–98. doi: 10.1084/jem.20190344
12. Schwerd T, Twigg SRF, Aschenbrenner D, Manrique S, Miller KA, Taylor IB, et al. A biallelic mutation in IL6ST encoding the GP130 co-receptor causes immunodeficiency and craniosynostosis. *J Exp Med.* (2017) 214:2547–62. doi: 10.1084/jem.20161810
13. Freeman AF, Holland SM. The hyper-IgE syndromes. *Immunol Allergy Clin North Am.* (2008) 28:277–91. doi: 10.1016/j.iac.2008.01.005
14. Kopf M, Baumann H, Freer G, Freudenberg M, Lamers M, Kishimoto T, et al. Impaired immune and acute-phase responses in interleukin-6-deficient mice. *Nature.* (1994) 368:339–42. doi: 10.1038/368339a0
15. Barcenas-Morales G, Cortes-Acevedo, P, Doffinger R. Anticytokine autoantibodies leading to infection early recognition, diagnosis and treatment options. *Curr Opin Infect Dis.* (2019) 32:330–6. doi: 10.1097/QCO.0000000000000561
16. Galle P, Svenson M, Bendtzen K, Hansen MB. High levels of neutralizing IL-6 autoantibodies in 0.1% of apparently healthy blood donors. *Eur J Immunol.* (2004) 34:3267–75. doi: 10.1002/eji.200425268
17. Rutherford AI, Subesinghe S, Hyrich KL, Galloway JB. Serious infection across biologic-treated patients with rheumatoid arthritis: results from the British Society for Rheumatology Biologics Register for Rheumatoid Arthritis. *Ann Rheum Dis.* (2018) 77:905–10. doi: 10.1136/annrheumdis-2017-212825
18. Pawar A, Desai RJ, Solomon DH, Santiago Ortiz AJ, Gale S, Bao M, et al. Risk of serious infections in tocilizumab versus other biologic drugs in patients with rheumatoid arthritis: a multidatabase cohort study. *Ann Rheum Dis.* (2019) 78:456–64. doi: 10.1136/annrheumdis-2018-214367
19. Nishimoto N, Ito K, Takagi N. Safety and efficacy profiles of tocilizumab monotherapy in Japanese patients with rheumatoid arthritis: meta-analysis of six initial trials and five long-term extensions. *Mod Rheumatol.* (2010) 20:222–32. doi: 10.1007/s10165-010-0279-5
20. Kojima T, Yabe Y, Kaneko A, Hirano Y, Ishikawa H, Hayashi M, Miyake H, Takagi H, Kato T, Terabe K, et al. Monitoring C-reactive protein levels to predict favourable clinical outcomes from tocilizumab treatment in patients with rheumatoid arthritis. *Mod Rheumatol.* (2013) 23:977–85. doi: 10.3109/s10165-012-0782-y
21. Bari SF, Khan A, Lawson T. C reactive protein may not be reliable as a marker of severe bacterial infection in patients receiving tocilizumab. *Case Reports.* (2013) 2013:bcr2013010423. doi: 10.1136/bcr-2013-010423

ORIGINAL ARTICLE

Nationwide observational study of paediatric inflammatory multisystem syndrome temporally associated with SARS-CoV-2 (PIMS-TS) in the Czech Republic

Jan David[1] · Veronika Stara[1] · Ondrej Hradsky[1] · Jana Tuckova[2] · Katerina Slaba[2] · Petr Jabandziev[2,3] · Lumir Sasek[4] · Michal Huml[4] · Iveta Zidkova[5] · Jan Pavlicek[5] · Alzbeta Palatova[6] · Eva Klaskova[6] · Karina Banszka[7] · Eva Terifajova[7] · Radim Vyhnanek[8] · Marketa Bloomfield[8,9] · Sarka Fingerhutova[10] · Pavla Dolezalova[10] · Lucie Prochazkova[11] · Gabriela Chramostova[12] · Filip Fencl[1] · Jan Lebl[1]

Abstract

The worldwide outbreak of the novel 2019 coronavirus disease (COVID-19) has led to recognition of a new immunopathological condition: paediatric inflammatory multisystem syndrome (PIMS-TS). The Czech Republic (CZ) suffered from one of the highest incidences of individuals who tested positive during pandemic waves. The aim of this study was to analyse epidemiological, clinical, and laboratory characteristics of all cases of paediatric inflammatory multisystem syndrome (PIMS-TS) in the Czech Republic (CZ) and their predictors of severe course. We performed a retrospective-prospective nationwide observational study based on patients hospitalised with PIMS-TS in CZ between 1 November 2020 and 31 May 2021. The anonymised data of patients were abstracted from medical record review. Using the inclusion criteria according to World Health Organization definition, 207 patients with PIMS-TS were enrolled in this study. The incidence of PIMS-TS out of all SARS-CoV-2-positive children was 0.9:1,000. The estimated delay between the occurrence of PIMS-TS and the COVID-19 pandemic wave was 3 weeks. The significant initial predictors of myocardial dysfunction included mainly cardiovascular signs (hypotension, oedema, oliguria/anuria, and prolonged capillary refill). During follow-up, most patients (98.8%) had normal cardiac function, with no residual findings. No fatal cases were reported.

Conclusions: A 3-week interval in combination with incidence of COVID-19 could help increase pre-test probability of PIMS-TS during pandemic waves in the suspected cases. Although the parameters of the models do not allow one to completely divide patients into high and low risk groups, knowing the most important predictors surely could help clinical management.

What is Known:
- *Preliminary evidence, majority from relatively small, and mostly single-centre patient cohorts, has shown some insights in the basic epidemiological and clinical data of children with a paediatric inflammatory multisystem syndrome temporally associated with SARS-CoV-2 (PIMS-TS).*

What is New:
- *To our knowledge, this is the unique published national population-wide cohort allowing to study the epidemiology (including overall incidence), time gap between viral exposure and clinical symptoms of PIMS-TS, and clinical presentations and outcomes within the individual pandemic waves of COVID-19 that were characterised by various prevailing genetic variants of SARS-CoV-2.*
- *We estimated 3-week interval as a most probable period between SARS-CoV-2 infection and PIMS-TS based on nationwide population data using cross-correlation method.*

Jan David, Veronika Stara and Ondrej Hradsky shared first authorship.

Filip Fencl and Jan Lebl are senior authors who contributed equally.

✉ Jan David
jan.david@centrum.cz

Extended author information available on the last page of the article

Springer

Introduction

Following a temporary success within the first wave of the worldwide pandemic of the novel 2019 coronavirus disease (COVID-19) with very few positive cases in spring 2020, the Czech Republic (CZ) suffered from one of the highest incidences of individuals who tested positive for severe acute respiratory syndrome coronavirus 2 (SARS-CoV-2) during the second and third pandemic waves in late 2020 and in early 2021 (with predominant B.1.258 and B.1.1.7 variants) [1–3]. By May 2021, the number of confirmed COVID-19 cases exceeded 155,873 per one million people (total 1.6 million cases, 15.6% of the population), and the number of deaths hit the 30,000 mark (cumulative mortality 2,829 per one million) according to data of the Institute of Health Information and Statistics (IHIS) of CZ [1, 2]. During the most devastating third wave of the pandemic in January–March 2021, the numbers of newly infected patients reached almost 18,000 per day [1–3].

In parallel, paediatricians faced a serious wave of cases of the multisystem condition resulting from an aberrant immune response to SARS-CoV-2 in children that was already recognised as a novel paediatric disease in spring 2020 [4]. This condition partially resembling Kawasaki disease (KD) was assigned the name paediatric inflammatory multisystem syndrome temporally associated with SARS-CoV-2 (PIMS-TS) or multisystem inflammatory syndrome in children (MIS-C) [4].

PIMS-TS is a severe, heterogeneous disease characterised by multiorgan involvement. Several factors linked to disease severity were described, namely age (older than 5 years), higher concentrations of troponin, brain natriuretic peptide (BNP), ferritin, C-reactive protein (CRP), and D-dimer [5]. However, the majority of previously published studies included relatively small and mostly single-centre patient cohorts [6].

The aim of this study was to analyse epidemiological, clinical, and laboratory characteristics of all cases of PIMS-TS in CZ [7]. We also aimed to identify predictors of a severe course of PIMS-TS.

Materials and methods

We performed a retrospective-prospective nationwide observational study based on patients hospitalised with PIMS-TS in CZ. Data were obtained from nine university hospitals and eight regional hospitals in CZ, which is a middle-sized country with a total population of 10.7 million (2.1 million children and adolescents under 19 years of age) [1]. Data on positive reverse transcription-polymerase chain reaction (RT-PCR) SARS-CoV-2 individuals were retrieved from reviews according to the IHIS of CZ [1–3].

Medical training procedures, data sheet collection, and results evaluation within this study were conducted under the authorisation of the Czech Paediatric Society. Soon after the occurrence of the first cases of PIMS-TS in October 2020, diagnostic and therapeutic guidelines using the already available recommendations were updated [8]. Medical staff from all 59 paediatric departments within CZ participated in an online training programme on the recognition and treatment of PIMS-TS. The recommendations were published using multiple information channels and were also available for all primary care paediatricians. All representative physicians were instructed to collect and report a standard set of data (Supplementary table 1) on all children diagnosed with PIMS-TS.

Patients with PIMS-TS according to World Health Organization definition (Supplementary Fig. 1) [7] who were admitted to the hospital between 1 November 2020 and 31 May 2021 were included in the study (Fig. 1). The anonymised data of patients (demographic and clinical data, laboratory test results, imaging and echocardiographic findings, and treatments) were abstracted by medical record review. Laboratory evidence of SARS-CoV-2 exposure or a history of contact with a SARS-CoV-2-positive person in the preceding 2 months was required. From each patient, we obtained one nasopharyngeal swab to test for SARS-CoV-2 using RT-PCR and took blood samples to test for IgG antibodies against SARS-CoV-2. Standard cardiology investigations included electrocardiography and echocardiography (initially and 1–6 months apart, individually according to paediatrics department). We defined a coronary artery dilatation as a z-score 2.0–2.5 and an aneurysm as a z-score 2.5 and higher (by the Lopez method) [9]. Myocardial dysfunction was defined by a decreased left ventricular ejection fraction (< 55.0%). Resistance to intravenous immunoglobulin (IVIG) treatment was defined as a persistent fever or laboratory evidence of inflammation 36 h of the first immunoglobulin infusion [9].

To ascertain the completeness of the nationwide dataset of patients hospitalised with PIMS-TS, at the end of the observation period, chairs of all inpatient paediatric departments were re-contacted by an e-mail and/or by a direct phone call, which led to identification of an additional five yet unreported cases that were consequently added to the study cohort.

All data were analysed using R statistical software (version 4.0.4). Missing data were imputed using multiple imputation methods within the r package mice (version 3.13.0); missing data in continuous variables were imputed using Predictive Mean Matching Imputation algorithm and categorical variables using Random Forest imputation algorithm. The number of missing values in original dataset were stated in Supplementary table 2. Continuous variables were described as medians and interquartile ranges (IQRs). Categorical variables were described as absolute

Fig. 1 Study profile
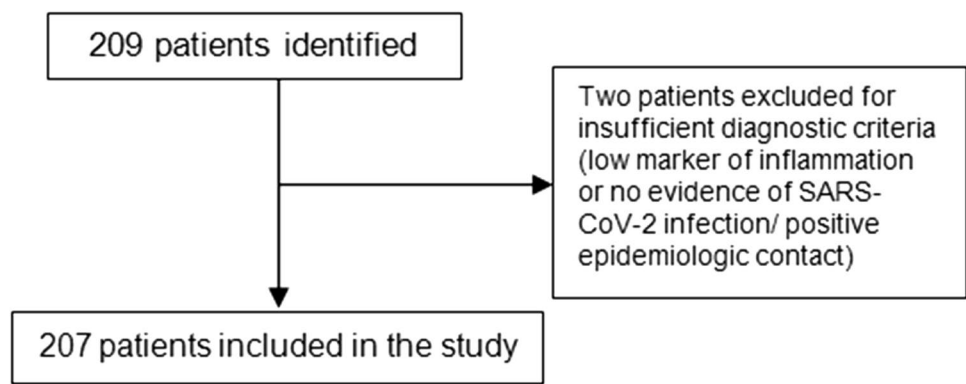
frequencies and percentages. Incidence rate and 95% confidence intervals (CI) were calculated using the epiR package (version 2.0.26). The difference between age categories (0–5 as a reference category) and sex (male sex as a reference category) was tested by generalized linear regression models. The interval between peak of RT-PCR SARS-CoV-2 positivity in children and development of PIMS-TS was estimated using cross-correlation plots. The estimated value was confirmed by comparison of multiple regression models with the most probable intervals as a predictor (based on cross-correlation plots).

The heatmap with dendrogram (based on matrix similarity computation) of the symptom co-occurrence was constructed using R packages "proxy" and "plots". The difference between patients with and without myocardial dysfunction was tested by unadjusted generalized linear regression model. For the purpose of the prediction, categorical data were converted to dummy variables and all missing data of predictors were imputed using k-nearest neighbours algorithm. The prediction models were constructed using R package "caret". Data were divided into training (65.0%) and testing (35.0%) parts. For construction of the models, the modified random forest method, minimising the distance to the perfect model with cross-validation and resampling, was used. The accuracies of these particular models and receiver operator curves (ROCs) were estimated on the testing parts of the datasets.

Results

Using the inclusion criteria, 207 patients with PIMS-TS were enrolled in this study. In the monitored period, the overall incidence of PIMS-TS was 0.1:1,000 of general paediatric population aged 0–19 years and was dependent on age and gender (1:7,400 in 0–5 years; 1:7,200 in 5–10 years; 1:13,900 in 10–15 years; 1:23,900 in 15–19 years; 1:8,100 in males; and 1:13,700 in females). The incidence based on 207 patients with PIMS-TS out of 233,289 SARS-CoV-2 RT-PCR positive children was 0.9:1,000. The incidence rate was 99.0 (95% CI 86.0, 113.0) per 1,000,000 SARS-CoV-2 RT-PCR positive person-months (0–19 years). The incidence rate differed according to age category as follows: 0–5 years, 136.0 (95% CI 104.0, 174.0); 5–10 years, 140.0 (95% CI 110.0, 173.0); 10–15 years, 72.0 (95% CI 53.0, 96.0); and > 15 years, 42.0 (95% CI 24.0, 68.0) person-months. Using the generalised linear regression model, the frequency of PIMS-TS among SARS-CoV-2 RT-PCR-positive children was lower in the 10–15 years age group (odds ratio (OR) 0.5, 95% CI 0.36, 0.77) and > 15 years (OR 0.3, 95% CI 0.17, 0.52) age group. The estimated OR for girls was nearly half (0.6, 95% CI 0.44, 0.78) that for boys. The data also made it possible to estimate the period between the occurrence of PIMS-TS and the COVID-19 pandemic wave. According to the cross-correlation method, the most likely 3-week interval was found (Supplementary Fig. 2).

Median age at PIMS-TS presentation was 8 years, 132 (63.8%) patients were male and 75 (36.2%) patients were female. Most individuals (196 (94.7%)) were from the Caucasian ethnic group. The demographics, clinical, laboratory parameters, and treatment of patients are summarised in Table 1. The median duration of symptoms before initial treatment was 5 days (range 3–20). Forty-two (20.3%) patients had comorbidities, with the most common being allergies (7.7%) and cardiovascular (2.9%) disorders. An overview of symptom frequency and co-occurrence is displayed in Fig. 2. Among 207 patients, 71 (34.3%) patients had a clearly pathological electrocardiogram: repolarization abnormality ($n = 42$), atrioventricular (AV) block ($n = 11$), and prolonged QTc interval ($n = 2$). Eighty-two (39.6%) individuals had decreased myocardial function and 51 (24.6%) of them required inotropic support. Use of extracorporeal membrane oxygenation was not needed. Only 23 (11.1%) patients had involvement of the coronary arteries. All patients were hospitalised in paediatric departments with accessibility to intensive care monitoring.

Sixty-one (29.5%) patients had early neurological symptoms. The most frequent reported neurological symptoms were meningism ($n = 24$), disorders of consciousness ($n = 21$), headache ($n = 11$), and seizures ($n = 2$). Six children underwent lumbar puncture, five with negative findings and one with cerebrospinal pleocytosis. Three (1.5%) patients had neuroimaging (computed tomography or magnetic resonance imaging of brain), which revealed a spectrum of findings, including extrapontine myelinolysis, bilateral cortical and cortico-subcortical

hyperintensities, cortical swelling (in posterior reversible encephalopathy syndrome (PRES)), arterial thrombosis, and cerebral ischaemia. Two patients (without known associated risk factors) had major left ventricular thrombi with embolization to the cerebral artery. No known deaths occurred in our cohort. Over 1–6 months of follow-up ($n = 161$), 159 patients (98.8%) had normal cardiac function with no residual findings. Only two patients (1.2%) had persistent left coronary artery dilation, but with normal cardiac function.

In addition to the descriptive characteristics, the objective was to identify possible predictors of a severe course of PIMS-TS from two clinical perspectives: primary and secondary healthcare providers. Figure 3 shows the most important predictors for development of myocardial dysfunction in the training dataset. From the general practitioner's standpoint, cardiovascular signs (hypotension, oedema, oliguria/anuria, and prolonged capillary refill), decreased concentration of haemoglobin, elevated concentration of CRP, and thrombocytopenia have been shown to be the strongest predictors of a cardiac impairment (Fig. 3a). On the other hand, among the hospital healthcare providers with wider laboratory possibilities, these predictors were as follows: cardiovascular signs, elevated concentration of BNP, procalcitonin, troponin, or decreased concentration of haemoglobin (Fig. 3b). ROCs showed characteristics of the models in the testing part of the dataset (Fig. 4). The accuracy of the model from the general practitioner's point of view was 0.8 (95% CI 0.64, 0.87, sensitivity 0.6, specificity 0.9) and 0.8 (95% CI 0.70, 0.90, sensitivity 0.7, specificity 0.7) for the hospital healthcare provider.

Discussion

Thanks to a system of nationwide data collection, we succeeded to summarise data of all patients ($n = 207$) that manifested with clinical symptoms of PIMS-TS and were admitted to a hospital in the entire country within a defined time period of 7 months. To our knowledge, this is one of the first and unique published national population-wide cohort allowing to study the epidemiology (including overall incidence), time gap between viral exposure and clinical symptoms of PIMS-TS, and clinical presentations and outcomes within the individual waves of COVID-19 that were characterised by various prevailing genetic variants of SARS-CoV-2. We are aware that the incidence of PIMS-TS to confirmed paediatric infections is likely a gross overestimation of the true incidence (depending on testing strategy and possible asymptomatically infected children).

Several demographic and clinical characteristics were similar to those reported in previous studies, such as median age (8 years), duration of fever (5 days), and predominant severe multisystem involvement during initial illness (including gastrointestinal symptomatology (84.1%)) [6]. Additionally,

male predominance (63.8%), similarly to other published studies (59.0%), was confirmed [6]. A possible explanation is provided by the androgen-dependency of angiotensin-converting enzyme 2, which acts as a receptor for SARS-CoV-2 to enter the cell [10].

In our cohort, one third of patients showed neurological symptoms, similarly to other previously published studies (15.0–40.0%) [4, 11, 12]. Regarding PIMS-TS, both the peripheral and central nervous systems may be affected. Most commonly, signs include headaches, meningism, confusion, seizures, and unconsciousness [13]. In addition, we diagnosed a paediatric patient with PRES as a complication of PIMS-TS [14]. In contrast, several cases of PRES in acute SARS-CoV-2 infection in adults are described [15]. Nervous system damage associated with SARS-CoV-2 infection can occur through both direct and indirect mechanisms. The proposed aetiological mechanisms include the role of cytokines in endothelial cell dysfunction, failure of cerebral autoregulation, and cerebral ischaemia due to thrombosis [12]. Cerebrospinal fluid testing is usually negative [16].

The majority of patients (90.3%) had SARS-CoV-2 IgG-positive serology at admission. This value proves to be an important predictive diagnostic parameter, which partially allows to distinguish PIMS-TS from an acute course of COVID-19 or KD [17]. The diagnostic yield might drop if progressively more children (as the entire population) have been seroconverted through natural infection (or vaccination). Also, the platelet count may be helpful. In a recent report, compared to a "classical" KD cohort, patients with PIMS-TS had lower platelet counts (188×10^9/L versus 383×10^9/L) [18]. Similarly, in our study, the median of platelet count was 172×10^9/L (range 40–831). A possible explanation may lie within varied underlying immunopathogenesis of both diseases, which are currently intensely studied but not yet fully understood [18–20]. Additionally, the age at disease onset differs, being 4–17 years in PIMS-TS versus 0.5–5 years in KD [21]. Some theories suggest to address this age disparity, such as the protective function of the non-atrophied thymus in younger children [22].

Children with PIMS-TS are at risk for AV conduction disease, especially patients with ventricular dysfunction [23]. In our cohort, 34.3% patients were identified with pathological electrocardiogram findings, however, mostly with repolarization abnormalities ($n = 42$). Only ten patients had first-degree AV block, and one patient had second-degree AV block. These abnormal findings did not persist in any patient and were not detected during follow-up (1–6 months later).

COVID-19 is associated with thrombotic complications, but embolic events are rare in children, in contrast with adult COVID-19. Patients with PIMS-TS have the highest incidence (6.5%, in group > 12 years) versus COVID-19 (2.1%) or asymptomatic SARS-CoV-2 infection (0.7%) [24]. In our study, the median of D-dimer concentration was 2,263 µg/L (range 185–35,000), and only two patients (1.2%) had confirmed

Table 1 Patient demographic, clinical and laboratory characteristics, and treatment

Parameter	Normal myocardial function (n = 125)	Myocardial dysfunction (n = 82)	Odds ratio (confidence intervals)
Age, years (median, IQR)	7.0 (4–11)	8.4 (6–12)	1.1 (0.99, 1.12)
Male (n, %)	74 (59.2)	58 (70.7)	0.6 (0.33, 1.09)
Non-Caucasian ethnicity (n, %)	9 (7.2)	2 (2.4)	3.1 (0.65, 14.88)
SDS Height (median, IQR)	0.05 (-0.90–0.93)	0.29 (-0.60–1.04)	1.1 (0.91, 1.43)
SDS BMI (median, IQR)	-0.26 (-0.90–0.70)	-0.39 (-1.010–0.565)	0.9 (0.75, 1.17)
Comorbidities (n, %)	26 (20.8)	16 (19.5)	1.1 (0.54, 2.18)
Duration of fever, days (median, IQR)	4 (3–6)	5 (4–6)	1.0 (0.90, 1.15)
Cervical lymphadenopathy (n, %)	51 (40.8)	32 (39.0)	1.1 (0.61, 1.91)
Mucocutaneous lesions (n, %)	79 (63.2)	54 (65.9)	0.9 (0.50, 1.60)
Rash (n, %)	89 (71.2)	56 (68.3)	1.1 (0.62, 2.11)
Conjunctival injection (n, %)	87 (70.2)	60 (73.2)	0.9 (0.46, 1.61)
Vomiting (n, %)	45 (36.0)	24 (29.3)	1.3 (0.72, 2.43)
Diarrhoea (n, %)	57 (45.6)	38 (46.3)	0.9 (0.53, 1.64)
Nausea (n, %)	51 (42.1)	27 (32.9)	1.5 (0.82, 2.66)
Abdominal pain (n, %)	64 (51.2)	38 (46.3)	1.1 (0.64, 1.99)
Meningism (n, %)	11 (8.8)	13 (15.9)	0.5 (0.22, 1.21)
Headache (n, %)	3 (2.4)	8 (9.8)	0.2 (0.06, 0.89)
Disorders of consciousness (n, %)	9 (7.2)	12 (14.6)	0.5 (0.18, 1.14)
Seizures (n, %)	2 (1.6)	0 (0)	3,838,542.0 (0, Inf)
Normal electrocardiogram (n, %)	96 (76.8)	40 (48.8)	3.5 (1.90, 6.36)
Leukocytes, ×10⁹/L (median, IQR)	9.4 (6.5–12.5)	9.4 (7.0–11.0)	1.0 (0.93, 1.04)
Neutrophils, ×10⁹/L (median, IQR)	7.2 (4.6–9.8)	7.0 (4.5–9.1)	1.0 (0.92, 1.02)
Lymphocytes, ×10⁹/L (median, IQR)	1.1 (0.7–1.7)	0.9 (0.6–1.4)	0.8 (0.62, 1.03)
Haemoglobin, g/L (median, IQR)	114 (108–124)	115 (103–123)	1.0 (0.97, 1.00)
Platelets, ×10⁹/L (median, IQR)	178 (132–243)	163 (114–203)	1.0 (0.99, 1.00)
C-reactive protein, mg/L (median, IQR)	119.6 (70–178)	159.6 (108–212)	1.0 (1.00, 1.01)
Procalcitonin, μg/L (median, IQR)	1.61 (0.71–5.49)	4.90 (1.90–7.96)	1.0 (1.00, 1.04)
ESR (median, IQR)	54 (37–77)	49 (36–73)	1.0 (0.99, 1.01)
Ferritin, μg/L (median, IQR)	297.5 (167.8–575.0)	516.0 (260.0–887.5)	1.0 (1.00, 1.00)
NT-proBNP, ng/L (median, IQR)	1,500 (413–3,877)	5,013 (1,109–15,857)	1.0 (1.00, 1.00)
Troponin I, ng/L (median, IQR)	11.0 (5–46)	45.5 (13–100)	1.0 (1.00, 1.00)
Fibrinogen, g/L (median, IQR)	5.2 (4.5–6.7)	5.4 (4.6–6.2)	0.9 (0.79, 1.13)
D-dimer, μg/L (median, IQR)	1,992 (1,000–4,000)	2,937 (1,414–4,000)	1.0 (1.00, 1.00)
Urea, mmol/L (median, IQR)	3.9 (2.9–5.1)	4.3 (3.3–6.2)	1.1 (1.02, 1.21)
Creatinine, μmol/L (median, IQR)	41 (30–54)	46 (36–61)	1.0 (1.00, 1.02)
Triacylglycerol, mmol/L (median, IQR)	1.57 (1.23–2.13)	2.02 (1.41–2.74)	1.4 (1.00, 1.90)
Lactate dehydrogenase, μkat/L (median, IQR)	4.9 (4.1–5.7)	4.6 (3.8–5.9)	1.0 (0.80, 1.22)
ALT, μkat/L (median, IQR)	0.40 (0.27–0.70)	0.40 (0.26–0.67)	0.8 (0.53, 1.34)
AST, μkat/L (median, IQR)	0.54 (0.41–0.79)	0.49 (0.36–0.81)	0.8 (0.49, 1.40)
Positive epidemiologic contact in patient history (n, %)	88 (70.4)	56 (68.3)	1.1 (0.60, 2.03)
Symptomatology of COVID-19 in patient history (n, %)	38 (30.4)	24 (29.3)	1.1 (0.57, 1.95)
SARS-CoV-2 PCR positive at admission (n, %)	28 (22.4)	13 (15.9)	0.7 (0.31, 1.36)
SARS-CoV-2 IgG-positive at admission (n, %)	108 (86.4)	79 (96.3)	4.1 (1.17, 14.74)
Intravenous immunoglobulin (n, %)	114 (91.2)	76 (92.7)	0.8 (0.29, 2.32)
Resistance for intravenous immunoglobulin (n, %)	13 (10.4)	4 (4.9)	2.3 (0.71, 7.25)
Systemic corticosteroids (n, %)	97 (77.6)	77 (93.9)	0.2 (0.08, 0.61)
Anakinra (n, %)	5 (4.0)	1 (1.2)	3.4 (0.38, 29.81)
Mechanical ventilation (n, %)	3 (2.4)	7 (8.5)	0.3 (0.07, 1.06)
Inotropic support (n, %)	11 (8.8)	40 (48.8)	0.1 (0.05, 0.22)

Data are n (%), median or interquartile range (IQR). All demographic, clinical, and laboratory parameters were taken initially, before any therapeutic interventions. All data were analysed using R statistical software (version 4.0.4). Missing data were imputed using multiple imputation methods within the r package mice (version 3.13.0); missing data in continuous variables were imputed using Predictive Mean Matching Imputation algorithm and categorical variables using Random Forest imputation algorithm. The number of missing values in original dataset were stated in Supplementary Table 2

ALT alanine aminotransferase, *AST* aspartate aminotransferase, *COVID-19* Novel 2019 coronavirus disease (SARS-CoV-2 infection), *ESR* erythrocyte sedimentation rate, *NT-proBNP* N-terminal pro B-type brain natriuretic peptide, *PCR* polymerase chain reaction, *SDS BMI* standard deviation score of body mass index

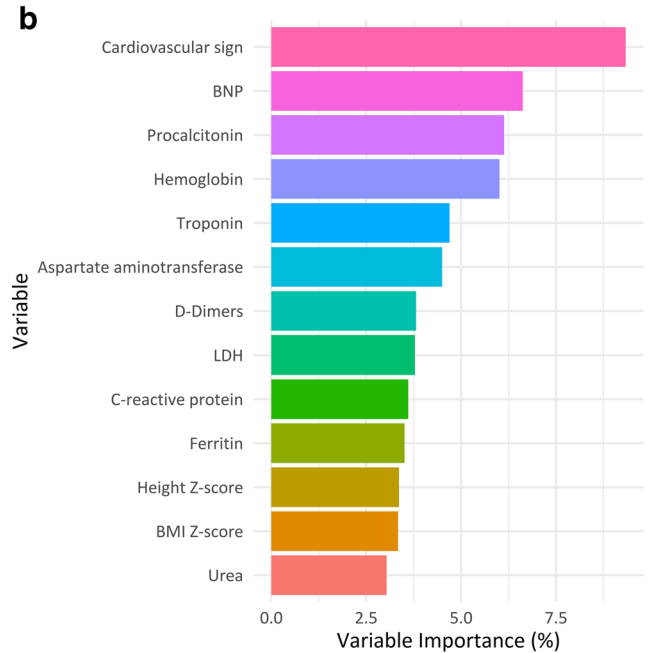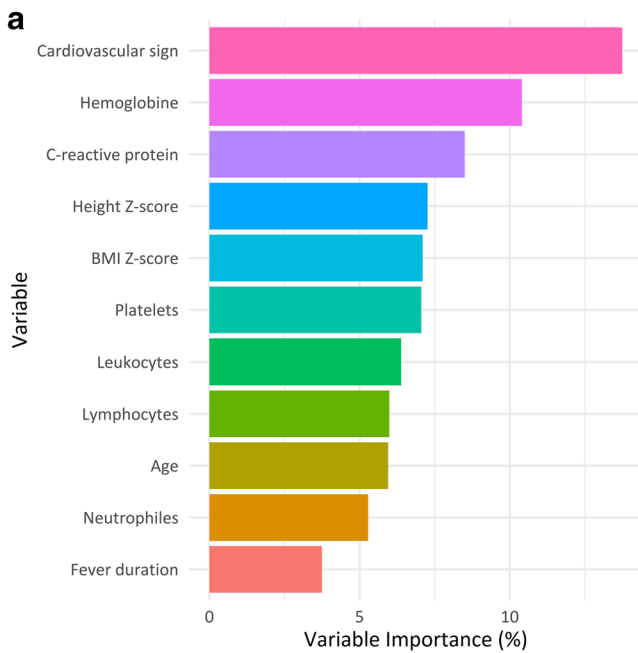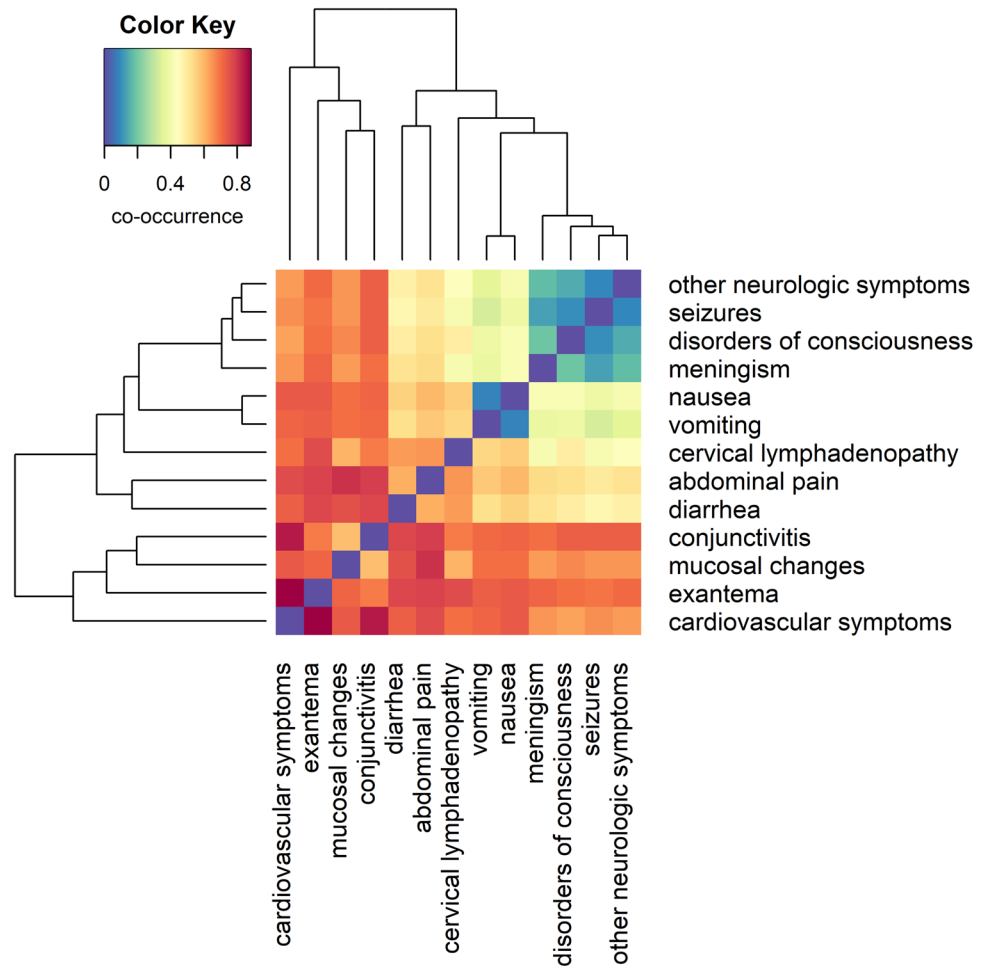**Fig. 2** Overview of symptom frequency and co-occurrence

Fig. 3 The most important predictors for development of myocardial dysfunction according to general practitioners (Fig. 3**a**) and hospital care providers (Fig. 3**b**). Predictors with importance less than 3% were not displayed. BMI = body mass index. BNP = brain natriuretic peptide. LDH = lactate dehydrogenase
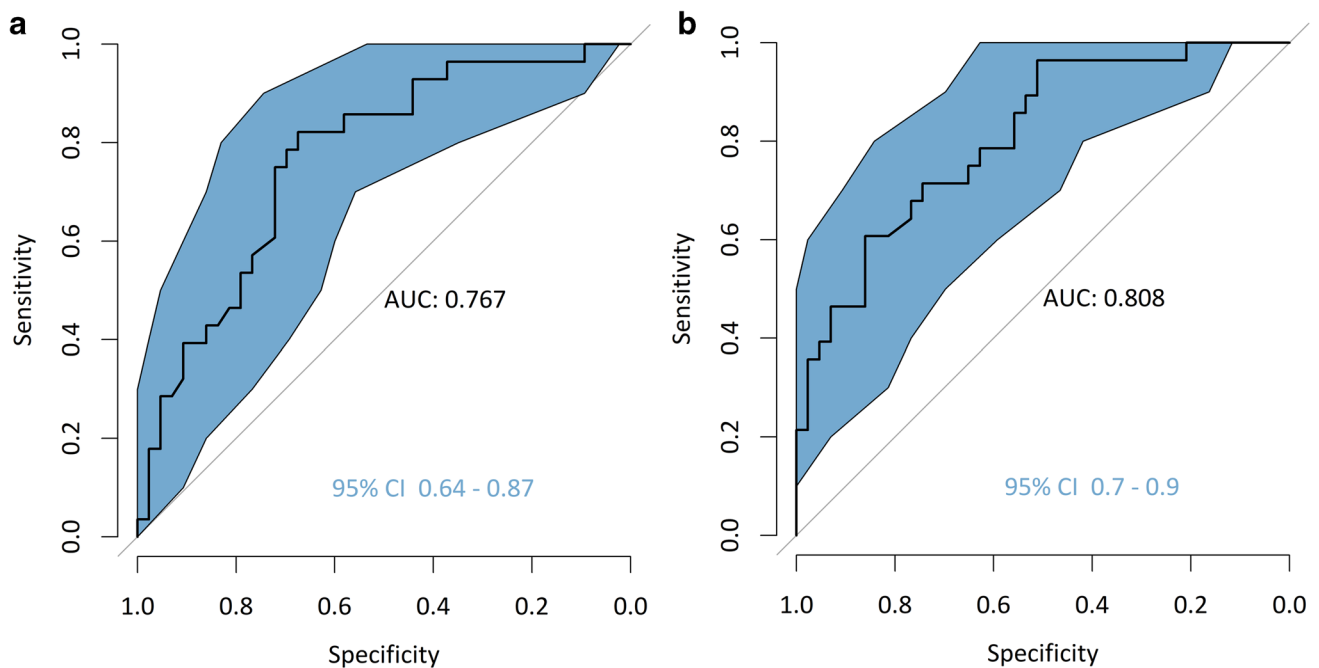
Fig. 4 Receiver operator curves (ROCs) with characteristics of the models on the testing parts of the datasets according to general practitioners (Fig. 4**a**) and hospital care providers (Fig. 4**b**). AUC = area under the curve. CI = confidence intervals

clinically relevant thrombosis (major left ventricular thrombi) at the time of admission: an 8-year-old girl and 17-year-old young man [25]. Both had an unremarkable medical and family history. We can speculate that a low incidence rate in our cohort is due to a combined anticoagulant and antiplatelet treatment that was administered routinely [8].

In a published systematic review on PIMS-TS ($n = 953$), 18 deaths occurred (1.9%) [6]. Unlike in other countries, in CZ, there was no report of a fatal case of PIMS-TS. However, residual cardiac finding was present only in two patients (1.2%, $n = 161$). This is less than the previously published data (7.3%) [6]. Except for one patient with neurological deficit, no other residual morbidity was reported.

In our cohort, 83.0% patients received combined treatment with IVIG (2 g/kg per dose) and systemic corticosteroids. According to local guidelines [8], a dual regimen in corticosteroids dosing was made possible. Higher doses of methylprednisolone (10–30 mg/kg per day) are earmarked for serious/life-threatening conditions. In less severe conditions, a lower dose of methylprednisolone (0.8–2.0 mg/kg per day) may be administered. This combination of IVIG and systemic corticosteroids could be associated with a better course of fever in PIMS-TS and can thus contribute to low morbidity and mortality in our national cohort [26]. It should also be noted that all reported patients were hospitalised in paediatric departments with accessibility to intensive care monitoring. This might have played an important role, due to rigorous monitoring and early detection of disease progression. Also, a later onset of a pandemic in CZ allowed to learn from international experiences.

According to our data, we propose several initial predictors of severe cardiac involvement in patients with PIMS-TS, such as cardiovascular signs, concentration of selected laboratory parameters of inflammation or cardiac impairment. These factors are similar to those reported previously [5, 27, 28]. However, our results allow specifying predictors according to the level of healthcare provider, which may be very beneficial for clinical practice. In particular, for primary care paediatricians, these predictors may be relevant if full PIMS-TS diagnostic criteria are not met and a decision is made on whether to refer the patient for hospital admission. However, it has to be mentioned that the accuracy of these models do not allow strictly selected patients who do not need intensive treatment [28]. Apart from the relatively low number of included patients, the relatively low accuracy could be explained by treatment titration according to actual patient condition.

In summary, individuals from our study had nearly 40.0% decreased myocardial function and 11.1% coronary artery involvement. Over 1–6 months of follow-up ($n = 161$), all patients had normal cardiac function. Only two patients (1.2%) had persistent left coronary artery dilation, which is much less than previously published [6]. It is important to keep in mind that the dilatation of coronary arteries could be a nonspecific consequence of increased coronary blood flow due to higher myocardial oxygen demand caused by febrile illness [29]. We speculate that the use of Z-scores of coronary artery dimensions may perhaps increase the threshold of abnormal findings on echocardiography in PIMS-TS. In a similar way, it

has increased the sensitivity of echocardiographic detection of coronary artery changes in KD [9].

The results of our study may have some practical consequences. Firstly, our data allowed clarification of the incidence of PIMS-TS out of all SARS-CoV-2 positive children, which was 0.9:1,000. Secondly, 3-week intervals in combination with incidence of COVID-19 could help increase pre-test probability of PIMS-TS during pandemic waves in the suspected cases. Thirdly, using information campaigns and an intensive treatment protocol (combined IVIG and systemic corticosteroids), there were no reported fatalities from PIMS-TS within the country in that monitored period. Fourthly, we confirmed predictors of PIMS-TS severity from two clinical perspectives. They may serve as a clue to an early detection of patients at higher risk of developing myocardial dysfunction. Finally, during follow-up, all patients had normal cardiac function. Only two patients (1.2%) had persistent left coronary artery dilation. Additionally, the PIMS-TS incidence this group has found (0.9:1,000 of SARS-CoV-2 positive children) is higher than previously reported [30]. It emphasizes importance of COVID-19 vaccination strategies in young and healthy children.

Study limitations

This study had several limitations that are partly linked to the combined retrospective and prospective design. The data were collected from 17 paediatric departments from all over the country and no specific standardisation of laboratory testing methodology could be done. Despite the online training of all medical staff, mild differences in establishing diagnosis, evaluating clinical findings, and thus individualising treatment procedures cannot be excluded. However, all potential participating hospital staff were trained according to national diagnostic and treatment guidelines. As a nationwide study, validation on an external group was not possible. Also, the exact distribution of SARS-CoV-2 variants in the Czech population was not known, so we could only estimate by dominant variant in individual pandemic waves. The strength of this study includes the country-wide surveillance of all affected patients, detected by a double-checked method, and evaluated on the background of the national epidemiological data on COVID-19.

Abbreviations AV: Atrioventricular; BNP: Brain natriuretic peptide; CI: Confidence interval; COVID-19: The novel 2019 coronavirus disease; CRP: C-reactive protein; CZ: Czech Republic; IHIS: Institute of Health Information and Statistics; IQRs: Interquartile ranges; IVIG: Intravenous immunoglobulin; KD: Kawasaki disease; MIS-C: Multisystem inflammatory syndrome in children; OR: Odds ratio; PIMS-TS: Paediatric inflammatory multisystem syndrome temporally associated with SARS-CoV-2; PRES: Posterior reversible encephalopathy syndrome; ROCs: Receiver operator curves; RT-PCR: Reverse transcription-polymerase chain reaction; SARS-CoV-2: Severe acute respiratory syndrome coronavirus 2

Authors' contributions All authors contributed to the study conception, design, material preparation, and data collection. Analysis were performed by Ondrej Hradsky and Jan David. The first draft of the manuscript was written by Jan David, Ondrej Hradsky, Filip Fencl, and Jan Lebl, and all authors commented on previous versions of the manuscript. All authors read and approved the final manuscript.

Data availability Any reasonable requests to share deidentified data (including study protocol) will be considered by the senior authors and corresponding author subject to institutional agreements and ethics approvals. Data requests should be sent to the corresponding author (jan.david@fnmotol.cz). Authors whose names appear on the submission have contributed sufficiently to the scientific work and therefore share collective responsibility and accountability for the results.

Declarations

Ethics approval The observational study was approved by the Ethics Committee of the University Hospital Motol (number 705/21).

Consent to participate Data were collected from clinical reviews only and further analysed in the anonymous form, consent from patients (parents) was not required.

Competing interests The authors declare no competing interests.

References

1. Institute of Health Information and Statistics of the Czech Republic (2021). https://www.uzis.cz. Accessed 7 May 2021
2. Komenda M, Bulhart V, Karolyi M et al (2020) Complex reporting of coronavirus disease (COVID-19) epidemic in the Czech Republic: use of interactive web-based application in practice. J Med Internet Res 22:e19367. https://doi.org/10.2196/19367
3. Jirincova H, Nagy A (2021) SARS-CoV-2 variant surveillance in the Czech Republic. http://www.szu.cz/uploads/Epidemiologie/Coronavirus/WGS_covid/SARSvariantS_surveillance_final_CZ_ECDC.pdf. Accessed 7 May 2021
4. Feldstein L (2021) Characteristics and outcomes of US children and adolescents with multisystem inflammatory syndrome in children (MIS-C) compared with severe acute COVID-19. JAMA 325:1074–1087
5. Abrams JY, Oster ME, Godfred-Cato SE et al (2021) Factors linked to severe outcomes in multisystem inflammatory syndrome in children (MIS-C) in the USA: a retrospective surveillance study. Lancet Child Adolesc Health 5:323–331

6. Hoste L, Van Paemel R, Haerynck F (2021) Multisystem inflammatory syndrome in children related to COVID-19: a systematic review. Eur J Pediatr 180:2019–2034

7. World Health Organization (2020) Multisystem inflammatory syndrome in children and adolescents with COVID-19. https://www.who.int/publications/i/item/multisystem-inflammatory-syndrome-in-children-and-adolescents-with-covid-19. Accessed 7 May 2021

8. Fencl F, Sibikova M, David J, Malcova H (2021) Pediatric inflammatory multisystem syndrome temporally associated with SARS-CoV-2. Czech guidelines. (in Czech, Syndrom multisystémové zánětlivé odpovědi asociovaný s COVID-19 u dětí. Doporučený postup ČPS ČLS JEP). Ces-slov Pediat 76:4–9

9. McCrindle BW, Rowley AH, Newburger JW et al (2017) Diagnosis, treatment, and long-term management of Kawasaki disease: a scientific statement for health professionals from the American Heart Association. Circulation 135:e927-999

10. Mihalopoulos M, Levine AC, Marayati NF, Chubak BM, Archer M, Badani KK, Tewari AK, Mohamed N, Ferrer F, Kyprianou N (2020) The resilient child: sex-steroid hormones and COVID-19 incidence in pediatric patients. J Endocr Soc 4:bvaa106

11. Chen TH (2020) Neurological involvement associated with COVID-19 infection in children. J Neurol Sci 418:117096

12. Aghagoli G, Gallo Marin B, Katchur NJ, Chaves-Sell F, Asaad WF, Murphy SA (2021) Neurological involvement in COVID-19 and potential mechanisms: a review. Neurocrit Care 34:1062–1071

13. Abdel-Mannan O, Eyre M, Löbel U, Bamford A, Eltze C, Hameed B, Hemingway C, Hacohen Y (2020) Neurologic and radiographic findings associated with COVID-19 infection in children. JAMA Neurol 77:1440–1445

14. Lindan CE, Mankad K, Ram D et al (2021) Neuroimaging manifestations in children with SARS-CoV-2 infection: a multinational, multicentre collaborative study. Lancet Child Adolesc Health 5:167–177

15. Kishfy L, Casasola M, Banankhah P, Parvez A, Jan YJ, Shenoy AM, Thomson C, AbdelRazek MA (2020) Posterior reversible encephalopathy syndrome (PRES) as a neurological association in severe Covid-19. J Neurol Sci 414:116943

16. Lad SS, Kait SP, Suryawanshi PB et al (2021) Neurological manifestations in pediatric inflammatory multisystem syndrome temporally associated with SARS-CoV-2 (PIMS-TS). Indian J Pediatr 88:294–295

17. Rostad CA, Chahroudi A, Mantus G et al (2020) Quantitative SARS-CoV-2 serology in children with multisystem inflammatory syndrome (MIS-C). Pediatrics 146:e2020018242

18. Yeo WS, Ng QX (2020) Distinguishing between typical Kawasaki disease and multisystem inflammatory syndrome in children (MIS-C) associated with SARS-CoV-2. Med Hypotheses 144:110263

19. Sancho-Shimizu V, Brodin P, Cobat A et al (2021) SARS-CoV-2-related MIS-C: A key to the viral and genetic causes of Kawasaki disease? J Exp Med 218:e20210446. https://doi.org/10.1084/jem.20210446

20. Consiglio CR, Cotugno N, Sardh F et al (2020) The Immunology of Multisystem Inflammatory Syndrome in Children with COVID-19. Cell 183:968–981

21. Toubiana J, Poirault C, Corsia A et al (2020) Kawasaki-like multisystem inflammatory syndrome in children during the covid-19 pandemic in Paris, France: prospective observational study. BMJ 369:m2094. https://doi.org/10.1136/bmj.m2094

22. Güneş H, Dinçer S, Acıpayam C, Yurttutan S, Özkars MY (2021) What chances do children have against COVID-19? Is the answer hidden within the thymus? Eur J Pediatr 180:983–986

23. Dionne A, Mah DY, Son MBF et al (2020) Atrioventricular block in children with multisystem inflammatory syndrome. Pediatrics 146:e2020009704

24. Whitworth HB, Sartain SE, Kumar R et al (2021) Rate of thrombosis in children and adolescents hospitalized with COVID-19 or MIS-C. Blood 138:190–198. https://doi.org/10.1182/blood.2020010218

25. Materna O, Koubský K, Pádr R, Janoušek J (2021) Major left ventricular thrombi in an adolescent with COVID-19-associated inflammatory syndrome. Eur Heart J ehab165. https://doi.org/10.1093/eurheartj/ehab165

26. Ouldali N, Toubiana J, Antona D et al (2021) Association of intravenous immunoglobulins plus methylprednisolone vs immunoglobulins alone with course of fever in multisystem inflammatory syndrome in children. JAMA 325:855–864

27. Pignatelli R, Antona CV, Rivera IR et al (2021) Pediatric multisystem SARS COV2 with versus without cardiac involvement: a multicenter study from Latin America. Eur J Pediatr 180:2879–2888

28. Ward JL, Harwood R, Smith C et al (2022) Risk factors for PICU admission and death among children and young people hospitalized with COVID-19 and PIMS-TS in England during the first pandemic year. Nat Med 28:193–200

29. Muniz JC, Dummer K, Gauvreau K, Colan SD, Fulton DR, Newburger JW (2013) Coronary artery dimensions in febrile children without Kawasaki disease. Circ Cardiovasc Imaging 6:239–244

30. Payne AB, Gilani Z, Godfred-Cato S et al (2021) Incidence of multisystem inflammatory syndrome in children among US persons infected with SARS-CoV-2. JAMA Netw Open 4:e2116420. https://doi.org/10.1001/jamanetworkopen.2021.16420

Authors and Affiliations

Jan David[1] · Veronika Stara[1] · Ondrej Hradsky[1] · Jana Tuckova[2] · Katerina Slaba[2] · Petr Jabandziev[2,3] ·
Lumir Sasek[4] · Michal Huml[4] · Iveta Zidkova[5] · Jan Pavlicek[5] · Alzbeta Palatova[6] · Eva Klaskova[6] · Karina Banszka[7] ·
Eva Terifajova[7] · Radim Vyhnanek[8] · Marketa Bloomfield[8,9] · Sarka Fingerhutova[10] · Pavla Dolezalova[10] ·
Lucie Prochazkova[11] · Gabriela Chramostova[12] · Filip Fencl[1] · Jan Lebl[1]

[1] Department of Paediatrics, Second Faculty of Medicine, Charles University and University Hospital Motol, V Úvalu 84, 150 06, Prague, Czech Republic

[2] Department of Paediatrics, Faculty of Medicine, Masaryk University and University Hospital Brno, Brno, Czech Republic

[3] Central European Institute of Technology, Masaryk University, Brno, Czech Republic

[4] Department of Paediatrics, Faculty of Medicine, Charles University and University Hospital Plzeň, Plzeň, Czech Republic

[5] Department of Paediatrics, Faculty of Medicine, University of Ostrava and University Hospital Ostrava, Ostrava, Czech Republic

[6] Department of Paediatrics, Faculty of Medicine, Palacky University and University Hospital Olomouc, Olomouc, Czech Republic

[7] Department of Paediatrics, Faculty of Medicine, Charles University and University Hospital Hradec Králové, Hradec Králové, Czech Republic

[8] Department of Paediatrics, First Faculty of Medicine, Charles University and University Thomayer Hospital, Prague, Czech Republic

[9] Department of Immunology, Second Faculty of Medicine, Charles University and University Hospital Motol, Prague, Czech Republic

[10] Department of Paediatrics and Inherited Metabolic Disorders, First Faculty of Medicine, Charles University and General University Hospital, Prague, Czech Republic

[11] Department of Paediatrics, Regional Bata Hospital, Zlín, Czech Republic

[12] Department of Paediatrics, Regional Hospital, Kolín, Czech Republic

EAACI statement and guideline on the pathogenesis, immunology, and immune-targeted management of the Multisystem Inflammatory Syndrome in Children (MIS-C) or Pediatric Inflammatory Multisystem Syndrome (PIMS).

Wojciech Feleszko [1], Magdalena Okarska-Napierała [2], Emilie Pauline Buddingh [3], Marketa Bloomfield [4], Anna Sediva [4], Carles Bautista-Rodriguez [5,6], Helen A Brough [7, 8, 9], Philippe A. Eigenmann [10], Thomas Eiwegger [11], Andrzej Eljaszewicz [12], Stefanie Eyerich [13], Cristina Gomez-Casado [14], Alain Fraisse [5,6], Jozef Janda [15], Rodrigo Jiméeneéz-Saiz [16,17,18,19], Tilmann Kallinich [20], Inge Kortekaas Krohn [21,22], Charlotte G Mortz [23], Carmen Riggioni [24], Joaquin Sastre [25], Milena Sokolowska [26,27], Ziemowit Strzelczyk [1], Eva Untersmayr [28], Gerdien Tramper-Stranders [29,30]
for the Immunology Section and Working Group Infections of the EAACI

[1] Department of Pediatric Pneumology and Allergy. The Medical University of Warsaw, Żwirki i Wigury 61, 02-091 Warsaw, Poland

[2] Department of Pediatrics with Clinical Assessment Unit, Medical University of Warsaw, Żwirki i Wigury 61, 02-091 Warsaw, Poland.

[3] Department of Pediatrics, Willem-Alexander Children's Hospital, Leiden University Medical Centre, The Netherlands

[4] Department of Immunology, Motol University Hospital, 2nd Faculty of Medicine, Charles University, Prague, Czech Republic

[5] Pediatric Cardiology Services, Royal Brompton Hospital, London, United Kingdom.

[6] National Heart and Lung Institute, Imperial College London, London, United Kingdom.

[7] Paediatric Allergy Group, Department of Women and Children's Health, School of Life Course Sciences, St. Thomas' Hospital, King's College London, London, UK

[8] Children's Allergy Service, Evelina Children's Hospital, Guy's and St.Thomas' Hospital NHS Foundation Trust, London, UK

[9] Paediatric Allergy Group, Peter Gorer Department of Immunobiology, School of Immunology and Microbial Sciences, Guys' Hospital, King's College London, London, UK

[10] Department of Women-Children-Teenagers, University Hospital of Geneva, Geneva, Switzerland.

[11] Division of Immunology and Allergy, Food Allergy and Anaphylaxis Program, The Hospital for Sick Children, Toronto, ON, Canada; Translational Medicine, Research Institute, The Hospital for Sick Children, Toronto, ON, Canada; Department of Immunology, University of Toronto, Toronto, ON, Canada.

[12] Department of Regenerative Medicine and Immune Regulation, Medical University of Bialystok, Bialystok, Poland

[13] Center for Allergy and Environment (ZAUM), Technical University and Helmholtz Center Munich, Munich, Germany

[14] Department of Dermatology, Medical Faculty, University Hospital Düsseldorf, Heinrich-Heine-University Düsseldorf, Düsseldorf, Germany

[15] Faculty of Science, Charles University, Prague, Czech Republic

[16] Department of Immunology, Instituto de Investigación Sanitaria Hospital Universitario de La Princesa (IIS-Princesa), Madrid, Spain

[17] Department of Immunology and Oncology, Centro Nacional de Biotecnología (CNB-CSIC), Madrid, Spain

[18] Faculty of Experimental Sciences, Universidad Francisco de Vitoria (UFV), Madrid, Spain

[19] McMaster Immunology Research Centre, Department of Medicine, McMaster University, Hamilton, ON, Canada

20 Pediatric Pneumology, Immunology and Critical Care Medicine, Charité - Universitätsmedizin Berlin and Deutsches Rheuma-Forschungszentrum (DRFZ), an Institute of the Leibniz Association, Berlin, Germany. Berlin, Germany

21 Vrije Univeristeit Brussel (VUB), SKIN Research Group, Laarbeeklaan 103, 1090 Brussels, Belgium

22 Vrije Universiteit Brussel (VUB), Universitair Ziekenhuis Brussel (UZ Brussel), Department of Dermatology, Laarbeeklaan 101, 1090 Brussels, Belgium

23 Department of Dermatology and Allergy Center, Odense Research Center for Anaphylaxis (ORCA), Odense University Hospital, Odense, Denmark

24 Allergy, Immunology and Rheumatology Division Department of Paediatrics, Yong Loo Lin School of Medicine, National University of Singapore, Singapore

25 Fundacion Jimenez Diaz and CIBER de Enfermedades Respiratorias (CIBERES), Instituto de Salud Carlos III, 28029 Madrid, Spain.

26 Swiss Institute of Allergy and Asthma Research (SIAF), University of Zurich, Davos, Switzerland

27 Christine Kühne - Center for Allergy Research and Education (CK-CARE), Davos, Switzerland

28 Institute of Pathophysiology and Allergy Research, Center of Pathophysiology, Infectiology and Immunology, Medical University of Vienna, Vienna, Austria

29 Dept of Paediatric Medicine, Franciscus Gasthuis & Vlietland, Rotterdam, The Netherlands.

30 Dept of Neonatology, Erasmus MC-Sophia, Rotterdam, The Netherlands

AUTHOURS CONFLICT OF INTEREST DECLARATION:

MANUSCRIPT

[I] Introduction

Since the beginning of the severe acute respiratory syndrome coronavirus 2 (SARS-CoV-2) pandemic, children have been relatively spared from severe coronavirus disease 2019 (COVID-19). In children, COVID-19 is usually asymptomatic or shows mild disease course. Interestingly, despite growing COVID-19 incidence among children due to the emergence of new, more contagious SARS-CoV-2 variants, severe disease develops in a minority of children, mostly those with chronic medical conditions.[1–4] However, in mid-March 2020, physicians in the countries particularly hit by the first COVID-19 pandemic wave, noticed a sudden rise in the number of children with fever and hyperinflammatory multisystem injury quickly progressing to shock.[5–9] This new pediatric entity appeared to develop

approximately four weeks after SARS-CoV-2 infection.[7,10,11] It was named pediatric inflammatory multisystem syndrome temporally associated with SARS-CoV-2 (PIMS-TS)[12] or multisystem inflammatory syndrome in children (MIS-C) [13,14]. Most children with MIS-C demonstrate anti-SARS-CoV-2 antibodies,[11,15–21] which were found to be higher compared to pediatric patients with acute COVID-19. [22] Delayed symptom onset and high antibody titers suggest that MIS-C is a late immunological hyperactivation in response to SARS-CoV-2 rather than a severe presentation of an acute infection.

The clinical and laboratory picture of MIS-C resemble Kawasaki disease (KD), toxic shock syndrome (TSS), and macrophage activation syndrome (MAS) despite some significant differences from those three entities. [23,24] Thus, KD, TSS, and MAS may be seen as essential points of reference when investigating the pathomechanism of MIS-C, its differential diagnosis or treatment.

In response to the emergence of MIS-C, the European Academy of Allergy and Clinical Immunology (EAACI) established a task force (TF) within the Immunology Section in May 2021. The goal of this TF was to describe state-of-the-art immune phenomena in MIS- C and provide guidance to clinicians in the evaluation and management of MIS-C. An international multidisciplinary group was mandated to propose a unified clinical management algorithm to diagnose and treat children with MIS-C.

Clinical guidance generated from this effort is intended to aid in the care of individual patients, without supplanting clinical decision-making. Modifications to treatment plans, particularly in patients with complex conditions, are highly disease-, patient-, geography-, and time-specific, and therefore, these must be individualized as part of a shared decision-making process.

[II] Methodology

TF members were selected by the Task Force leadership (WF, GTS) based on their expertise in basic and clinical immunology, infectious diseases, cardiology, pediatrics, dermatology, and rheumatology, as well as their experience in managing MIS-C and hyperinflammation in acute SARS-CoV-2 infection. The multidisciplinary TF was composed of basic researchers and clinicians from 10 European Countries (A, BE, CH, CZ, D, DK, ES, NL, PL, UK), Canada and Singapore. All specialists who were approached to develop this position paper agreed to participate. Initially, TF members were subdivided into 9 work groups to address the full spectrum of topics related to MIS-C: definition, clinical description, differential diagnosis, role of the virus, immunology (including the role of innate and adaptive immunology), diagnostic evaluation of MIS-C and the treatment of MIS-C with a special focus on immunomodulation and management of hyperinflammation.

During the first round in May 2021, participants agreed with the importance of addressing these topics and the structure of the work groups.

A preliminary guidance document was generated, and the entire TF was given an opportunity to review and edit the final document. Individual approval was obtained from each member on <mark>DD.MM, 2022</mark> and by the EAACI Executive Committee on <mark>DD.MM, 2022</mark>.

[III] Case definition

Several MIS-C case definitions have been published in May 2020[12–14] and are presented in Table 1. As the disease was new and potentially dangerous, the definitions were relatively broad. The World Health Organization (WHO) and Centers for Disease Control and Prevention (CDC) definitions are commonly used in the studies concerning MIS-C. Despite some differences, all published definitions involve six major categories: (i) young age, (ii) fever, (iii) high inflammatory markers, (iv) multisystem injury, (v) exclusion of other plausible diagnoses, and (vi) SARS-CoV-2 exposure. Considering that definitions are broad and SARS-CoV-2 seropositivity is becoming universal, cautious differential diagnosis is crucial in children suspected to have MIS-C.

Table 1. Multisystem inflammatory syndrome in children (MIS-C) definitions according to the Royal College of Paediatrics and Child Health (RCPCH), the Centers for Disease Control and Prevention (CDC), and the World Health Organization (WHO).

		RCPCH (01.05.2020)	CDC (14.05.2020)	WHO (15.05.2020)
1)	**Age**	<18 years	<21 years	<19 years
2)	**Fever**	Persistent	Fever >38.0°C for ≥24 hours	≥3 days
3)	**Inflammation**	↑ CRP, neutrophils and ↓ lymphocytes	≥ 1: ↑ CRP, PCT, ESR, fibrinogen, D-dimer, ferritin, LDH, IL-6, neutrophils. ↓ lymphocytes, albumin	↑ ESR, CRP, PCT
4)	**Multi- (single-) system involvement**	≥ 1: shock, cardiac, respiratory, renal, gastrointestinal, or neurological disorder	≥ 2: cardiac, renal, respiratory, hematologic, gastrointestinal, dermatological, or neurological involvement	≥ 2: muco-cutaneous inflammation signs, hypotension or shock, cardiac involvement, coagulopathy, acute gastrointestinal problems
5)	**Other causes excluded**	Infectious	Infectious and non-infectious	Infectious
6)	**COVID-19 history**	Positive or negative	Positive for SARS-CoV-2 by PCR, serology, or antigen test; or exposure to a suspected or confirmed COVID-19 case within the 4 weeks prior to the onset of symptoms	Evidence of COVID-19 (PCR, antigen test or serology positive), or likely contact with COVID-19 patients with

Additional comments	This may include children fulfilling full or partial criteria for Kawasaki disease	Clinically severe illness requiring hospitalization	

CDC, Centers for Disease Control and Prevention; COVID-19, coronavirus disease 2019; CRP, C-reactive protein; ESR, erythrocyte sedimentation rate; IL, interleukin; LDH, lactate dehydrogenase; PCR, polymerase chain reaction; PCT, procalcitonin; RCPCH, Royal College of Paediatrics and Child Health; SARS-CoV-2, severe acute respiratory syndrome coronavirus 2; WHO, World Health Organization.

[IV] Clinical description

The first reports about MIS-C came from the United Kingdom (UK)[25] and Italy,[6] though the largest cohorts published thus far are from the United States of America (USA),[26–28] where 7880 cases have been registered, as of March 2022.[29] Hundreds of more MIS-C patients have been reported worldwide after that. Intriguingly, there are no MIS-C reports in China, and only five cases were published from Japan.[30]

Published cohorts of MIS-C are heterogenous and challenging to compare due to varying definitions of the disease and its complications, different inclusion criteria, and incomplete data. However, the clinical picture of MIS-C, emerging from those publications, is relatively reproducible (Table 2).

Table 2A. Clinical characteristics of MIS-C children from the largest cohorts published worldwide.

Study ID	Belay, USA[11]	Relvas-Brandt, Brasil[16]	Ciftdogan, Turkey[31]	Ludwikowska, Poland[15]	Flood, UK[17]	Kahn, Sweden[18]	Mamishi, Iran[20]	Garcia-Salido, Spain†[21]	Tiwari, India[32]	Belhadjer, France, Switzerland†[24]	Webb, South Africa[33]
Study time	III.20-I.21	II.-XII.20	XI.20-VI.21	III.20-II.21	III.20-VI.20	XII.20-V.21	III.20-VI.20	III.20-VI.20	III.20-IV.21	III.20-IV.20	-
Case definition used	CDC	WHO	CDC/WHO	WHO	BPSU	WHO	CDC	RCPCH	CDC	‡	-
Number of patients	**1733**	**652**	**614**	**274**	**268**	**133**	**45**	**45**	**41**	**35**	**23**
Age, median (IQR, if available) [years]	9 (5-13)	5	7.4 (3.9-12)	8.8 (5.2-12.1)	8.2 (4-12.1)	9.3 (4.3)§	7 (4-9.9)	9.4 (5.5-11.8)	6.2	10	6.6 (4.8-8.4)
Sex, % male	57.6%	57.1%	57.7%	63%	60%	61%	53%	66.7%	56%	51%	73.9%
Comorbidities, % (No.)	-	**20.1% (131)**	**11.8% (73)**	**18% (38)**	**19% (51)**	-	**13% (6)**	**17.8% (8)**	**20% (8)**	**28% (10)**	-
Clinical picture, % (No.)											
Febrile days before admission, median	-	4	4	5	-	-	-	-	-	-	-
Rash	**55.6% (963)**	-	**54.4% (334)**	**83% (218)**	**52.6% (141)**	**51% (67)**	-	-		**57% (20)**	**87% (20)**
Conjunctivitis	**53.6% (929)**	-	**49.7% (305)**	**78% (207)**	**50.4% (135)**	**52% (69)**	**15.8% (12)**	-	**61% (25)**	**89% (31)**	**65.2% (15)**
Oral inflammation	-	-	**43.1% (265)**	**66% (173)**	**33.2% (89)**	**17% (22)**	**3.6% (2)**	-	**71% (29)**	**54% (19)**	-
Gastrointestinal involvement (any)	-	**87.6% (571)**	**77% (473)**	**93% (250)**	**99.3% (266)**	-	-	-	**27% (11)**	**83% (29)**	-
Respiratory involvement (any)	-	**66% (430)**	**34.6% (216)**	-	**17.9% (48)**	-	**44.7% (34)**	-	**78% (32)**	**34% (12)**	**43.5% (10)**
Neurological involvement (any)	-	**56.1% (366)**	-	**86% (220)**	**32.5% (87)**	-	**18.4% (14)**	-	**51% (21)**	**31% (11)**	**22.7% (5)**
Hypotension	**50.8% (880)**	**27.8% (181)**	**12.1% (74)¶**	**41% (99)**	**42.5% (114)**	-	-	**84.4% (38)¶**	**54% (22)¶**	-	**56.5% (13)**

ECHO findings, % (No.)											
Decreased myocardial contractility	**31%** (484)	-	-	**23%** (58)	**38.4%** (78)	**19%** (23)	-	**48.9%** (22)		**100%** (35)	**34.8%** (8)
Coronary arteries affected	**16.5%** (258)	-	**9.9%** (57)	**8%** (21)	**26.6%** (54)	**16%** (20)	**31%** (14)	**6.7%** (3)		**17%** (6)	**4.3%** (1)
SARS-CoV-2 status, % of tested (No.) unless otherwise											
SARS-CoV-2 PCR positive	**51.1%** (893)	**22.2%** (145)	**9.4%** (56)	**12.6%** (29)	**14.8%** (264)	**36%** (46) ‡‡	**22%** (10)	**40%** (18)		**34%** (12)	-
SARS-CoV-2 serology positive	**82.6%** (1432)	**61.2%** (399)	**94.2%** (520)	**94.5%** (241)	**63.6%** (75)	**80%** (107)	**78%** (35)	**63%** (17)††		**86%** (30)	-

BPSU, British Paediatric Surveillance Unit, CDC, Centers for Disease Control and Prevention, PCR, polymerase chain reaction, SARS-CoV-2, severe acute respiratory syndrome coronavirus 2, RCPCH, the Royal College of Paediatrics and Child Health; WHO, World Health Organization

† The study involved children hospitalized in pediatric intensive care unit (PICU) only

‡ Inclusion criteria: fever >38.5°C, cardiogenic shock or acute left ventricular dysfunction, and CRP >10 mg/dL

§ Mean (+/- SD)

¶ Reported as a shock

†† serology reported only in a subgroup with negative PCR for SARS-CoV-2

‡‡ PCR or antigen positive

Table 1B. Laboratory characteristics, treatment and outcome of MIS-C children from the largest cohorts published worldwide.

Study ID	Belay, USA[11]	Relvas-Brandt, Brasil[16]	Ciftdogan, Turkey[31]	Ludwikowska, Poland[15]	Flood, UK[17]	Kahn, Sweden[18]	Mamishi, Iran[20]	Garcia-Salido, Spain†[21]	Tiwari, India[32]	Belhadjer, France, Switzerland†[24]	Webb, South Africa[33]
Laboratory results, median (IQR, if available), mean (SD) or % (No.) outside normal limit (at respective peaks)											
CRP [mg/dL]	18.1 (10.2-26.1)	-	14 (8.3-20.7)	14 (8.4-19.5)	22.3 (16.2-28.9)	-	6.7 (3-10.2)	22.6	11.9 (7.9)	24.1 (15-31.1)	30 (19.9-36.4)
Procalcitonin [ug/L]	-	-	2 (0.54-9.0)	2.5 (1.0-6.9)	4.7 (1.9-15.9)	-	-	7.5	8.9 (1.6-51)	36 (8-99)	-

D-dimers [ug/L]	2350 (1250-4380)	-	2320 (1122-4241)	2600 (1500-4600)	3400 (1757-6921)	-	3909 (848-4528)	-	2500 (1100-4300)	-	-
Ferritin [ug/L]	475.9 (243-916.3)	-	302 (147-576)	331 (197.9-622.4)	542.6 (284-1049)	-	453 (179-1450)	-	350 (170-733)	-	-
Troponin [ng/mL]	0.06 (0.01-0.3)	-	10 (4-33)	28% (62)‡	-	-	0.6 (0.1-26)	0.06 (0.01-0.2)	50% (6)‡	0.35 (0.19-1.27)	-
NT-proBNP [ng/L]	2789 (491-8405)	-	1420 (355–5193)	86% (171)‡		2024 (461-5984)	-	5532 (1582-12783)	1845 (403–6840)	41484 (35811-52475)	7556 (1240-31225)
Lymphocyte count [x10^9/L]	0.88 (0.5-1.7)	-	1.2 (0.7–2.0)	1.0 (0.7-1.8)	0.8 (0.5-1.7)	-	1.26 (0.66-2.7)	0.7	-	-	-
Platelets [x10^9/L]	134 (94-200)	-	190 (131–285)	176 (127-248)	171.5 (112-266.5)	-	167 (89-275)	119.5	-	-	-
Albumin [g/dL]	-	-	3.43 (3–3.9)	3.3 (2.8-3.7)	2.5 (2.1-3.1)	-	3.4 (3-4.2)	-	2.9 (0.7)	-	-
Treatment and outcome, % (No.) unless otherwise											
Admitted to PICU	58.2% (1009)	44.5% (290)	31.3% (192)	8% (23)	44% (118)	16% (21)	-	100% (45)	-	100% (35)	52.2% (12)
Mechanical ventilation	-	19.6% (128)	13.5% (83)	4% (10)	16.4% (44)		-	13.3% (6)	-	62% (22)	26.1% (6)
Inotropes/vasopressors	-	27.8% (181)	19.1% (117)	-	29.9% (80)	-	-	66.7% (30)	-	80% (28)	39.1% (9)
IVIG	80.5% (1359)	67.9% (418)	93% (571)	93% (238)	70.5% (189)		48% (18)	51.1% (23)	-	71% (25)	100% (23)
Steroids	71% (1230)	62.3% (376)	83.8% (514)	67% (143)	55.6% (149)		60% (27)	80% (36)	-	34% (12)	65.2% (15)

Biologic agents	-	-	**6.4%** (39)	**1%** (3)	**9.3%** (25)	-	-	**24.4%** (11)	-	**8.6%** (3)	**9.1%** (2)
Median hospital stay [days]	-	9	9 (6-12)	-	8 (5-11)	-	8 (6-11)	-	-	10 (8-14)	7 (4.3-11.8)
Death	**1.4%** (24)	**6.4%** (42)	**1.8%** (11)	**0.7%** (2)	**1.1%** (3)	-	**11%** (5)	0	5% (2)	0	0

CRP, C-reactive protein; IQR, interquartile range; IVIG, intravenous immunoglobulin; IVIG, intravenous immunoglobulin; NT-proBNP, N-terminal prohormone of B type natriuretic peptide; PICU, pediatric intensive care unit;

† The study involved children hospitalized in pediatric intensive care unit (PICU) only

‡ Percentage increased

MIS-C presents with fever and multisystem injury, with predominant gastrointestinal and mucocutaneous involvement, and laboratory markers of severe inflammation. Table 3 summarizes the clinical features and laboratory hallmarks of MIS-C, KD, TSS, sepsis, appendicitis, and MAS for differential diagnosis. Despite clinical resemblance to KD, TSS or MAS, MIS-C remains a distinct, unique entity[23,24] (for more details see chapter VII - The role of the virus in the context of other hyperinflammatory diseases).

Table 3. Differential diagnosis of MIS-C

		MIS-C	KD	TSS	Sepsis	Appendicitis	HLH/MAS
CLINICAL FEATURES	Prevailing age group	School-age	Infants and toddlers	Any age	Any age	School-age, adolescents	Any age
	Persistent fever	+++	+++	+++	++	+	+++
	Cheilitis/red lips	++	+++	+	+	0	0
	Nonexudative conjunctivitis	++	+++	+	0	0	+
	Lymphadenopathy	+++	+++	0	+	0	++
	GIS involvement	+++	+/-	++	+	+++	+/-
	Hypotension	++	+/-	+++	++	0	+
	Heart failure	++	+	+/-	+/-	0	+/-
	Coronary aneurysms	+	++	0	0	0	0
LABORATORY MARKERS	Elevated plasma CRP	+++	+++	+++	+++	+++	++
	Elevated plasma Ferritin	+++	+	No data	++	+/-	+++
	Lymphopenia	++	0	0	+++	0	++
	Neutrophilia	++	+++	+++	+++	+++	0
	Thrombocytopenia	++	+/-	+++	++	+	++
	Hypertriglyceridemia	++	++	0	0	0	++

CRP, C-reactive protein; GIS, gastrointestinal system; HLH/MAS, hemophagocytic lymphohistiocytosis/macrophage activation syndrome; KD, Kawasaki disease; MIS-C, multisystem inflammatory syndrome in children; TSS, toxic shock syndrome.
Meaning of symbols: +++ typical; ++ common; + possible; +/- rare; 0 no.

Some children with MIS-C develop life-threatening complications, mostly related to cardiovascular failure, with hypotension and decreased left ventricle contractility[5,6,17,21,23,24,27,34,35]. Older age, black race, higher inflammatory markers, and lower lymphocyte and platelet counts correlate with clinical deterioration and the need for intensive care treatment. [27,34,36] Despite the severe clinical course in a substantial proportion of MIS-C patients, immunomodulatory treatment is highly effective; most children recover within a week, and the mortality rate is relatively low (Table 2B). Coronary artery dilations and aneurysms comprise another significant MIS-C complication, though their prevalence and persistence are difficult to establish. Fortunately, coronary arteries abnormalities seem to resolve in

most patients, too. [19,24,28] This may result from transient coronary dilation due to inflammation and/or histamine release.[37]

Some studies on MIS-C aimed to distinguish separate phenotypes of MIS-C using latent class analysis. Godfred-Cato et al. identified three classes of patients: Class I, with multiorgan failure and shock; Class II, with predominant respiratory involvement, likely overlapping with severe COVID-19 in a fraction of older teenagers, and Class III, characterized by predominant mucocutaneous involvement in the youngest age group, suggestive of KD overlap.[8] Similarly, Flood et al. identified three subgroups of patients: Class 1 – with the most benign clinical course, and Classes 2 and 3, which matched Class III and I, respectively, as described by Godfred-Cato.[17] Also other research groups have described an association between the clinical picture of MIS-C and age, with mucocutaneous involvement more common in younger children and myocarditis more prevalent in the older age group. [10,31,38] On the other hand, Belay et al. found the clinical presentation of MIS-C may depend on the symptomatic course of the preceding SARS-CoV-2 infection. Cardiovascular complications were more common in children who had asymptomatic COVID-19 before developing MIS-C in their cohort.[11]

[V] MIS-A

Although the multisystem inflammatory syndrome is mainly observed in children, adults also might suffer from this condition (MIS-A). Scarcely described in case reports, this condition specifically affects young adults and resembles the childhood condition with a hyperinflammation and extra-pulmonary organ dysfunction. The overlapping symptoms of acute COVID-19 and MIS-A make differentiation of the 2 diagnoses challenging.[39,40]

[VI] Association with SARS-CoV-2 and COVID-19

MIS-C develops three to six weeks after SARS-CoV-2 infection. Waves of MIS-C usually emerge approximately four weeks after the COVID-19 waves observed in the general population (Figure 1). According to Belay et al., 95% of those children who develop MIS-C will generate symptoms within 60 days after experiencing SARS-CoV-2 infection.[11] The preceding infection may be symptomatic or asymptomatic. The risk of developing MIS-C following SARS-CoV-2 exposure is estimated to be 1:3000-4000 based on studies from Denmark,[41] Germany,[42] and the US.[43] The incidence of MIS-C is higher in Black, Hispanic or Latino, and Asian or Pacific Islander children as compared to Caucasians.[43] Interestingly, MIS-C incidence decreases in consecutive COVID-19 waves, possibly due to changing predominant SARS-CoV-2 variants together with growing immunity in the society.[44]
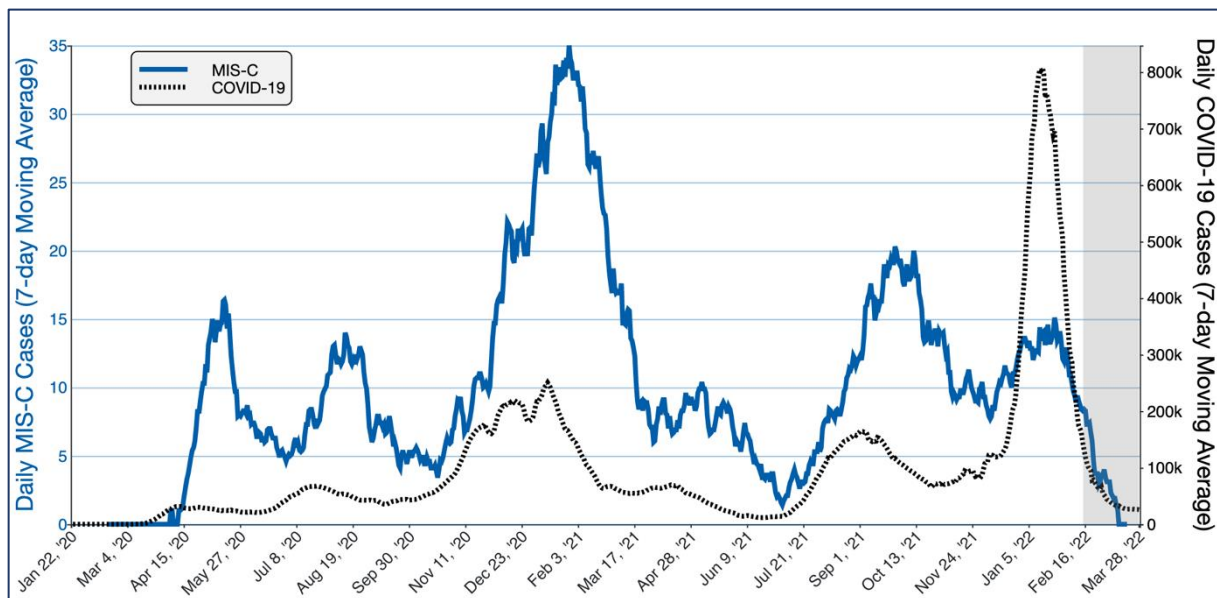
Figure 1. Daily US MIS-C and COVID-19 cases reported to CDC (7-day moving average) (Source: CDC; Materials developed by CDC; https://covid.cdc.gov/covid-data-tracker/#mis-national-surveillance)

Some children (up to 50%) with MIS-C have positive nasopharyngeal polymerase chain reaction (PCR) test results for SARS-CoV-2 (Table 2), whereas the majority (60-95%) have anti-SARS-CoV-2 antibodies. PCR-positive children with MIS-C had significantly higher cycle threshold (Ct) values than patients with acute COVID-19, suggestive of past rather than ongoing infection. [45–47] Importantly, MIS-C and severe acute COVID-19 share some clinical and laboratory characteristics[48] and some children may present with overlapping features of both diseases.[8] Nevertheless, MIS-C differs from acute COVID-19. MIS-C develops in otherwise healthy children as opposed to severe COVID-19, which mainly affects children with chronic conditions. Children with MIS-C are more likely to have cardiovascular and mucocutaneous involvement, whereas respiratory injury is more common in severe COVID-19. Children with MIS-C more often need intensive care than children with severe COVID-19.[28]

[VII] The role of the virus in the context of other hyperinflammatory diseases

Many children with MIS-C fulfill KD diagnostic criteria.[6,8,15,23] KD is a vasculitis that affects mostly children under the age of 5 years.[49] KD is thought to result from a hyperinflammatory response to an environmental factor in a genetically susceptible host. No single factor triggering KD has been identified till now, but an infectious agent can be a potential causative factor. With a peak in winter and early spring, the incidence of seasonal KD matches seasonal waves of viral infections. Interestingly, various undefined antigens and particles of possible viral origin have been found in the tissues of KD children.[50,51]

Similarly, SARS-CoV-2 antigens were detected in the tissues of several organs (lungs, heart, kidneys, liver, spleen, and brain) of children who died from MIS-C.[52] This surprising finding suggests a direct effect of SARS-CoV-2 on the tissues involved in the hyperinflammatory reaction. Persistent immune dysfunction or exhaustion induced by chronic antigen exposure is one of the proposed mechanisms.[53,54]

MIS-C shares many clinical features with TSS, particularly highly prevalent gastrointestinal involvement, peripheral edema, hypotension, and mucocutaneous signs. TSS results from massive T-cell activation and cytokine production in response to staphylococcal or streptococcal toxins with superantigenic properties.[55] A superantigenic pathomechanism has been hypothesized in MIS-C as well. Through structure-based computational modeling, Noval-Rivas et al. identified a motif near the S1/S2 cleavage site of the SARS-CoV-2 spike protein that resembled the staphylococcal enterotoxin B of *Staphylococcus aureus*.[56] Uncontrolled cytokine production in response to SARS-CoV-2 spike protein could be involved in both severe COVID-19 and MIS-C pathogenesis. Indeed, severe COVID-19 adult patients presented a T cell receptor (TCR) β chain skewing towards fragments that can be bound by superantigens.[57]

[VIII] Vaccination and MIS-C

The introduction of COVID-19 vaccinations in children did not result in rise of MIS-C cases in the USA[29] and case reports of vaccine-induced MIS (called MIS-V) are only anecdotal.[58,59] Moreover, Pfizer-BioNtech vaccine was found to be 91% effective in preventing MIS-C in adolescents 12-18 years old.[60] Similar findings were observed in teenagers in France, too.[61] Interestingly, rare cases of MIS-C despite previous COVID-19 vaccination in teenagers seem to be of milder clinical course, with no need for intensive care.[60] Vaccine-induced immunity may play a role in decreasing MIS-C incidence in consecutive COVID-19 waves and some authors predict that in future MIS-C will be a rare disease affecting only young unimmunized children, similarly as KD.[44]

There are many knowledge gaps though; it is still unclear whether vaccine-induced protection against MIS-C applies to younger age groups, how long it lasts and whether it is going to be as effective in newly emerging SARS-CoV-2 variants.

Despite unknown risk of either re-infection with SARS-CoV-2 or COVID-19 vaccination after MIS-C, CDC experts consider benefits from COVID-19 vaccination to outweigh its risks in children after MIS-C. The recommended interval from MIS-C diagnosis to COVID-19 vaccination is at least 3 months.

> **CLINICAL STATEMENT 1.**
>
> **COVID-19 vaccination is a safe and effective prophylaxis of MIS-C. Children who underwent MIS-C may be vaccinated against COVID-19 at least 3 months since MIS-C diagnosis.**

[IX] Immunology of MIS-C

An abnormal immune response plays a central role in MIS-C. In the following section, we discuss hypotheses on MIS-C pathogenesis and the contribution of innate and adaptive immunity to inflammation. Although these three systems are deeply interrelated, for simplicity, the innate, the adaptive humoral, and cellular responses are considered separately.

**9.1. Four main hypotheses for the pathogenic etiology of MIS-C (Figure 2)**

The first hypothesis is based on the above-mentioned superantigenic properties of protein S.[56,57,62] Superantigen-induced generalized and polyclonal T cell activation leads to cytokine storm and multiorgan injury which clinically resembles TSS. Interestingly, a profound expansion of *TRBV11-2* gene corresponding to superantigen-specific TCR skewing, was found in CD4(+) T cells of children with MIS-C.[62,63] Moreover, polyclonal *TRBV11-2* expansion was correlated with HLA class I alleles A02, B35, C04, which may reflect genetic susceptibility to such uncontrolled immunologic response to SARS-CoV-2.[63]

The second hypothesis involves a chronic inflammatory response to continuous viral antigen exposure and subsequent T-cell exhaustion due to prolonged antigenic stimulation.[53,54,64] Both transcriptional signatures[65] and surface markers of T cells exhaustion[64] were found in children with MIS-C.

The third hypothesis regards involvement of the gastrointestinal tract. Severe gastrointestinal symptoms have been observed in 90% of MIS-C patients, likely due to the extended presence of SARS-CoV-2 in the gastrointestinal tract,[66] which may lead to increased intestinal permeability and viral translocation into the circulation. This theory is supported by increased concentration of zonulin – serum marker of intestinal barrier disfunction – in children with MIS-C.[66]

Finally, a fourth plausible mechanism involves the production of autoantibodies, as indicated by several reports. Clinical data have demonstrated not only increased percentages of CD19+CD27+CD38+ plasmablastic cells during the acute period of the disease,[64,67] but also elevated levels of specific target autoantibodies in patients with MIS-C. Their generation may result from the tissue damage, but also may be regarded as one of the triggers of the disease. These potential markers of an autoimmune response include autoantibodies directed against myocardial tissue, endothelium, gastrointestinal epithelium, cellular immune mediators, and endoglin, which maintains the structural integrity of arteries. [53,68,69]

Equally plausible is the sequential succession of these four mechanisms, that is: the initial persistence of the virus in the gut, which leads to antigenemia, with the abundance of superantigens and prolonged, excessive activation of immune mechanisms with autoantibody generation.

Figure 2. Descriptive flowchart synthesizing the hypothesized immunologic mechanisms underlying the development of multisystem inflammatory syndrome in children (MIS-C).
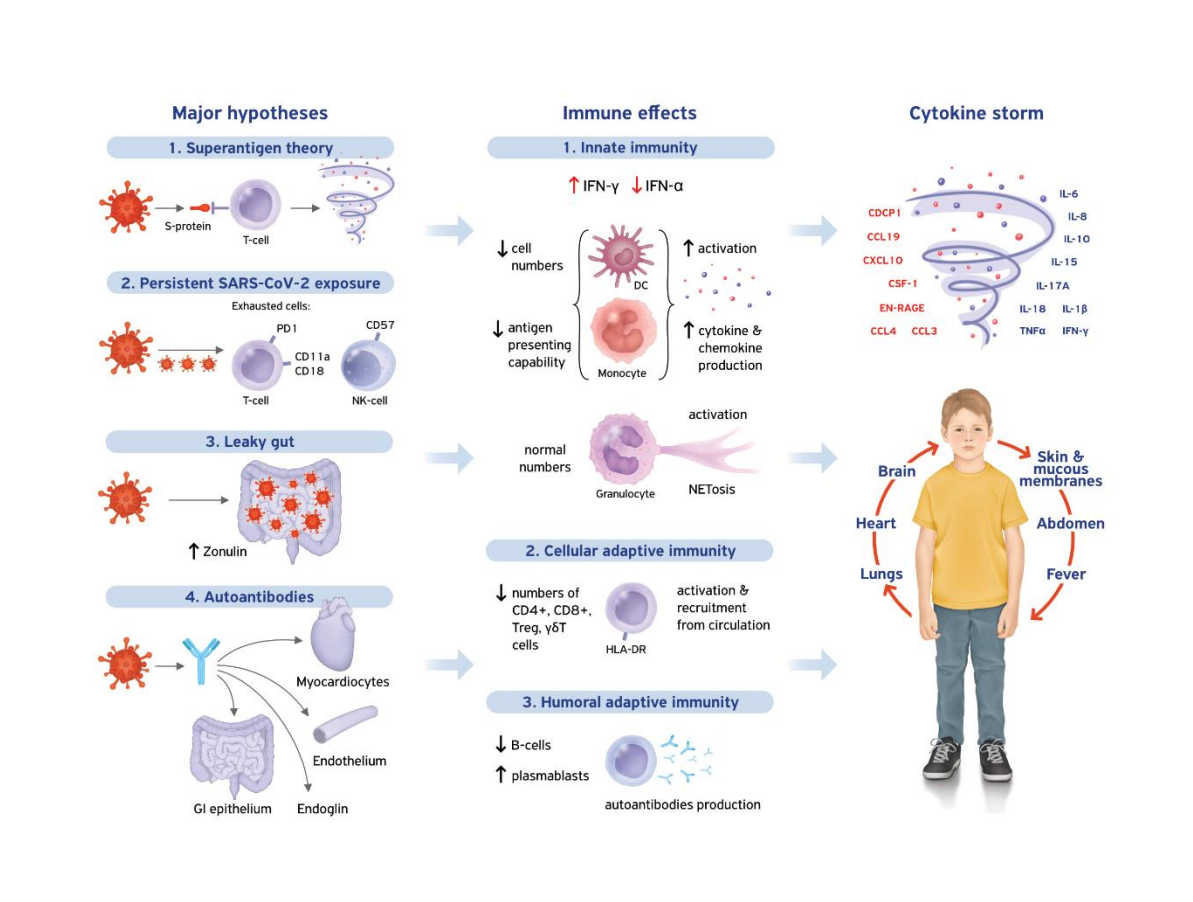
CCL, C-C motif ligand; CD, cluster of differentiation; CDCP1, CUB domain-containing protein 1; CSF, colony stimulating factor; CXCL C-X-C motif ligand; DC, dendritic cell; EN-RAGE, extracellular receptor for advanced glycation end products binding protein; HLA, human leukocyte antigen; IFN, interferon; IL, interleukin, IL-1RA = interleukin-1 receptor antagonist; NK, Natural Killer; PD, programmed cell death protein, SARS-CoV-2, severe acute respiratory syndrome coronavirus 2; TNF, tumor necrosis factor.

9.2. Contribution of innate immunity to MIS-C pathology

The role of the innate immune system in MIS-C is complex. Imbalanced interferon (IFN) signaling pathways, depletion and concomitant hyperactivation of dendritic cells (DCs) and monocytes, together with activated neutrophils contribute to cytokine storm and hyperinflammation.

I.   **The role of IFNs**

Several studies underline the central role of IFN-γ in MIS-C pathogenesis. IFN-γ concentration correlates with the disease severity[70] and IFN-γ-induced chemokines, CXCL9 and CXCL10 are disproportionately high in MIS-C patients.[62,71,72] The cytokine profiles of children with MIS-C are characterized by elevated IFN-γ, IL-18, GM-CSF, CCL5, CXCL9 and CXCL10, and inflammatory monocyte activation markers including MCP-1, IL-1α, and IL-1RA.[70,72] This cytokine profile positions an IFN-γ induced response as the main trigger of inflammation. In addition, an important negative regulator of IFN-γ mediated immunity, TWEAK (TNF-like weak inducer of apoptosis), is downregulated in acute MIS-C patients.[69]

On the other hand, MIS-C is characterized by depleted type I IFN response, possibly due to decreased frequencies of plasmacytoid dendritic cells (pDCs) which constitute the major source of IFN-α.[53,72,73] Low levels of IFN-α correlate with severe course and poor outcome of acute COVID-19 in adult patients.[74,75] Interestingly, haploinsufficiency in suppressor of cytokine signaling (SOCS) 1, an essential negative regulator of type I and type II IFN signaling, was identified in some children with MIS-C.[76,77]

II.   The role of dendritic cells and monocytes

An inflammatory profile with reduced numbers of circulating myeloid (conventional) and plasmacytoid DCs, and monocytes in MIS-C patients were reported by different groups.[53,72,73] Moreover, de Cevins et al. showed significant heterogeneity in classical and intermediate monocytes in severe MIS-C cases.[73] Using multiparametric large-scale analyses, they found upregulated TNF signaling, overexpression of HIF-1a, low type I and II IFN responses, and decreased expression of NF-κB inhibitors, specifically in monocytes and DCs. Thus, it is possible that sustained NF-κB signaling leads to overexpression of monocyte and DC-derived inflammatory mediators that are crucial in the severe phase of MIS-C. In fact, classical monocytes from MIS-C patients showed increased CD64 and CD54 expression concomitant with CD14 and TLR4 downregulation, characteristic for activated cells and cytokine production.[67,73,78] Notably, MIS-C, like other cytokine storm syndromes, such as KD, is manifested with elevated levels of monocyte-derived and DC-derived inflammatory mediators, including cytokines (IL-1α, IL-6, IL-8, IL-10) and chemokines (CXCL9, CXCL10, CCL2, CCL3, CCL4, CCL19, CDCP1, and CSF-1).[53,69,71,72] Furthermore, decreased levels of costimulatory molecules and HLA-DR in monocytes and DCs, indicate impaired antigen presentation capacity, which affects the development of adaptive immunity.[67]

III.   The role of natural killer cells and neutrophils

Both children with MIS-C and acute COVID-19 had reduced numbers of natural killer (NK) cells, cytolytic NK subset, and unconventional mucosal associate invariant T-cells (MAITs), whereas innate lymphoid

cells frequencies are similar to those in healthy adults.[64] Similarly, transcriptional signatures of exhausted CD56^{dim}CD57^{+} NK cells were found in MIS-C patients.[65]

Carter et al. demonstrated that absolute neutrophil counts were similar during the acute, resolution and convalescence phases of MIS-C and comparable to counts in healthy controls.[79] However, neutrophils of MIS-C patients had an increased expression of CD64 combined with a decreased expression of CD10 during the acute phase, indicating neutrophil activation and a reduction of mature neutrophils.[79] The acute pediatric COVID-19 neutrophil response is governed by a robust anti-viral interferon-stimulated gene signature.[80] However, the MIS-C neutrophils demonstrate a different phenotype. Boribong et al. found a strong granulocytic myeloid-derived suppressor cell (G-MDSC) enrichment with altered metabolism towards activation degranulation, reactive oxygen species (ROS) generation and formation of neutrophil extracellular traps (NETosis).[72,80] NETosis, which can be stimulated by immune complexes of S protein with specific anti-S antibodies,[80] contributes to vascular damage.[72] Thus, given the possible antigenemia due to the leaky gut theory in MIS-C pathogenesis, chronic intravascular neutrophil activation and NETs formation may be directly linked to endothelial damage and cardiovascular complications. Therefore, neutrophils may play a crucial role in the pathogenesis of MIS-C.

IV.   Hyperinflammation in MIS-C

Several studies investigated the plasma proteome in MIS-C patients highlighting an increase in IL-6, IL-8, IL-10, IL-15, IL-17A, IL-18, IL-1β, TNF-α and IFN-γ. [47,53,67,81] In addition, chemokines important for NK-/T-cell (CCL19, CXCL10) and monocyte/neutrophil (CCL3, CCL4) recruitment and factors for their differentiation and activation (EN-RAGE, CSF-1) were enhanced.[53,69] Further, soluble PD1-L1 and IL-18R1 were increased pointing to immune exhaustion and reflecting a host-driven immune compensation.[53] Interestingly, hyperinflammation in MIS-C patients was not driven by CXCL-8 as it is the case in adult COVID-19.[82]

9.3. Humoral Adaptive Immunity

Pronounced lymphopenia has been consistently observed in MIS-C children. [23,67,83,84] In the acute phase of the disease, total B cell numbers are decreased.[67,83] The frequencies of naïve-, CD27-IgD-, non-switched, and switched memory B cells do not differ between active pediatric COVID-19 and MIS-C.[64,67] Although MIS-C develops late after acute infection, the frequency of plasmablasts is still as high as in the active COVID-19 patients indicating ongoing and prolonged humoral responses in MIS-C. [64,67] The frequencies of follicular T helper cells (Tfh) are unaltered. However, the expression of the Tfh homing

chemokine CXCR5 is reduced on these cells, indicating potential alterations in the generation of germinal centers and subsequent humoral responses.[64]

Interestingly, several reports indicated the presence of autoantibodies in MIS-C.[53,68,69] The autoantibody profile consisted of target structures already known e.g., lupus erythematosus or Sjogren's disease (anti-La, anti-Jo-1)[53] or hereditary hemorrhagic telangiectasia (anti-endoglin) [69] and of several proteins not attributed to auto-inflammation. Autoantibodies targeting myocardial and endothelial tissue, as well as gastrointestinal epithelium and cellular immune mediator targets, were also identified.[53] However, it must be determined if the occurrence of autoantibodies is a direct effect of SARS-CoV-2 infection or an epiphenomenon due to substantial tissue damage.

9.4. Cellular adaptive immunity

In line with reduced B cell numbers in MIS-C patients, also the total number of T cells is lower than in healthy controls and is restored during clinical improvement.[53,67,83,84] Noteworthy, shifts in lymphocyte counts in MIS-C correlate with the disease severity markers, particularly hypotension.[53,67,83,84] A general lymphopenia results from a decreased numbers of T helper cells (CD4+), cytotoxic T cells (CD8+), γδ T cells and Treg cells.[67,84] The antiviral and cytotoxic γδ T cells expressed higher HLA-DR levels in the acute phase of MIS-C, suggestive of cell activation.[53,67] Also naïve memory CD4+CCR7+T cells expressed high amount of HLA-DR in the acute phase of MIS-C.[67] However, overall relative distribution of all T cell subpopulations seem to be normal in MIS-C patients. Importantly, all those subpopulations returned to control levels during clinical improvement or convalescence.[67,83] In a few MIS-C patients, increased phosphorylation of Signal Transducer and Activator of Transcription (STAT3) in naïve and memory CD4+ and CD8+ T cells was noted.[53] In addition, serum protein profiling revealed a profound induction of cytokines and chemokines responsible for recruiting T cells from circulation and modifying their functions, such as CCL19, CXCL10, and CDCP1, in MIS-C patients.[53,72]

CLINICAL STATEMENT 2.

The immunological mechanism leading to MIS-C is unclear and depends on activating multiple pathways leading to hyperinflammation. The treatment should include immunosuppressive agents, such as glucocorticosteroids (GCS) or high-dose intravenous immunoglobulins (IVIG).


[X] Diagnostic Workup

Diagnosis of MIS-C is based on the characteristic constellation of clinical, laboratory, and imaging findings and exclusion of other infectious and non-infectious causes of hyperinflammation.

Epidemiological context is important – diagnosis is more likely at the time of the MIS-C wave. However, it cannot be excluded at a time of low COVID-19 incidence.[17,85] Diagnostic workup in MIS-C patients aims at confirming the diagnosis and assessing the extent of multiorgan involvement. Here, we propose a simple diagnostic algorithm (Figure 3). Most MIS-C patients exhibit some degree of cardiac involvement. The most severe manifestation is left ventricle systolic failure and subsequent cardiac shock.[86] Therefore, every patient with high MIS-C suspicion should have immediate (preferably within 12 hours from admission) electrocardiography (ECG) and echocardiography (ECHO) performed. The frequency of subsequent ECGs and ECHOs should be consulted closely with a pediatric cardiologist, preferably at least every 2-3 days during the acute phase of the disease. After hospital discharge, follow-up studies should be performed within 1-2 and 4-6 weeks with further monitoring for selected patients.

CLINICAL STATEMENT 3.

MIS-C diagnosis is based on clinical and laboratory picture with exclusion of other plausible diagnoses. Prompt and regular electro- and echocardiographic evaluation is particularly important.

Figure 3. Diagnostic workup in patients suspected for MIS-C.
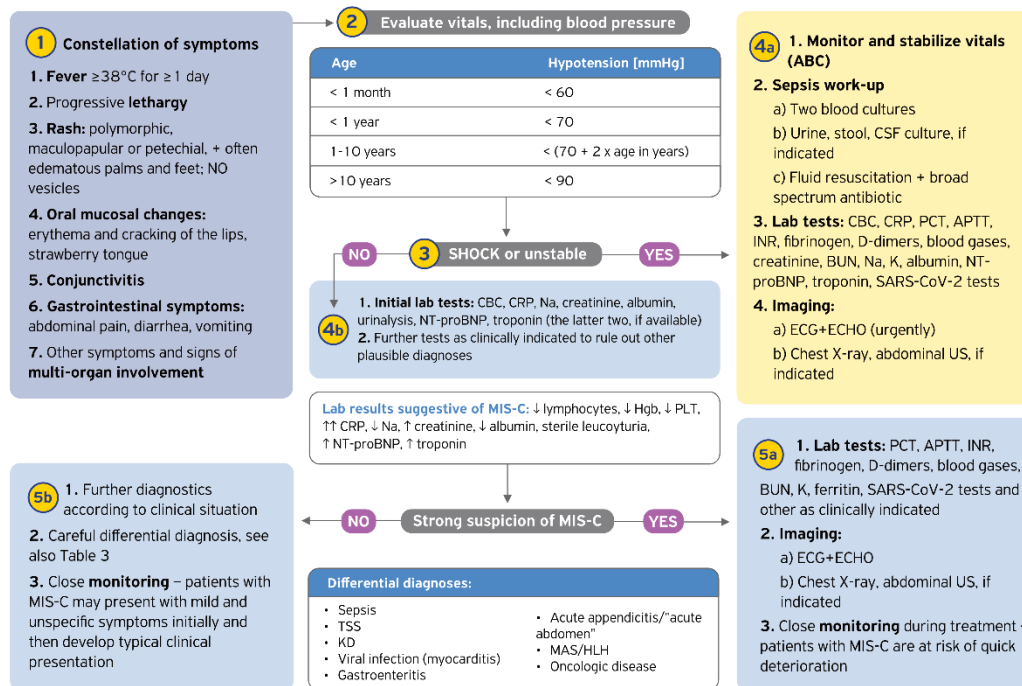
APTT, activated partial thromboplastin time; BUN, blood urea nitrogen; CBC, complete blood count; CRP, C-reactive protein; CSF, cerebrospinal fluid; ECG, electrocardiogram; ECHO, echocardiogram; Hgb, hemoglobin; INR, international normalized ratio; K, potassium; KD, Kawasaki disease; MAS/HLH, macrophage activation syndrome/ hemophagocytic lymphohistiocytosis; MIS-C, multisystem inflammatory syndrome in children; Na, sodium; NT-proBNP, N-terminal prohormone of natriuretic peptide type B; PCT, procalcitonin; PLT, platelets; SARS-CoV-2, severe acute respiratory syndrome coronavirus 2; TSS, toxic shock syndrome; US, ultrasonography

[XI] MIS-C treatment

Immunomodulation has been the mainstay of MIS-C treatment since the first reports concerning the disease [5,17,23,28]. However, MIS-C therapy is complex and involves anti-thrombotic therapies, anti-microbials in the suspicion of sepsis, and all sorts of organ dysfunction support. There are several published guidelines on MIS-C patients management, though all of them are based on observational studies.[87–90] Here we focus on immunomodulatory and anti-thrombotic therapies in MIS-C.

11.1. Immunomodulation

The post-infectious, immunological nature of MIS-C, hyperinflammatory character, and its close clinical resemblance to KD formed the basis for MIS-C treatment with intravenous immunoglobulin (IVIG) and glucocorticosteroids (GCS).

I. IVIG

IVIG in a dose ranging from 1 to 2 g/kg and, according to some sources, not exceeding 100 g has been used in most MIS-C patients (see Table 2). On the one hand, coronary arteries aneurysms (CAAs) have been reported as a complication of MIS-C[17,23,28,36] and, on the other, IVIG has a well-documented efficacy in reducing the risk of CAAs in KD.[91] However, neither the exact risk of CAAs in MIS-C is known nor IVIG efficacy in this indication. Unlike in KD, most patients with MIS-C receive GCS (Table 2), which could be partially due to unsatisfactory response to IVIG alone. Nevertheless, IVIG is included in most recommendations as a first-line treatment (Figure 4).[87–90]

Figure 4. Treatment algorithm for MIS-C
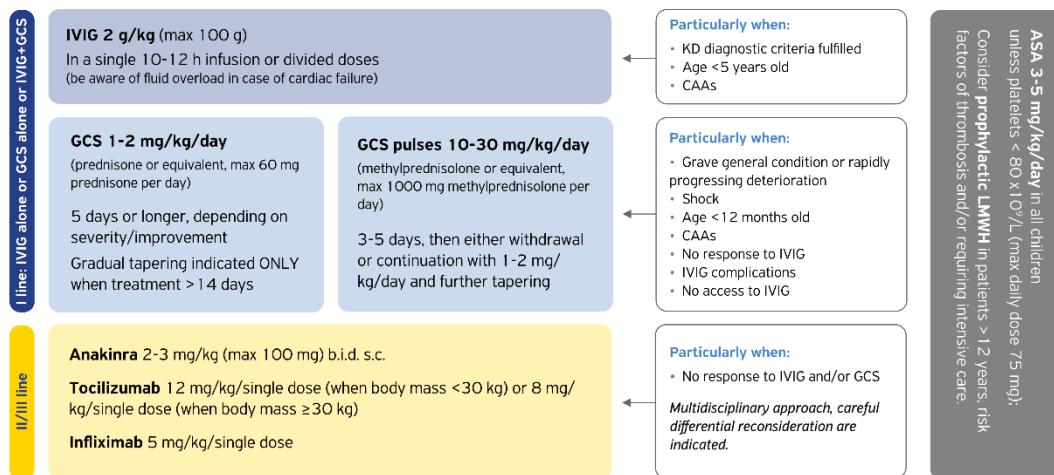
ASA, acetylsalicylic acid; B.i.d., twice a day; CAAs, coronary arteries aneurysms; GCS, glucocorticosteroids; IVIG, intravenous immunoglobulins; LMWH, low molecular weight heparin; MIS-C, multisystem inflammatory syndrome in children; KD, Kawasaki disease; PLT, platelets; s.c., subcutaneous

II. GCS

GCS administered either as prednisolone (2 mg/kg/day) or pulsed methylprednisolone (10-30 mg/kg/day for 1-3 days), are used as a first-line treatment in patients with shock or particularly severe disease and as a second line in non-responders to IVIG.[87–90] Interestingly, in an Italian study, GCS were used as a single first-line treatment in MIS-C, and 74% needed no step-up therapy.[92] The optimal GCS treatment length is also debatable. Whereas some of the guidelines recommend stepwise dose reduction within 2-3 weeks,[76–79] in a study by Ouldali, most patients received five days of therapy, which appeared effective, too.[93]

Several retrospective studies comparing different treatment strategies with IVIG, and GCS were published in 2021. Ouldali et al. compared IVIG alone to combined IVIG and GCS as first-line therapy.[93] They found that IVIG alone was associated with a higher risk of treatment failure and progression to cardiovascular complications. Similar results were revealed by the Overcoming COVID-19 Investigators group. They observed that initial IVIG and GCS treatment was associated with a lower risk of new or persistent cardiovascular dysfunction than with IVIG alone.[94] In contrast, the British Best Available Treatment Study group (BATS) found no significant difference between three primary treatment options: IVIG alone, GCS alone, or combined IVIG and GCS, in terms of recovery from the disease.[95] These discrepancies may be due to different inclusion criteria, different disease severity (with a milder course in patients included in the BATS), and different outcomes measured. What is particularly interesting is that in a smaller study from the UK involving pediatric intensive care unit (PICU) patients only, no short-term benefit from any kind of treatment was found compared to supportive treatment only.[96] It must be emphasized that MIS-C severity may vary in different populations, as was found by Polish authors.[36] Thus, the immunomodulatory treatment strategy may need to be adjusted to a specific population.

CLINICAL STATEMENT 4.

In the light of current knowledge, either intravenous immunoglobulin (IVIG) alone, glucocorticosteroids (GCS) alone, or both IVIG and GCS, are acceptable I-line therapy in children with MIS-C.

CLINICAL STATEMENT 5.

IVIG is particularly indicated in young children with Kawasaki disease phenotype and cases of coronary artery aneurysms. GCS are particularly indicated in children with the grave general condition, rapidly progressing deterioration, and shock.

11.2 Biological treatment

A minority of patients with MIS-C do not respond to IVIG and GCS and receive immunosuppressive biological agents (e.g., human interleukin-1 receptor antagonist (anakinra), humanized monoclonal antibody against the interleukin-6 receptor (tocilizumab), a chimeric monoclonal antibody that blocks TNF-α (infliximab)). Of particular importance, before initiating such treatment, a multidisciplinary consultation should take place to rule out other possible diagnoses that may underlie such an unusual clinical presentation.[89] Anakinra appears to have an advantage over other alternatives due to its

shorter half-life and upstream effects. For this reason, its use may be preferable to other biologics, particularly in an off-label situation and due to the safety reasons of using biologicals in young children.

CLINICAL STATEMENT 6.

Biological treatment is the II/III-line treatment in MIS-C. It should always be preceded by careful differential re-evaluation and multidisciplinary consultation. Anakinra is a preferable biological agent for children with MIS-C.

11.3 Anti-thrombotic treatment

Thrombotic complications have been observed since the earliest reports about MIS-C[5,17,97], and laboratory markers of coagulopathy (high D-dimers and fibrinogen, low platelets) are typical for this hyperinflammatory disease.[17,23,28] Whitworth et al. found that age ≥12 years, cancer, central venous catheter, and MIS-C were independent risk factors for thrombosis in children hospitalized for COVID-19 and/or MIS-C.[97] According to the guidelines, anti-coagulation prophylaxis with low molecular weight or unfractionated heparin should be administered based on individual risk profiles (including obesity, immobility, history of thrombo-embolism and other known risk factors), with patients hospitalized in intensive care units considered the most vulnerable.[87–90]

On the other hand, due to similarities to KD mentioned above, anti-platelet low-dose aspirin (3-5 mg/kg/day, maximum dose of 75 mg) is recommended in all children with MIS-C unless they have active bleeding or their platelet level falls <80.000/μL.[87,89,90]

CLINICAL STATEMENT 7.

Anti-thrombotic prophylaxis involves routine acetylsalicylic acid (ASA) in an anti-platelet dose unless contraindicated and low molecular weight or unfractionated heparin in selected cases with an elevated risk of thrombotic complications.

[XII] Follow up

Despite MIS-C being a life-threatening condition, the overall outcome appears to be good across the reported cohorts (see Table 2A). However, long-term data are scarce. While a substantial proportion of children need intensive care and at least several days of PICU management, the overall mortality is low,[9,11,15,17] even amongst the youngest infants[98] and those with organ failures. The most common direct causes of death are cardiac dysfunction, shock, or multiorgan failure.

Mid- and long-term outcomes are unknown. The cardiac dysfunction and the CAAs appear to be the most severe sequelae of MIS-C. However, the emerging evidence shows a very high early resolution rate, ranging from 80 to 90%, within weeks from MIS-C.[28]

The disease heterogeneity and, consequently, the multitude of specialties involved in managing MIS-C patients present a challenge in establishing a unified follow-up protocol. To date, no universal consensus exists, and much of the post-discharge care is practiced according to institutional or regional recommendations. Cardiovascular pathology appears to be the main determinator of individual follow-up scheduling, along with the markers of inflammatory activity, which are monitored variedly by rheumatologists, immunologists, or infectious diseases specialists.

CLINICAL STATEMENT 8.

The overall short-term outcome of MIS-C is good. Most children recover without clinical or laboratory sequalae within weeks post-discharge. There is insufficient data on long-term outcomes.

CLINICAL STATEMENT 9.

MIS-C patients should be followed-up at regular intervals after discharge, focusing on cardiac disease, organ damage, inflammatory activity, and immune reconstruction.

[XIII] Future directions

Given the significant advances in research over the past year, we believe that there is sufficient evidence to support the current therapeutic options. Nevertheless, there is still a need for further research. The following research gaps are of particular importance:

Immunology and Diagnostics:

- Identification of a sensitive and specific diagnostic marker
- Identification of risk factors that predict clinical deterioration
- Revealing the genetic basis of the disease
- Evaluation of incidence and extinction of MIS-C with subsequent SARS-CoV-2 virus variants.

Management and treatment:

- Identification of new treatment strategies
- Mechanisms of response or non-response to treatment
- Verification of the optimal therapeutic option in prospective, preferably randomized, controlled trials

-   Further evaluation of the role of vaccination in the prevention of MIS-C.

[XIV] Conclusions

MIS-C is a new and rare manifestation of SARS-CoV-2 infection in children, that is clinically distinct to COVID-19 but shares features with other severe pediatric diseases, e.g., KD, TSS, and MAS. Case definition is broad and necessitates careful differential diagnosis. The exact pathomechanism of the disease is unknown, but the immune system dysregulation affecting both innate and adaptive immunity plays a central role. Current management of MIS-C relies on supportive care in combination with immunosuppressive agents. The most frequently used agents are systemic steroids and IVIG. Intensive studies in recent months have provided sufficient data to elaborate on the origins of the disease; however, mechanistic studies are still lacking. In anticipation of further research, we also propose a convenient and clinically practical algorithm for managing MIS-C developed by the Immunology Section of the European Academy of Allergology and Clinical Immunology.

References

1. Edward PR, Lorenzo-Redondo R, Reyna ME, et al. Severity of Illness Caused by Severe Acute Respiratory Syndrome Coronavirus 2 Variants of Concern in Children: A Single-Center Retrospective Cohort Study. *medRxiv*. Published online October 26, 2021. doi:10.1101/2021.10.23.21265402
2. Delahoy MJ, Ujamaa D, Whitaker M, et al. Hospitalizations Associated with COVID-19 Among Children and Adolescents — COVID-NET, 14 States, March 1, 2020–August 14, 2021. *MMWR Morbidity and Mortality Weekly Report*. 2021;70(36):1255-1260. doi:10.15585/MMWR.MM7036E2
3. Molteni E, Sudre CH, Canas LS, et al. Illness characteristics of COVID-19 in children infected with the SARS-CoV-2 Delta variant. *medRxiv*. Published online October 7, 2021:2021.10.06.21264467. doi:10.1101/2021.10.06.21264467
4. Wang L, Berger NA, Kaelber DC, Davis PB, Volkow ND, Xu R. COVID infection severity in children under 5 years old before and after Omicron emergence in the US. *medRxiv*. Published online January 13, 2022:2022.01.12.22269179. doi:10.1101/2022.01.12.22269179
5. Riphagen S, Gomez X, Gonzalez-Martinez C, Wilkinson N, Theocharis P. Hyperinflammatory shock in children during COVID-19 pandemic. *The Lancet*. 2020;395(10237):1607-1608. doi:10.1016/S0140-6736(20)31094-1
6. Verdoni L, Mazza A, Gervasoni A, et al. An outbreak of severe Kawasaki-like disease at the Italian epicentre of the SARS-CoV-2 epidemic: an observational cohort study. *The Lancet*. 2020;395(10239):1771-1778. doi:10.1016/S0140-6736(20)31103-X
7. Belot A, Antona D, Renolleau S, et al. SARS-CoV-2-related paediatric inflammatory multisystem syndrome, an epidemiological study, France, 1 March to 17 May 2020. *Eurosurveillance*. 2020;25(22):2001010. doi:10.2807/1560-7917.ES.2020.25.22.2001010
8. Godfred-Cato S, Bryant B, Leung J, et al. COVID-19–Associated Multisystem Inflammatory Syndrome in Children — United States, March–July 2020. *MMWR*

Morbidity and Mortality Weekly Report. 2020;69(32):1074-1080. doi:10.15585/mmwr.mm6932e2

9. Davies P, Evans C, Kanthimathinathan HK, et al. Intensive care admissions of children with paediatric inflammatory multisystem syndrome temporally associated with SARS-CoV-2 (PIMS-TS) in the UK: a multicentre observational study. *The Lancet Child and Adolescent Health*. 2020;4(9):669-677. doi:10.1016/S2352-4642(20)30215-7

10. Feldstein LR, Rose EB, Horwitz SM, et al. Multisystem Inflammatory Syndrome in U.S. Children and Adolescents. *New England Journal of Medicine*. 2020;383(4):334-346. doi:10.1056/nejmoa2021680

11. Belay ED, Abrams J, Oster ME, et al. Trends in Geographic and Temporal Distribution of US Children with Multisystem Inflammatory Syndrome during the COVID-19 Pandemic. *JAMA Pediatrics*. 2021;175(8):837-845. doi:10.1001/jamapediatrics.2021.0630

12. Paediatric multisystem inflammatory syndrome temporally associated with COVID-19 (PIMS) - guidance for clinicians | RCPCH. Accessed January 21, 2022. https://www.rcpch.ac.uk/resources/paediatric-multisystem-inflammatory-syndrome-temporally-associated-covid-19-pims-guidance

13. HAN Archive - 00432 | Health Alert Network (HAN). Accessed January 21, 2022. https://emergency.cdc.gov/han/2020/han00432.asp

14. Multisystem inflammatory syndrome in children and adolescents with COVID-19. Accessed January 21, 2022. https://www.who.int/publications/i/item/multisystem-inflammatory-syndrome-in-children-and-adolescents-with-covid-19

15. Ludwikowska KM, Okarska-Napierała M, Dudek N, et al. Distinct characteristics of multisystem inflammatory syndrome in children in Poland. *Scientific Reports 2021 11:1*. 2021;11(1):1-13. doi:10.1038/s41598-021-02669-2

16. Relvas-Brandt L de A, Gava C, Camelo FS, et al. Síndrome inflamatória multissistêmica pediátrica: estudo seccional dos casos e fatores associados aos óbitos durante a pandemia de COVID-19 no Brasil, 2020. *Epidemiologia e Serviços de Saúde*. 2021;30(4):1-14. doi:10.1590/s1679-49742021000400005

17. Flood J, Shingleton J, Bennett E, et al. Paediatric multisystem inflammatory syndrome temporally associated with SARS-CoV-2 (PIMS-TS): Prospective, national surveillance, United Kingdom and Ireland, 2020. *The Lancet Regional Health - Europe*. 2021;3:100075. doi:10.1016/j.lanepe.2021.100075

18. Kahn R, Berg S, Berntson L, et al. Population-based study of multisystem inflammatory syndrome associated with COVID-19 found that 36% of children had persistent symptoms. *Acta Paediatrica, International Journal of Paediatrics*. Published online 2021. doi:10.1111/apa.16191

19. Haslak F, Barut K, Durak C, et al. Clinical features and outcomes of 76 patients with COVID-19-related multi-system inflammatory syndrome in children. *Clinical Rheumatology*. Published online June 5, 2021. doi:10.1007/s10067-021-05780-x

20. Mamishi S, Movahedi Z, Mohammadi M, et al. Multisystem Inflammatory Syndrome Associated with SARS-CoV-2 Infection in 45 Children: A First Report from Iran. *Epidemiology and Infection*. Published online 2020. doi:10.1017/S095026882000196X

21. García-Salido A, de Carlos Vicente JC, Belda Hofheinz S, et al. Severe manifestations of SARS-CoV-2 in children and adolescents: from COVID-19 pneumonia to multisystem inflammatory syndrome: a multicentre study in pediatric intensive care units in Spain. *Crit Care*. 2020;24(1):666. doi:10.1186/s13054-020-03332-4

22. Anderson EM, Diorio C, Goodwin EC, et al. SARS-CoV-2 antibody responses in children with MIS-C and mild and severe COVID-19.

23. Whittaker E, Bamford A, Kenny J, et al. Clinical Characteristics of 58 Children with a Pediatric Inflammatory Multisystem Syndrome Temporally Associated with SARS-CoV-2. *JAMA - Journal of the American Medical Association*. 2020;324(3):259-269. doi:10.1001/jama.2020.10369

24. Belhadjer Z, Méot M, Bajolle F, et al. Acute Heart Failure in Multisystem Inflammatory Syndrome in Children in the Context of Global SARS-CoV-2 Pandemic. *Circulation*. 2020;142(5):429-436. doi:10.1161/CIRCULATIONAHA.120.048360

25. Riphagen S, Gomez X, Gonzalez-Martinez C, Wilkinson N, Theocharis P. Hyperinflammatory shock in children during COVID-19 pandemic. *The Lancet*. 2020;395(10237):1607-1608. doi:10.1016/S0140-6736(20)31094-1

26. Belay ED, Abrams J, Oster ME, et al. Trends in Geographic and Temporal Distribution of US Children with Multisystem Inflammatory Syndrome during the COVID-19 Pandemic. *JAMA Pediatrics*. Published online 2021. doi:10.1001/jamapediatrics.2021.0630

27. Abrams JY, Oster ME, Godfred-Cato SE, et al. Factors linked to severe outcomes in multisystem inflammatory syndrome in children (MIS-C) in the USA: a retrospective surveillance study. *The Lancet Child and Adolescent Health*. 2021;5(5):323-331. doi:10.1016/S2352-4642(21)00050-X

28. Feldstein LR, Tenforde MW, Friedman KG, et al. Characteristics and Outcomes of US Children and Adolescents with Multisystem Inflammatory Syndrome in Children (MIS-C) Compared with Severe Acute COVID-19. *JAMA - Journal of the American Medical Association*. 2021;325(11):1074-1087. doi:10.1001/jama.2021.2091

29. CDC COVID Data Tracker. Accessed September 27, 2021. https://covid.cdc.gov/covid-data-tracker/#mis-national-surveillance

30. Yamaguchi Y, Takasawa K, Irabu H, et al. Infliximab treatment for refractory COVID-19-associated multisystem inflammatory syndrome in a Japanese child. *Journal of Infection and Chemotherapy*. Published online 2022. doi:10.1016/J.JIAC.2022.01.011

31. Yilmaz Ciftdogan D, Ekemen Keles Y, Cetin BS, et al. COVID-19 associated multisystemic inflammatory syndrome in 614 children with and without overlap with Kawasaki disease-Turk MIS-C study group. *European Journal of Pediatrics*. 2022;29:1. doi:10.1007/S00431-022-04390-2

32. Tiwari A, Balan S, Rauf A, et al. COVID-19 related multisystem inflammatory syndrome in children (MIS-C): a hospital-based prospective cohort study from Kerala, India. *BMJ Paediatrics Open*. 2021;5(1):e001195. doi:10.1136/BMJPO-2021-001195

33. Webb K, Abraham DR, Faleye A, McCulloch M, Rabie H, Scott C. Multisystem inflammatory syndrome in children in South Africa. *The Lancet Child and Adolescent Health*. 2020;4(10):e38. doi:10.1016/S2352-4642(20)30272-8

34. Swann O v., Holden KA, Turtle L, et al. Clinical characteristics of children and young people admitted to hospital with covid-19 in United Kingdom: Prospective multicentre observational cohort study. *The BMJ*. 2020;370. doi:10.1136/bmj.m3249

35. Lima-Setta F, Magalhães-Barbosa MC de, Rodrigues-Santos G, et al. Multisystem inflammatory syndrome in children (MIS-C) during SARS-CoV-2 pandemic in Brazil: a multicenter, prospective cohort study. *Jornal de Pediatria*. 2021;97(3):354-361. doi:10.1016/j.jped.2020.10.008

36.   Ludwikowska KM, Okarska-Napierała M, Dudek N, et al. Multisystem inflammatory syndrome in European White children – study of 274 cases. doi:10.1101/2021.03.30.21254584

37.   Ricke DO, Gherlone N, Smith F, Tisdall P, Fremont-Smith P, Kawasaki Disease M. Kawasaki Disease, Multisystem Inflammatory Syndrome in Children: Antibody-Induced Mast Cell Activation Hypothesis. *Multisystem Inflammatory Syndrome in Children: Antibody-Induced Mast Cell Activation Hypothesis J Pediatrics & Pediatr Med*. 2020;4(2):1-7.

38.   Dufort EM, Koumans EH, Chow EJ, et al. Multisystem Inflammatory Syndrome in Children in New York State. *New England Journal of Medicine*. 2020;383(4):347-358. doi:10.1056/nejmoa2021756

39.   Lawrensia S, Henrina J, Cahyadi A. Multisystem inflammatory syndrome in adults: A systematic review and meta-analysis of the rheumatological spectrum of complications post COVID-19 infection. *Revista Colombiana de Reumatología*. Published online September 28, 2021. doi:10.1016/J.RCREU.2021.09.002

40.   Patel P, Decuir J, Abrams J, Campbell AP, Godfred-Cato S, Belay ED. Clinical Characteristics of Multisystem Inflammatory Syndrome in Adults: A Systematic Review. *JAMA Netw Open*. 2021;4(9). doi:10.1001/JAMANETWORKOPEN.2021.26456

41.   Holm M, Hartling UB, Schmidt LS, et al. Multisystem inflammatory syndrome in children occurred in one of four thousand children with severe acute respiratory syndrome coronavirus 2. *Acta Paediatrica*. 2021;110(9):2581-2583. doi:10.1111/APA.15985

42.   Sorg A, Hufnagel M, Doenhardt M, et al. Risk of Hospitalization, severe disease, and mortality due to COVID-19 and PIMS-TS in children with SARS-CoV-2 infection in Germany. *medRxiv*. Published online November 30, 2021:2021.11.30.21267048. doi:10.1101/2021.11.30.21267048

43.   Payne AB, Gilani Z, Godfred-Cato S, et al. Incidence of Multisystem Inflammatory Syndrome in Children Among US Persons Infected With SARS-CoV-2. *JAMA Netw Open*. 2021;4(6):e2116420. doi:10.1001/jamanetworkopen.2021.16420

44.   Cohen JM, Carter MJ, Cheung CR, Ladhani S, Group EPTS. Lower Risk of Multisystem Inflammatory Syndrome in Children (MIS-C) with the Delta and Omicron variants of SARS-CoV-2. *medRxiv*. Published online March 31, 2022:2022.03.13.22272267. doi:10.1101/2022.03.13.22272267

45.   Anderson EM, Diorio C, Goodwin EC, et al. SARS-CoV-2 antibody responses in children with MIS-C and mild and severe COVID-19. *J Pediatric Infect Dis Soc*. 2021;10(5):669-673. doi:10.1093/JPIDS/PIAA161

46.   Diorio C, Henrickson SE, Vella LA, et al. Multisystem inflammatory syndrome in children and COVID-19 are distinct presentations of SARS–CoV-2. *The Journal of Clinical Investigation*. 2020;130(11):5967-5975. doi:10.1172/JCI140970

47.   DeBiasi RL, Harahsheh AS, Srinivasalu H, et al. Multisystem Inflammatory Syndrome of Children: Subphenotypes, Risk Factors, Biomarkers, Cytokine Profiles, and Viral Sequencing. *Journal of Pediatrics*. 2021;237:125-135.e18. doi:10.1016/j.jpeds.2021.06.002

48.   Most ZM, Hendren N, Drazner MH, Perl TM. Striking Similarities of Multisystem Inflammatory Syndrome in Children and a Myocarditis-Like Syndrome in Adults: Overlapping Manifestations of COVID-19. *Circulation*. 2021;143:4-6. doi:10.1161/CIRCULATIONAHA.120.050166/FORMAT/EPUB

49. McCrindle BW, Rowley AH, Newburger JW, et al. Diagnosis, Treatment, and Long-Term Management of Kawasaki Disease: A Scientific Statement for Health Professionals From the American Heart Association. *Circulation*. 2017;135(17):e927-e999. doi:10.1161/CIR.0000000000000484

50. Rowley AH, Baker SC, Shulman ST, et al. Cytoplasmic inclusion bodies are detected by synthetic antibody in ciliated bronchial epithelium during acute Kawasaki disease. *Journal of Infectious Diseases*. 2005;192(10):1757-1766. doi:10.1086/497171

51. Rowley AH, Baker SC, Shulman ST, et al. Detection of antigen in bronchial epithelium and macrophages in acute Kawasaki disease by use of synthetic antibody. *J Infect Dis*. 2004;190(4):856-865. doi:10.1086/422648

52. Duarte-Neto AN, Caldini EG, Gomes-Gouvêa MS, et al. An autopsy study of the spectrum of severe COVID-19 in children: From SARS to different phenotypes of MIS-C. *EClinicalMedicine*. 2021;35. doi:10.1016/J.ECLINM.2021.100850/ATTACHMENT/849A1CDE-57A6-4001-A741-75FF2F78CE3C/MMC3.DOCX

53. Gruber CN, Patel RS, Trachtman R, et al. Mapping Systemic Inflammation and Antibody Responses in Multisystem Inflammatory Syndrome in Children (MIS-C). *Cell*. 2020;183(4):982-995.e14. doi:10.1016/J.CELL.2020.09.034

54. Martinez OM, Bridges ND, Goldmuntz E, Pascual V. The immune roadmap for understanding multi-system inflammatory syndrome in children: opportunities and challenges. *Nature Medicine 2020 26:12*. 2020;26(12):1819-1824. doi:10.1038/s41591-020-1140-9

55. Schlievert PM. Role of superantigens in human disease. *J Infect Dis*. 1993;167(5):997-1002. doi:10.1093/INFDIS/167.5.997

56. Noval Rivas M, Porritt RA, Cheng MH, Bahar I, Arditi M. COVID-19–associated multisystem inflammatory syndrome in children (MIS-C): A novel disease that mimics toxic shock syndrome—the superantigen hypothesis. *The Journal of Allergy and Clinical Immunology*. 2021;147(1):57. doi:10.1016/J.JACI.2020.10.008

57. Cheng MH, Zhang S, Porritt RA, et al. Superantigenic character of an insert unique to SARS-CoV-2 spike supported by skewed TCR repertoire in patients with hyperinflammation. *Proc Natl Acad Sci U S A*. 2020;117(41):25254-25262. doi:10.1073/pnas.2010722117

58. Yousaf AR, Cortese MM, Taylor AW, et al. Reported cases of multisystem inflammatory syndrome in children aged 12–20 years in the USA who received a COVID-19 vaccine, December, 2020, through August, 2021: a surveillance investigation. *The Lancet Child & Adolescent Health*. 2022;0(0). doi:10.1016/S2352-4642(22)00028-1

59. Iyengar KP, Nune A, Ish P, Botchu R, Shashidhara MK, Jain VK. Multisystem inflammatory syndrome after SARS-CoV-2 vaccination (MIS-V), to interpret with caution. *Postgraduate Medical Journal*. 2022;98(e2):e91-e91. doi:10.1136/POSTGRADMEDJ-2021-140869

60. Zambrano LD, Newhams MM, Olson SM, et al. Effectiveness of BNT162b2 (Pfizer-BioNTech) mRNA Vaccination Against Multisystem Inflammatory Syndrome in Children Among Persons Aged 12–18 Years — United States, July–December 2021. *MMWR Morbidity and Mortality Weekly Report*. 2022;71(2):52-58. doi:10.15585/MMWR.MM7102E1

61. Levy M, Recher M, Hubert H, et al. Multisystem Inflammatory Syndrome in Children by COVID-19 Vaccination Status of Adolescents in France. *JAMA*. 2022;327(3):281-283. doi:10.1001/JAMA.2021.23262

62. Sacco K, Castagnoli R, Vakkilainen S, et al. Immunopathological signatures in multisystem inflammatory syndrome in children and pediatric COVID-19. *Nature Medicine 2022*. Published online February 17, 2022:1-13. doi:10.1038/s41591-022-01724-3

63. Porritt RA, Paschold L, Rivas MN, et al. HLA class I–associated expansion of TRBV11-2 T cells in multisystem inflammatory syndrome in children. *The Journal of Clinical Investigation*. 2021;131(10). doi:10.1172/JCI146614

64. Vella LA, Giles JR, Baxter AE, et al. Deep immune profiling of MIS-C demonstrates marked but transient immune activation compared to adult and pediatric COVID-19. *Science Immunology*. 2021;6(57). doi:10.1126/SCIIMMUNOL.ABF7570

65. Beckmann ND, Comella PH, Cheng E, et al. Cytotoxic lymphocytes are dysregulated in multisystem inflammatory syndrome in children. *Seunghee Kim-Schulze*. 5(5):18. doi:10.1101/2020.08.29.20182899

66. Yonker LM, Gilboa T, Ogata AF, et al. Multisystem inflammatory syndrome in children is driven by zonulin-dependent loss of gut mucosal barrier. *The Journal of Clinical Investigation*. 2021;131(14). doi:10.1172/JCI149633

67. Carter MJ, Fish M, Jennings A, et al. Peripheral immunophenotypes in children with multisystem inflammatory syndrome associated with SARS-CoV-2 infection. *Nature Medicine 2020 26:11*. 2020;26(11):1701-1707. doi:10.1038/s41591-020-1054-6

68. Ramaswamy A, Brodsky NN, Sumida TS, et al. Post-infectious inflammatory disease in MIS-C features elevated cytotoxicity signatures and autoreactivity that correlates with severity. *medRxiv*. Published online April 3, 2020:2020.12.01.20241364. doi:10.1101/2020.12.01.20241364

69. Consiglio CR, Cotugno N, Sardh F, et al. The Immunology of Multisystem Inflammatory Syndrome in Children with COVID-19. *Cell*. 2020;183(4):968-981.e7. doi:10.1016/J.CELL.2020.09.016

70. Esteve-Sole A, Anton J, Pino-Ramirez RM, et al. Similarities and differences between the immunopathogenesis of COVID-19-related pediatric multisystem inflammatory syndrome and Kawasaki disease. *J Clin Invest*. 2021;131(6). doi:10.1172/JCI144554

71. Diorio C, Shraim R, Vella LA, et al. Proteomic Profiling of MIS-C Patients Reveals Heterogeneity Relating to Interferon Gamma Dysregulation and Vascular Endothelial Dysfunction. *medRxiv*. Published online April 20, 2021. doi:10.1101/2021.04.13.21255439

72. Caldarale F, Giacomelli M, Garrafa E, et al. Plasmacytoid Dendritic Cells Depletion and Elevation of IFN-γ Dependent Chemokines CXCL9 and CXCL10 in Children With Multisystem Inflammatory Syndrome. *Frontiers in Immunology*. 2021;12. doi:10.3389/FIMMU.2021.654587/FULL

73. de Cevins C, Luka M, Smith N, et al. A monocyte/dendritic cell molecular signature of SARS-CoV-2-related multisystem inflammatory syndrome in children with severe myocarditis. *Med*. 2021;2(9):1072-1092.e7. doi:10.1016/J.MEDJ.2021.08.002

74. Zhang Q, Liu Z, Moncada-Velez M, et al. Inborn errors of type I IFN immunity in patients with life-threatening COVID-19. *Science*. 2020;370(6515). doi:10.1126/SCIENCE.ABD4570

75. Trouillet-Assant S, Viel S, Gaymard A, et al. Type I IFN immunoprofiling in COVID-19 patients. *J Allergy Clin Immunol*. 2020;146(1):206-208.e2. doi:10.1016/J.JACI.2020.04.029

76. Lee PY, Platt CD, Weeks S, et al. Immune dysregulation and multisystem inflammatory syndrome in children (MIS-C) in individuals with haploinsufficiency of SOCS1. *J Allergy Clin Immunol*. 2020;146(5):1194-1200.e1. doi:10.1016/J.JACI.2020.07.033

77. Chou J, Platt CD, Habiballah S, et al. Mechanisms underlying genetic susceptibility to multisystem inflammatory syndrome in children (MIS-C). *Journal of Allergy and Clinical Immunology*. 2021;148(3):732-738.e1. doi:10.1016/j.jaci.2021.06.024

78. Zanoni I, Granucci F. Role of CD14 in host protection against infections and in metabolism regulation. *Frontiers in Cellular and Infection Microbiology*. 2013;3(JUL). doi:10.3389/FCIMB.2013.00032

79. Carter MJ, Fish M, Jennings A, et al. Peripheral immunophenotypes in children with multisystem inflammatory syndrome associated with SARS-CoV-2 infection. *Nature Medicine 2020 26:11*. 2020;26(11):1701-1707. doi:10.1038/s41591-020-1054-6

80. Boribong BP, Lasalle TJ, Bartsch YC, et al. Neutrophil Profiles of Pediatric COVID-19 and Multisystem Inflammatory Syndrome in Children. *BioRxiv*. Published online 2021. doi:10.1101/2021.12.18.473308

81. Peart Akindele N, Kouo T, Karaba AH, et al. Distinct Cytokine and Chemokine Dysregulation in Hospitalized Children With Acute Coronavirus Disease 2019 and Multisystem Inflammatory Syndrome With Similar Levels of Nasopharyngeal Severe Acute Respiratory Syndrome Coronavirus 2 Shedding. *J Infect Dis*. 2021;224(4):606-615. doi:10.1093/INFDIS/JIAB285

82. Sokolowska M, Lukasik ZM, Agache I, et al. Immunology of COVID-19: Mechanisms, clinical outcome, diagnostics, and perspectives-A report of the European Academy of Allergy and Clinical Immunology (EAACI). *Allergy*. 2020;75(10):2445-2476. doi:10.1111/ALL.14462

83. Okarska-Napierała M, Mańdziuk J, Feleszko W, et al. Recurrent assessment of lymphocyte subsets in 32 patients with multisystem inflammatory syndrome in children (MIS-C). *Pediatr Allergy Immunol*. 2021;32(8):1857-1865. doi:10.1111/PAI.13611

84. Lee PY, Day-Lewis M, Henderson LA, et al. Distinct clinical and immunological features of SARS-CoV-2-induced multisystem inflammatory syndrome in children. *J Clin Invest*. 2020;130(11):5942-5950. doi:10.1172/JCI141113

85. Okarska-Napierała M, Ludwikowska KM, Szenborn L, et al. Pediatric Inflammatory Multisystem Syndrome (PIMS) Did Occur in Poland during Months with Low COVID-19 Prevalence, Preliminary Results of a Nationwide Register. *J Clin Med*. 2020;9(11):1-14. doi:10.3390/JCM9113386

86. Sperotto F, Friedman KG, Son MBF, VanderPluym CJ, Newburger JW, Dionne A. Cardiac manifestations in SARS-CoV-2-associated multisystem inflammatory syndrome in children: a comprehensive review and proposed clinical approach. *Eur J Pediatr*. 2021;180(2):307-322. doi:10.1007/S00431-020-03766-6

87. American College of Rheumatology MIS-C and COVID-19 Related Hyperinflammation Task Force. Clinical Guidance for Pediatric Patients with Multisystem Inflammatory Syndrome in Children (MIS-C) Associated with SARS-CoV-2 and Hyperinflammation in COVID-19. *American college of Rheumatology*. 2020;(Version 1):1-5.

88. Harwood R, Allin B, Jones CE, et al. A national consensus management pathway for paediatric inflammatory multisystem syndrome temporally associated with COVID-19

(PIMS-TS): results of a national Delphi process. *Review Lancet Child Adolesc Health*. 2021;5:133-174. doi:10.1016/S2352-4642(20)30304-7

89. Schlapbach LJ, Andre MC, Grazioli S, et al. Best Practice Recommendations for the Diagnosis and Management of Children With Pediatric Inflammatory Multisystem Syndrome Temporally Associated With SARS-CoV-2 (PIMS-TS; Multisystem Inflammatory Syndrome in Children, MIS-C) in Switzerland. *Frontiers in Pediatrics*. 2021;0:396. doi:10.3389/FPED.2021.667507

90. Okarska-Napierała M, Ludwikowska K, Jackowska T, et al. Approach to a child with Multisystem Inflammatory Syndrome associated with COVID19. Recommendations by the Polish Paediatric Society Expert Group. Update – February 2021. *Pediatria Polska - Polish Journal of Paediatrics*. 2021;96(2):121-128. doi:10.5114/POLP.2021.107395

91. Newburger JW, Takahashi M, Burns JC, et al. The Treatment of Kawasaki Syndrome with Intravenous Gamma Globulin. *http://dx.doi.org/101056/NEJM198608073150601*. 2009;315(6):341-347. doi:10.1056/NEJM198608073150601

92. Licciardi F, Baldini L, Dellepiane M, et al. MIS-C Treatment: Is IVIG Always Necessary? *Frontiers in Pediatrics*. 2021;9:1202. doi:10.3389/FPED.2021.753123/BIBTEX

93. Ouldali N, Toubiana J, Antona D, et al. Association of Intravenous Immunoglobulins Plus Methylprednisolone vs Immunoglobulins Alone With Course of Fever in Multisystem Inflammatory Syndrome in Children. *JAMA*. 2021;325(9):855-864. doi:10.1001/JAMA.2021.0694

94. Son MBF, Murray N, Friedman K, et al. Multisystem Inflammatory Syndrome in Children — Initial Therapy and Outcomes. *https://doi.org/101056/NEJMoa2102605*. 2021;385(1):23-34. doi:10.1056/NEJMOA2102605

95. McArdle AJ, Vito O, Patel H, et al. Treatment of Multisystem Inflammatory Syndrome in Children. *https://doi.org/101056/NEJMoa2102968*. 2021;385(1):11-22. doi:10.1056/NEJMOA2102968

96. Davies P, Lillie J, Prayle A, et al. Association Between Treatments and Short-Term Biochemical Improvements and Clinical Outcomes in Post-Severe Acute Respiratory Syndrome Coronavirus-2 Inflammatory Syndrome. *Pediatric Critical Care Medicine*. 2021;22(5):e285. doi:10.1097/PCC.0000000000002728

97. Whitworth H, Sartain SE, Kumar R, et al. Rate of thrombosis in children and adolescents hospitalized with COVID-19 or MIS-C. *Blood*. 2021;138(2):190-198. doi:10.1182/BLOOD.2020010218

98. Godfred-Cato S, Tsang CA, Giovanni J, et al. Multisystem Inflammatory Syndrome in Infants <12 months of Age, United States, May 2020–January 2021. *Pediatric Infectious Disease Journal*. 2021;40(7):601-605. doi:10.1097/inf.0000000000003149

B cells, BAFF and interferons in MIS-C

Adam Klocperk[1,$], Marketa Bloomfield[1,$], Zuzana Parackova[1], Ludovic Aillot[2], Jiri Fremuth[3], Lumir Sasek[3], Jan David[4], Filip Fencl[4], Aneta Skotnicova[5], Katerina Rejlova[5], Martin Magner[6,7], Ondrej Hrusak[5], Anna Sediva[1]

[1]Department of Immunology, 2nd Faculty of Medicine, Charles University and University Hospital in Motol, Prague, Czech Republic

[2]Institute of Organic Chemistry and Biochemistry of the Czech Academy of Sciences, IOCB Gilead Research Center, Prague, Czech Republic

[3]Department of Paediatrics - PICU, Faculty of Medicine in Pilsen, Charles University in Prague, Pilsen, Czech Republic

[4]Department of Paediatrics, 2nd Faculty of Medicine, Charles University and University Hospital in Motol, Prague, Czech Republic

[5]CLIP - Childhood Leukaemia Investigation Prague, Czech Republic; Department of Pediatric Hematology, Charles University and University Hospital Motol, Prague, Czech Republic

[6]Department of Paediatrics, 1st Faculty of Medicine, Charles University and Thomayer University Hospital, Prague, Czech Republic

[7]Department of Paediatrics and Inherited Metabolic Disorders, General University Hospital and First Faculty of Medicine, Charles University, Prague, Czech Republic

[$]These authors contributed equally and share first authorship.

Summary sentence

Elevated serum BAFF in children with MIS-C supports the state of polyclonal B cell activation and autoimmune phenomena characterizing this disease.

Running title

Corresponding author

Adam Klocperk

Department of Immunology, 2nd Faculty of Medicine, Charles University and University Hospital in Motol

V Uvalu 84

150 06, Prague

Czech Republic

+420 702 013 154

adam.klocperk@fnmotol.cz

Key words

PIMS-TS; COVID-19; interferon; APRIL

Abstract

Multisystem Inflammatory Syndrome in Children associated with COVID-19 (MIS-C) is a late complication of pediatric COVID-19, which follows weeks after original SARS-CoV-2 infection, regardless of its severity. It is characterized by hyperinflammation, neutrophilia, lymphopenia and activation of T cells with elevated IFN-γ. Observing production of autoantibodies and parallels with systemic autoimmune disorders, such as systemic lupus erythematodes (SLE), we explored B cell phenotype and serum levels of type I, II and III interferons, as well as the cytokines BAFF and APRIL in a cohort of MIS-C patients and healthy children after COVID-19.

We documented a significant elevation of IFN-γ, but not IFN-α and IFN-λ in MIS-C patients. BAFF was elevated in MIS-C patient sera and accompanied by decreased BAFFR expression on all B cell subtypes. The proportion of plasmablasts was significantly lower in patients compared to healthy post-COVID children. We noted the presence of ENA Ro60 autoantibodies in 4/35 tested MIS-C patients.

Our work shows the involvement of humoral immunity in MIS-C and hints at parallels with the pathophysiology of SLE, with autoreactive B cells driven towards autoantibody production by elevated BAFF.

Graphical abstract
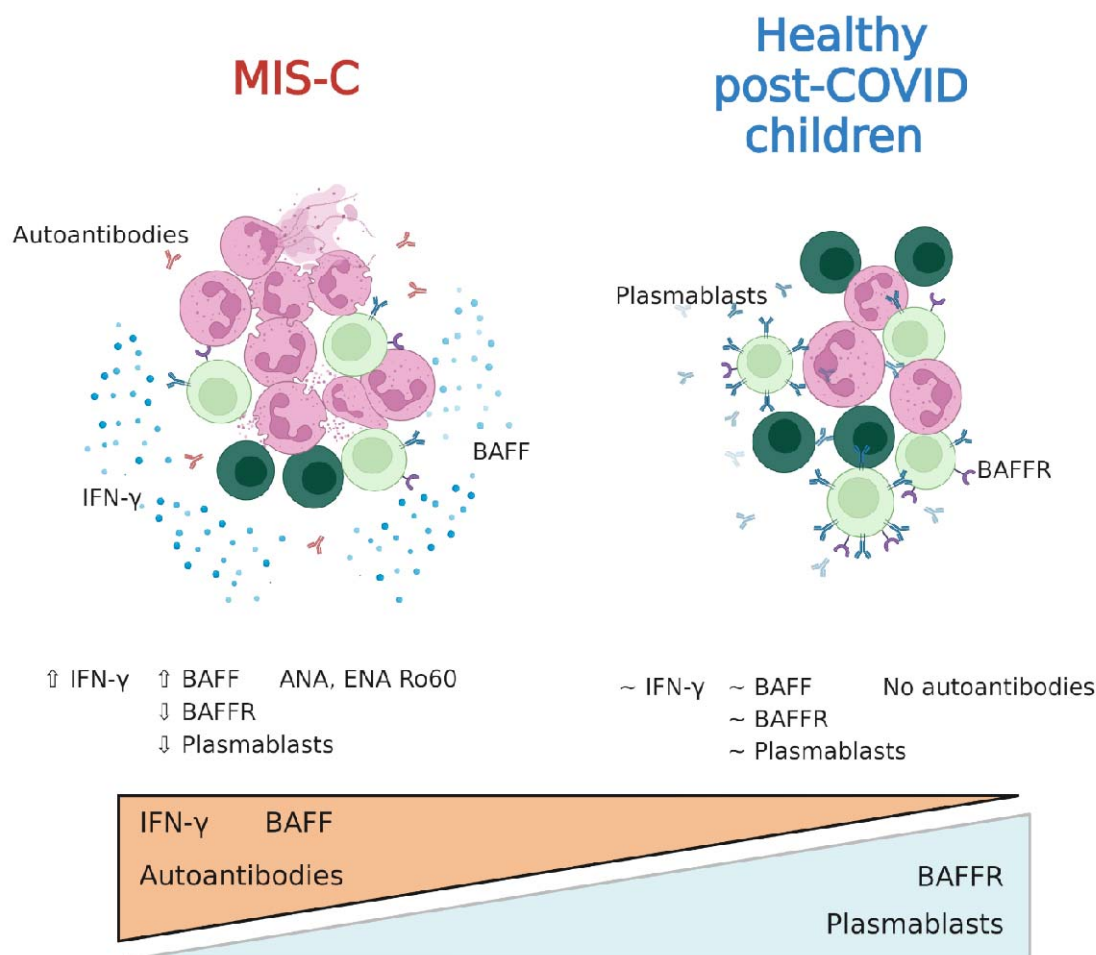
Introduction

Multisystem Inflammatory Syndrome in Children associated with COVID-19 (MIS-C) is now a well specified entity described in a number of excellent publications that map in detail the immune / autoimmune / inflammatory responses accompanying this condition [1–4]. All these works point to a significant pro-inflammatory state, accompanied by alterations in cellular populations of innate and acquired immunity, with prominent lymphopenia during the acute state of the disease, which typically lags several weeks after acute SARS-CoV-2 infection, regardless of its severity. This lymphopenia is characterized by a decrease in T cells, but at the same time with their activation and clonal proliferation [4]. Significant alterations were shown in T-cell subpopulations in MIS-C and recent reports also show their clonality and exhaustion [5,6].

B cells, on the other hand, are less studied in the context of MIS-C. Absolute B-cell counts were reported normal or decreased, in line with the general MIS-C-associated lymphopenia [3,7], however they seem to be less suppressed than T cells, with elevated proportion of B cells within the lymphocyte compartment [4]. Some studies taking a closer look at B cell subpopulations have shown an increase in plasmablasts, as well as IgD⁻CD27⁻ double negative B cells among peripheral blood mononuclear cells [4,8,9]. Similar IgD⁻CD27⁻ activated B cells were previously documented in systemic lupus erthematodes (SLE) in association with disease activity and autoantibody secretion [10]. This points to a potential parallel with autoreactive B cell activation in both systemic autoimmune diseases such as SLE, and MIS-C. Consistently, a number of publications document the presence of autoimmune phenomena and autoantibodies in MIS-C patients, targeting both systemic and tissue- or organ-specific antigens[8,11]. These findings suggest a strong polyclonal antibody response driven by activated B cells. In SLE, these events are driven by the serum cytokine BAFF and APRIL [12,13], however, such association has not yet been studied in MIS-C.

Other shared features of SLE and MIS-C may involve interferon activation. While increased IFN-γ response has been demonstrated to be a feature shared by MIS-C and SLE [14–16], the activity of type I and type III interferons has only been shown in lupus [17,18], but not in MIS-C. Interestingly, antibodies against type I interferons have been demonstrated to contribute to COVID-19 mortality and severity [19].

To explore these immune factors contributing to the hyperinflammation in MIS-C we set out to assess type I, II and III interferons, serum BAFF, APRIL, and B cell phenotype and BAFFR expression in children with acute MIS-C and in healthy children after uncomplicated COVID-19.

3

Patients and methods

Patients and controls

The MIS-C cohort was recruited from patients admitted to the Department of Pediatrics, University Hospital in Motol, Prague, Department of Pediatrics, Thomayer University Hospital, Prague, and Department of Pediatrics, University Hospital in Pilsen, Pilsen, Czech Republic. Informed consent with participation in this study was signed by the participants' legal guardians in accordance with the Declaration of Helsinki and the study was approved by the Ethical Committee of the University Hospital in Motol, reference no. EK-1376/21. Data on demographics, clinical manifestations, routine laboratory features and other investigations, therapeutic management, and outcomes were collected retrospectively from medical records of the patient, or obtained via patient/parent interview.

In MIS-C patients, samples were obtained through peripheral venepuncture after the establishment of MIS-C diagnosis, before administration of corticosteroids or immunoglobulins. Patients were included in the study based on their MIS-C diagnosis consistent with WHO criteria [20]. In total, 50 MIS-C patients were recruited during the inclusion period between October 2020 and April 2021, 24 female, age 11 months to 18 years (7.8 ± 4.35 years, mean ± SD). The alpha (B.1.1.7) SARS-CoV-2 variant was dominant in Czechia during this period.

As a control cohort, 7 healthy children who previously underwent COVID-19, 2 female, age 1 to 14 years (9.9 ± 3.9 years), were recruited into the study (hereafter referred to as healthy post-COVID children). These healthy donors were sampled 4-6 weeks after their SARS-CoV-2 PCR positivity.

For assessment of BAFF and APRIL, 4 MIS-C patients, 2 female, age 1.4 to 5.5 years (3.5 ± 1.4 years), were re-evaluated 6 months after discharge from hospital (hereafter referred to as MIS-C convalescent). Further, 8 healthy donor children with no history of COVID-19, 5 female, age 11.6 to 17.2 years (13.7 ± 1.9 years) were included for comparison (hereafter referred to as healthy children).

Description of cohorts summarized in Table 1.

Flow cytometry

For evaluation of peripheral blood B cell phenotype, blood was taken into EDTA-coated tubes as described above. PBMCs were obtained using Ficoll-Paque (Pharmacia, Uppsala, Sweden) and cryopreserved in liquid nitrogen.

After thawing, PBMCs were incubated in the presence of recombinant human DNAse I (Pulmozyme, Roche, Prague, Czechia; final concentration was 10 IU/mL) in complete media (RPMI 1640 supplemented with 10% of heat inactivated fetal calf serum, penicillin (50 U/mL), streptomycine (50 U/mL) and 1,7mM sodium glutamate) for 30 minutes at 37°C in a CO2 incubator. One million cells were resuspended in 100 μL PBS (Sigma-Aldrich, St. Louis, MO) and stained for 30 min in the dark at room temperature with CD5 BV421 (Cat No. 562646, BD Biosciences, San Jose, CA), IgM BV510 (Cat No. 314522, Biolegend, San Diego, CA), BAFFR BV711 (Cat No. 743573, BD Biosciences) and a dried mixture of IgD FITC, CD27 PE, CD24 PerCP-Cy5.5, CD19 PE-Cy7, CD21 APC, and CD38 APC-Cy7 (Custom-design dry reagent tube, Exbio Praha, Vestec, Czechia). Then, 2 mL of BD FACS™ Lysing Solution (BD Biosciences) were added and cells were incubated for 10 minutes in the dark, room temperature. At the end, cells were washed once in PBS with 1% BSA and pellets were resuspended in 150 μL PBS.

Flow cytometry measurement was performed on BD FACSLyrics (BD Immunocytometry Systems, San Jose, CA). FlowJo software was used for data analysis (TreeStar, Ashland, OR).

ELISA

For evaluation of serum cytokine levels, blood was taken into uncoated tubes as described above, serum was separated by centrifugation and stored frozen at -80°C until further evaluation. BAFF and APRIL was measured according to manufacturer's specifications using pre-made ELISA kits (BAFF from R&D Systems, Minneapolis, USA, APRIL from abcam, Cambridge, UK). Type I, II and III interferons (specifically, pan-IFN-α, IFN-γ and IFN-λ1) were quantified following manufacturer's protocols of Human ELISA Basic KIT (HRP) (MABTECH , Sweden) using Nunc MaxiSorp flat-bottom 96-well plates (Invitrogen). Absorbance 450nm was read by multimode plate reader EnVision 2105 (PerkinElmer).

Statistics

Statistical analysis was performed using using Brown-Forsythe and Welch one-way analysis of variance (ANOVA) and unpaired t-tests with Welch's correction in GraphPad Prism 8.0 (San Diego, CA, USA). Values of $p = 0.01$-0.05 (*), $p = 0.001$-0.01 (**), $p < 0.001$ (***) and $p < 0.0001$ (****) were considered statistically significant.

Results and discussion

To explore the hyperinflammatory signature of MIS-C we measured IFN-α, IFN-γ and IFN-λ in the serum of 50 patients with MIS-C sampled shortly after admission to hospital, before administration of immunosuppressive therapy, and compared them to the sera of healthy children who underwent COVID-19 4-6 weeks prior to sampling and had no signs of MIS-C. We saw no significant changes in IFN-α (t test with Welch's correction p = 0.27) and IFN-λ levels (p = 0.33) (Fig 1A, C), therefore our data suggests that lingering type I and III interferon inflammation are not robust driving factors behind MIS-C pathogenesis, despite their role in fight against the SARS-CoV-2 infection proper [19,21,22]. On the other hand, IFN-γ was significantly elevated in MIS-C compared to healthy post-COVID children (p = 0.0004) (Fig 1B). This elevation of IFN-γ has been described in MIS-C previously [14,15,22] and may reflect the concurrent T cell activation [15,22].

As discussed earlier, the elevation of IFN-γ and presence of autoimmune phenomena in MIS-C is reminiscent of SLE and warrants exploration of B cell immunity in these patients [16,23]. Thus, we measured the serum concentration of BAFF and APRIL, two cytokines supporting the development and survival of B cells. The serum levels of APRIL were largely below the assay detection limit, although in a subset of MIS-C patients we detected elevated APRIL levels, which were missing in healthy post-COVID children, healthy children, and even in convalescent MIS-C patients sampled several months after full recovery (Figure 1D). Nevertheless, the majority of samples tested APRIL-negative and as such the differences were not significant.

The serum BAFF levels, on the other hand, varied significantly among the MIS-C, convalescent MIS-C, healthy post-COVID and the healthy children (Brown-Forsythe ANOVA p < 0.0001) (Figure 1E). The MIS-C patients had the highest BAFF levels of all cohorts, which in particular were higher than those in healthy post-COVID children (t test with Welch's correction p < 0.0001), but also than those in convalescent MIS-C patients (p < 0.0001). Interestingly, even healthy post-COVID children had elevated serum BAFF levels compared to healthy children without history of COVID-19 (p = 0.0093). In both MIS-C patients and healthy children, the trend remained identical, with higher BAFF during/after disease, and lower BAFF after full recovery or in times of full health. To the best of our knowledge, BAFF has not yet been studied in connection with MIS-C and no comparison with other studies is therefore available.

The significant increase of BAFF levels in MIS-C is in line with polyclonal B cell activation, which may underlie the genesis of MIS-C-related autoantibodies and its clinical manifestations, i.e. the autoimmune systemic and organ inflammation. In our cohort, of 35 patients in whom autoantibodies were tested, 4/35 (11%) had positive Ro60 antibodies and further 4/35 (11%) had positive extractable nuclear antigen (ENA) screening but none of the tested individual antigens were positive. Previous studies in MIS-C patients reported the presence of anti-La, a characteristic autoantigen of SLE and Sjogren's disease, and anti-Jo-1, characteristic for idiopathic inflammatory myopathies [24]. In addition, a number of other non-routine autoantibodies directed against various autoantigens were detected, confirming the autoimmune disposition accompanying the acute stage of MIS-C [24]. Furthermore, the combination of increased IFN-γ and a consequent increase in BAFF has been previously described in SLE, representing another analogy with MIS-C [25]. Interestingly, in case of SLE, it has been shown that neutrophils can contribute to an increase in BAFF and augment the autoimmune process. In the case of COVID-19 and especially MIS-C, characterized by marked neutrophilia, a similar parallel might contribute to the induction of autoimmune phenomena [26].

Evaluating the impact of upregulated BAFF signalling on B cell subpopulations, we saw a highly significant decrease of circulating plasmablasts (p < 0.0001) and less significant decrease of transitional B cells (p = 0.029), whereas other developmental subsets did not differ significantly (Figure 2A, B). The highly significant lack of plasmablasts is of particular note given their comparatively lower reliance on BAFF for survival, which can also be bolstered by APRIL [27].

The decrease seems to be in contrast to some previous publications [2,4], however, the samples analyzed here were obtained strictly before the initiation of immunomodulatory therapy (immunoglobulins or steroids), which was not always the case with the previously mentioned works. Furthermore, we calculate these subpopulations as proportion of total B cells, rather than all lymphocytes or the whole PBMC compartment, which are both disproportionately affected by the profound T cell lymphopenia characteristic for MIS-C. Indeed, our dataset also documented a relative expansion of B cells in lymphocytes (Supplementary Figure 1), which resulted in falsely comparable proportion of plasmablasts and elevated naïve B cells when calculating these subsets as proportion of all lymphocytes (Supplementary Figure 2). In the context of the absolute peripheral blood B cell lymphopenia seen in MIS-C [3], however, it becomes clear that plasmablasts are in fact decreased, and that not only T and B cells, but even specifically B cell subsets are differentially affected by MIS-C.

Naïve and transitional B cells are also highly dependent on BAFF for survival [28], however all MIS-C B cells had strikingly suppressed BAFF receptor (BAFFR) expression (Figure 2C). This was true in all B-cell subsets, including naïve and transitional forms. These results are consistent with the similar situation observed in SLE and Sjögren syndrome, where high levels of BAFF are associated with decreased BAFFR expression on all B cell subtypes [29,30]. This inverse correlation may be attributed to down-regulation of BAFFR resulting from chronic exposure to elevated BAFF levels, which was suggested to be mediated via unspecified post-transcriptional mechanisms [30].

In summary, our brief report highlights the dysregulation of humoral immunity with autoimmune bias in MIS-C and suggests a role of the BAFF-BAFFR axis, which warrants further exploration.

Authorship

AK co-designed the study, processed samples, gathered clinical data, analysed the data and co-wrote the manuscript. MB co-designed the study, recruited patients and healthy donors, gathered clinical data, reviewed and edited the manuscript. ZP and LA performed experiments. MM, JF, LS, JD and FF recruited patients and provided clinical data. AS, KR and OH performed experiments and analysed data. AS designed the study and co-wrote the manuscript.

Acknowledgements

Conflict of Interest Disclosure

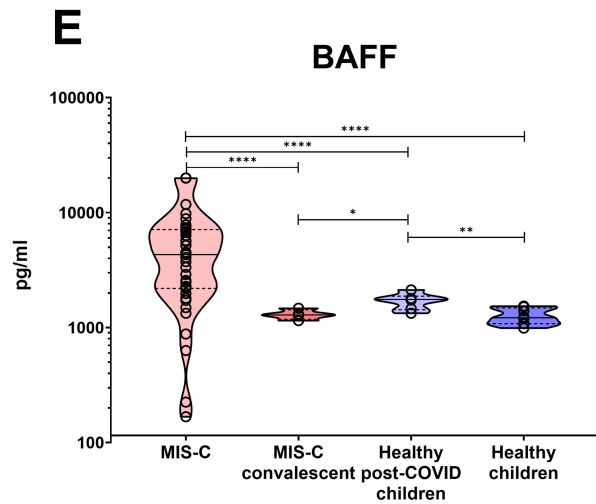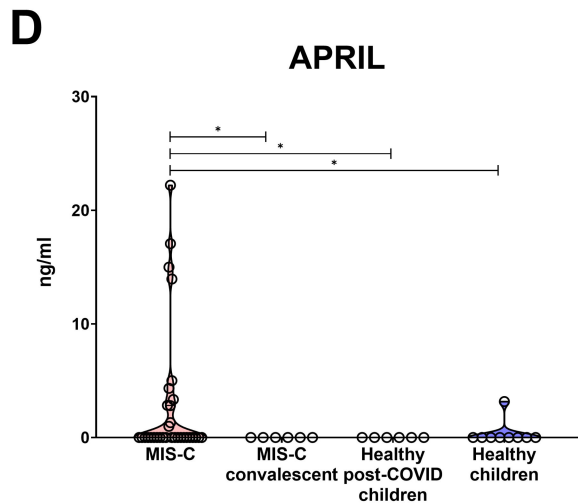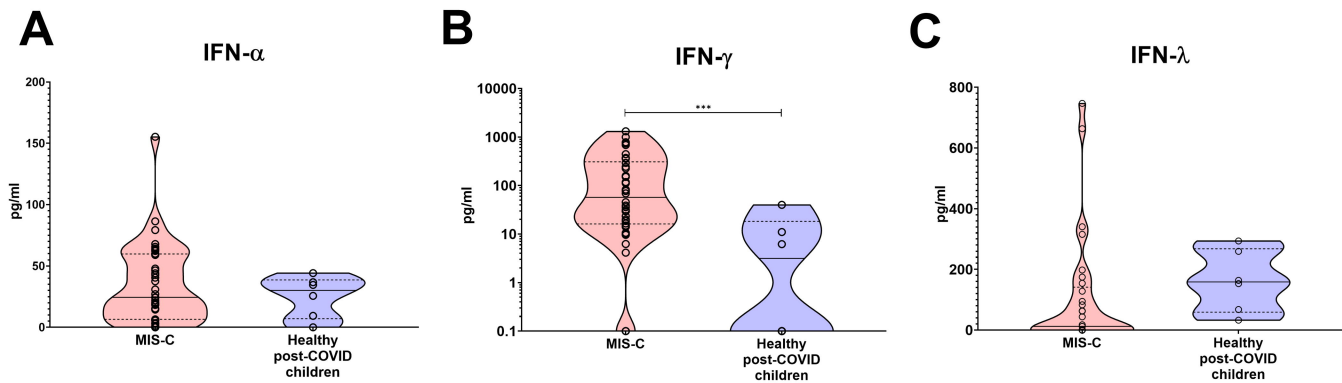The authors declare no conflict of interest.

References

1. Henderson LA, Yeung RSM. MIS-C: early lessons from immune profiling. *Nat Rev Rheumatol*. 2021;17:75–76.

2. Consiglio CR, Cotugno N, Sardh F, et al. The Immunology of Multisystem Inflammatory Syndrome in Children with COVID-19. *Cell*. 2020;183:968-981.e7.

3. Carter MJ, Fish M, Jennings A, et al. Peripheral immunophenotypes in children with multisystem inflammatory syndrome associated with SARS-CoV-2 infection. *Nat Med*. 2020;26:1701–1707.

4. Vella LA, Giles JR, Baxter AE, et al. Deep immune profiling of MIS-C demonstrates marked but transient immune activation compared with adult and pediatric COVID-19. *Science Immunology*. 2021;6:eabf7570.

5. Porritt RA, Paschold L, Rivas MN, et al. HLA class I–associated expansion of TRBV11-2 T cells in multisystem inflammatory syndrome in children. *J Clin Invest*;131 . Epub ahead of print 5 2021. DOI: 10.1172/JCI146614.

6. Beckmann ND, Comella PH, Cheng E, et al. Downregulation of exhausted cytotoxic T cells in gene expression networks of multisystem inflammatory syndrome in children. *Nat Commun*. 2021;12:4854.

7. Okarska-Napierała M, Mańdziuk J, Feleszko W, et al. Recurrent assessment of lymphocyte subsets in 32 patients with multisystem inflammatory syndrome in children (MIS-C). *Pediatr Allergy Immunol*. 2021;32:1857–1865.

8. Ramaswamy A, Brodsky NN, Sumida TS, et al. Immune dysregulation and autoreactivity correlate with disease severity in SARS-CoV-2-associated multisystem inflammatory syndrome in children. *Immunity*. 2021;54:1083-1095.e7.

9. Syrimi E, Fennell E, Richter A, et al. The immune landscape of SARS-CoV-2-associated Multisystem Inflammatory Syndrome in Children (MIS-C) from acute disease to recovery. *iScience*. 2021;24:103215.

10. Tanaka Y, Kubo S, Iwata S, et al. B cell phenotypes, signaling and their roles in secretion of antibodies in systemic lupus erythematosus. *Clin Immunol*. 2018;186:21–25.

11. Porritt RA, Binek A, Paschold L, et al. The autoimmune signature of hyperinflammatory multisystem inflammatory syndrome in children. *J Clin Invest*;131 . Epub ahead of print October 15, 2021. DOI: 10.1172/JCI151520.

12. Pers J-O, Daridon C, Devauchelle V, et al. BAFF overexpression is associated with autoantibody production in autoimmune diseases. *Ann N Y Acad Sci*. 2005;1050:34–39.

13. Vincent FB, Morand EF, Schneider P, et al. The BAFF/APRIL system in SLE pathogenesis. *Nat Rev Rheumatol*. 2014;10:365–373.

14. Diorio C, Shraim R, Vella LA, et al. Proteomic profiling of MIS-C patients indicates heterogeneity relating to interferon gamma dysregulation and vascular endothelial dysfunction. *Nat Commun*. 2021;12:7222.

15. Diorio C, Henrickson SE, Vella LA, et al. Multisystem inflammatory syndrome in children and COVID-19 are distinct presentations of SARS-CoV-2. *J Clin Invest*. 2020;130:5967–5975.

16. Munroe ME, Lu R, Zhao YD, et al. Altered type II interferon precedes autoantibody accrual and elevated type I interferon activity prior to systemic lupus erythematosus classification. *Ann Rheum Dis*. 2016;75:2014–2021.

17. Bengtsson AA, Sturfelt G, Truedsson L, et al. Activation of type I interferon system in systemic lupus erythematosus correlates with disease activity but not with antiretroviral antibodies. *Lupus*. 2000;9:664–671.

18. Crow YJ. Type I interferonopathies: A novel set of inborn errors of immunity. *Ann N Y Acad Sci*. 2011;1238:91–98.
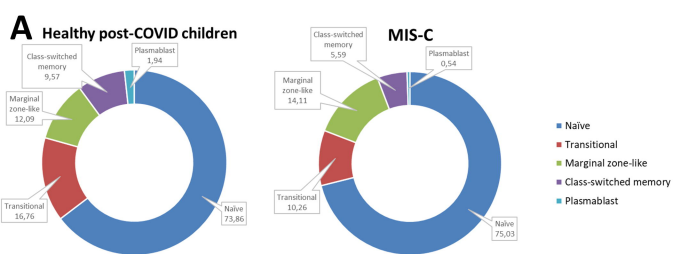
19. Bastard P, Rosen LB, Zhang Q, et al. Autoantibodies against type I IFNs in patients with life-threatening COVID-19. *Science*. 2020;370:eabd4585.

20. WHO Headquarters. Multisystem inflammatory syndrome in children and adolescents with COVID-19 Available from: https://www.who.int/publications/i/item/multisystem-inflammatory-syndrome-in-children-and-adolescents-with-covid-19. 2020. Accessed February 17, 2022.

21. Schuhenn J, Meister TL, Todt D, et al. Differential interferon-α subtype induced immune signatures are associated with suppression of SARS-CoV-2 infection. *Proc Natl Acad Sci U S A*;119 . Epub ahead of print February 22, 2022. DOI: 10.1073/pnas.2111600119.

22. Sacco K, Castagnoli R, Vakkilainen S, et al. Immunopathological signatures in multisystem inflammatory syndrome in children and pediatric COVID-19. *Nat Med* . Epub ahead of print February 17, 2022. DOI: 10.1038/s41591-022-01724-3.

23. Theofilopoulos AN, Koundouris S, Kono DH, et al. The role of IFN-gamma in systemic lupus erythematosus: a challenge to the Th1/Th2 paradigm in autoimmunity. *Arthritis Res*. 2001;3:136–141.

24. Gruber CN, Patel RS, Trachtman R, et al. Mapping Systemic Inflammation and Antibody Responses in Multisystem Inflammatory Syndrome in Children (MIS-C). *Cell*. 2020;183:982-995.e14.

25. Harigai M, Kawamoto M, Hara M, et al. Excessive production of IFN-γ in patients with systemic lupus erythematosus and its contribution to induction of B lymphocyte stimulator/B cell-activating factor/TNF ligand superfamily-13B. *The Journal of Immunology*. 2008;181:2211–2219.

26. Coquery CM, Wade NS, Loo WM, et al. Neutrophils contribute to excess serum BAFF levels and promote CD4+ T cell and B cell responses in lupus-prone mice. *PLoS One*. 2014;9:e102284.

27. Belnoue E, Pihlgren M, McGaha TL, et al. APRIL is critical for plasmablast survival in the bone marrow and poorly expressed by early-life bone marrow stromal cells. *Blood*. 2008;111:2755–2764.

28. Schiemann B, Gommerman JL, Vora K, et al. An essential role for BAFF in the normal development of B cells through a BCMA-independent pathway. *Science*. 2001;293:2111–2114.

29. Salazar-Camarena DC, Ortiz-Lazareno PC, Cruz A, et al. Association of BAFF, APRIL serum levels, BAFF-R, TACI and BCMA expression on peripheral B-cell subsets with clinical manifestations in systemic lupus erythematosus. *Lupus*. 2016;25:582–592.

30. Sellam J, Miceli-Richard C, Gottenberg J-E, et al. Decreased B cell activating factor receptor expression on peripheral lymphocytes associated with increased disease activity in primary Sjögren's syndrome and systemic lupus erythematosus. *Ann Rheum Dis*. 2007;66:790–797.

Figure legends

Figure 1 Cytokines in MIS-C patients. A, IFN-α, B, IFN-γ and C, IFN-λ in MIS-C patients and healthy post-COVID children. D, APRIL and E, BAFF in MIS-C patients, convalescent MIS-C patients 6 months after disease resolution, healthy post-COVID children and healthy donor children with no history of COVID-19 or MIS-C.
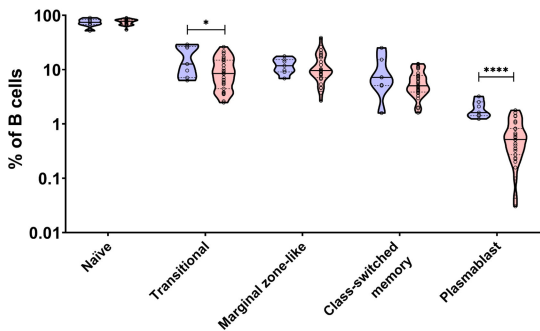
Figure 2 B cell phenotype in MIS-C patients. A and B, B cell subpopulations in MIS-C patients and healthy post-COVID children. C, BAFFR expression in naive, transitional, MZ-like, switched memory and plasmablast B cells of MIS-C patients and healthy post-COVID children.

A IFN-α

B IFN-γ

C IFN-λ

D APRIL

E BAFF

A

Healthy post-COVID children

Class-switched memory 9,57

Marginal zone-like 12,09

Transitional 16,76

Naïve 73,86

Plasmablast 1,94

MIS-C

Class-switched memory 5,59

Marginal zone-like 14,11

Transitional 10,26

Naïve 75,03

Plasmablast 0,54

- Naïve
- Transitional
- Marginal zone-like
- Class-switched memory
- Plasmablast

B

B-cell subpopulations

% of B cells

Naïve · Transitional · Marginal zone-like · Class-switched memory · Plasmablast

*

****

C

BAFFR expression

BAFFR MFI

Naïve · Transitional · Marginal zone-like · Class-switched memory · Plasmablast

*** *** *** ** *

- MIS-C
- Healthy post-COVID children